Insane in the brain:

How neuroparasites manipulate the insect's brain function and behaviour

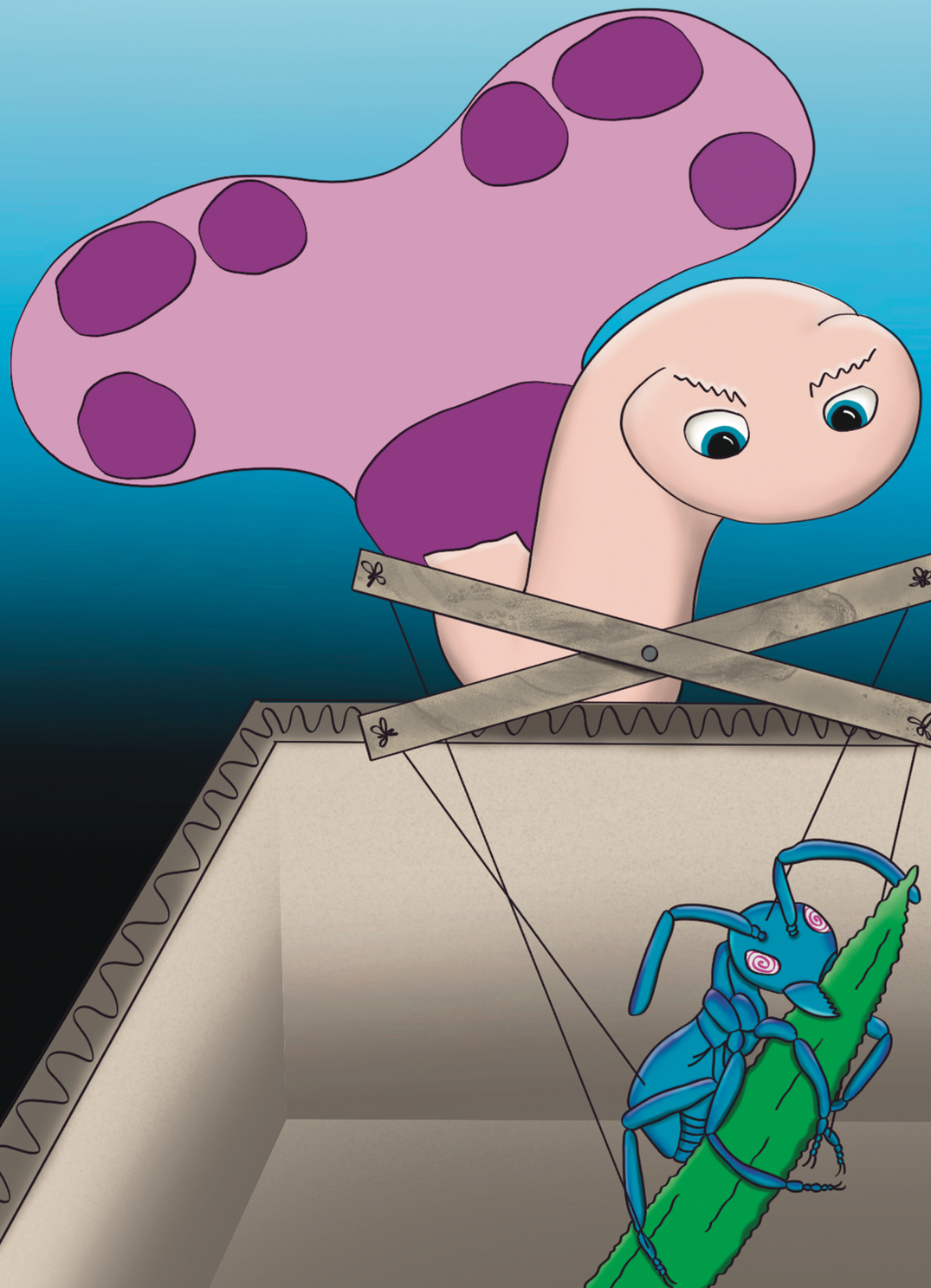

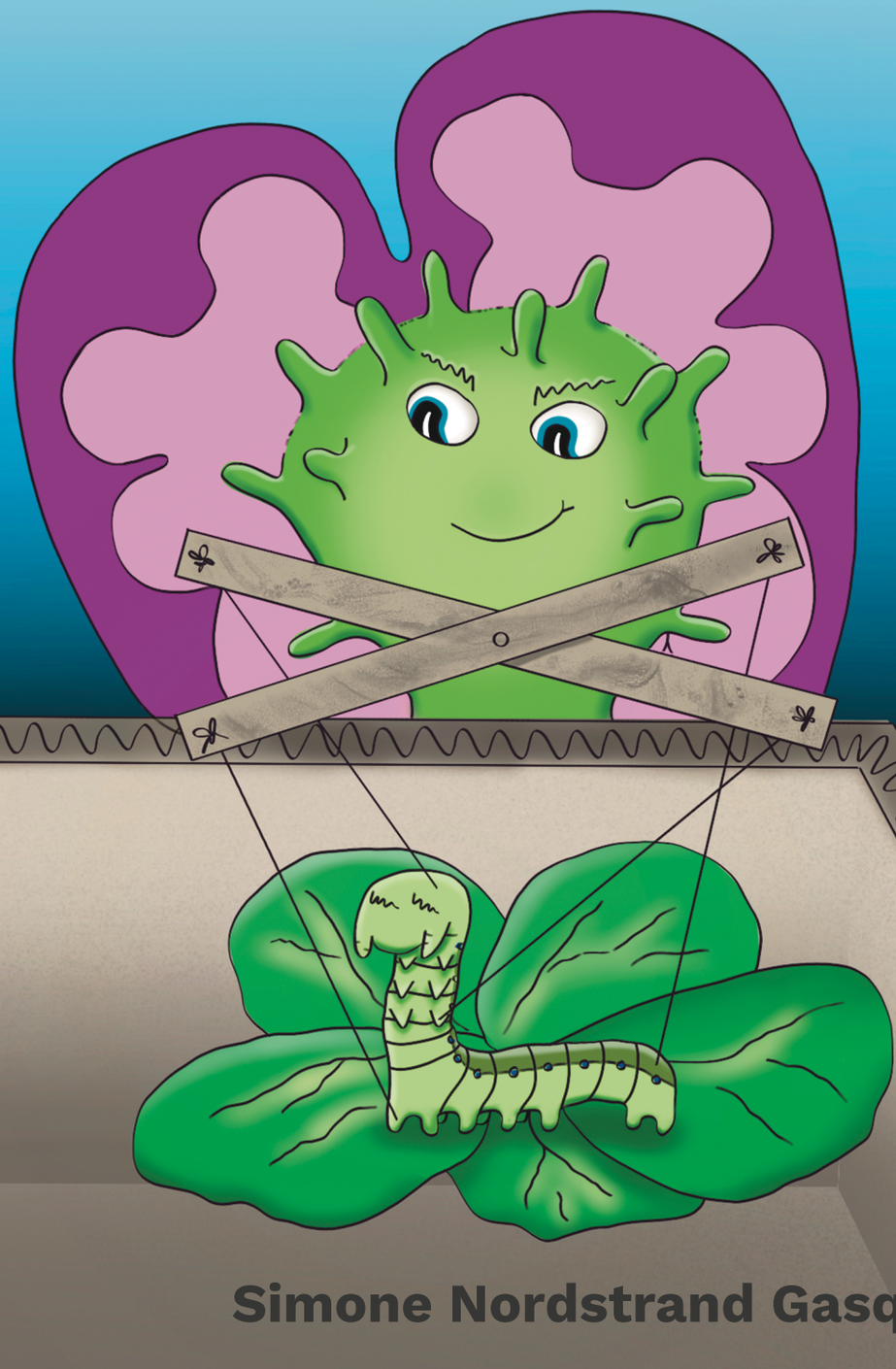

Insane in the brain

Simone N. Gasque 2024

Simone Nordstrand Gasque

Propositions

1. Data on behavioural alterations expressed by naturally parasite-infected host systems are easier to interpret than data from systems in a laboratory setting.
   (this thesis)

2. Being alive is not a prerequisite for having an infection strategy.
   (this thesis)

3. Parasite biodiversity needs protection.

4. Being awarded an Ig Nobel Prize is a greater honour than graduating cum laude.

5. Pandemic lockdowns revitalise scientists to publish research that was otherwise left in the drawer (drawer research).

6. Like dog owners tend to resemble their pet over time, PhD-candidates become like their projects.

7. The healthy finalisation of a PhD-project requires activities that provide a different state of mind than the project.

8. Neurodiversity was neglected when open office spaces were invented.

Propositions belonging to the PhD thesis entitled

Insane in the brain: how neuroparasites manipulate the insect's brain function and behaviour

Simone Nordstrand Gasque
Wageningen, March 26, 2024

Insane in the brain:

How neuroparasites manipulate the insect's brain function and behaviour

Simone Nordstrand Gasque

Insane in the brain:

How neuroparasites manipulate the insect's brain function and behaviour

Simone Nordstrand Gasque

Thesis committee

Promotor
Prof. Dr M.M. van Oers
Professor of Virology
Wageningen University & Research

Co-promotors
Dr V.I.D. Ros
Associate professor, Laboratory of Virology
Wageningen University & Research

Dr A. Haverkamp
Assistant professor, Laboratory of Entomology
Wageningen University & Research

Other members
Prof. Dr C.H.J. van Oers, Wageningen University & Research, and Netherlands Institute of Ecology (NIOO-KNAW), Wageningen
Dr C. de Bekker, Utrecht University
Prof. Dr S. Herrero, Universitat de València, Spain
Prof. Dr A.T. Groot, University of Amsterdam

This research was conducted under the auspices of the Graduate School for Production Ecology and Resource Conservation.

Thesis
submitted in fulfilment of the requirements for
the degree of doctorat Wageningen University
by the authority of the Rector Magnificus
Prof. Dr C. Kroeze,
in the presence of the
Thesis Committee appointed by the Academic Board
to be defended in public
on Tuesday March 26, 2024
at 4 p.m. in the Omnia Auditorium.

Simone Nordstrand Gasque
Insane in the brain: How neuroparasites manipulate the insect's brain function and behaviour
238 pages
PhD thesis, Wageningen University, Wageningen, the Netherlands (2024)
With references, with summaries in English, Dutch, and Danish
Doi: 10.18174/649696

At turde, er at miste fodfæste for en stund.
Ikke at turde, er at miste sig selv.
To dare it to lose one's footing momentarily.
Not to dare is to lose oneself.

Søren Kierkegaard

Table of contents

Chapter 1 9
General introduction

Chapter 2 23
Where the baculoviruses lead, the caterpillars follow:
Baculovirus-induced alterations in caterpillar behaviour

Chapter 3 37
Expression of trematode-induced zombie-ant behaviour is strongly associated with temperature

Chapter 4 73
In the mind of a caterpillar: Immunoreactive areas of the major biogenic amines in the larval *Spodoptera exigua* central nervous system

Chapter 5 105
Baculovirus entry into the central nervous system of *Spodoptera exigua* caterpillars is independent of the viral protein tyrosine phosphatase

Chapter 6 131
Untangling the strings of the puppet master: Investigating the role of biogenic amine signalling cascades in AcMNPV-infected *Spodoptera exigua* caterpillars

Chapter 7 167
General discussion

References 185
Summary 209
Sammenvatting 213
Referat 217
Publications 221
About the author 223
Training and education statement 227
Acknowledgements 231

It is we who are the parasites,
and earth the host.

Carl Zimmer

CHAPTER 1

General introduction and thesis outline

Symbionts and parasites: No existence without

All life exists in context and relation to other lifeforms, as no natural lifeform will complete its lifecycle without interacting with others. This is especially true for entities like viruses that I include here in the term lifeforms, although it is arguable whether they are alive or not. The interaction between two lifeforms is termed biological interaction or symbiosis, which is any of the many close and long-term interactions between two lifeforms. Symbiosis is a topic of immense importance, which is fundamental to many aspects of the current live on earth. Without the evolutionary event of phagocytosis of prokaryotic bacteria by eukaryotic cells (the endosymbiont hypothesis), now indispensable organelles encompassed in eukaryotic cells (chloroplasts and mitochondria) would not be present (Sagan 1967; Karnkowska *et al.* 2016; Lazcano and Peretó 2017) and life as we know it would not exist. Mutualism, commensalism, amensalism, neutralism, competition, and exploitation (predation and parasitism) are regarded as the different forms of symbiosis. In this thesis, I focus on parasitism. Parasitism has evolved independently at least 223 times in the animal kingdom alone, and is estimated to be the way of life of about half of the species on earth (Windsor 1998; Meeûs and Renaud 2002; Weinstein and Kuris 2016). Parasitism is defined as the interaction of an organism that receives energy from another organism, indicated as the host, with an advantage to the parasite and a negative consequence to the host (Meeûs and Renaud 2002). In other words, parasites are organisms that live at the expense of a host (Eilenberg *et al.* 2017). Furthermore, the host is providing the conditions needed for the parasite to reproduce and fulfil its lifecycle, at least in the cases where the parasite is an obligate and not a facultative parasite. Lines cannot always be fully drawn of whether a given interaction is parasitic, commensalistic etc. (Eilenberg *et al.* 2017). Parasites can live on the exterior of the host (ecto-) or within (endoparasites), and even inside the cells of the host as intracellular parasites. Parasites can fulfil their lifecycle in two forms; in the direct form at the expense of a single host or in complex cycles, where multiple hosts are required. For parasites with multiple hosts, the host in which the mature parasite lives and reproduces is termed the definitive host, and the preceding hosts in the lifecycle are called intermediate hosts. The parasite-host relationship has previously been regarded as a population inhabiting an island (Zimmer 2001). Getting from one host to the next or from one environment to another is figuratively speaking like crossing an ocean of different matter to get to an inhabitable island yet again. This voyage is termed transmission. To enable transmission, or to increase it, manipulation of the host may occur. The manipulation can be a phenotypical change, such as in the examples of abnormal and additional limb development in amphibians due to an infection with the trematode *Ribeiroia ondatrae* (Johnson *et al.* 2002), or the conspicuous change of appearance of host snails by *Leucochloridium paradoxum*-sporocyst placement in the tentacles (Wesołowska and Wesołowski 2014). Even more

marvellous and bizarre are the cases where parasites induce altered host behaviour as described in detail below.

Parasitic manipulation

For obligate parasites (that might cause fatal illness of the host), we are dealing with an evolutionary arms race (Dawkins 1982; Dawkins and Krebs 1979) that is under the highest level of evolutionary pressure as both parties are running and fighting for their lives. The only way to survive is to keep evolving, and each party is increasing its forces, weaponry or strategies to win the battle. This has also been referred to as the Red Queen hypothesis, as inspired by the story 'Through the looking glass' (1871) by Lewis Carroll (Caroll 1871; van Valen 1973). "It takes all the running you can do, to keep at the same place". As originally referred to by Richard Dawkins (the Extended Phenotype, 1982), animals, and especially parasites, tend to manipulate objects in the world around them (Tain *et al.* 2006). These parasites manipulate the hosts in which they exist, to increase the change of being transmitted to a new physical environment or literally to the next host. Despite what one might think, the cases of hosts serving under behavioural alteration by a manipulating parasite in the animal kingdom is not rare. An extensive example of this is the behavioural change induced by the injection of an iflavirus during oviposition by the braconid parasitoid *Dinocampus coccinellae* into the ladybeetle host (*Coleomegilla maculata*). Here the parasitoid larvae will emerge from the ladybeetle after which the ladybeetle will protect the wasp cocoon (bodyguarding behaviour). Although the wasp offspring benefits from this behavioural alteration, the inducer of this behavioural change is in fact the iflavirus (Dheilly *et al.* 2015). Other examples are the parasitic barnacles *Sacculina spp.*, e.g. *Sacculina carcini*, which upon infection can change its crab host's phenotype and behaviour by feminisation of male crabs (Kristensen *et al.* 2012).

Neuroparasitology, the invertebrate CNS, biogenic amines and the blood-brain barrier

Neuroparasitology is a recently introduced term for the research field covering parasites that manipulate the behaviour of the host, where it is expected that this manipulation is executed by infection of the central nervous system (CNS) of the host (Hughes and Libersat 2018). At the time the term was introduced, trematodes and viruses were the only two groups that were recognised as infecting the CNS (Romig *et al.* 1980; Knebel-Mörsdorf *et al.* 1996; Herz *et al.* 2003; Torquato *et al.* 2006; Katsu-

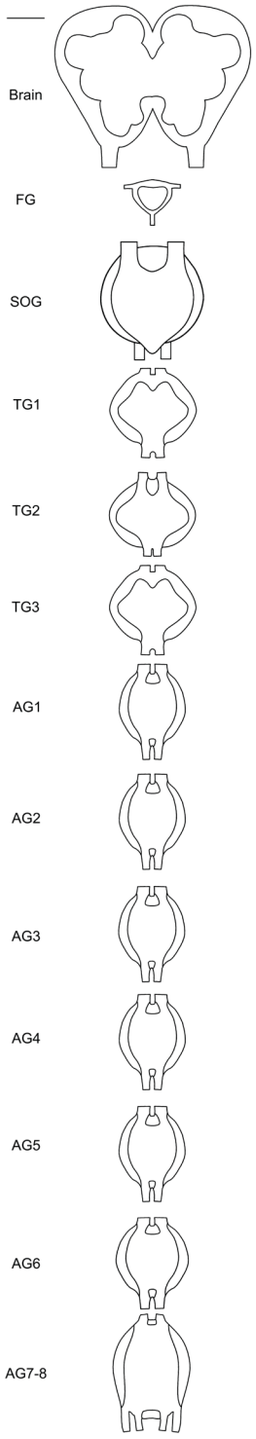

ma *et al.* 2012; Martín-Vega *et al.* 2018), where for example the unencysted metacercariae of *Dicrocoelium dendriticum* (or *Dicrocoelium hospes*) lodge onto the suboesophageal ganglion (SOG) of ants (see detailed description of the lifecycle later in this chapter and in Chapter 3, Figure 1). Parasitic barnacles have been described to infect the host's CNS by goblet-shaped organs, more specifically, they localise inside the thoracic and abdominal ganglia and the connectives between the ganglia (Lianguzova *et al.* 2020; Miroliubov *et al.* 2020). Following the definition of neuroparasites, the goblet cells from parasitic barnacles infecting the abdominal and thoracic ganglia in crabs (Lianguzova *et al.* 2020; Miroliubov *et al.* 2020) should be regarded as neuroparasites. Organisms that inject venom into the CNS of their offspring's host, such as the jewel wasps, are not regarded neuroparasites as they themselves do not invade the brain. However, the iflavirus that is injected along with the venom by the *D. coccinellae* wasp can be considered a neuroparasite, since it was found to invade the beetle's CNS (Dheilly *et al.* 2015). We will furthermore not use the term neuroparasitism for organisms that infect the CNS after the death of the host, such as the hypocrealean fungi (Fredericksen *et al.* 2017), whereas entomophthoralean species should be regarded as neuroparasites in my opinion due to the recent evidence suggesting they can infiltrate the CNS tissue while the host is still alive (Elya *et al.* 2018). The insect CNS is placed ventrally in the body cavity of the insect and is structured from the tip of the head (rostrally or cranially) to the end (caudally) by the supraoesophageal ganglion (brain), suboesophageal ganglion (SOG), the thoracic ganglia, and ending with the abdominal ganglia. As insects are segmented, these ganglia receive and send signals within the segment in which they are localised and are connected by the connectives, similar to a long string of pearls (Figure 1; see more detail in Chapter 4; and Chapter 5).

Figure 1. Schematic overview of the central nervous system of a mid-third instar *S. exigua* caterpillar, consisting of the supraoesophageal ganglion (brain), followed by the suboesophageal ganglion (SOG), three thoracic ganglia (TG1 to TG3), and seven abdominal ganglia (AG1 to AG7-8; abdominal ganglia 7 and 8 are fused). Each ganglion is connected to the adjacent ganglion by two connectives (not fully depicted). The much smaller frontal ganglion (FG) is connected to the brain which it is placed acutely caudally to. Scalebar (top left) represents 50 µm.

For protection against any parasites and pathogens a barrier of the brain exists, this barrier is termed the blood- brain barrier (BBB) (Dunton *et al.* 2021). The invertebrate BBB consists of the exterior extracellular basement membrane known as the neural lamella (NL) along with two types of glial cells; the subperineurial glia (SPG) and the apical perineurial glia (PG) cells (Hindle and Bainton 2014). This barrier also needs to be somewhat permeable to permit entry for molecules such as oxygen and carbohydrates that are needed in the brain. Signal molecules mediate the transport of nerve signals between nerve endings, for example in the form of biogenic amines. Biogenic amines are important neuroactive molecules that can act physiologically as neurotransmitters, neuromodulators or neurohormones (Blenau and Baumann 2001). For invertebrates (and more specifically insects) the four major biogenic amines are tyramine, octopamine, dopamine and serotonin (Figure 2; see further details in Chapter 4) (Blenau and Baumann 2001).

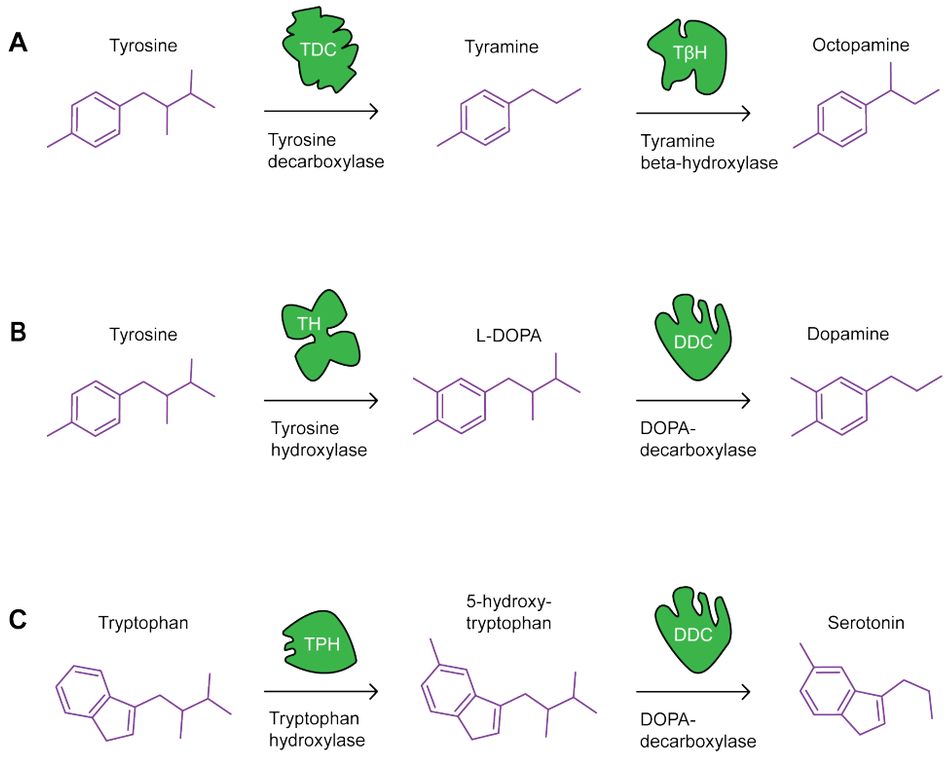

Figure 2. Graphical visualisation of the biosynthesis pathways of the four major biogenic amines, along with the enzymes catalysing these processes. A) biosynthesis pathway of tyrosine to tyramine (TA) and octopamine (OA), catalysed by tyrosine decarboxylase (TDC) and tyramine beta-hydroxylase (TβH). B) biosynthesis pathway of tyrosine to dopamine (DA), catalysed by tyrosine hydroxylase (TH) and DOPA-decarboxylase (DDC). C) biosynthesis pathway of tryptophan to serotonin (5HT), catalysed by tryptophan hydroxylase (TPH) and DDC.

These amines have shown importance in a wide range of traits, including learning, locomotion, memory formation, retrieving stored information, feeding, mating, aggression and recognition of nestmates for social insects (Akasaka *et al.* 2010; Thamm *et al.* 2010; Kamhi and Traniello 2013; Waddell 2013; Momohara *et al.* 2018; Xu *et al.* 2018).

Study systems

Viruses, baculoviruses and AcMNPV

Viruses are the simplest and smallest form of "life" on the planet. For example, porcine circovirus 1 (PCV1; family *Circoviridae*) is 17-20 nm in size with a genome of 1.7-2.3 kilobases (kb) (ICTV 2023a; NCBI: GCA_004041335.1) or viruses from the families of *Parvoviridae* or *Picornaviridae* with capsid sizes of about 20 and 30 nm, respectively (ICTV 2023b; ICTV 2023c)). Viruses have single stranded or double stranded RNA- or DNA-genomes that are protected by a protein coat composed of capsid proteins (this is the most simple form of a virus, many viruses are more complex with lipid membranes surrounding the nucleocapsids). Viruses fully rely on their host for protein synthesis as they do not contain ribosomes. The majority of viruses do not contain enzyme systems producing the buildings blocks of life (lipids, amino acids, carbohydrates etc.) or generating chemical energy, and neither do they contain the protein complexes needed for protein synthesis or molecules involved in metabolism and growth (Acheson 2011; with the exception of e.g. Mimiviruses as reviewed by Kalafati *et al.* 2022). This raises the issue and question of whether viruses can be termed as living entities or if they are inanimate. When their genome is packed in virions they are inanimate, whereas upon cell infection they share many similarities with living organisms, such as the ability to evolve, mutate and reproduce. The discussion of whether viruses are living entities or inanimate might serve a whole dissertation in itself. Nevertheless, one thing is certain, as viruses require host cells for replication, there is no other way of describing them than as obligate intracellular (micro-) -parasites or -pathogens. Baculoviruses (*Baculoviridae*) are large insect viruses (Williams *et al.* 2017a). They encapsulate virus particles in large occlusion bodies (OBs), also called polyhedra. The virus particles released from these OBs upon oral infection are described as occlusion derived virions (ODVs). Baculoviruses also produce a second virion form, the budded virion (BV), which is essential for cell-to-cell infection. The genetic material has the form of large circular double stranded DNA-genomes of 81-178 kilo base pairs (Ros 2021). These genomes are packed in rod-shaped nucleocapsids (therefor their name "baculo", derived from the Latin word baculum which mean staff or stick) of around 30-60 nm in width and 250-300 nm in length (Williams *et al.* 2017a; Harrison *et al.* 2018). All members of the family share 38 homologous core genes (Javed *et al.* 2017; Ros 2021; Chen *et. al.* 2023), and

the family has been subdivided into four genera based on phylogenetic relatedness; *Alphabaculovirus*, *Betabaculovirus*, *Gammabaculovirus* and *Deltabaculovirus* (Jehle *et al.* 2006; Ros 2021). The most well studied alphabaculovirus is Autographa californica multiple nucleopolyhedrovirus (AcMNPV) with a genome size of 133,894 base pairs encoding around 152 proteins (Ayres *et al.* 1994). In this dissertation the focus is on AcMNPV. Natural baculovirus infections occur as caterpillars ingest vegetation contaminated with baculovirus OBs (Figure 3).

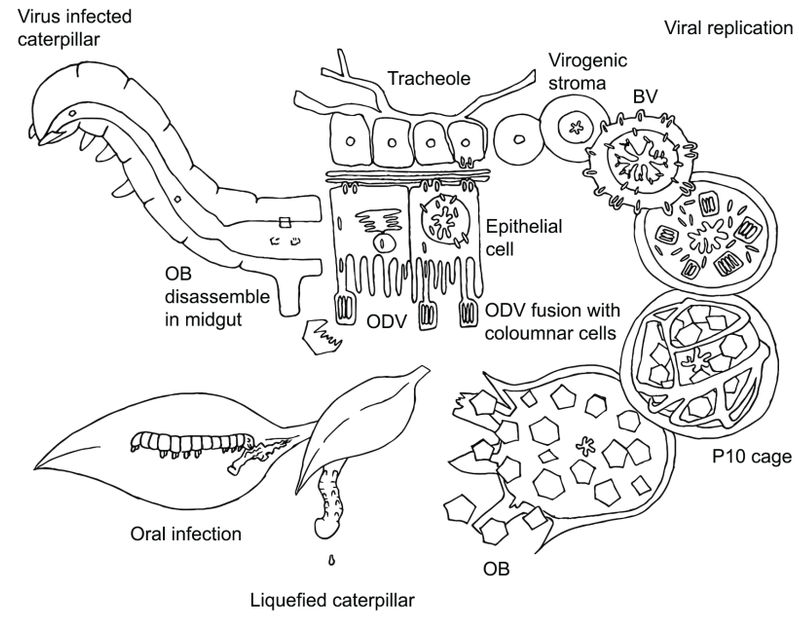

Figure 3. Replication cycle of baculoviruses, e.g. Autographa californica multiple nucleopolyhedrovirus (AcMNPV). Caterpillars get orally infected, and the occlusion bodies (OBs, or polyhedra from the polyhedral shape) disassemble in the alkaline environment of the caterpillar midgut (cross section through caterpillar only showing some of the intestinal tract and the outer shape of the caterpillar). Occlusion derived virions (ODV) bind to midgut epithelial cells. After the viral envelope and the cell membrane fuse, nucleocapsids enter these cells and can either bypass viral replication (left epithelial cell) or initiate viral replication (right epithelial cell) forming new nucleocapsids. Nucleocapsids leave the cell by budding, forming budded viruses (BVs). The BVs pass over the basal lamina (illustrated above the epithelial cells) into other tissues, here represented as midgut regenerative cells and tracheal cells represented as a tracheole. On the right side of the figure the viral replication is illustrated. Showing the virogenic stroma (amoeboid shape inside nucleus), the progression of production of BVs, ODVs and finally production of OBs. The P10-cage surrounding the nucleus is illustrated; this structure is pivotal for breakage of the nucleus and therefor for OB release. OBs escape the enclosure of the caterpillars' body by means of liquefaction of the host, and new caterpillars can get infected by ingesting contaminated vegetation or by cannibalism of liquefied caterpillars. Drawing by Simone N. Gasque.

After the OBs disassemble in the alkaline environment of the caterpillar's midgut, the ODVs bind and fuse with the microvilli of the midgut epithelial cells and release nucleocapsids into the cytoplasm of these cells (initial phase of baculoviral infection). Nucleocapsids are transported to the cell nucleus where the DNA is unpacked and replicated. Progeny nucleocapsids are formed, that are subsequently transported to the cell envelope where they egress by budding (obtaining an envelope), leading to the formation of budded virions (BVs). In the midgut cells, some nucleocapsids directly pass towards the other end of the cell (without replication), where they egress by budding. Neighbouring cells can get infected, or a secondary phase can progress with infections of other cell types, initially mainly tracheal cells and haemocytes. Through the haemolymph the infection can spread to other tissues, such as muscles and fat body (Slack and Arif 2007; Williams *et al.* 2017b). AcMNPV can infect a broad range of lepidopteran host species (30 species, possibly accounting 95 species) (Cory 2003; Clem and Passarelli 2013), including *Spodoptera exigua*; this combination constitutes the virus-host system under study in this dissertation.

Spodoptera exigua

Spodoptera exigua, the beet army worm, is a polyphagous pest insect (Azidah and Sofian-Azirun 2006). It originated from Asia, but is now a serious pest in greenhouses in colder locations (e.g. Europe). The greenhouses provide an option for these insects to survive the otherwise too cold winters. *Spodoptera exigua* neonate larvae hatch from eggs and go through five larval instars (L1 to L5; some studies report an optional sixth instar) (Simon *et al.* 2021). Lepidopterans are holometabolous insects and they undergo complete metamorphosis. At the end of the fifth instar the caterpillars dig into the ground where they pupate, after which the imago (adult) emerges. Caterpillars feed gregarious (L1 and L2) and solitarily (L3-L5) (Azidah and Sofian-Azirun 2006). *Spodoptera exigua* caterpillars can be reared on an artificial diet in a laboratory setting (Smits 1987) as is described in most detail in chapter 5. The larval instars of *S. exigua* can get infected by AcMNPV, which can lead to the behavioural alteration expressed as tree-top disease and hyperactivity, the latter being the topic of this dissertation (see more detail on baculoviral induced behavioural alteration in Chapter 2). It is expected that these behavioural changes are induced from the infection of the CNS.

Formica polyctena and *Dicrocoelium dendriticum*

The other host organism used for conducting part of the research included in this dissertation, is the European red wood ant, *Formica polyctena*, *in situ* infected with the lancet liver fluke *Dicrocoelium dendriticum* (order Trematoda, class Digenea). On the contrary to the laboratory kept population of *S. exigua,* which I manually infected with AcMNPV, the *D. dendriticum*-infected *F. polyctena* population concerns

a wild population found in the Bidstrup Forests in Denmark. *Formica polyctena* are, like other ants, true eusocial insects, defined by their big complex societies, which can be seen on the forest floor by their large anthills (Kamhi *et al.* 2016). The trematode *D. dendriticum* serves a well-known example of an inducer of behavioural alteration expressed in the second intermediate ant host (Figure 4; and Chapter 3). In an altruistic act one to two of the metacercariae of the lancet liver flukes migrate to and lodge onto the SOG of the ant where they remain in an unencysted state (Tarry 1969; Romig *et al.* 1980; Manga-González *et al.* 2001; Martín-Vega *et al.* 2018; Criscione *et al.* 2020). This movement to the CNS is expected to be the reason for the altered behaviour of the host.

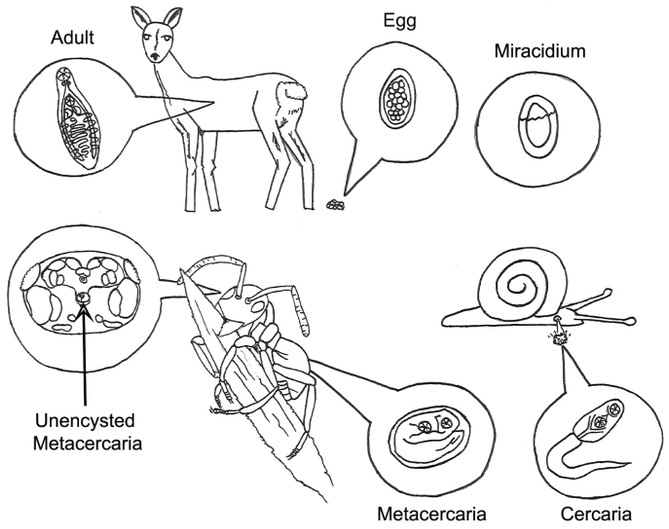

Figure 4. Lifecycle of *Dicrocoelium dendriticum.* Eggs are excreted from an herbivorous mammal serving as the definitive host, and hatch into a miracidium when ingested by a terrestrial snail. Mother and daughter sporocysts develop in the hepatopancreas of the snail (not shown), producing the cercaria stage. Cercariae are released from the snail via slimeballs excreted from the pneumostome. Ants eat the slimeballs containing infective cercariae, which develop into metacercariae in the hemocoel of the gaster of the ant. However, one or more cercariae penetrates the lining of the crop upon ingestion and migrates to the suboesophageal ganglion (depicted in the head capsule of the ant by arrow; Martín-Vega *et al.* 2018), where it induces a reversible biting behaviour of the ants where the mandibles are locked to vegetation leaving the ant exposed to ingestion by a suitable definitive host. Following ingestion, the metacercariae excyst in the duodenum, migrate to the bile ducts of the liver and mature to become adult worms producing large numbers of eggs by sexual reproduction. Drawing by Simone N. Gasque.

In the 1970-80s anecdotal observations were made describing how infected ants bite onto vegetation early in the morning and late in the evening (Badie 1975; Spindler *et al.* 1986), with postulations that the time of day or temperature play a major role for the expression of this reversible behavioural alteration.

Objectives and research questions

The main goal of this dissertation is to better understand the mechanisms behind parasite-induced behavioural alteration, including both the internal aspects of the host in the form of the role of the CNS and what happens on a molecular level, but also the outer abiotic factors that influence the expression of this behavioural alteration. Focusing on two great examples of neuroparasites, which are known to lodge onto or infect the CNS of the host, I intend to answer a range of questions and thereby hopefully aid in advancing our understanding of parasites that alter the behaviour of the host.
The following research questions will be addressed in this PhD dissertation:

1. Which of the abiotic factors has the biggest influence on the behavioural expression of *D. dendriticum*-infected *F. polyctena* ants in the field? (Chapter 3)

2. Where are the brain cells expressing the major nerve signalling molecules and their rate limiting enzymes located in the CNS of *S. exigua* caterpillars? Which differences and similarities are observable between the above-mentioned targets? (Chapter 4

3. When and where can we identify AcMNPV in the CNS of *S. exigua* caterpillars? And how does AcMNPV-PTP play a role in the CNS entry? (Chapter 5)

4. Which mechanisms play a role in the induction of behavioural alteration of AcMNPV-infected *S. exigua* caterpillars? (Chapter 6)

5. Which similarities can be detected in the locations of AcMNPV and the different biogenic amines in the CNS of *S. exigua*? (Chapter 7)

Outline of the thesis

This project was originally named “Insane in the brain” and set out to study “How a virus manipulates a caterpillars brain function and behaviour to enhance transmission”, with focus on the infected and uninfected central nervous system and unravelling the underlying mechanisms behind the altered behavioural hyperactivity (Figure 5). During the course of time another system was included for widening of the overall scope. From focusing on the direct infection of caterpillars by baculoviruses, another CNS infecting parasite going through a complex lifecycle (opposite to baculoviruses) was included.

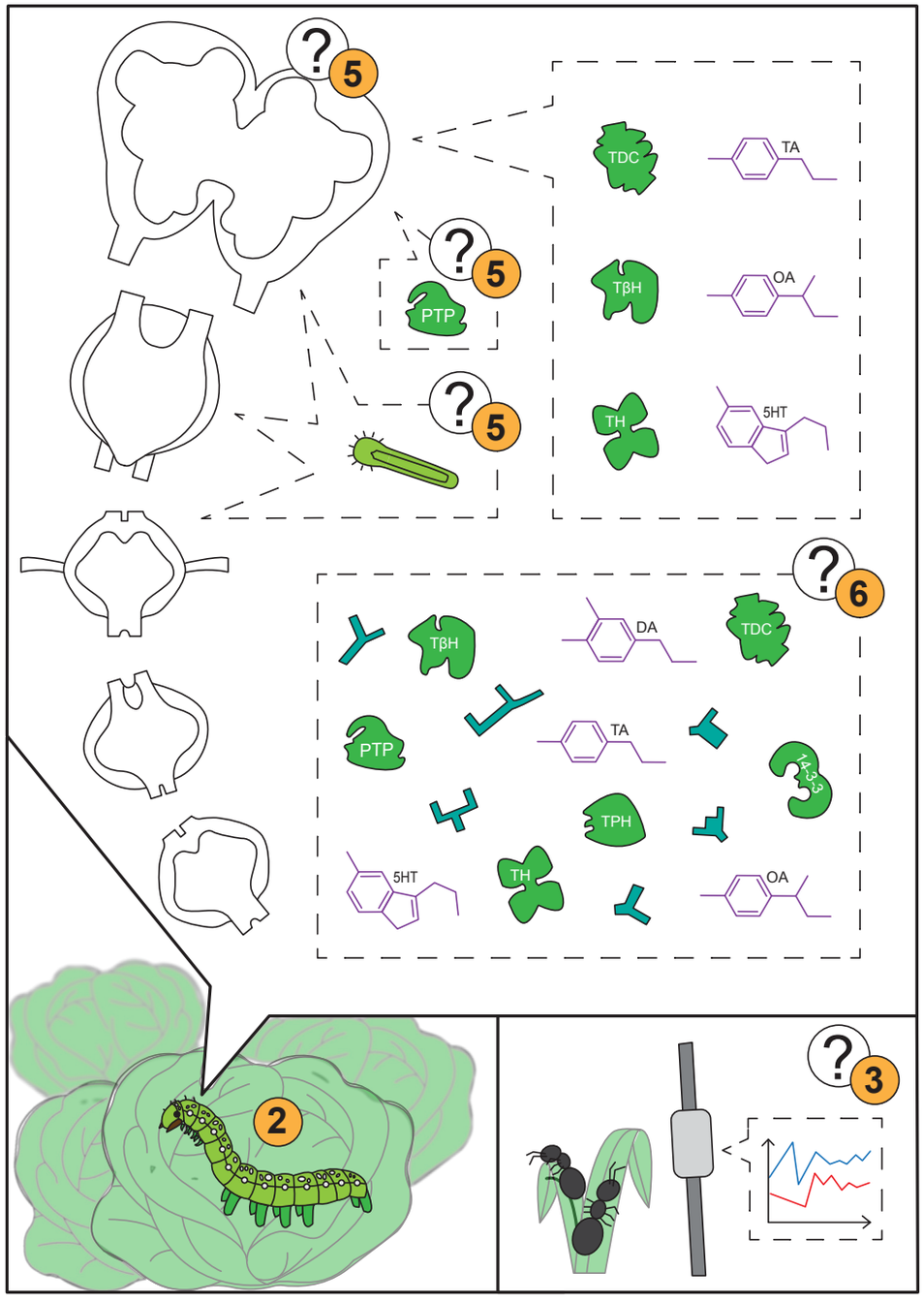

Figure 5. Graphical overview of the outline of this dissertation. Chapter 2 reviews what was known at the time about behavioural alteration of caterpillars by baculoviruses. Chapter 3 investigates which of the studied abiotic factors in the field has the highest influence on the expression of trematode induced be-

havioural alteration in forest ants. The following chapters zoomed in on the internal aspects of the *Spodoptera exigua* caterpillars. Chapter 4 studies where some of the major biogenic amines and their rate limiting enzymes are located in the central nervous system (CNS). In Chapter 5 an investigation of if, how, when and where Autographa californica multiple nucleopolyhedrovirus (AcMNPV) enters and localise in the CNS was conducted. Furthermore, the role of AcMNPV protein tyrosine phosphatase (PTP) in CNS entry was studied. In Chapter 6 the concentrations of biogenic amines and the gene expression of their enzymes and receptors were studied under AcMNPV infection. Important molecules and proteins for this dissertation are abbreviated, and orange circles indicates the chapter where the content of the visuals can be found in. Idea and initial draft by Simone N. Gasque, and full digital illustration by Frederik N. Gasque.

In Chapter 2 an overview of what was known at the start of this project on baculovirus-induced alteration of caterpillar behaviour is given, with special focus on already discovered players in the host, such as protein tyrosine phosphatase (PTP) and its influence on hyperactivity, and ecdysteroid UDP-glucosyl transferase (EGT) and its influence on tree-top disease. The influence of light in the behavioural-altered cases and future methods of detecting the underlying mechanism in the alteration are also touched upon. In Chapter 3, a clear example of induction of negative geotactic behaviour induced in the *D. dendriticum*-ant system, is thoroughly analysed *in situ*, in order to find the main abiotic driver of the typical biting behaviour of the parasitised ants observed in the field. In Chapter 4 as many as six different targets are identified and analysed in the CNS of third instar *Spodoptera exigua* caterpillars, to get insight into biogenic amines in larval lepidopteran CNS. This is a descriptive chapter, to lay the foundation wherefrom further studies of viral locations within the CNS can build upon. The four major nerve signalling molecules (tyramine, octopamine, dopamine (indirectly through rate limiting enzyme) and serotonin) in invertebrates along with enzymes involved in the biosynthesis process leading to these biogenic amines are targeted. Tyrosine decarboxylase, tyramine, tyramine beta-hydroxylase and octopamine are analysed, representing both the tyraminergic and octopaminergic pathways. Tyrosine hydroxylase (as indirect targeting of dopamine, the dopaminergic pathway) and serotonin (serotonergic pathway) are also targeted. This results in options for seeing differences between the locations of the immunoreactive cell bodies and projections of each of these, but also drawing parallels of similarities between the locations of the targets. In Chapter 5 it is investigated if, how and when AcMNPV can infect the different ganglia of the CNS. The findings are used to test the previous postulated idea of baculoviruses infecting and crossing into the CNS over the blood-brain barrier through means of the trachea. Lastly for this chapter, I analyse whether the entry into the CNS is dependent of the viral protein PTP, a protein which enzymatic activity is known to be required for the behavioural expression of hyperactivity during AcMNPV-infections of *S. exigua*. Next, we dive into the underlying molecular mechanisms that might be involved in the behavioural change induced by AcMNPV in the *S. exigua* host in Chapter 6. Quantities of some of the major nerve signalling molecules, dopamine, octopamine and serotonin, are measured and differences in expression of the rate limiting enzymes needed for the synthesis of these biogenic amines (including also tyramine) and the receptors these bind to, along with extra candidate genes (e.g. *14-3-3*) are measured. Results and conclusions from the previous chapters are being discussed and placed in a broader perspective in Chapter 7, forming the general discussion of this PhD dissertation.

Acknowledgements

I would like to thank Vera I.D. Ros, Alexander Haverkamp and Monique M. van Oers for constructive feedback on an earlier version of this chapter. I would also extend my gratitude to Frederik N. Gasque for visualising my ideas on a sketch into the visual overview of this dissertation in Figure 5.

The important thing is to never stop questioning.

Marie Skłodowska-Curie
and Albert Einstein

CHAPTER 2

Where the baculoviruses lead, the caterpillars follow: Baculovirus-induced alterations in caterpillar behaviour

Simone N. Gasque, Monique M. van Oers and Vera I.D. Ros

Laboratory of Virology, Wageningen University and Research, Droevendaalsesteeg 1, 6708 PB Wageningen, The Netherlands.

Published as:
Gasque SN, van Oers MM, Ros VID. 2019. Where the baculoviruses lead, the caterpillars follow: baculovirus-induced alterations in caterpillar behaviour. Curr Opin Insect Sci. 33: 30-36. doi: 10.1016/j.cois.2019.02.008.

Abstract

Baculoviruses are well-known for altering the behaviour of their caterpillar hosts by inducing hyperactivity (enhanced locomotion) and/or tree-top disease (climbing to elevated positions prior to death). These features, along with the genomic small size of baculoviruses compared to non-viral parasites and the at hand techniques for producing mutants, imply that baculoviruses are excellent tools for unravelling the molecular mechanisms underlying parasitic alteration of host behaviour. Baculoviruses can be easily mutated, allowing an optimal experimental setup in comparative studies, where for instance host gene expression can be compared between insects infected with wild-type viruses or with mutant viruses lacking genes involved in behavioural manipulation. Recent studies have revealed the first insight into the underlying molecular pathways that lead to the typical behaviour of baculovirus-infected caterpillars and into the role of light therein. Since host behaviour in general is mediated through the host's central nervous system (CNS), a promising future step will be to study how baculoviruses regulate the neuronal activity of the host.

Parasite-induced alterations in host locomotory behaviour

Many parasites alter the locomotory behaviour of their invertebrate hosts to increase their transmission, by changing the speed of locomotion (hence the total distance covered), the direction of movement (e.g. horizontally or vertically, by photo- or geotaxis), or the nature of the movement itself (e.g. twitching) (Bethel and Holmes 1973; Helluy 1984; Vasconcelos *et al.* 1996; van Houte *et al.* 2013). Nematomorphs (horsehair worms) manipulate their insect hosts to seek water and to jump into it in a seemingly suicidal action (Schmidt-Rhaesa and Ehrmann 2001; Thomas *et al.* 2002). The so-called 'zombie ants' are infected with flukes (e.g. *Dicrocoelium dendriticum*) or fungi (e.g. *Pandora formicae* or *Ophiocordyceps unilateralis sensu lato*). These ants express negative geotaxis (Hughes *et al.* 2011; Botnevik *et al.* 2016; Małagocka *et al.* 2017) migrating to elevated heights in vegetation, where they lock their mandibles in a reversible tetany when infected by flukes or in a fatal death grip when infected by fungi (Hughes *et al.* 2011; S.N. Gasque, MSc thesis, University of Copenhagen, 2017). The altered ant behaviour enhances transmission of flukes to the definitive host (Manga-González *et al.* 2001) and increases the spread of fungal spores (Andersen *et al.* 2009; Hughes *et al.* 2011; Małagocka *et al.* 2015). Changes in locomotion are also frequently observed in caterpillars infected with baculoviruses (see Box 1). Infected caterpillars show increased locomotion (Figure 1A) [termed in the literature as hyperactivity, hypermobility or enhanced locomotor activity (ELA)] and/or a preferred direction of movement in their elevation-seeking behaviour to the top of branches or leaves (Figure 1B; Supplementary File), just prior to death (termed as 'Wipfelkrankheit' or tree-top disease) (Kamita *et al.* 2005; Hoover *et al.* 2011; van Houte *et al.* 2012; Ros *et al.* 2015).

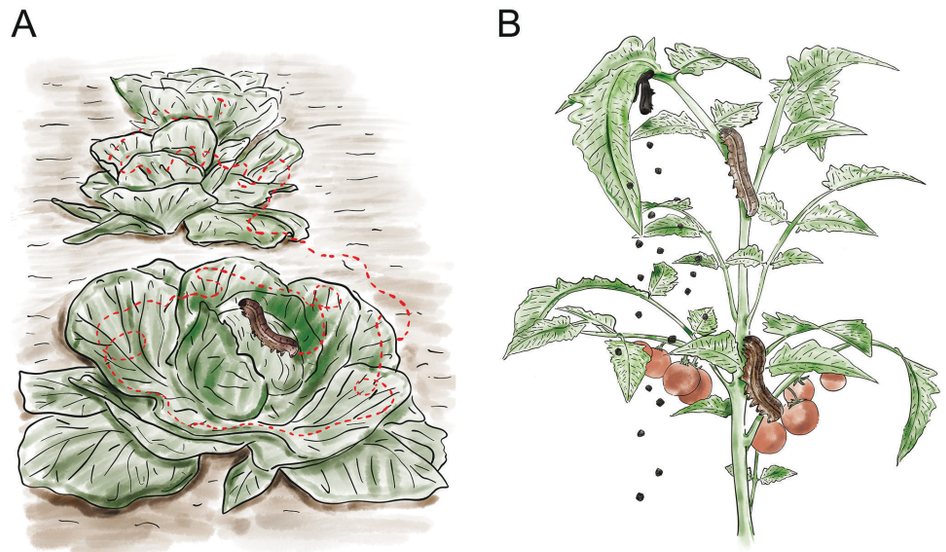

Figure 1. Graphical representation of behavioural manipulation in baculovirus-infected caterpillars. A) Infected caterpillars express increased locomotion (hyperactivity, ELA), thereby moving in the horizontal plane (here in a cabbage field) and/or tree-top disease B), where the infected caterpillars move to elevated positions, typically to the top of vegetation (here on a tomato plant). Over time, the caterpillar becomes paler before it attaches itself with its abdominal prolegs, dies and liquefies. Subsequently, viral occlusion bodies are dispersed over the vegetation and soil underneath. Claus Gasque ('by GASQUE') drew the images.

These behavioural changes are assumed to increase the area over which the progeny virus is spread. For instance, tree-top disease can enhance the distribution of progeny virus over the underlying foliage, thereby increasing the chance of transmission to other caterpillars (Vasconcelos *et al.* 1996; Goulson 1997). In addition, the resulting cadavers at the top of plants are more visible to birds predating on caterpillars, enhancing long-distance dispersal of the virus (Entwistle *et al.* 1993; Vasconcelos *et al.* 1996). Furthermore, the elevated positions of diseased larvae (often close to the central plant stem) increase the frequency of encounters with healthy larvae foraging for young foliage at the top of plants, resulting in a high incidence of intraspecific necrophagy, that ultimately results in enhanced virus transmission (Rebolledo *et al.* 2015).

Initial studies on baculovirus-induced behavioural manipulation

The earliest reported observation of an illness-related behavioural alteration in caterpillars was by Hoffmann in 1891 (as mentioned in Goulson 1997). Hoffmann explained how caterpillars of the nun moth, *Lymantria monacha*, in a state of 'Schlafsucht' or 'Flacherie' lost their appetite and migrated to the top of trees or branches ('wipfeln'). Due to this 'Wipfelkrankheit' or 'tree-top disease' (as it was later named) the nun moths died up in the trees hanging by their abdominal prolegs (Figure 2) (Glaser and Chapman 1916; Steinhaus 1946; Smirnoff 1965).

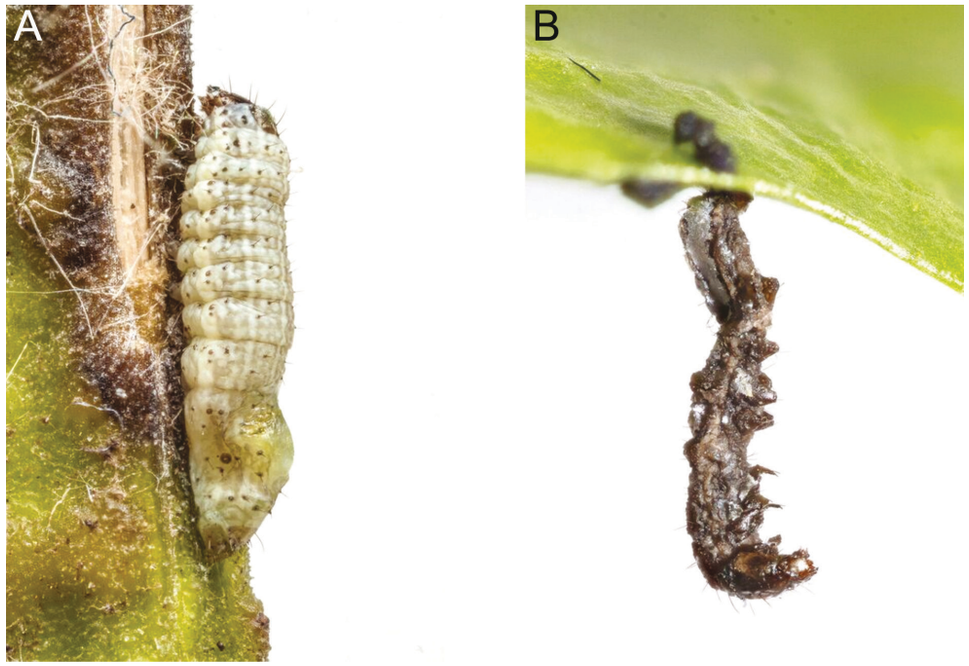

Figure 2. SeMNPV-infected third instar *Spodoptera exigua* caterpillars. A) An infected caterpillar on a plant stem showing the characteristic paleness and the start of liquefaction at 3 days post infection (dpi). B) A liquefied cadaver hanging from a leaf at 6 dpi. The photographs were taken with a canon MP-e65 lens mounted on a Canon M5 camera. Several photographs were taken at different focal distances using a Stackshot automated macro rail and combined in Zerene focus stacking software v 1.04. Pictures produced by Hans M. Smid, Laboratory of Entomology, Wageningen University and Research.

This tree-top disease was later proven to be caused by baculoviruses (Bergold 1943). Several studies conducted in the middle of the 1990's showed that *Mamestra brassicae* caterpillars infected with the alphabaculovirus M. brassicae multiple nucleopolyhedrovirus (MbMNPV) dispersed over larger distances than their uninfected conspecifics (Vasconcelos *et al.* 1996; Goulson 1997). The mobility of MbNPV-infected *M. brassicae* larvae changed over the course of the infection; infected larvae moved further than uninfected individuals 4 days post infection (dpi), but moved less than their healthy counterparts at 7 dpi (Vasconcelos *et al.* 1996). Goulson (1997) also described higher dispersal rates of MbNPV-infected fifth instars compared to uninfected larvae, both in the laboratory and in the field.

Box 1: Baculoviruses

Baculoviruses (family *Baculoviridae*) are enveloped viruses with rod-shaped nucleocapsids and a large (81-178 kilo base pairs) circular double-stranded DNA genome (Williams *et al.* 2017a). Baculoviruses are the most well-studied insect viruses, infecting over 700 (mainly lepidopteran) insect species and being widely used as biocontrol agents (Lacey *et al.* 2015; Williams *et al.* 2017a). Baculoviruses have two virion phenotypes; budded virions (BVs) and occlusion-derived virions (ODVs) (reviewed by Harrison and Hoover 2012; and Blissard and Theilmann 2018). To persist in the harsh environment outside of the insect body, the ODVs are embedded in a protective protein matrix, forming occlusion bodies (OBs) (Figure 3). The protective matrix is composed of either polyhedrin (for nucleopolyhedroviruses, NPVs) or granulin (for granuloviruses, GVs). When ingested by a susceptible insect host, the OBs disassemble in the alkaline environment of the larval midgut, releasing the ODVs, which subsequently bind and fuse with the columnar cells in the larval midgut epithelium. The nucleocapsids then enter the midgut cells and initiate viral replication to generate BVs that spread to other tissues of the larva. During the final stage of infection, new OBs are produced and released by cell lysis, which ultimately causes complete liquefaction of the host (Figure 2). Currently, the family *Baculoviridae* contains four genera: *Alphabaculovirus* (lepidopteran specific NPVs), *Betabaculovirus* (lepidopteran specific GVs), *Gammabaculovirus* (hymenopteran specific NPVs) and *Deltabaculovirus* (with currently a single dipteran specific NPV) (Jehle *et al.* 2006).

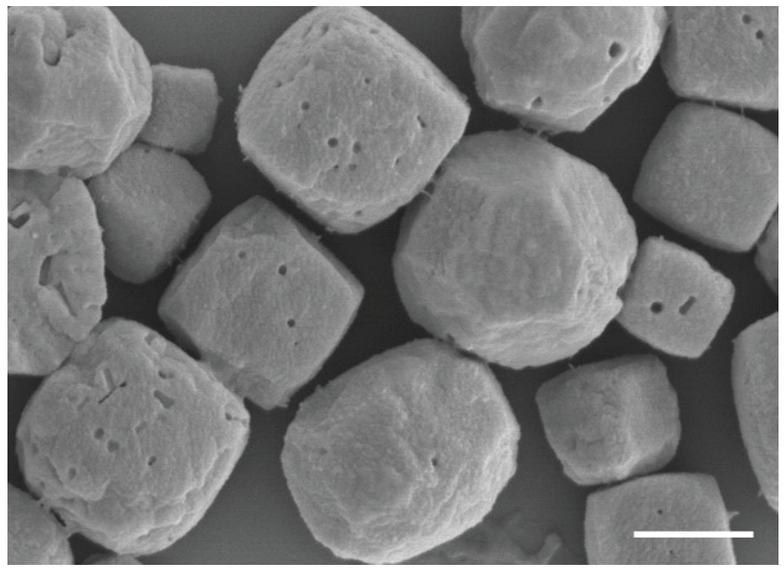

Figure 3. Baculovirus occlusion bodies. Bar represents 1 µm.
[Photo credits: Wageningen Electron Microscopy Centre (WEMC)].

Baculovirus-induced hyperactivity

While observational reports of baculovirus-induced behavioural manipulations were abundant, not much was known for a long time on the causative mechanisms leading to these behavioural changes. In 2005, Kamita *et al.* (2005) demonstrated that the Bombyx mori nucleopolyhedrovirus (BmNPV) *ptp* gene [encoding for a protein tyrosine phosphatase (PTP)] was required for the hyperactivity of neonate *B. mori* larvae. Subsequently, van Houte *et al.* (2012) showed that hyperactivity was also observed in third instar *Spodoptera exigua* larvae infected with Autographa californica (Ac)MNPV and that the AcMNPV *ptp* gene played a key role in the induction of hyperactivity in this system. Homologues of *ptp* are present in a subset of baculoviruses (a clade within the genus *Alphabaculovirus*, named group I NPVs) (van Houte *et al.* 2012). Based on phylogenetic studies, it seemed evident that the *ptp* gene was acquired from a lepidopteran host by a baculovirus ancestral to the group I NPVs. Furthermore, *ptp*-induced hyperactivity may be a conserved strategy within group I NPVs (van Houte *et al.* 2012). However, further studies demonstrated that the exact mechanism of *ptp*-induced hyperactivity may depend on the virus and host species involved. In AcMNPV-infected *S. exigua* larvae, hyperactivity was only observed when the virus expressed an enzymatically active form of PTP, indicating that the PTP phosphatase activity was required for hyperactivity (van Houte *et al.* 2012). In contrast, *B. mori* larvae infected with a BmNPV-mutant that produced an enzymatically inactive PTP (achieved by mutating its catalytic site) still exhibited hyperactivity (Katsuma *et al.* 2012; Katsuma 2015). Since PTP was found to primarily copurify with the envelope fraction of BmNPV budded virions, it was suggested that BmNPV PTP has a role in hyperactivity as a virion-associated structural protein rather than as a phosphatase (Katsuma *et al.* 2012). It was further suggested that PTP aids baculovirus infection of the brain and possible other tissues, and that this specific tissue tropism might play a role in the induction of hyperactivity.

The above-mentioned studies suggest that two closely related baculoviruses may exhibit different mechanisms to achieve PTP-induced hyperactivity. As indicated above, *ptp* is restricted to group I NPVs, however, hyperactivity has also been observed for larvae infected with group II NPVs, as seen for MbNPV infecting *M. brassicae* larvae (Vasconcelos *et al.* 1996; Goulson 1997). This implies that baculoviruses possess additional mechanisms, not involving the *ptp* gene, to induce hyperactivity.

Baculovirus-induced tree-top disease – the role of the *egt* gene

The observation that baculovirus-infected caterpillars die at elevated positions on plants or trees has been frequently made in the past century, and during the last decade this phenomenon has been studied in more detail. Several studies have focused on the involvement of the viral *egt* gene in this process and the results suggest that similarly to the induction of hyperactivity, baculoviruses possess multiple mechanisms to induce tree-top disease. The *egt* gene, present in nearly all baculoviruses (Ros *et al.* 2015), encodes for ecdysteroid UDP-glucosyl transferase (EGT), an enzyme that catalyses the conjugation of a sugar molecule (UDP-glucose or UDP-galactose) with ecdysteroids (O'Reilly and Miller 1989). As a consequence, the moulting hormone 20-hydroxyecdysone (20E) becomes inactivated, thereby blocking the normal moulting processes in virus-infected insects (O'Reilly and Miller 1991; Cory *et al.* 2004). In addition, *egt* was found to extend the time until the host dies, keeping the host longer in an active feeding state (O'Reilly and Miller 1991; O'Reilly 1999; Cory *et al.* 2004), although such an effect was not universally found, as a prolonged feeding stage was absent for some virus-host combinations or for certain host instars (Cory *et al.* 2001; Ros *et al.* 2015).

Several studies have demonstrated that the role of the *egt* gene in tree-top disease might be a consequence of the effect of EGT on moulting and moulting- or feeding-associated behaviours (Hoover *et al.* 2011; Han *et al.* 2015b; Ros *et al.* 2015). Hoover *et al.* (2011) showed that the *egt* gene of Lymantria dispar (Ld)MNPV was required for tree-top disease in gypsy moth (*L. dispar*) larvae. Healthy *L. dispar* larvae feed up in the tree at night, and crawl down during daytime to hide in bark crevices to avoid predation (Hoover *et al.* 2011). Once EGT titres are high enough in LdMNPV-infected larvae to reduce host 20E level, the moulting cycle and the daily movement and feeding patterns may be interrupted. Wildtype infected larvae remain up in the tree and continue eating. Subsequently, they die at elevated positions. Larvae infected with a mutant virus lacking *egt* continue their daily movement patterns and are found dead at low positions (Hoover *et al.* 2011). Also, in AcMNPV-infected *S. exigua* and *Trichoplusia ni* larvae, EGT was found to affect moulting and moulting-related behaviour. These larvae climb to elevated positions prior to moulting when healthy, but this behaviour was absent in wild type (WT) AcMNPV-infected larvae, where EGT blocked moulting. Larvae infected with a mutant virus (lacking the *egt* gene) did exhibit premoult climbing behaviour. However, in these AcMNPV-infected larvae, death occurred at a later time point than moulting (as seen for mutant-infected larvae) and both WT- and mutant AcMNPV-infected larvae climbed to elevated positions prior to death, indicating that tree-top disease was not affected by EGT (Ros *et al.* 2015). *Spodoptera exigua* larvae infected with S. exigua (Se)MNPV also expressed tree-top

disease (van Houte *et al.* 2014b), but here the extended time to death impelled by EGT played a crucial role in this process. While WT-infected larvae died at elevated positions and mutant (without *egt*)-infected larvae died at low positions, this difference was due to a different time point of death (Han *et al.* 2015a). Larvae infected with the mutant virus lacking *egt* died before the time point at which tree-top disease was induced in WT-infected larvae. Therefore, it was concluded that SeMNPV EGT facilitates tree-top disease indirectly by prolonging the host's time to death.

In a recent paper, Zhang *et al.* (2018) demonstrated that tree-top disease of *Helicoverpa armigera* larvae infected with H. armigera (Hear)NPV was linked to the activity of both juvenile hormone (JH) and 20E, two main regulators of insect moulting and metamorphosis (Riddiford *et al.* 2003). In *H. armigera* larvae displaying tree-top disease, 20E signalling was blocked, while JH signalling was triggered. Both JH and 20E interact downstream with Broad isoform Z2 (BrZ2), which was downregulated after HearNPV infection. Two host micro RNAs (miRNAs), miR-8 and miR-429, were found to regulate expression of *BrZ2* and are most likely involved in the 20E- and JH-regulated tree-top disease (Zhang *et al.* 2018). Since EGT directly affects 20E by blocking its function (O'Reilly and Miller 1991), possibly the viral EGT is involved in HearNPV-induced tree-top disease in *H. armigera*, although Georgievska *et al.* (2010) found no evidence for the involvement of EGT in tree-top disease in this system. Since JH and 20E are involved in the regulation of moulting, tree-top disease might also be linked to moulting-related behaviour.

Based on the reviewed studies we argue that the *egt* gene might play a role in tree-top disease in some species, and that EGT exerts its effects through interference with host moulting and therefore with moulting-related behaviour, and/or through extending the time until the host dies. Hence, the observed tree-top disease is a consequence of a delicate interplay between virus and host and further depends on factors including the stage of the host, the time point of infection, the viral dose and the intrinsic behaviour of the host species (Han *et al.* 2015b; Ros *et al.* 2015). The displayed manipulation is likely to be adapted to the specific life cycle characteristics, feeding habits and (moulting-related) movement patterns of the host species involved (Rebolledo *et al.* 2015; Ros *et al.* 2015). Furthermore, the fact that the presence or absence of the *egt* gene did not affect tree-top disease in AcMNPV infected *S. exigua* and *T. ni* larvae suggests that additional viral genes play a role in inducing tree-top disease in these noctuid species.

Baculoviruses may induce both hyperactivity and tree-top disease in their caterpillar hosts, and this may occur sequentially. In LdMNPV-infected *L. dispar asiatica* larvae, hyperactivity was observed from 3 to 6 dpi (Bhattarai *et al.* 2018b) while tree-top disease occurred at 6 dpi (starting at 144 hpi) (Bhattarai *et al.* 2018c) (although a slightly different virus dose was used). Strikingly, in these studies (Bhattarai *et al.* 2018b; Bhattarai *et al.* 2018c) an identical, vertical, set-up was used to measure both behavioural traits, which means that hypermobility was not measured as horizontal movement, making it difficult to interpret their findings. In *S. exigua* larvae infected with AcMNPV during their third instar tree-top disease was observed later in time than hyperactivity; hyperactivity was generally observed at 3 dpi (around 70 hpi) (van Houte *et al.* 2012), whereas the climbing to elevated positions occurred at 75 hpi or later, but only when larvae had moulted to the fourth instar (Ros *et al.* 2015). Furthermore, it seems plausible that different molecular mechanisms underlie hyperactivity and tree-top disease; while the *ptp* gene of AcMNPV was found to be involved in inducing hyperactivity in *S. exigua* larvae, it was not required for the induction of tree-top disease in this system (van Houte *et al.* 2014a).

Baculovirus-induced tree-top disease – the role of light

Light was found to play a pivotal role in baculovirus-induced tree-top disease (van Houte *et al.* 2014b; van Houte *et al.* 2015; Bhattarai *et al.* 2018a; Bhattarai *et al.* 2018c). Third instar larvae of *S. exigua* infected with SeMNPV, *H. armigera* infected with HearNPV and *L. dispar asiatica* infected with LdMNPV displayed positive phototaxis, with infected larvae dying at elevated positions when light was applied from above, while larvae died at low positions in complete dark conditions or when light was provided from below. Uninfected larvae showed no phototactic behaviour as larvae displayed similar movement patterns in light and dark conditions (van Houte *et al.* 2014b; Bhattarai *et al.* 2018a; Bhattarai *et al.* 2018c). Han *et al.* (2018c) further demonstrated that SeMNPV-infected *S. exigua* larvae needed to be exposed to light provided from above during a defined time period [43 to 50 hours post infection (hpi) for third instars] to exhibit tree-top disease. This so-called trigger period was required before, but not during the actual climbing phase (between 57 and 67 hpi), which took place in the dark (Han *et al.* 2018c). Possibly, molecular pathways leading to phototactic behaviour are activated during the determined trigger period (Han *et al.* 2018c). In LdMNPV-infected *L. dispar asiatica* larvae, expression of the host's core circadian genes (*per* and *tim*) was increased during the night, however a clear link with tree-top disease was not shown (Bhattarai *et al.* 2018c). Bhattarai *et al.* (2018a) further investigated the response of infected larvae to different light spectra and found that HearNPV-infected *H. armigera* larvae are attracted to blue (450-490nm), white (broad-spectrum) and UVA (320-400nm) light, but not to UVB (290-320nm) light. Although positive phototaxis prior to death is found for different virus-host combinations, light does not always play a role; AcMNPV-infected *T. ni* larvae (V.I.D. Ros, unpublished) died at high positions even when they were kept in complete darkness throughout the experiment (Han *et al.* 2015b), indicating that in

these virus-host combinations larvae display negative geotaxis. These findings further support the hypothesis that different baculoviruses may have evolved different mechanisms to achieve virus-induced behavioural manipulations.

Future directions to reveal the underlying world of behavioural manipulation

Parasite-induced behavioural modifications may in many cases involve the host central nervous system (CNS) (Perrot-Minnot and Cezilly 2013; Hughes and Libersat 2018). Parasites can either directly evoke changes in the host CNS, e.g. by injecting hormone homologues or venom (like seen for parasitic wasps) (Adamo 2002; Libersat *et al.* 2009), or they may indirectly affect neurological activity by altering the host's gene expression and protein profile (Biron *et al.* 2006; Adamo 2013). Several studies on behavioural manipulation have revealed changes in levels of biogenic amines (as reviewed in Adamo 2002, Perrot-Minnot and Cezilly 2013, and van Houte *et al.* 2013), indicating that parasites may interfere with the synthesis or release of these agents in the host CNS (Perrot-Minnot and Cezilly 2013; van Houte *et al.* 2013; Hughes and Libersat 2018). Helluy and Holmes (1990) were the first to reveal the involvement of a biogenic amine in parasitic manipulation of host behaviour, while studying gammarids infected with *Polymorphus paradoxus* cystacanths. Out of a series of individually injected biogenic amines (GABA, noradrenalin, serotonin, serotonin creatinine sulphate, dopamine, octopamine), only serotonin made uninfected individuals express the same clinging behaviour as infected gammarids.

The previously mentioned studies - revealing which baculovirus genes may be involved in inducing behavioural alterations (Kamita *et al.* 2005; Hoover *et al.* 2011; van Houte *et al.* 2012; Ros *et al.* 2015) and which host genes may be acting in downstream pathways (Zhang *et al.* 2018) - present a first step to unravel the underlying world of manipulative forces that these viruses use to change their caterpillar host's behaviour. However, the underlying mechanisms are likely to be more complex and may involve modifications within the host CNS. Several studies have shown the presence of baculoviruses in the brain of infected caterpillars (Knebel-Mörsdorf *et al.* 1996; Herz *et al.* 2003; Torquato *et al.* 2006; Katsuma *et al.* 2012). Future studies should attempt to use histological approaches with infected caterpillar brains to link parasitology and neurology. Such neuroparasitological studies (Hughes and Libersat 2018; Libersat *et al.* 2018) could reveal to what extent and through which mechanisms baculoviruses control the neuronal activity of their hosts. Due to advances in recent years in the available molecular biology tools (such as transcriptomic, proteomic and metabolomic approaches), bioimaging and neuroscience, we can now move even further in order to elucidate the pathways hijacked by baculoviruses and other parasites (Hughes and Libersat 2018). So far, few studies have used –omics approaches to unravel mechanisms underlying parasitic manipulation (Biron *et al.* 2005a; Biron *et al.* 2006; Ponton *et al.* 2006; de Bekker *et al.* 2015), but recently initial transcriptomics studies on baculoviral-induced hyperactivity or tree-top disease have been performed (Wang *et al.* 2015; Bhattarai *et al.* 2018b; Bhattarai *et al.* 2018c). However, the set-up of these studies, comparing infected to uninfected (healthy) hosts, makes it difficult to link differentially expressed genes to specific behavioural displays, since the differential expression may simply be a consequence of the viral infection. Future studies should include comparisons between manipulative (WT) parasites and non-manipulative (mutant) parasites, providing the possibility to control for generalised responses to infection. The baculovirus-host system provides an excellent platform for such comparisons, since well-developed genetic tools allow easy engineering of baculovirus strains, enabling the use of mutant viruses. Since the causative viral genes for host behavioural manipulation have been identified (see above), -omics approaches can be applied comparing WT viruses and mutant viruses lacking these causative genes.

Conclusions

Baculoviruses infecting caterpillars have proven to be an excellent model system to study the mechanisms underlying parasite-induced behavioural manipulations. Baculoviruses can be easily genetically modified in the laboratory (e.g. Hoover *et al.* 2011, Han *et al.* 2015a, Katsuma 2015, and Ros *et al.* 2015), allowing functional studies of potential viral genes involved. Furthermore, this unique system will facilitate future -omics studies to unravel the host pathways involved. Now that we have identified viral genes that are crucial for particular behavioural displays, such as the AcMNPV *ptp* gene, we have the tools at hand for comparative -omics studies that can help us to reveal the downstream pathways. By combining -omics studies with insect brain scanning and ethopharmacological experiments, we will be able to integrate histology, -omics, manipulative and behavioural studies in settings similar to the *in situ* environment – which is an important prerequisite for future neuroparasitological studies (Hughes and Libersat 2018).

Acknowledgements

This work was supported by the Netherlands Organisation for Scientific Research (NWO; grant number ALWOP.362). We thank Claus Gasque ('by GASQUE') for drawing the illustrations of tree-top disease and hyperactivity in Figure 1 and Hans

M. Smid (Laboratory of Entomology, Wageningen University and Research) for critically reading the manuscript and for his expertise and help in making the photos for Figure 2 and the Supplementary File. We thank Kelli Hoover for useful discussions and two anonymous reviewers for their suggestions.

Supplementary files

Supplementary File. Time lapse of tree-top disease. Third instar SeMNPV-infected *Spodoptera exigua* caterpillars crawl to the top of a pepper plant (*Capsicum annuum*) at 3 days post infection (dpi). Photographs at the end of the time lapse show the initial expression of tree-top disease with a bloated appearance and a glossy exoskeleton and a more advanced stage of tree-top disease, after liquefaction and desiccation of the cadaver.

https://www.youtube.com/watch?v=DAtUEfTUnHM&feature=youtu.be

Science is the language in which we converse with nature, and its truths are revealed through the language of evidence.

Mary Anning

CHAPTER 3

Expression of trematode-induced zombie-ant behaviour is strongly associated with temperature

Simone N. Gasque[1,2] and Brian L. Fredensborg[1]
[1]Section for Organismal Biology, Department of Plant and Environmental Sciences, University of Copenhagen, Thorvaldsensvej 40, 1871 Frederiksberg C, Denmark

[2] Current location: Laboratory of Virology, Wageningen University and Research, Droevendaalsesteeg 1, 6708 PB Wageningen, The Netherlands

Published as:
Gasque SN and Fredensborg BL. 2023. Expression of trematode-induced zombie-ant behavior is strongly associated with temperature. Behav Ecol. 34: 960-968. doi: 10.1093/beheco/arad064.

Abstract

Parasite-induced modification of host behaviour increasing transmission to a next host is a common phenomenon. However, field-based studies are rare and the role of environmental factors in eliciting host behavioural modification is often not considered. We examined the effects of temperature, relative humidity (RH), time of day, date, and an irradiation-proxy on behavioural modification of the ant *Formica polyctena* (Förster 1850) by the brain-encysting lancet liver fluke *Dicrocoelium dendriticum* (Rudolphi 1819). This fluke induces ants to climb and bite to vegetation by the mandibles in a state of temporary tetany. A total of 1264 individual ants expressing the modified behaviour were observed over 13 non-consecutive days during one year in the Bidstrup Forests, Denmark. A sub-set of those ants (N=172) was individually marked to track attachment and release of infected ants in relation to variation in temperature. Infected ants primarily attached to vegetation early and late in the day corresponding to low temperature and high RH, presumably coinciding with the grazing activity of potential herbivorous definitive hosts. Temperature was the single most important determinant for the induced phenotypic change. On warm days, infected ants altered between the manipulated and non-manipulated state multiple times, while on cool days many infected ants remained attached to the vegetation all day. Our results suggest that temperature-sensitivity of the infected ants serves the dual-purpose of exposing infected ants to the next host at an opportune time, while protecting them from exposure to high temperatures, which might increase host (and parasite) mortality.

1 Introduction

Parasite manipulation of the host phenotype (appearance and/or behaviour) to increase transmission to a new host is a widespread phenomenon across host and parasite phyla (Moore 2002). The phenotypic changes of the infected host may involve dispersal of infective propagules to favourable locations and at favourable times, or, among parasites with a complex life cycle, facilitate an increase in the predation rate of the infected host by the next host in the life cycle of the parasite (i.e. trophic transmission) (Combes 2001; Poulin 2007). Thus, the phenomenon of host phenotypic manipulation is the result of a strong selection pressure on the parasite to enhance the otherwise very small chance of completing its life cycle (Poulin 2007; Froelick *et al.* 2021). Many cases of host phenotypic manipulation by parasites have been reported (Lafferty and Shaw 2013), but environmental or physiological factors that regulate the expression of the manipulated behaviour in infected hosts remain undescribed in most cases (Moore 2002; Lafferty and Shaw 2013; Hughes and Libersat 2018). Field studies of host behaviour in relation to parasite infection are complex and extremely rare since the parasitised host usually displays alterations of already existing behaviours, and parasite contribution to those behaviours may be difficult to quantify under natural conditions (Poulin 1995). The commonality of trophically-transmitted parasites in natural ecosystems, and their potentially great effect on food web properties (Lafferty *et al.* 2008) call for a much better understanding of the environmental factors associated with their transmission. We studied *Dicrocoelium dendriticum,* the lancet liver fluke, which induces a radical but temporary behavioural change in the ant intermediate host, making it easy to phenotypically distinguish infected from uninfected individuals. This quintessential example therefore serves as an appropriate model to investigate factors involved in eliciting and maintaining parasite-induced behavioural manipulation under field conditions.

Dicrocoelium dendriticum has a complex life cycle including a terrestrial snail as the first intermediate host, worker ants as the second intermediate host, and herbivorous mammals as the definitive host (Figure 1). *Dicrocoelium dendriticum* relies on trophic transmission for the completion of its life cycle. Individual larval parasites (metacercariae) migrate in an act of altruistic kin selection behaviour (Criscione *et al.* 2020) to the suboesophageal ganglion of the ant (Romig *et al.* 1980; Martín-Vega *et al.* 2018),) where they elicit a reversible and radical behavioural change, which is unique to infected hosts (Botnevik *et al.* 2016). Hence, the infected ant climbs and locks its mandibles to vegetation (Badie and Rondelaud 1988) in a state of tetany that leaves the ant susceptible for ingestion by an herbivorous mammalian definitive host (Tarry 1969). If not ingested by the herbivorous host, the mandibles unlock, and the infected ant is free to return to the forest floor.

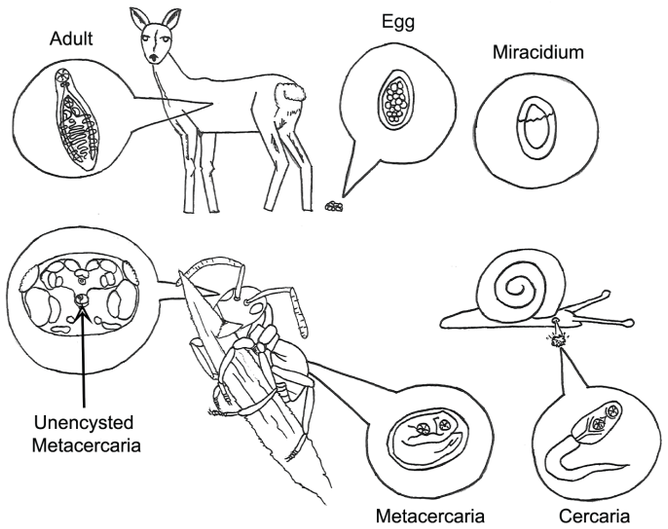

Figure 1. Lifecycle of *Dicrocoelium dendriticum.* Eggs are excreted from an herbivorous mammal serving as the definitive host, and hatch into a miracidium when ingested by a terrestrial snail. Mother and daughter sporocysts develop in the hepatopancreas of the snail (not shown), producing the cercaria stage. Cercariae are released from the snail via slimeballs excreted from the pneumostome. Ants eat the slimeballs containing infective cercariae, which develop into metacercariae in the hemocoel of the gaster of the ant. However, one or more cercariae penetrates the lining of the crop upon ingestion and migrates to the suboesophageal ganglion (depicted in the head capsule of the ant by arrow; Martín-Vega *et al.* 2018), where it induces a reversible biting behaviour of the ants where the mandibles are locked to vegetation leaving the ant exposed to ingestion by a suitable definitive host. Following ingestion, the metacercariae excyst in the duodenum, migrate to the bile ducts of the liver and mature to become adult worms producing large numbers of eggs by sexual reproduction. Drawing by Simone N. Gasque.

In other host-parasite associations the behavioural change is also radical but precedes the inevitable death of the host (e.g. tree-top disease by baculoviruses and death grip by *Ophiocordyceps*- or *Pandora*-infected ants) (reviewed by Gasque *et al.* 2019). Thus, in fungal- and viral-induced behaviours where the spores/viral progeny can persist in the environment, the host normally dies within hours/days after the induction of the altered behaviour. Contrary to this, *D. dendriticum* cannot survive outside the intermediate ant host and transmission is dependent on the direct ingestion of infected ants by herbivorous definitive hosts. The likelihood that an infected ant is eaten upon initial display of parasite-induced biting behaviour may be very small. The chance of transmission of *D. dendriticum* will however increase with prolonged exposure to the definitive host, and thus depend on ant host longevity. Thus, it is likely that natural selection favours increased exposure to the definitive host, but disfavours exposure to pre-mature predation or hazardous environmental conditions, which could kill the ant host and therefore the parasite (Fritz 1982; Parker *et al.* 2009).

Studies dating back to the 1970s and 1980s reported anecdotal observations of *D. dendriticum* infected ants biting in the morning and evening, leading to speculations on the possible role of time of day, temperature, or other environmental factors related to increased transmission success to grazing ruminant definitive hosts, but this was not investigated further (Tarry 1969; Badie *et al.* 1973; Badie 1975; Spindler *et al.* 1986; Badie and Rondelaud 1988). The chronobiology and effects of light have been shown to play a role in the expression of parasite induced behavioural changes in other systems. In the case of *Ophiocordyceps unilateralis s.l.,* -infected carpenter ants climb around solar noon, and bite the vegetation in locations and orientations which would lead to optimal humidity conditions for spore-formation and -release (Andersen *et al.* 2009; Hughes *et al.* 2011). Another host-parasite system similarly dependent on trophic transmission to *D. dendriticum*, is the brain-encysting trematode *Microphallus papillorobustus* and acanthocephalans infecting gammarids. Infected gammarids seek light and cling to submerged macrophytes in the habitat of dabbling ducks which serve as definitive hosts (Bethel and Holmes 1973; Helluy 1983).

A previous laboratory study indicated that the biting behaviour of *D. dendriticum* infected ants was determined by a negative relationship between increasing temperature and the probability that infected ants would bite to a leaf (Botnevik *et al.* 2016). However, the effect of temperature on *D. dendriticum* infected ant's biting behaviour has, so far, not been tested under natural conditions, where ants are exposed to multiple environmental variables with potential effects on ant behaviour.

In this study, we recorded the manipulated phenotype of the second intermediate host, the European Red Wood Ant, *Formica polyctena*, naturally infected with *D. dendriticum*, concurrent with *in situ* measurements of temperature, relative humidity (RH), and time of day. In addition, we quantified the frequency of changes to and from the manipulated phenotype in relation to temperature on individually marked ants on seven different days from August-October and at two separate sites. We hypothesised that temperature was the most important factor to infected ants expressing the manipulated behaviour in line with the previous laboratory study (Botnevik *et al.* 2016) and with circumstantial evidence from previous field observations (Badie *et al.* 1973; Paraschivescu and Raicev 1980; Spindler 1986). To our knowledge, this is the first study to individually label and track the behaviour of infected ants in the field, which rendered the option to recatch individual ants and study their behavioural expression of infections over 24-hours, and on longer term.

2 Materials and methods

2.1 Field site and execution of fieldwork

Fieldwork took place in the Bidstrup Forests in Hvalsø, approximately 45 km South-west of Copenhagen, Denmark, in 2016-2017. The forests contain a mixture of hard-wood and coniferous trees in a hilly terrain and the *D. dendriticum-F. polyctena* system inhabits the forests (Botnevik *et al.* 2016). The aims of the fieldwork were to: 1) Investigate the relative contribution of temperature and RH (measured in the microclimate of infected ants), time of day, date and an irradiation-proxy in inducing and maintaining the altered phenotype (biting to vegetation). 2) Track biting behaviour of individually marked infected ants to observe the dynamics of initiation, maintenance, and termination of the altered phenotype. Four anthills were included in the observations each day (except in April 2017, see below) and were from two different sites (s and h). Three anthills; Anthill 1 (55°34'41"N 11°52'22"E), Anthill 2 (55°34'40"N 11°52'22"E) and Anthill 3 (55°34'40"N 11°52'23"E) were located in a line at approximately one meter distance from each other (site s). Anthill 4 was located approximately 300 m from site s (55°34'37"N 11°52'43"E) and termed site h.

2.2 Ant observations

Fieldwork was avoided on days with precipitation to standardise the conditions for ant behavioural studies. Ant observations were conducted from early morning to late afternoon/evening on nine days from 16/8/2016 until 12/10/2016, and on three days from 6/4/2017 to 16/8/2017. On one occasion, ant observations continued until sunset and continued the following morning, to cover a 24-hours cycle (22/9 - 23/9/2016). A total of 131.5 hours of field observations were conducted from 12 occurrences, with one stretching two days giving a total of 13 observation days from 16/8/2016 to 16/8/2017. On each field day, the vegetation within a perimeter of 2 m from each anthill (3 m from Anthill 4 due to the dispersed vegetation at this site) was examined for ants biting to vegetation at a minimum of six times every day. A temperature/humidity -logger (OM-EL-USB-2, Omega engineering Inc.) was attached with two plastic strips to a one-meter-long marker stick and placed in the ground at the same height and in close proximity to the majority of ants biting to vegetation at the first observation time point (Figure 2).

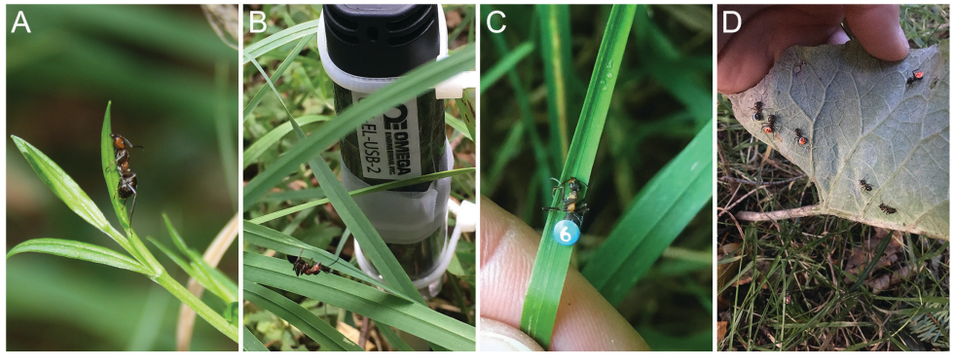

Figure 2. Photographs of *Formica polyctena* ants expressing the behavioural alteration induced by *Dicrocoelium dendriticum* in the Bidstrup Forests, Denmark in 2016 and 2017. A) shows an ant expressing the biting behaviour (on probably *Stellaria holostea*), and in B) a temperature/humidity- logger seen placed in close proximity to an ant expressing the altered behaviour, biting onto cocksfoot grass, *Dactylis glomerata*. C) with a number tag glued to the dorsal part of gaster (individual B6, also biting onto a piece of *Dactylis glomerata*). In D) an assembly of six infected ants were found under a big leave (undefined *Arctium* species), four of these with a number tag on (R33, R63, R76 and a B-tag not readable from this angle).

Temperature and RH were recorded continually by the temperature/humidity-logger in intervals of two minutes. For the analysis, the median temperature and median RH was used for the minutes that did not have a recorded temperature and RH linked to it. For Anthill 2 the mean values from the surrounding anthills (1 and 3) were used for each timepoint. Five factors that potentially influenced the proportion of infected ants biting to vegetation were included in the analysis of ant activity: temperature, RH, date, time of day (day length divided in three equal groups of the total day length), and an irradiation-proxy (calculated from official records of sunrise and sunset, www.soltider.dk), indicating the level of solar irradiance that biting ants could be exposed to. Thus, concurrent measures of temperature, RH, and the number of ants biting the vegetation were recorded at each of the minimally six observation time-points per field day. In August-October 2016, 172 ants were individually marked (after the final observation time-point of the day, of these were 126 ants observed again at the same anthills as they were at when tagged) by numbered and coloured tags (Swienty A/S) glued to the dorsal part of the gaster of the ants observed biting to vegetation (see Figure 2C, D; in depth description of procedure in supplementary; data in Dataset S3; and further analysis in section 3.2).

Ants biting to vegetation received a touch stimulus, which induced slight movement in ants harbouring *D. dendriticum* (Paraschivescu and Raicev 1980; Gasque and Fredensborg pers. obs.) to distinguish them from infections by the entomopathogenic fungus *Pandora formicae* (de Bekker *et al.* 2018), which also inhabits the Bidstrup Forests (Małagocka *et al.* 2015; Małagocka *et al.* 2017). *Pandora formicae* initially induces a similar behaviour but infected ants remain motionless.

2.3 Orientation of infected ants and infection patterns

On two separate days (15/9/16 and 22/9/16, recorded respectively in the afternoon and in the morning), the orientation of infected ants biting onto grass blades were noted. It was noted for each recording whether the ant was facing downwards towards the roots or facing upwards to the tip of the grass blade (see Figure 2C). A total of 174 ants expressing biting behaviour were collected on different dates (Table S2) from the four observed anthills and transported back to the laboratory in individual 15 ml centrifuge tubes for dissection and verification of infection. Eighty ants collected randomly by the use of a handkerchief placed on the nest (Botnevik *et al.* 2016) were used as a negative control. Ants were stored at 5°C until they were measured from mandible to the tip of gaster to the nearest 1 mm and dissected. Dissections were performed in a 0.9% saline solution under a Leica MZ12 stereomicroscope (X20), and the presence and number of metacercariae in the gaster were recorded (for the first two groups). For the last group collected 16/8/2017 dissections were conducted only to verify infection status of the ants.

2.4 Statistical analysis

The number of ants biting onto the vegetation at the different observations were considered independent observations since the probability of expressing parasite-induced behaviour was determined by the environmental factors at the time of observation (Dataset S1). The number of ants expressing the altered phenotype fluctuated considerably between sampling days at a given anthill from a few individuals to 116. We, therefore, used the proportion of ants biting to vegetation (the number of ants biting at said timepoint relative to the maximum number of ants observed biting to vegetation at the same anthill that day) on each day as the dependent variable. Temperature, RH, date, an irradiation-proxy and time of day (interval) were used as explanatory variables

We do not have an individual ID on the majority of the ants (only the 126 tagged ants mentioned earlier). Therefore, it was not possible to include individual ID as an independent variable in the analysis. With a proportional response variable, the data followed a binomial distribution, and we used logistic regression in a generalised linear model (GENMOD, SAS) to assess the associations (see 'extra supplementary' for the codes in SAS). Initially, all five explanatory variables were included in the model (Table S1). By including or excluding date in the model it was possible to assess the significance level of the other variables operating within and among dates, respectively. The significance levels of all the variables were compared between the two runs (including date: Table S1 vs excluding date: Table 1), to estimate which factor was the one explaining most of the expressed parasite-induced behaviour of the ants

within a day as well as across observation dates. By comparing the models with AIC, BIC, Deviance, Pearson chi-square and more, the different tests pointed at the two different models of being the best fitting model. So, to further analyse which factor had the biggest influence on the expression of the proportion of infection in our data set, we performed a regression analysis based on the Random Forest method. As date itself was not regarded correctly we instead included it in the format of year, month and days per year as separate columns utilising the R packages Dplyr (version 1.0.8) and Lubridate (v 1.8.0). The initially run included all the variables in Dataset S1, besides the two used to calculate proportion of infection (infection and maximum) as they obviously would skew the test. Lastly excluding all the factors used to calculate irradiation proxy. We utilised the R package Boruta (v 8.0.0) to perform feature selection and ranking as a regression to predict the proportion of infection, based on 100 iterations of 20000 trees. R package Caret (v 6.0-94) was utilised to split train and test datasets, and also train and test the models to predict proportion of infection. Train and test splitting separated the data randomly, with 30% of the data retained as a testing set. We trained the model with 5-fold cross-validation repeated 10 times, utilising forests with 2000 trees and four tuning length options. Model performance was evaluated with R^2 and RMSE.

The number of ants maintaining their attachment throughout the day (Dataset S2) was used as a proportion to the maximum of ants at each anthill in relation to first; date, anthill, average RH and average temperature, and later solely average temperature and average RH at each anthill per day, in both cases a generalised linear model with binomial errors (GENMOD) was chosen and tested in SAS. The orientation-data of ants biting onto grass, were analysed by chi-square test compared to the equal chance of orientation to either direction. Graphs were made in GraphPad Prism (v 9.5.1.), besides Supplementary Figure S1, which was generated in R and improved in Inkscape (v 1.2), and Supplementary Figure S2 was generated in Excel (v 2208).

3 Results

3.1 Factors determining parasite-induced behaviour modification

Temperature (Den DF=437, χ^2=120.94, P<0.0001) was strongly associated with the proportion of infected ants expressing the manipulated phenotype (Table 1).

Table 1. Results of generalised linear model examining the effects of environmental factors and time on the expression of biting behaviour in *Dicrocoelium dendriticum*-infected *Formica polyctena* given as the

proportion of ants displaying the behaviour at each observation in relation to the maximum number of ants observed displaying biting behaviour on that day. 'Irradiation-proxy' indicates the solar position on the sky and 'Time of day' representing an interval as daylength is divided in three groups.

Factor	Den DF	Estimate	χ^2	P-value
Temperature	437	-0.1090	120.94	<0.0001
Relative humidity	437	0.0145	26.17	<0.0001
Time of day	437	0.0544	0.50	0.4786
Irradiation-proxy	437	-0.0012	3.28	0.0703

As seen from the estimates from the maximum likelihood parameters in the test excluding the date-variable, temperature explains most of the variation in our dataset (Dataset S1), as a 1°C increase, makes 11% of the ants let go of their biting (estimate -0.1090, SE ±0.0106) and when including date (Table S1) in the test the same accounts for 14% of the ants (estimate -0.1384, SE ±0.0268). Both estimates are comparable as they fall within the same standard error. With the comparison between the date-included and -excluded runs, temperature was the only variable of high importance in all tested models which kept a high χ^2 -value, and highly significant p-value (P<0.0001). In the excluded-date run, relative humidity (Den DF=437, χ^2=26.17, P<0.0001) was highly associated with the proportion of ants expressing the *D. dendriticum*-infection. However, RH was not significantly related to ant biting behaviour within date, and the significant effect of RH observed across dates was likely an artefact of a negative correlation between RH and temperature with the latter being the main explanatory factor of ant biting behaviour (see above). Irradiation-proxy or time of day (by interval) showed no significant relationship to the induced behavioural modification in either of the runs. In a Random Forest regression modelled to predict the proportion of infection, temperature was ranked as the most important factor for prediction (Figure S1). The trained model could predict roughly half of the proportion of infection in the test set (R^2 = 0.5297, RMSE = 0.2029), while a linear regression between proportion of infection and temperature presented an R^2 of ~0.25 in the full dataset.

3.2 Persistence of biting behaviour

The number of switches to and from biting behaviour was strongly and positively related to the daily temperature range (difference between maximum and minimum temperatures) in individually marked infected ants across the observation days (Linear Regression: F = 61.1, df = 1, P <0.001) (Figure 3). Thus, the larger the difference between maximum and minimum temperature, the less persistent the manipulated biting behaviour. Labelled ants that were used in a 24-hour study from 22/9/2016 to 23/9/2016 showed that of the numbered ants biting to vegetation in the evening (N=30) 96.67% were observed in the same state at the same location the following morning.

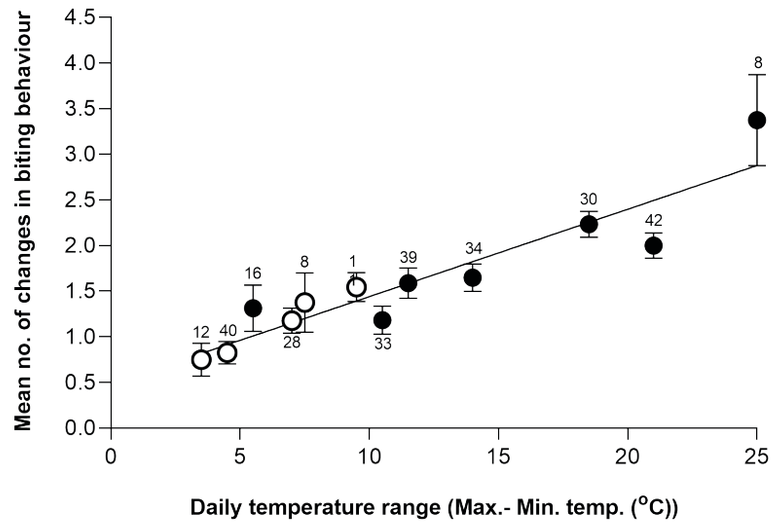

Figure 3. Number of changes in biting behaviour (mean ± SEM) of individually marked *Formica polyctena* ants infected with *Dicrocoelium dendriticum* in relation to the observed temperature range (difference between maximum and minimum temperature) on seven (Anthill 1-3, closed circle), or five observation days (Anthill 4, open circle) between August and October 2016, in the Bidstrup Forests, Denmark (see Dataset S3: 'GasqueFredensborg_2023_S3_Individually_marked_ants'). The number of individually marked ants observed per site per day is indicated at each error bar. A significant positive relationship was observed between temperature range and the number of changes to the manipulated behaviour for both sites (Anthill 1-3, R^2=0.77, Anthill 4, R^2= 0.98, combined R^2 = 0.86 (regression line: mean number of changes in behaviour = 0.484 + (0.0957 * temperature range)), all P<0.001).

3.3 Seasonality

The number of biting ants counted on each observation day varied greatly (Figure S2). However, a seasonal difference was observed from summer 2016 to summer 2017 when plotting the maximum number of infected ants counted on each day from the two sites (Figure 4). In April 2017 up to five times the number of ants biting the vegetation were observed in comparison to the other recorded months at the same site.

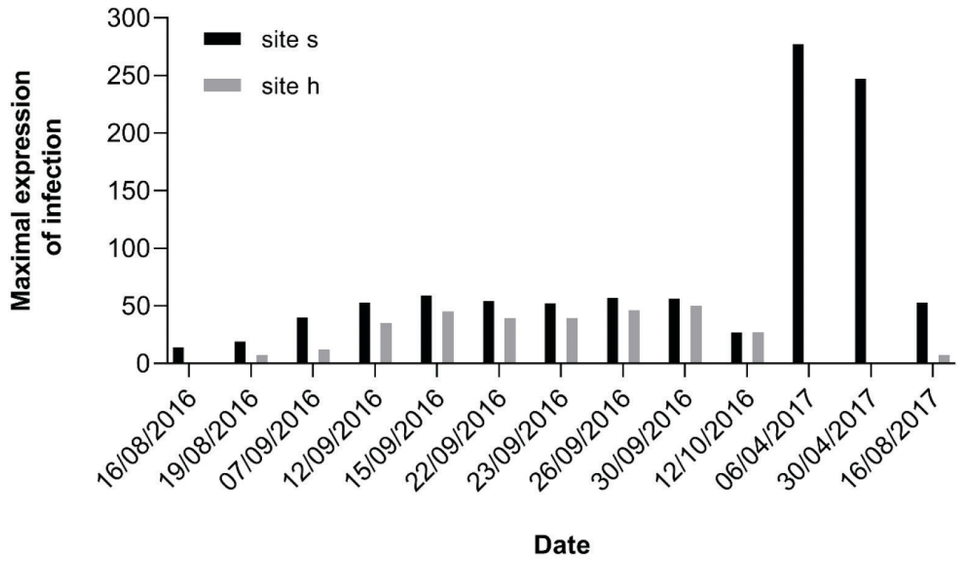

Figure 4. Bar chart representing the seasonal variation in the expression of *Dicrocoelium dendriticum*-induced biting behaviour of *Formica polyctena* from two sampling sites (site s (Anthill 1-3) and Anthill 4, from site h) on 13 observation days (16/8/2016 - 16/8/2017) within one year at the Bidstrup Forests, Denmark. The bars represent the maximum counted number of ants expressing the manipulated state at any of the counting time-points during each date as a total for both the sites (for site h: one number, for site s: maxima for Anthill 1-3 added together) (see Dataset: 'GasqueFredensborg_2023_S1_Abiotic_factors'). In two days of April at the h site, no ants were observed.

3.4 All-day attachment

At the end of September/start of October 2016 we observed that a great majority (up to 1/3) of the ants stayed in the biting state for the whole day of observations (Figure 5), in contrast to observations made earlier in the season (where none remained attached during all the observation times of the day). When analysed, date showed a positive correlation to the proportion of the maintenance of biting (Num DF=4, χ^2= 20.26, P=0.0004). Considering only the influence of the abiotic factors (average temperature and average RH for the individual anthills), average temperature showed the highest correlation to the maintenance of biting during the day (Num DF=1, χ^2 = 17.05, P<0.0001), whereas average RH showed no significant relationship to the proportion of ants biting to vegetation.

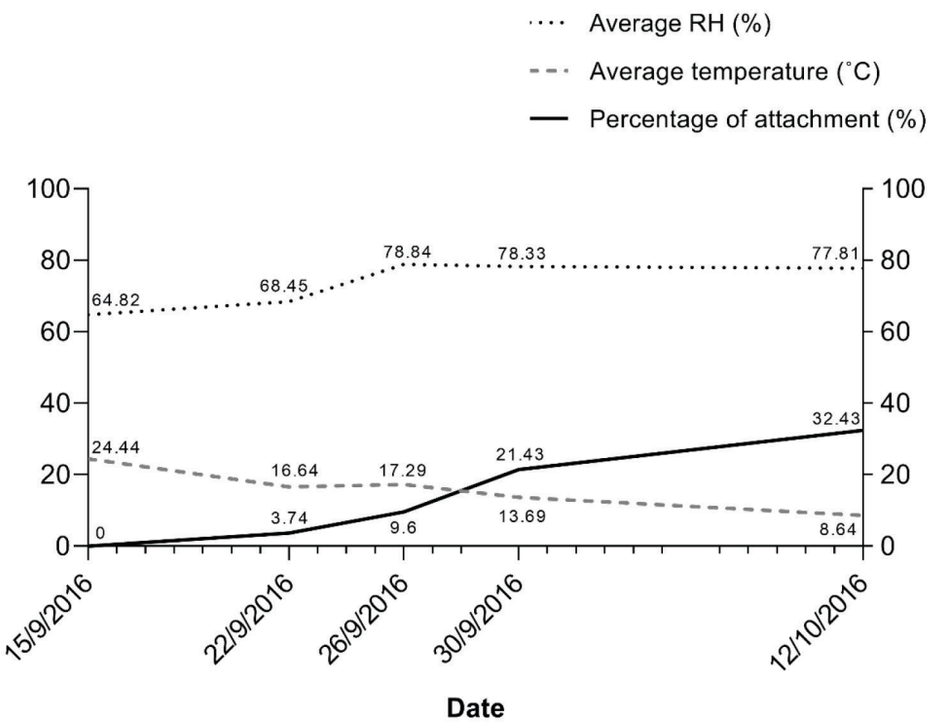

Figure 5. The percentage of maintained all-day attachment of *Dicrocoelium dendriticum* infected *Formica polyctena* ants (%, filled dark grey line) to the total of ants observed at all the anthills per day, throughout the observation time-points of the assigned days (15/9/2016 - 12/10/2016), in relation to the average temperature (°Celsius) (dashed light grey line) and the average relative humidity (RH, %) (dotted line) measured in the microclimate of the ants that day (see Dataset S2: 'GasqueFredensborg_2023_S2_All-day_attachment'). The exact values of the three parameters for each day are given near the lines. On earlier dates (16/8/2016 - 15/9/2016) the percentage of all-day attachment were also 0% as shown for 15/9/2016. (N total; 15/9: N=166, 22/9: N=187, 26/9: N=177, 30/9: N=168 and 12/10: N=74).

3.5 Orientation of infected ants and infection patterns

None of 80 ants randomly collected from the anthills were infected with *D. dendriticum* metacercaria (Table S2). A majority of the ants (70%) expressing infection by biting on to vegetation were facing downwards (n=144, df=1, χ^2= 23.36, P<0.0001). Combining all dissections, a metacercariae prevalence of 97% (N=174) was found in ants collected when biting to the vegetation in the field.

4 Discussion

There is a need for studies on how parasitic manipulation of animal behaviour responds to changes in environmental conditions (Loreto *et al.* 2018). However, it is inherently challenging to study the effects of individual environmental factors on animal behaviour under natural conditions, as many of them cannot be controlled and/or may co-vary. In this study, we succeeded to monitor the biting behaviour of the ant host in relation to individual environmental factors under natural conditions. We usually observed the greatest numbers of ants in the biting state in the early morning and in the late afternoon/evening similar to previous studies (Figure S2) (Badie *et al.* 1973; Badie 1975; Spindler 1986; Badie and Rondelaud 1988; Manga-González *et al.* 2001). However, our analysis clearly demonstrated that temperature, not the time of day itself, explained the switch to a biting state observed in the manipulated phenotype (biting to vegetation). Thus, low temperature facilitated the biting behaviour while higher temperatures reduced it (Table 1; Figure 3; Figure 5). We also found a significant positive relationship between the daily temperature range and the number of times infected ants switched biting behaviour between the manipulated and non-manipulated phenotype (Figure 3). This indicates that persistence of the biting behaviour was greatly reduced when ants experienced large variation in the temperatures during a day. The results from this field study therefore corroborates with results from a previous laboratory-based study, in which temperature determined the probability that infected ants were found biting to grass leaves (Botnevik *et al.* 2016).

In further support of temperature as the main driver of the induced biting behaviour, the proportion of infected ants maintaining all-day attachment significantly increased from the middle of September until the middle of October concurrent with a decrease in daily average temperature (Figure 5). Thus, in October, infected ants were more likely to remain attached to the vegetation the entire day when the maximum temperature was 11.5°C. Termination of the parasite-induced behaviour therefore seems to be determined by temperature, and not by time of day, RH, or a proxy for irradiation. Similarly, as indicated by our 24-hour study, ants presumably remain attached all-night. It is from late evening to early morning that we measured the lowest temperatures. In April 2017 there were up to five times as many ants observed exhibiting the manipulated phenotype than in other months (Figure 4), suggesting that infected ants survive the winter in the nest and continue to express the manipulated behaviour the following spring as transmission between snail and ant host primarily takes place during late spring and summer (Tarry 1969; Manga-González and González-Lanza 2005). Interestingly, late May to early June is when female roe deer express the highest total daily activity time (56.7% of the day, Cederlund 1989) in central Sweden (similar latitude to our study). The largest proportion of infected ants biting may therefore not only coincide with the daily activity of potential definitive hosts (Stache *et al.* 2013) through the indication by temperature, but potentially also be synchronised with the seasonal activity of potential other definitive hosts (Cederlund 1989). Temperature seems to be an appropriate indicator of parasite transmission success and thus parasite fitness, as it relates to both host longevity and the encounter possibility with potential definitive hosts. Hence, biting to vegetation could be lethal to ants and thereby the *D. dendriticum* metacercariae at peak temperatures. In addition to host mortality, temperature also provides an indicator for the most opportune daily transmission window to potential definitive hosts since low temperature coincides with the crepuscular activity of herbivorous definitive hosts e.g. the European roe deer (Stache *et al.* 2013).

The exact mechanism linking temperature to climbing and biting behaviour of *D. dendriticum* infected ants remains unknown. However, it is known that one or few metacercariae lodge at the suboesophageal ganglion in the ant host (Romig *et al.* 1980; Martín-Vega *et al.* 2018, see arrow in Figure 1), which controls the initiation of mandibular abductor and adductor movement (Chapman 2013). Changes in temperature might affect parasite or host secretion of molecules, an inflammatory response or the mechanical pressure of the parasite on mandibular nervous tissue may in turn provoke a biting behaviour at low temperature conditions. Penetration of muscles by the fungus *O. kimflemingiae* may lead to the hypercontractions seen in the mandibles of infected carpenter ants (Mangold *et al.* 2019). However, in contrast to behaviour-manipulating trematodes and viruses (termed neuroparasites; Hughes and Libersat 2018), hypocrealean fungi do not invade the CNS of the living host (Fredericksen *et al.* 2017), whereas recent evidence suggests that entomophthorelean species can infiltrate the CNS tissue while the host is still alive (Elya *et al.* 2018; Elya *et al.* 2023). This all suggests that similar behaviours may be regulated by different underlying mechanisms across parasite phyla (Mangold and Hughes 2021).

In accordance with previous studies, we also found that most of the infected ants were facing head downwards (Badie and Rondelaud 1988; Manga-González *et al.* 2001). The reason is unknown, although we wonder if the final orientation is the result of a method for seeking out the optimal conditions of the attachment for the trematode-host or to provide shading at least for the head part, where the SOG-attached metacercaria is located (Gullan and Cranston 2010). Our analysis indicates that the effect of RH on *D. dendriticum* infected ants expressing biting behaviour in the field is smaller than that of temperature in line with previous studies, conducted under controlled laboratory conditions where no interaction between relative humidity and biting behaviour could be detected (Botnevik *et al.* 2016).

We indirectly assessed the effect of solar irradiation, by including a proxy for solar position in the analysis, on biting behaviour of ants infected with *D. dendriticum*. We did not find any evidence that the solar position had an effect on biting behaviour, similar to a study on the effect of artificial light (Botnevik *et al.* 2016). Light plays an important role in other systems, where parasites initially induce the same attachment to foliage, such as fungi from the genera *Pandora* and *Ophiocordyceps*. *O. unilateralis s.l.,* makes the infected *Camponotus leonardi* ants attach approximately 25 cm above the forest floor, which should be the optimal microclimate for the post-mortem development of the stalk and subsequent spore release (Andersen *et al.* 2009; Hughes *et al.* 2011). Transition to the so-called death grip in naturally infected *Camponotus* ants is synchronised to solar noon in the field (Hughes *et al.* 2011; Will *et al.* 2020), and comparisons between *O. camponoti-atricipis* infected *Camponoti atricipis* ants in shaded and control areas indicated a strong positive phototactic influence (Andriolli *et al.* 2019). These results combined suggest that illumination is an essential cue for fungus infected ants to locate the optimal microclimate for progeny development and dispersal (Chung *et al.* 2017). Light has a pivotal role, not only in fungal-systems but also for the expression of other parasite-induced behavioural alterations. Studies on aquatic gammarids infected with larval trematodes or acanthocephalans demonstrated positive phototaxis of infected individuals presumably increasing predation of infected gammarids by duck final hosts (Bethel and Holmes 1973; Helluy 1983). In that system temperature had no effect on parasite-induced host behaviour manipulation since light and not temperature presumably determined the encounter possibility with the definitive host (Labaude *et al.* 2020). For both of the baculoviral-induced phenotypic changes (hyperactivity and tree-top disease) the expressions are influenced by light (Kamita *et al.* 2005; van Houte *et al.* 2014b; Bhattarai *et al.* 2018c). Therefore, in future field studies it would be relevant to test the effect of light intensity on the timing of behavioural alteration in ants infected with *D. dendriticum* including a broader range of seasons.

For most host-parasite systems the underlying mechanisms of induced parasitic manipulation are to a great extend unknown. The same accounts for the *D. dendriticum-Formica* ant host system. By comparing similarly expressed behavioural manipulations across phyla we speculate that the parasite encoded protein tyrosine phosphatase (PTP) could be a potential regulating factor in the *D. dendriticum* case. PTP is linked to a change of movement and positive phototaxis, which is induced in hosts by several manipulating parasites. This enzyme has been found to play a role in the induction of hyperactivity of caterpillars when infected with baculoviruses (Kamita *et al.* 2005; Katsuma *et al.* 2012; van Houte *et al.* 2012). Fungal encoded PTP is also upregulated during the manipulated state (death grip) of *Ophiocordyceps*-infected ants (de Bekker *et al.* 2015; de Bekker *et al.* 2017; Will *et al.* 2020). Since the initial part of the *Ophiocordyceps*- and *Dicrocoelium*-induced behaviours in the ant host (the at minimum negative geotaxism (or positive phototaxis in *Ophiocordyceps* case) and the attachment to the vegetation by mouthparts) are similar to each other, PTP could have evolved convergently (Will *et al.* 2020). Currently it is unknown whether the phenotypical similarities of infected host behaviour have evolved independently across a taxonomically diverse range of parasites, or if they have evolved to exploit the same ancient host trait of biting to vegetation while sleeping (Lovett *et al.* 2020). In any case, investigating the possible role of PTP and other actors in the manipulated state of ants infected with *Dicrocoelium* would be very interesting to include in future quantitative studies such as transcriptomic or proteomic approaches (Biron *et al.* 2005b; Biron *et al.* 2006; Małagocka *et al.* 2015; de Bekker *et al.* 2017).

Conclusion

This study provided rare field evidence on the effects of environmental factors on parasite-induced behavioural changes in the host. We found that temperature was the driving factor influencing parasite-induced ant biting behaviour in the field. We propose that temperature sensitivity is an adaptation to increase transmission to the definitive mammalian host, while at the same time protecting the intermediate host from exposure to lethal temperatures. Investigating the biochemical underlying mechanisms and comparing these to other parasites inducing similar behaviour in ants and other insects will be an important next step.

Acknowledgements

We thank Per M. Jensen for fruitful theoretical discussions and for statistical assistance, the management at Bidstrup Forests for access to field sites, Pedro B. Costa for cross validation of GLM test results by application of the Random Forest method and Vera I.D. Ros and Julia Friman for comments on earlier drafts of the manuscript. Lastly, we also thank two anonymous reviewers whose constructive criticism improved the quality of the manuscript.

Funding

This work was supported by Villum Fonden (grant number 00007457).

Data accessibility

Analyses reported in this article can be reproduced using the data provided by:
Dataset S1; GasqueFredensborg_2023_S1_Abiotic_factors
Dataset S2; GasqueFredensborg_2023_S2_All-day_attachment
Dataset S3; GasqueFredensborg_2023_S3_Individually_marked_ants

Supplementary files

Supplementary Table S1. Results of generalised linear model examining the effects of environmental factors and time on the expression of biting behaviour in *Dicrocoelium dendriticum*-infected *Formica polyctena* given as the proportion of ants displaying the behaviour at each observation in relation to the maximum number of ants observed displaying biting behaviour on that day, when including date as an explanatory variable. 'Irradiation-proxy' indicates the solar position on the sky and 'Time of day' representing an interval as daylength is divided in three groups.

Factor	Num DF	Den DF	Estimate	X^2	P-value
Temperature	1	437	-0.1384	27.32	<0.0001
Relative humidity	1	437	-0.0051	0.20	0.6511
Time of day	1	437	0.0617	0.66	0.4183
Irradiation-proxy	1	437	-0.0001	0.01	0.9130
Date	11	437	Diff. Per date	59.69	<0.0001

Supplementary Table S2. Overview of infection patterns of ants gathered on location at different dates. The negative control (n=80) was gathered randomly with handkerchief method, and the collected ants biting the vegetation was first picked after checked with a touch stimulus. Length measurements were made from the tip of the mandibles to the end of gaster of ants collected from each group (negative control and biting group) on the 12/10/2016. The negative control measured 5-9 mm (n=80, average 6.63), whereas the biting group measured 6-8 mm (n=49, average 6.63). The negative control group showed 0% infections, whereas metacercariae were observed by dissections of gaster in 97% (n=174) of ants sampled while biting the vegetation. During dissections a parasitoid Neoneurinae wasp was found in the gaster of one of the ants gathered on the 12/10/2016. This record led to the first authenticated record of *F. polyctena* ants serving as host for a Neoneurinae wasp (Gasque *et al.* 2018). The infection ranges found in this study are congruent with previous reports from Mapes and Krull (1952) (6-103), Martín-Vega *et al.* (2018) (6-98), and Botnevik *et al.* (2016) (1-216). As the latter is from collected ants in 2014 at the same locations in the Bidstrup Forests as our study, it suggests limited interannual variation in the abundance of *D. dendriticum.* C = confirmation of infection.

Group	Date	Collected ants	Infection status	Number of infection (mean (range))
Neg. Control	12/10/2016	80	0%	0
Biting	12/10/2016	49	98%	56 (2-225)
Biting	18/6/2017	52	98%	53 (5-183)
Biting	16/8/2017	73	96% (C)	-
Biting combined		174	97%	54.5 (2-225)

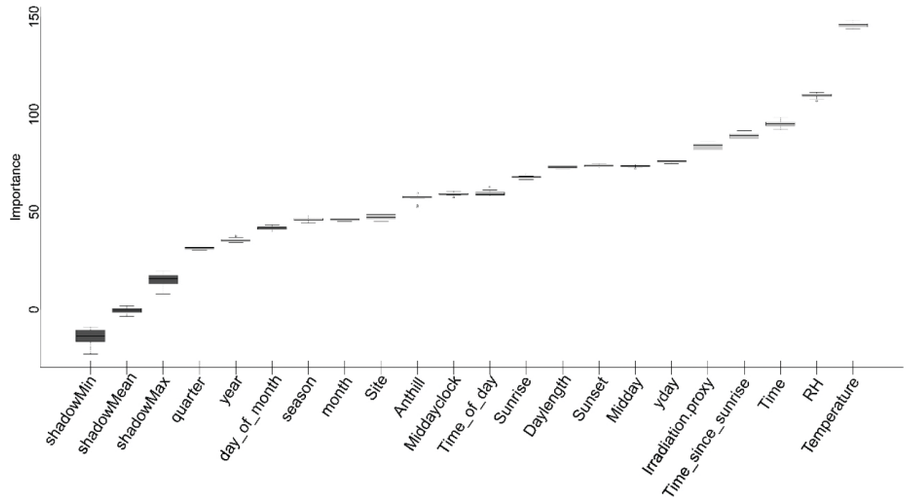

Supplementary figures S1. Relative importance of variables on the prediction of proportion of infection by regression test (Random Forest method). The variables are ranging from lowest importance in prediction (left on x-axis) to the highest importance in prediction (temperature, on the right of x-axis). Date was split in different variables for correct reading into R (quarter, year, day of month, season, month, yday (year day); see 'extra supplementary' for the R codes). The shadow features generated from the dataset (shadow min, shadow mean and shadow max; random permutations of the measured variables) are below importance of any of the measured variables (dark grey boxes) indicating that all measured variables are important predictors of proportion of infection (light grey boxes) (Dataset S1).

19/8/2016

A

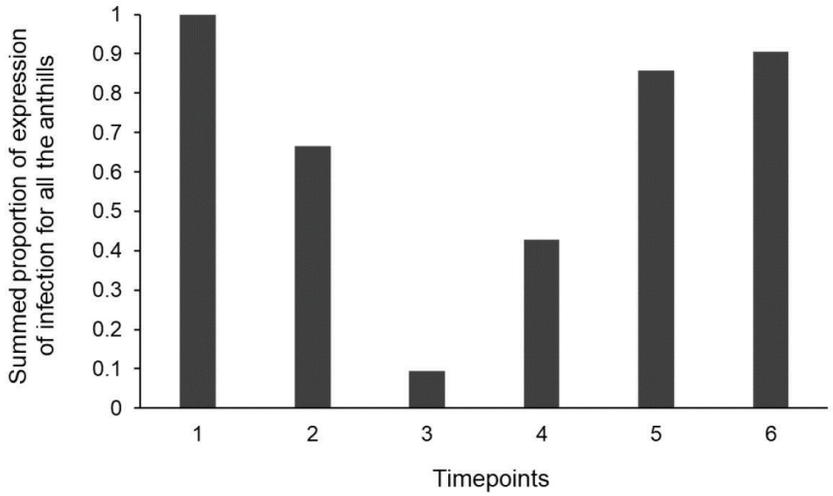

B

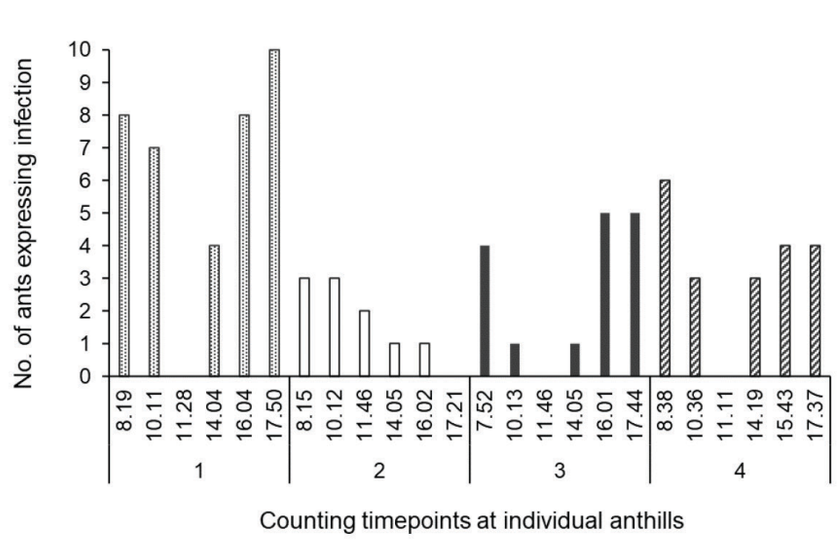

7/9/2016

A

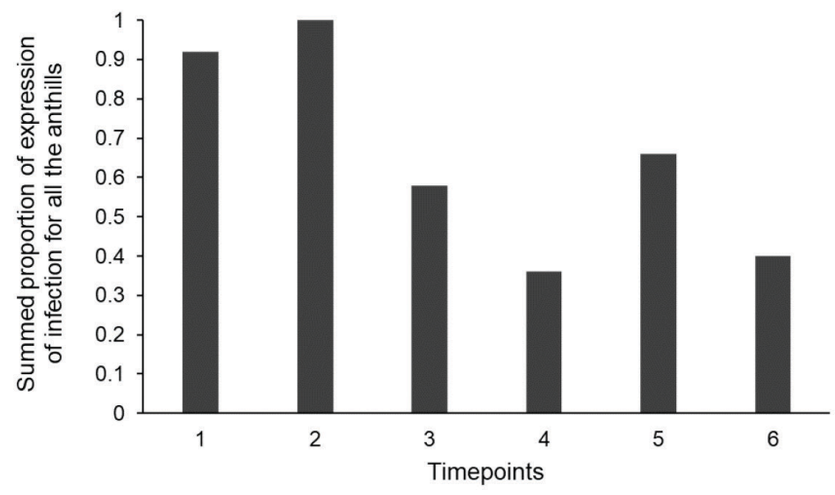

B

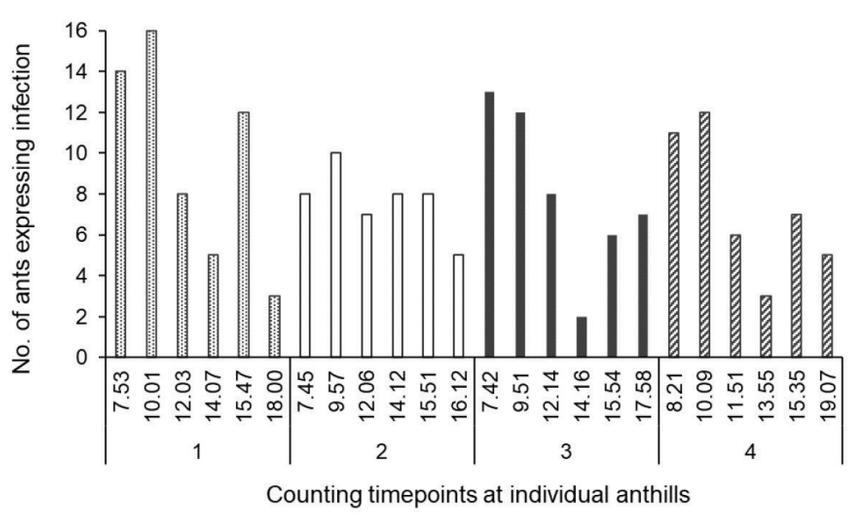

12/9/2016

A

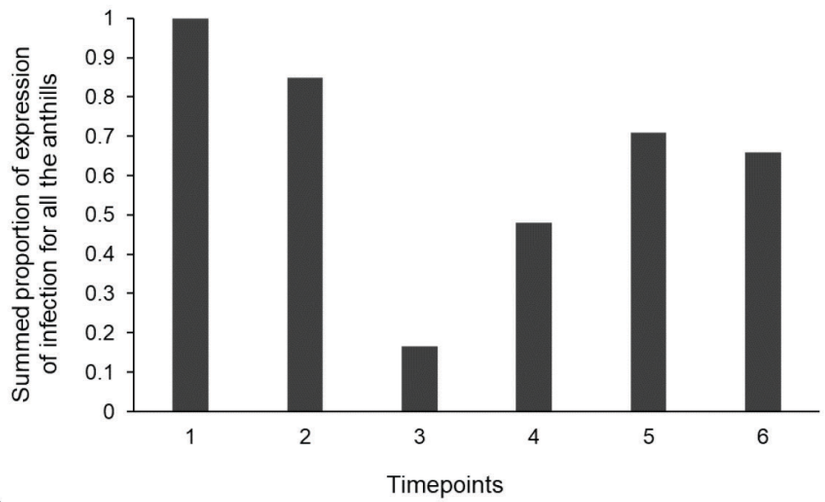

B

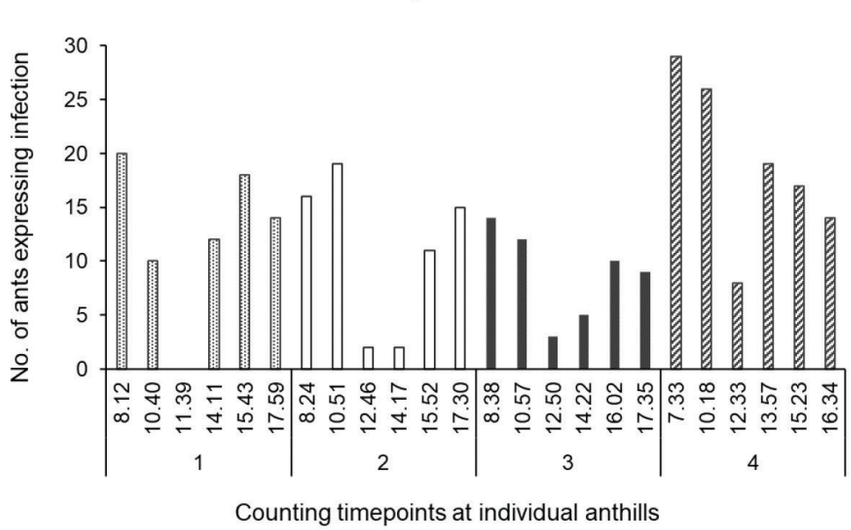

15/9/2016

A

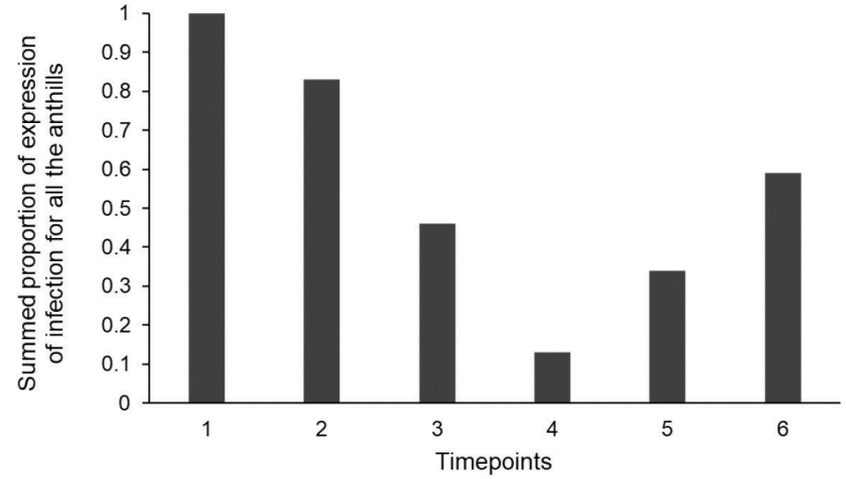

B

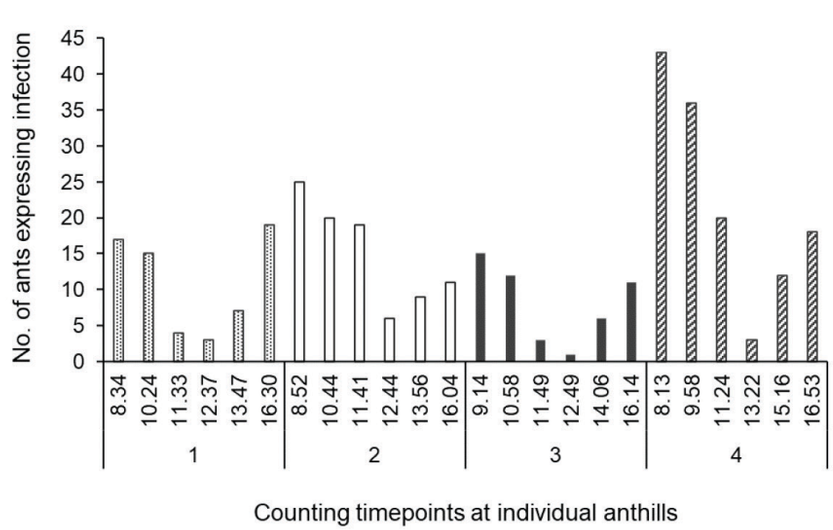

22/9/2016

A

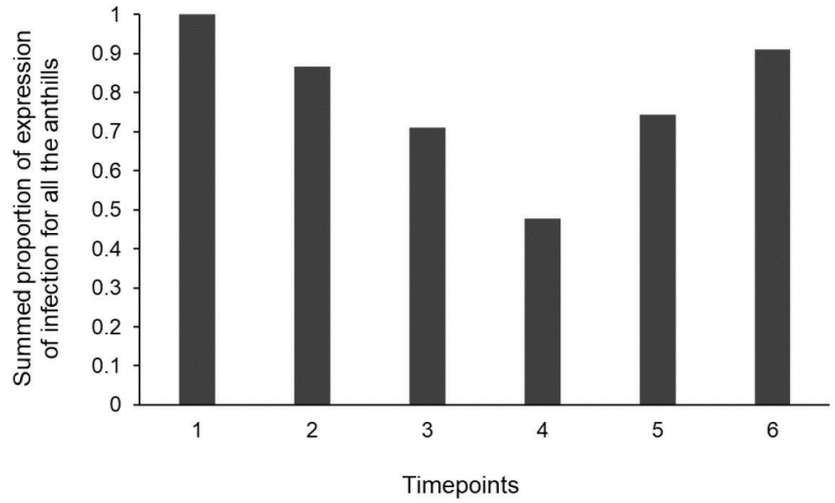

B

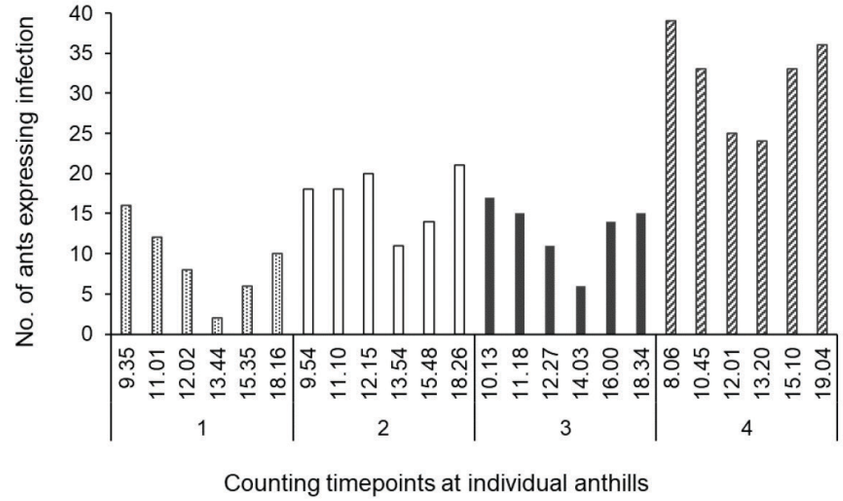

26/9/2016

A

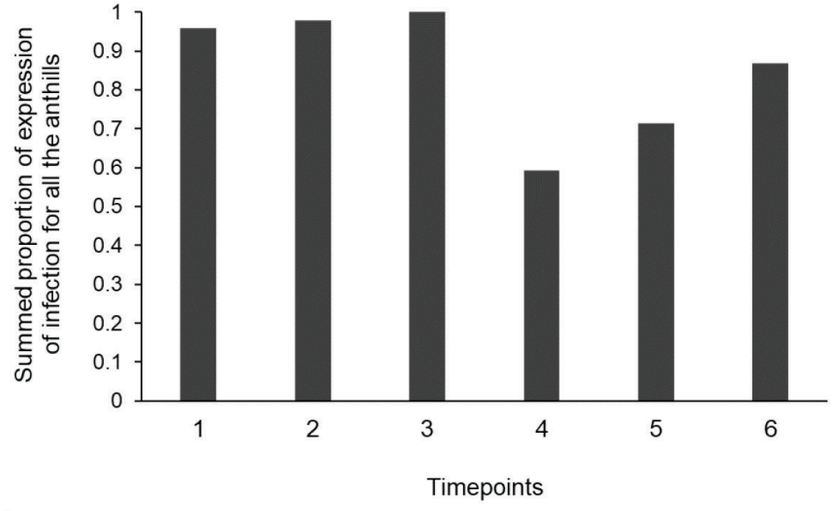

B

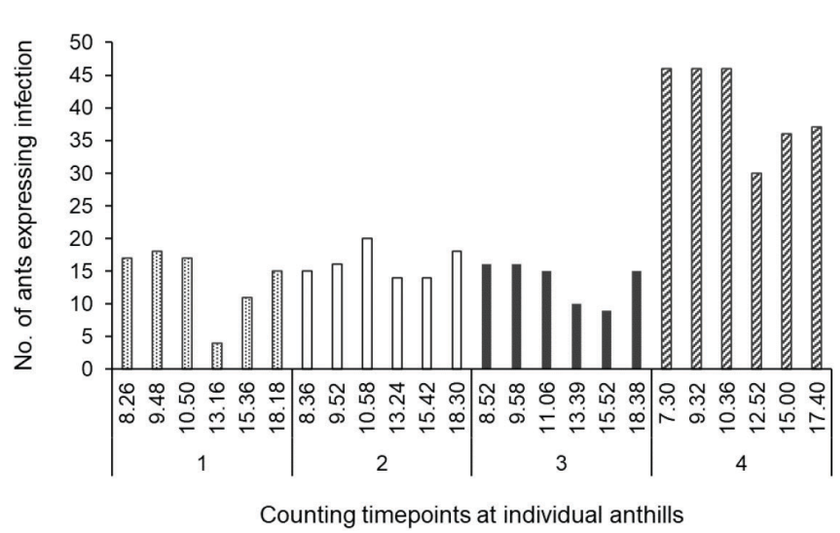

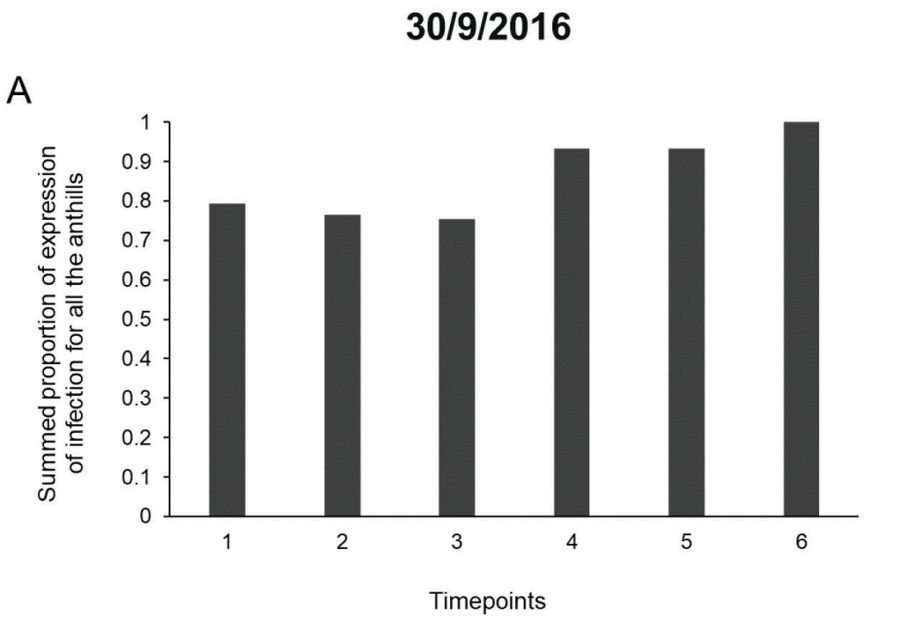
30/9/2016
A
Summed proportion of expression of infection for all the anthills
1
0.9
0.8
0.7
0.6
0.5
0.4
0.3
0.2
0.1
0
1
2
3
4
5
6
Timepoints
B
No. of ants expressing infection
50
45
40
35
30
25
20
15
10
5
0
8.36
10.27
11.54
13.37
15.12
16.26
9.04
10.36
12.02
13.50
15.18
16.32
9.21
10.48
12.14
14.06
15.26
16.40
7.42
10.10
11.26
13.00
14.52
15.56
1
2
3
4
Counting timepoints at individual anthills

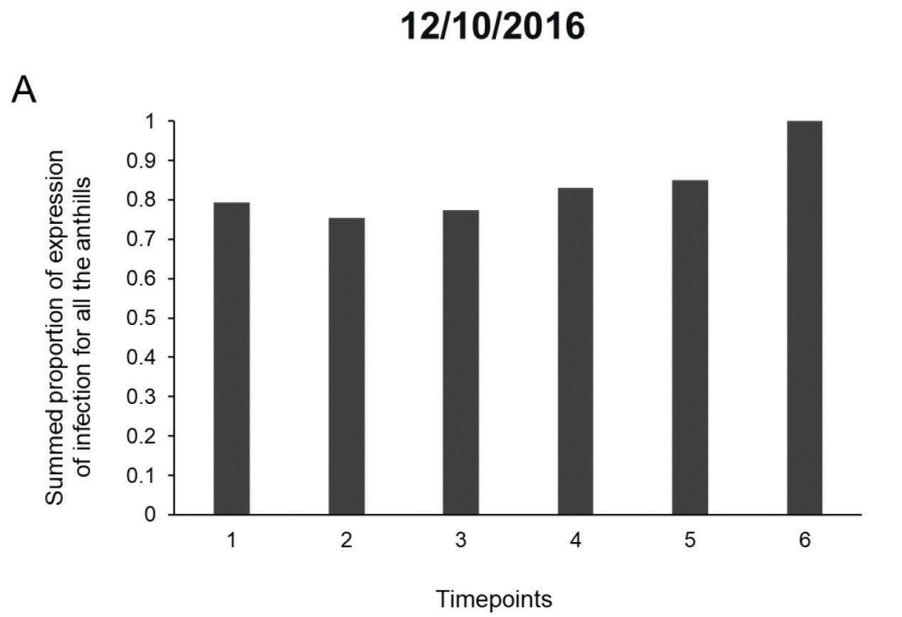
12/10/2016
A
Summed proportion of expression of infection for all the anthills
1
0.9
0.8
0.7
0.6
0.5
0.4
0.3
0.2
0.1
0
1
2
3
4
5
6
Timepoints
B
No. of ants expressing infection
30
25
20
15
10
5
0
9.06
10.50
11.29
12.38
14.05
16.03
9.32
10.54
11.34
12.50
14.16
16.12
9.47
10.58
11.39
13.00
14.27
16.32
8.12
10.38
11.14
12.14
13.46
15.26
1
2
3
4
Counting timepoints at individual anthills

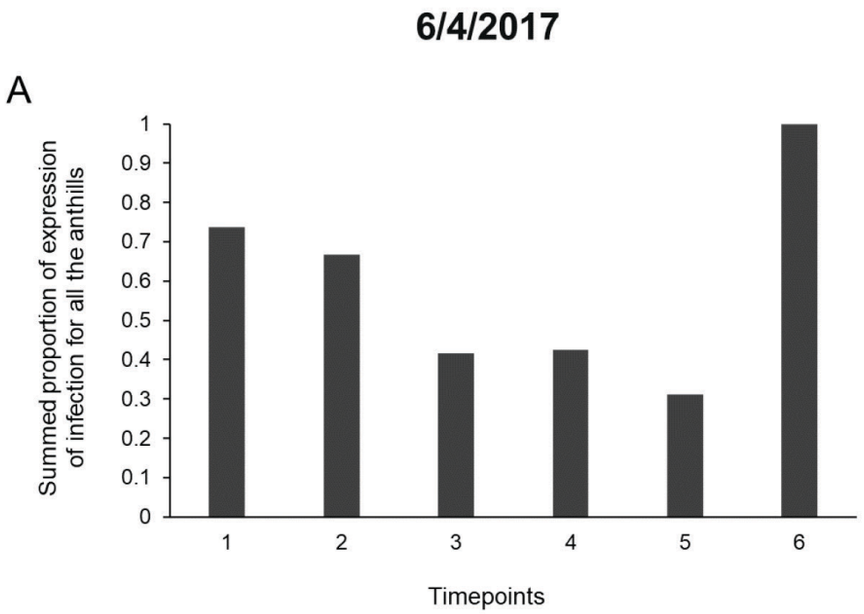
6/4/2017
A
Summed proportion of expression of infection for all the anthills
0
0.1
0.2
0.3
0.4
0.5
0.6
0.7
0.8
0.9
1
1
2
3
4
5
6
Timepoints
B
No. of ants expressing infection
0
20
40
60
80
100
120
7.16
9.06
10.28
11.24
12.30
14.40
7.40
9.14
10.34
11.38
12.48
14.52
8.02
9.22
10.42
11.48
12.56
15.04
1
2
3
Counting timepoints at individual anthills

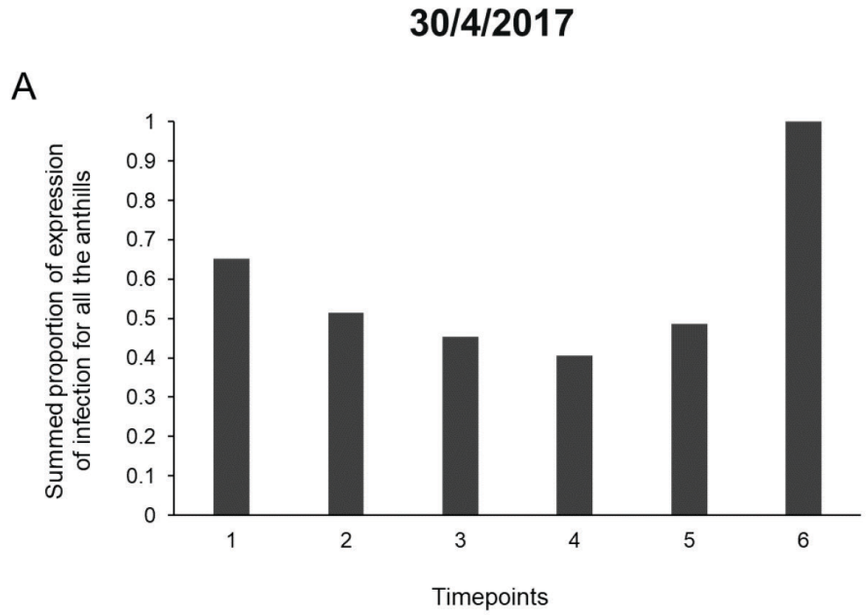
30/4/2017
A
Summed proportion of expression of infection for all the anthills
0
0.1
0.2
0.3
0.4
0.5
0.6
0.7
0.8
0.9
1
1
2
3
4
5
6
Timepoints
B
No. of ants expressing infection
0
20
40
60
80
100
120
7.34
8.58
10.04
11.12
12.50
15.56
7.44
9.10
10.14
11.28
13.02
14.48
8.00
9.20
10.32
11.38
13.22
15.08
1
2
3
Counting timepoints at individual anthills

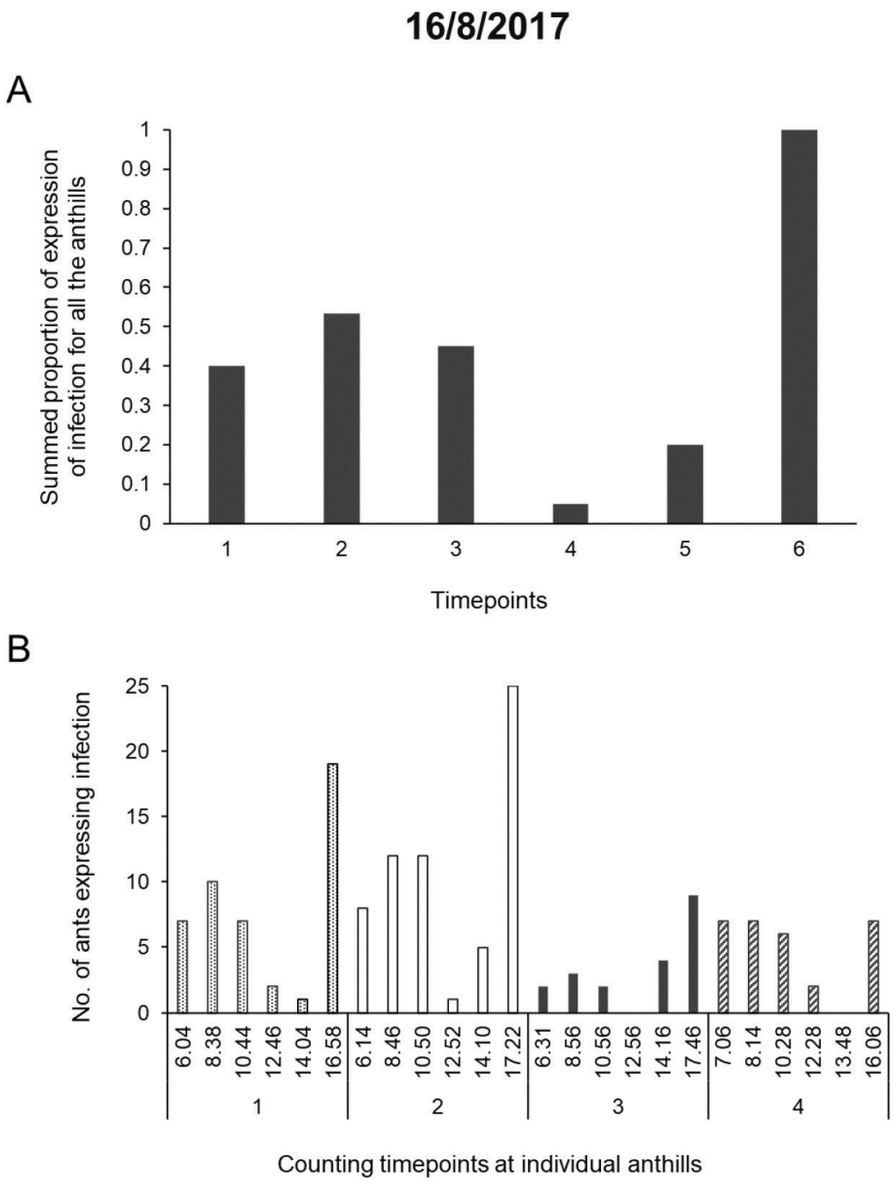

Supplementary figures S2. Overview of the infection status at six timepoints during the day of 11 dates in the field with data fitting the criteria*. Each figure for the separate dates consists of a top A) part and a bottom B) part. B) shows the exact numbers (varying maximum on secondary axis) of ants biting to vegetation at individual anthills recorded at the Bidstrup Forests, Denmark. The exact time of counting is indicated at respectively Anthill 1, 2, 3 and 4 (when applicable). Part A), expresses the summed proportion of biting ants at the six timepoints during the day, grouped from the row of timepoints in part B) underneath. This summed proportion is to the max (1) at the day of all the anthills recorded and represents the bigger picture of the tendencies of the proportion of expressed infection at the individual dates.

*The criteria were set to a recording frequency of at least six time points per observation day and including evenly distributed timepoints over the day in the field. Including measurements of around 7/8 in the morning, 10, 12/13, 14, 16/17 in the afternoon when applicable was intended. Pick was for proximity in time amongst the anthills, rather than representing extreme outliers of the day (e.g. first timepoint or very last timepoint, these can be seen in 'GasqueFredensborg_2023_S1_Abiotic_factors'). The 06/4/2017 and 30/4/2017 are included in the figure although there were no ants found at Anthill 4 on these dates, the rest of the anthills followed the criteria listed above.

Extra supplementary

Procedure for gluing number plates on gaster of ants in the field

The number plate was held with a pair of forceps in such a way that it would be placed on the ant orienting in a readable way (when looking at the ant with the head facing upwards). A small amount of insect glue was placed on the back of the number plate with a toothpick. An ant that was expressing the infection state (still biting onto the vegetation) was gently held on the head and thorax with a thumb. The plate was glued to the gaster of the ant by applying a light pressure on the plate for a few seconds, while at the same time removing the thumb holding the head and the thorax. With this technique most ants did not unlock their mandibles from the vegetation during the procedure, as seen with other techniques tested in the field (indicating the least amount of stress).

Codes used for SAS

Factors determining parasite-induced behavior modification

```
proc univariate plot normal;
var infection;
run;
proc genmod;
class date time time_of_day anthill site;
model infection/maximum = temperature RH time_of_day irradiation-proxy date / dist=binomial link =logit scale=pearson
type3;
output out = values pred=pred upper=upper lower=lower stdreschi=res;
run;
```

All-day attachment

```
proc univariate plot normal;
var maintain;
run;
proc genmod;
```

```
class date anthill;
model maintain/total = date anthill average_temperature average_rh/ dist=binomial link=logit
scale=pearson type3;
output out = values pred=pred upper=upper lower=lower;
run;
```

Codes used for R and Random Forest method

```
install.packages("Boruta")
install.packages("caret")
install.packages("dplyr")
install.packages("lubridate")
install.packages("forecast")
```
```{r}

library(Boruta)
library(caret)
library(dplyr)
library(lubridate)
library(forecast)
Data <- read.csv2(file = "../Data/GasqueFredensborg_2023_S1_Abiotic_factors.csv")
```
```{r}
str(Data)
hist(Data$Proportion_of_infection, breaks = 10)
Data_filtered <- select(.data = Data, c( -Maximum, -Infection))
Data_filtered$Date<-as.Date(Data_filtered$Date,format = '%d/%m/%Y')
Data_filtered$year = as.factor(lubridate::year(Data_filtered$Date))
Data_filtered$yday = yday(Data_filtered$Date)
Data_filtered$quarter = as.factor(quarter(Data_filtered$Date))
Data_filtered$month = as.factor(lubridate::month(Data_filtered$Date))
Data_filtered$day_of_month = lubridate::day(Data_filtered$Date)

season <- function(timedate, convention = "month_initials") {
  s_terms <- switch(convention,
                    "northern_hemisphere" = c("spring", "summer", "autumn", "winter"),
                    "southern_hemisphere" = c("autumn", "winter", "spring", "summer"),
                    "month_initials"      = c("MAM",    "JJA",    "SON",    "DJF"),
                    stop("Wrong value of convention")
  )

  m <- month(timedate)
  s <- factor(character(length(m)), levels = s_terms)
```



```
  s[m %in% c( 3,  4,  5)] <- s_terms[1]
  s[m %in% c( 6,  7,  8)] <- s_terms[2]
  s[m %in% c( 9, 10, 11)] <- s_terms[3]
  s[m %in% c(12,  1,  2)] <- s_terms[4]
  s
}
Data_filtered$season<-season(timedate = Data_filtered$Date)
Data_filtered<-na.omit(Data_filtered)
Data_filtered <- select(.data = Data_filtered, -Date)
Data_filtered_2<-select(.data = Data_filtered, c(-Middayclock, -quarter, -Sunrise, -Daylength, -Midday,
-Sunset, -Time_since_sunrise))

Data_filtered_3<-select(.data = Data_filtered, c(-quarter,-Irradiation.proxy))
```
```{r}
set.seed(101)
boruta_output<-
 Boruta(Proportion_of_infection~.,
        data = Data_filtered,
        doTrace=2,
        maxRuns = 100,
        ntree = 20000,
        getImp=imputeTransdapter(getImpRfZ))

plot(boruta_output)
plotImpHistory(boruta_output)
attribute_df<-attStats(boruta_output)
boruta_formula<-getConfirmedFormula(boruta_output)
```
```{r}
set.seed(101)
  trainIndex<- createDataPartition(y = Data_filtered$Proportion_of_infection,
                                   p = .70,
                                   list = FALSE,
                                   times = 1)
  # set train and test sets
  data_Train <- Data_filtered [ trainIndex,]
  data_Test  <- Data_filtered [-trainIndex,]
```
```{r}
train.control <- caret::trainControl(method = "repeatedcv",
                                     number = 5,
                                     repeats = 10,
```

```
                                allowParallel = TRUE)
  set.seed(101)
  model_borutized <- caret::train(form = boruta_formula,
                                  data = data_Train,
                                  method = “rf”,
                                  trControl = train.control,
                                  ntree= 2000, time
                                  tuneLength = 4)
```
```{r}
  prediction<-caret::predict.train(object = model_borutized,
                                   newdata = data_Test)
     error<- prediction - data_Test$Proportion_of_infection

  r2_output<-cor(data_Test$Proportion_of_infection, prediction)^2
  RMSE_output<-sqrt(mean(error ^ 2))
  ```

```{r}
  #R2 of RF prediction
  r2_output
  RMSE_output
  plot(data_Test$Proportion_of_infection, prediction)
```
  ```{r}

  cor(Data_filtered_3$Proportion_of_infection, Data_filtered_3$Temperature)^2
  plot(Data_filtered_3$Proportion_of_infection, Data_filtered_3$Temperature)

  cor(Data_filtered_3$Proportion_of_infection, Data_filtered_3$yday)^2
  plot(Data_filtered_3$Proportion_of_infection, Data_filtered_3$yday)

  cor(Data_filtered_3$Proportion_of_infection, Data_filtered_3$Time)^2
  plot(Data_filtered_3$Proportion_of_infection, Data_filtered_3$Time)

  cor(Data_filtered_3$Proportion_of_infection, Data_filtered_3$RH)^2
  plot(Data_filtered_3$Proportion_of_infection, Data_filtered_3$RH)
```

... the brain of an ant is one of the most marvellous atoms of matter in the world, perhaps more so than that of a man...

Charles Darwin
The Descent of Man 1871

CHAPTER 4

In the mind of a caterpillar: immunoreactive areas of the major biogenic amines in the larval *Spodoptera exigua* central nervous system

Simone N. Gasque[1], Sarah N. Kalisvaart[2], Hanneke A.C. Suijkerbuijk[2], Hans M. Smid[2], Vera I.D. Ros[1], and Alexander Haverkamp[2]

[1]Laboratory of Virology, Wageningen University and Research, Droevendaalsesteeg 1, 6708 PB Wageningen, The Netherlands
[2] Laboratory of Entomology, Wageningen University and Research, Droevendaalsesteeg 1, 6708 PB Wageningen, The Netherlands

Abstract

While the central nervous system (CNS) of insects has been studied to some extent, the focus has been mainly on brains of adult insects, and the larval CNS has received little attention so far. In lepidopteran insects, it is especially the larval instar, the caterpillar which causes the destruction of crop plants. In this research we constructed an overview of immunoreactive areas of the major biogenic amines in the CNS of mid third instar larvae of the beet armyworm *Spodoptera exigua*. The caterpillars of this polyphagous insect are a major pest with a worldwide distribution, affecting the production of many economically important crops and are a model system for examining the effects of baculoviruses on insect behaviour. We targeted the major biogenic amines of insects and the rate limiting enzymes involved in their biosynthesis, as it has been suggested that these are involved in the induction of a wide range of behaviours. We identified and described the immunoreactive neurons and projections and their location in the CNS of *S. exigua* for tyrosine decarboxylase (TDC), tyramine (TA), tyramine beta-hydroxylase (TβH), octopamine (OA), tyrosine hydroxylase (TH) and serotonin (5HT). With this study we started to fill the knowledge gap for the CNS of larval insects, and thereby we facilitate future research on lepidopteran larvae, their CNS and their behaviour.

1 Introduction

The human fascination of animals and the world around us stretches centuries back (Aubert *et al.* 2018). Animals can move around (after animus – from being animated), and it is speculated that due to this animation and avoidance of dangers the central nervous system (CNS) developed in animals (Greenfield 1998). The CNS of vertebrates is far more studied, compared to their invertebrate counter species (Dunton *et al.* 2021). Within invertebrates, mainly the CNS of adult insects has been studied (Hörner *et al.* 1995; Dacks *et al.* 2005; Tsuji *et al.* 2007; Mao and Davis 2009; Bao *et al.* 2010; Haverkamp and Smid 2014; van der Woude and Smid 2017; Tedjakumala *et al.* 2017; Xie *et al.* 2019), but little is known about the CNS of insect larvae. Larval instars (caterpillars) of the worldwide distributed beet armyworm *Spodoptera exigua* have devastating effects on economically important crop species (Dingha *et al.* 2004; Kwon *et al.* 2006; Robinson *et al.* 2023). Different methods have been applied to combat this pest, amongst others the usage of baculoviruses (Haase *et al.* 2015) which naturally infect the caterpillars. Interestingly, these viruses also induce behavioural changes in these caterpillars (reviewed by Gasque *et al.* 2019). However, little is known about the mechanisms behind such behavioural alterations, but it is evident that biogenic amines may play a key role in the expression of parasite-induced behavioural manipulations (Bethel and Holmes 1973; Helluy 1983; Øverli *et al.* 2001; Helluy and Thomas 2003; Ponton *et al.* 2006; Gaskell *et al.* 2009; Shaw *et al.* 2009). In mice infected with *Toxoplasma gondii*, a significant increase in dopamine (DA) metabolism was observed in neural cells and this increase was probably due to the release of the rate-limiting enzyme in the synthesis of DA, tyrosine hydroxylase (TH) (Prandovszky *et al.* 2011). In *Gammarus* species infected by the acanthocephalan *Polymorphus paradoxus*, serotonin (5HT, 5-hydroxytryptamine) may play a role, since injections with serotonin into uninfected individuals led to the same behavioural alteration (phototaxis and clinging behaviour to vegetation) as seen in *P. paradoxus*-infected individuals (Helluy and Holmes 1990). In addition, apparent differences in serotonin-like immunochemistry were seen between uninfected and infected *G. lacustris* (Maynard *et al.* 1996). In *Manduca sexta* caterpillars parasitised by *Cotesia congregata* octopamine (OA) levels were increased along with decreased feeding and locomotion (Adamo *et al.* 1997; Adamo and Shoemaker 2000). 5HT, DA, tyramine (TA) and OA are the major biogenic amines in invertebrates (and more specifically insects) (Blenau and Baumann 2001). Biogenic amines act as neuromodulators and can be locally released near the target site within the CNS or act throughout the insect body when being released into the haemolymph (Adamo *et al.* 1995). 5HT neurons trigger internal nutrient responses due to sugar and bitter tastes (Yao and Scott 2022), and are involved in visual formation, e.g. in the form of phototactic behaviour through the 5HT1A-receptor in the honey bee *Apis mellifera* (Thamm *et al.* 2010). DA is involved in mating activities (Akasaka *et al.* 2010) and in aggressive behaviour (Szczuka *et al.* 2013; Momohara *et al.* 2018). Along with DA, TA has also been found to play a role in aggressive behaviour (Momohara *et al.* 2018). OA is known as the stress and fight or flight neuromodulator (Adamo *et al.* 1995; Adamo and Baker 2011) and as modulator of mobility and movement (Xu *et al.* 2018). Furthermore, OA is released into the haemolymph during flying (Orchard *et al.* 1993) and during activation of the immune system (Dunphy and Downer 1994; Adamo *et al.* 2017). In addition, 5HT, DA and OA also play various roles during learning and memory formation (Wright *et al.* 2010; Burke *et al.* 2012; Waddell 2013). All the biogenic amines are produced from different aromatic amino acids by a range of enzymes. Tryptophan hydroxylase (TPH) hydroxylates (L-)tryptophan to 5-hydroxytryptophan, with subsequent catalysation by DOPA-decarboxylase (DDC, also known as aromatic L-amino acid decarboxylase) to 5HT (Figure 1). DDC is also involved in the biosynthesis of DA. Here, TH catalyse the hydroxylation of tyrosine to 3,4-dihydroxy-L-phenyl-alanine (L-DOPA), which is subsequently decarboxylated to DA by DDC. Tyrosine is also the starting point for the production of yet another neurotransmitter, namely OA. Here, tyrosine decarboxylase (TDC) leads to the synthesis of TA (separately acting as a neuromodulator), which is subsequently hydroxylated by tyramine beta-hydroxylase (TβH) to OA (Blenau and Baumann 2001; Rang *et al.* 2016).

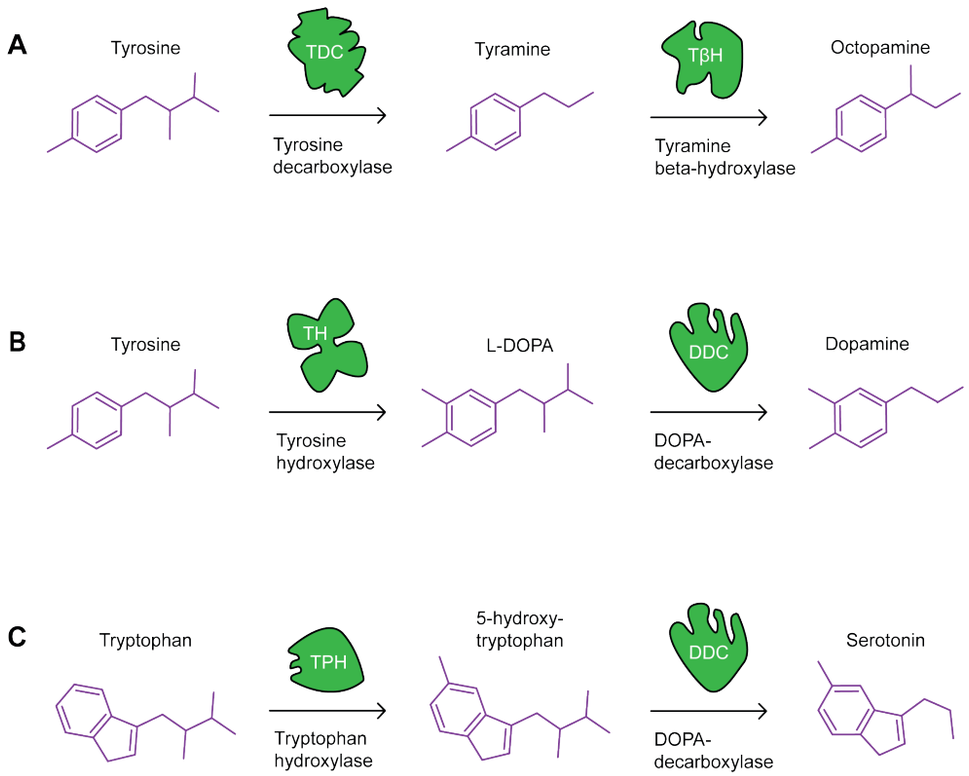

Figure 1. Graphical visualisation of the biosynthesis pathways of the four major biogenic amines, along with the enzymes catalysing these processes. A) biosynthesis pathway of tyrosine to tyramine (TA) and octopamine (OA), catalysed by tyrosine decarboxylase (TDC) and tyramine beta-hydroxylase (TβH). B) the biosynthesis of tyrosine to dopamine (DA) catalysed by tyrosine hydroxylase (TH) and DOPA-decarboxylase (DDC). C) the biosynthesis pathway to serotonin (5HT), involving the enzymes tryptophan hydroxylase (TPH) and DDC.

The CNS of *Spodoptera exigua* caterpillars (see chapter 1) is aligned as a sequence of ganglia which process and receive signals from different areas and can be involved in different functions (Chapman 2013). In short, the CNS is structured cranially to caudally starting with the supraoesophageal ganglion (brain) which contains the sections of neurons which are most comparable to a mammalian brain, with the areas sending and receiving signals from the ocelli (eyes) and the antennae, storing memory and combining sensory information. The suboesophageal ganglion (SOG) encompasses the neurons that send and receive signals to and from the mouth parts including the mandibles, and the maxillary and labial palps. The thoracic ganglia (TG1, TG2 and TG3) send and receive signals to and from the for-, mid- and hindlegs on the thorax, whereas the remaining ganglia send and receive signals to and from the abdominal prolegs and anal proleg (Chapman 2013). The aim of our study

was to target each of the four major biogenic amine pathways to provide an overview of the immunoreactivity (IR) in the brain, SOG and thoracic ganglia of *S. exigua* caterpillars. We identified and described the immunoreactive neurons and projections and their location in the CNS of the mid third instar (mL3) of *S. exigua* for each of the following targets: TDC, TA, TβH, OA, TH and 5HT. Thereby we provide, a detailed overview of immunoreactive areas of these major biogenic amines and their rate limiting enzymes in the CNS of insect larvae, more specifically for *S. exigua* third instar caterpillars.

2 Materials and methods

2.1 Insect rearing and CNS dissections

Spodoptera exigua larvae were reared on artificial diet until mid-third instar under a 14h : 10h light : dark regime at 25.5°C, 50% relative humidity as described before (Chapter 5).

Mid L3 larvae were immobilised by placement on ice and each larva was decapitated with a sharp sterile scalpel around the second or third leg pair. The remaining sample included the head capsule and the pro- and mesothorax (TG1 and TG2; in some cases also TG3). The CNS was dissected out, in either phosphate buffered saline (PBS, Oxoid, Dulbecco 'A' tablets) or directly in the fixative (see for each individual target 2.2-2.4), with sharpened forceps (Dumont No 5), by first making a ventral rupture on the larvae, removing access tissue and carefully tearing the oesophagus to facilitate intact circumoesophageal connectives. Each dissected CNS was carefully moved to the respective fixative (see below) in Eppendorf tubes placed on ice. The samples for TDC and 5HT analysis were fixed in 4% PFA (paraformaldehyde (Merck) in 0.1 M phosphate buffer or PBS (section 2.2), while the samples for TβH and TH analysis were fixed in freshly made Fix-M (8:1:1 of PBS (Oxoid, Dulbecco 'A' tablets), 100% methanol (Merck) and 36.5% formaldehyde (Sigma Aldrich)) (section 2.3). All samples were placed on a precooled cold plate installed at 1°C under a microscope (Olympus, SZX 12). The samples for TA and OA analysis were fixed on an objective slide in GPA fixative (2.5 ml 25% glutaraldehyde (Sigma Aldrich), 7.5 ml saturated picric acid (Gist-Brocades) and 100 µl 100% acetic acid (Sigma Aldrich)), followed by 30 minutes fixation in GPA in a dissection dish at room temperature (RT) (section 2.4). For each of the targets a minimum sample size of 15 CNSs was reached, with the aim of having around 10 high quality CNSs for confocal image scans.

2.2 4% PFA fixation protocol (TDC and 5HT)

The general outline of the immunohistochemical protocols has been described earlier (van der Woude and Smid 2017), but was optimised for *S. exigua*. Dissected out CNS were fixed overnight in 4% PFA at 4°C. To increase permeability the samples were dehydrated the day after dissection to 100% ethanol by a series of increasing alcohol percentage (70%, 90%, 96%, 100%, 100%) for 2 minutes each and subsequently degreased in xylene (first 50% xylene/50% ethanol, 100% xylene and lastly 50% xylene/50% ethanol again) and rehydrated for 2.5 minutes in each of a series of decreasing alcohol percentage (100%, 96%, 90%, 70%, 50%) to 50%. The alcohol was rinsed away by PBS in 5 rounds of 15 minutes, and the samples were incubated for 1 hour at RT by 0.5 mg/ml collagenase in PBS. The collagenase was washed away via 4 steps of 10 minutes with PBS-T (0.5% Triton-X), followed by a preincubation in PBS-T-NGS for 1 hour and an overnight incubation at 4°C (Rabbit anti 5HT (Millipore) diluted 1:200) or a 24 hours incubation at RT (or over weekend at 4°C, 1:100 dilution of Rabbit anti TDC, LSBio via bio-connect) in PBS-T-NGS. The primary antisera were washed away by rinsing 6 times in PBS-T for a total duration of 2 hours. Thereafter the samples were incubated in the secondary antisera at 4°C overnight (Goat anti-Rabbit antisera linked to Alexa Fluor 488 (GaR 488) (Invitrogen, Molecular probes) at a 1:100 dilution for the TDC treatment and 1:200 for 5HT) in PBS-T-NGS, including the counterstain To-Pro-3 (Life Technologies, Thermo Fisher Scientific) in a 1:500 dilution to label nuclei. The secondary antisera and counterstain were rinsed by several changes of PBS-T for the duration of 2 hours at RT, and 4 times in 2 hours in PBS, both steps conducted at RT (for 5HT last at 4°C). The samples were then dehydrated 2 minutes each in a series of 50%, 70%, 90%, 96%, 100%, 100% ethanol and then cleared by 50% xylene/50% ethanol, 100% xylene and lastly mounted in distyrene plasticiser xylene mixture (DPX, Merck) on microscope slides.

For 5HT the two rounds of both dehydration and rehydration series (one in the beginning and second described just above) led to the best staining of the cell bodies and projections in the brain. For the SOG the additional series of de- and rehydration led to the best staining of the projections, whereas without this step cells on the surface of the ganglia were visible. Staining of the TG worked best without these two additional series. Therefore, samples from both these procedures were used for the subsequent analysis of single cell, clusters and projections, to give the most accurate 5HT-IR cell and axon identifications in the brain, the SOG and the thoracic ganglia.

2.3 Fix-M fixation protocol (TßH and TH)

Immunohistochemical procedures for visualising TβH-IR and TH-IR are similar as described for visualising the TDC-IR and 5HT-IR, but differ at certain points as outlined below. Each dissected CNS was carefully moved to fix-M in Eppendorf tubes placed on ice and afterwards fixed overnight at 4°C (TH) or for about 30 minutes (for TβH most samples were fixed for 30 min, but a few in another round for 3 hours, with differences in the results in the brain samples, see result section). To wash off the fixative from the overnight TH fixation, 6 washing steps (for a total of 1 hour) were performed with PBS. For TβH an additional de- and rehydration series was conducted to increase the permeability of the samples and samples were subsequently cleared in xylene. This was done in the same manner as described above, although the samples were rehydrated for 3 minutes in each step. The alcohol was rinsed away by PBS in 5 rounds of 15 minutes each. Both the TβH and TH samples were incubated for 1 hour at RT with 0.5 mg/ml collagenase in PBS. The collagenase was washed away in 6 steps with PBS-T (total 1 hour), followed by a preincubation in PBS-T-NGS for 1 hour and a 24 hours incubation in a 1:100 dilution of the primary antisera in PBS-T-NGS (Rabbit anti TβH (Shiraz) and Rabbit anti TH (Bio-Techne LTD (original Novus biologicals)), at RT for TβH and at 4°C for TH. The primary antisera was washed away using PBS-T in 6 steps during 2 hours, and then the sample was incubated in the secondary antisera at 4°C overnight in GaR 488 (Invitrogen, Molecular probes) at a 1:100 dilution in PBS-T-NGS, together with To-Pro-3 (To-Pro-3 iodide 642/661, Life Technologies, Thermo Fisher Scientific) 1:500 as a nuclei counterstaining. The secondary antisera and counterstain were washed away at RT in 4 steps during 2 hours using PBS-T, and in 4 steps during 2 hours using PBS. The samples were then dehydrated 2 minutes each in a series of 50%, 70%, 90%, 96%, 100%, 100% and then cleared by 50% xylene/50% ethanol, 100% xylene and lastly mounted in distyrene plasticiser xylene mixture (DPX) on microscope slides.

2.4 GPA fixation protocol (TA and OA)

The direct TA and OA immunohistochemical procedure commenced with dissection of the CNSs in ice cold PBS. To prevent the CNS from curling up the CNSs were subsequently flattened out for 1 minute on an objective slide in GPA fixative, followed by 30 minutes fixation in GPA in a dissection dish at RT. To increase permeability the samples were dehydrated to 100% ethanol by a series of increasing alcohol percentage (50%, 70%, 90%, 96%, 100%, 100%) for 2 minutes each and subsequently degreased in xylene and rehydrated for 3 minutes in each of a series of decreasing alcohol percentage (100%, 96%, 90%, 70%, 50%) to 50%. For 20 minutes at RT the samples were incubated in 1% sodium borohydrate in PBS, which was subsequently washed away with PBS in 3 rounds of 15 minutes. The samples were then incubated for 45 minutes at RT with 5 mg/ml collagenase in PBS, and washed 4 times for 10 minutes in PBS-T. A 1 hour PBS-T-NGS (10%) preincubation step preceded the overnight incubation step in Rabbit anti TA (Chemicon) or OA (Mobitec) diluted 1:100 in PBS-T-NGS at RT. The following day the primary antibodies were washed away by PBS-T in 6 steps during a total duration of 2.5 hours at RT, and the samples were incubated overnight at RT in GaR 488 (Invitrogen, Molecular probes) 1:100

and 1:1000 of To-Pro-3 (Life Technologies, Thermo Fisher Scientific) in PBS-T-NGS. The subsequent day the secondary antibodies and the counterstain were washed away firstly with PBS-T and then PBS, each 4 times in a total of 2 hours for each of the treatments. The samples were then dehydrated in the same fashion as described in the two previous sections (2.2 and 2.3), followed by degrease in xylene for a minimum of 5 minutes and mounted on slides in DPX.

2.5 Antisera specificity

Specificities of the secondary antibodies of targets (TDC, TA, TβH, OA, TH and 5HT) were provided by the manufacturers (2.2-2.5). Each antiserum was tested on *S. exigua* CNSs, and if used for the first time in the laboratory, on *Drosophila melanogaster* brains as a positive control. In addition, a negative control was included for each antiserum, for which samples were prepared as above with omission of the primary antibody. All negative controls did not reveal any immunolabeling. The positive controls showed immunoreactivity for the targets.

The antisera against DA raised in mice, did not show affinity in *S. exigua*. We therefore used the rate limiting enzyme of DA, TH, to identify dopaminergic cell clusters (Tedjakumala *et al.* 2017; Hamanaka and Mizunami 2018). This method is based on the theory that the rate-liming enzyme towards the final neurotransmitter product and the neurotransmitter itself are produced in the same neurons (e.g. TH and DA in dopaminergic neurons) (Bao *et al.* 2010). The antisera against *Drosophila* TPH, the rate-limiting enzyme for 5HT showed no affinity in *S. exigua*.

2.6 Image acquisition, marking and brain nomenclature

For image acquisition, a Zeiss LSM 510 confocal laser scanning microscope (CLSM version 3.2 sp2) with a 458/488-nm argon laser to visualise Alexa Fluor 488, and a 633-nm HeNe laser to visualise TO-PRO-3 (iodide 642/661) was used. Alternatively, a Leica Stellaris 5 confocal LSM with a spectrally flexible white light laser was used for excitation of both the conjugates. Each CNS was scanned in parts (e.g. brain, SOG and the first, second and sometimes third thoracic ganglia) with oil immersion objectives; Plan-Neofluar 25x N.A. 0.8 and Plan-Neofluar 40x N.A. 1.3 for the LSM 510 was utilised. With Stellaris 5 a 40x N.A. 1.3 magnification was comparable to the 25x N.A. 0.8 from the LSM 510, and the LAS-X software package was used during the scanning process. The resolution was kept at 2048 × 2048 pixels and 8 bits, with a voxel size of 0.10-0.10-0.70 – 0.14-0.14-2 µm for all images. Each good quality sample was further used for the analysis. The stack was oriented correctly in the Fiji package of ImageJ (v 2.9.0, Fiji Distribution; Schindelin *et al.* 2012) and for most targets the analysis was conducted directly in ImageJ. For visualisation of different depths in one image, the z-projection was used with maximum intensity. Due to the high number of single cells and clusters in the brain visualised with TH-immunostaining, another approach was used to aid the differentiation for this target in these ganglia. The stack was imported into ImageJ, oriented correctly and subsequently only the primary target channel of the acquired images was imported into the TrakEM2 plugin (Cardona *et al.* 2012). Per brain of the TH immunostaining, one hemisphere was chosen for analysis and the diameter of each individual neuron was marked in all the image slides it was detected in. For all the targets, each of the ganglia the best stained side/hemisphere was analysed. This was done manually by the same person for the same target (e.g. TDC by S.N.K.) to keep identifications similar (all other target were analysed by S.N.G.).

The sample count for each ganglion (brain to TG2) ranged from 7-39 samples per target. For each of the good quality samples, the amount and location of single cells and projections were noted (Dataset S1-S6) and for the construction of datasets and tables, the minimum and maximum number of cells per cluster and of single cells were given, along with the arithmetic mean of cells per cluster (of positive scored cell counts, without the 0 inputs) as well as the overall cell count per ganglia. These data were the basis for the graphical representation of the locations and quantities for each rate limiting enzyme/biogenic amine and lastly combined in the overall graphical representation of the IR. In the result section below the data for the identified single cells and clusters are represented in parenthesis following the cluster name, the number of cells per cluster per side (if not stated otherwise), the arithmetic mean, and how many samples this single cell or cluster was observed in out of the total are given, for example (1-3, mean 1.7, 19/21). Since the head of *S. exigua* has a vertical orientation (with ventral mouthparts), we adapted the nomenclature (Ito *et al.* 2014) by referring to the location of cell bodies in the ventral-dorsal plane/body axis. In the abbreviations used, the first letter describes the direction in the ventral-dorsal plane (V or D), the middle letter describes the location in the anterior- posterior plane (A or P, if applicable), and the final letter indicates whether the single cell or cell cluster has a lateral, medial or central location (L, M or C) (Figure 2). In some cases, two or more individual cells or clusters are located at the same place according to the nomenclature, but due to visible space between them (or due to size or shape differences) they are not regarded as belonging to the same cluster. In those cases, a number was added to the name. These numbers are added from anteriorly to posteriorly.

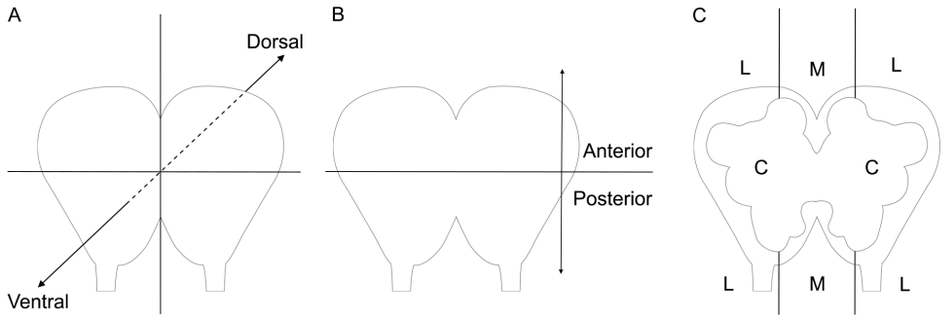

Figure 2. Nomenclature used for naming immunoreactive cells and projections. A) ventral (V) vs dorsal (D), B) anterior (A) vs posterior (P) and C) lateral (L), medial (M) or central (C).

3 Results

3.1 TDC immunoreactivity

The TDC-immunostaining revealed vesicle-like signal in certain parts of different neuropils. In addition, different cell clusters and single cells could be identified. TDC-IR was observed as a more cytoplasmic signal in comparison to e.g. 5HT-IR or TH-IR.

In the brain some single cells and clusters were detected medially (total per brain 6-14, mean 10, N=39). Described from anterior to posterior these were the VAM (1-3, mean 1.7, 15/39) and the VPM in all of the observed samples (3-6, mean 4.4) (Dataset S1) (Figure 3A, B). We also observed projections as a line of vesicle or as terminal like structures (not a clear continuous line as observed for some of the other targets) (Figure 3C, F, G, H). The VC projections were observed in almost all the samples (37/39) on the ventral side directing from a central medial to a lateral position across the superior neuropil (Figure 3C). The DPL projections were observed in the majority of the samples (28/39) on the dorsal side projecting from a central medial to a posterior lateral position going through the circumoesophageal connectives (cc) (Figure 3C).

Including the VA cluster (5-12 cells per side, mean 8, 12/21) on the ventral surface (Figure 3D), the SOG comprised seemingly more TDC-IR cells than the brain with a total of 6-36 cells and a mean of 18 (N=21). On the dorsal side single cells and clusters were found with a higher frequency. From anterior to posterior, the DAM cluster was observed in about half of the samples (1-2, mean 1.9, 9/21), the DAL cluster was found in most samples (1-3, mean 1.7, 19/21), and the DPL-1 single cell and DPL-2 cluster were observed in all of the samples (1 per SOG for DPL-1, and

1-2 per SOG, mean 1, for DPL-2) (Figure 3F). Two sets of projections were running longitudinal and seemingly parallel to the midline of the SOG. Most medially located, the DPM projections were observed in about half of the samples (11/21) and more lateral, the DL projection was seen in all of the samples (N=21) (Figure 3G). The projections in the SOG to TG3 were observed as a line of vesicles or neuron terminals, which indicated two parallel paired longitudinal tracts running through the neuropils, at different depth. These parallel-line projections were located more lateral than e.g. the TA signal (described below).

The DAL cluster was observed in all samples for TG1 (6-10, mean 8.4, 12/12) (Figure 3E) and for TG2 (7-10, mean 9.6, 7/7). In TG2, the single cell VAL (1, 6/7) was observed in a majority of the cases (Figure 3H). For both TG1 and TG2, VL, VM and DAM projections were observed (Figure 3H). For TG1 the VL projections were observed in all the samples, the VM projections in almost all (9/12) and the DAM projections in half of the samples. For TG2, VL was still seen in all samples (Figure 3H), VM and DAM in most cases (5/7 and 4/7, respectively).

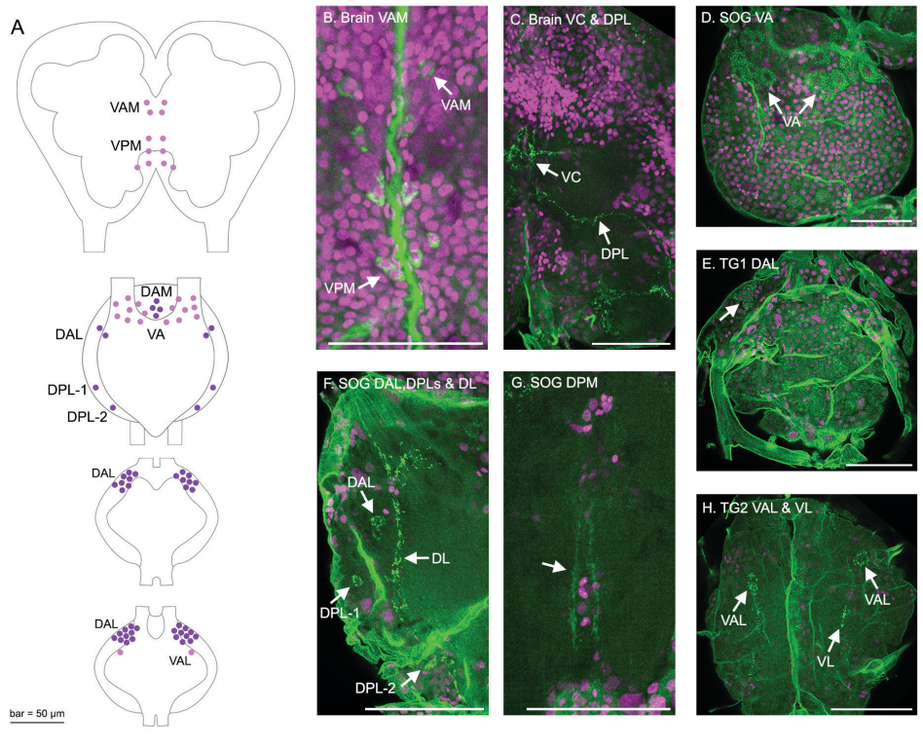

Figure 3. Tyrosine decarboxylase (TDC) immunoreactivity (IR) in *S. exigua* mid third instar caterpillars. A) overview of TDC-IR cell bodies and areas in the brain to the second thoracic ganglion (TG2). Pink dots for the ventral side, and purple dots for the dorsal side representing the cell clusters and single cells.

B-H) representative CLSM images of TDC-IR samples, with arrows indicating identified clusters and cells. B) VAM and VPM clusters in the brain. C) VC and DPL projections in the brain (z-projection of multiple images to visualise both projections). D) the VA cluster on the surface of the SOG. E) the TG-specific DAL cluster shown in TG1. F) the DAL, DPL-1 and DPL-2 clusters and single cells and the DL projection (z-projection of multiple images) and G) the DPM projections (z-projection of multiple images) in the SOG. H) the VL projection and the TG2-specific VAL single cells (z-projection of multiple images). Magenta signal for the TO-PRO-3 nuclei/dsDNA staining, green channel for TDC-IR. Scalebars represent 50 µm.

3.2 TA immunoreactivity

The TA-immunostaining revealed individual cells and projections, but also some vesicle-like structures by varicose terminals being labelled within certain brain areas (Dataset S2).

The TA-IR cell count in the brains resulted in a mean of 8.7 cells per brain (6-12, N=18). A VMC cluster of 3-6 cells per brain hemisphere was observed in most of the samples (11/18) (Figure 4A, B). In addition, a signal overarching the outer optical anlage (OOA; Huetteroth *et al.* 2010) was seen in all but one sample (Figure 4E). In few of the samples VL cells were observed (1-2, mean 1.3, 3/18). Furthermore, some projections and commissures (nerve tissues connecting the 2 hemispheres of a ganglion) were observed. The major projections were the PL to medial projection (17/18) (Figure 4E) along with the VPC projection (15/18). The latter branch into the most posteriorly located commissure (PC). PC and the anteriorly located commissure (AC) were observed in most of the samples (14/18 and 15/18, respectively), and these two were located respectively posteriorly and anteriorly to the central body (CB) (Figure 4E). The medially located commissure (MC) was observed in half of the samples.

In the SOG to TG3 we observed longitudinal tracts running through the length of the ganglia in all or all but one sample (SOG: 16/17, TG1: 17/17, TG2: 11/11, TG3: 6/6) (Figure 4C). TA signals were not observed located within specific cell bodies in the SOG. In TG1, TG2 and TG3 a DPM cluster ranging from 1 to 3 cells was observed in nearly all samples (TG1: 14/17, TG2: 9/11, TG3: 6/6), with increasing intensity and cell count in the more caudally located ganglia (TG1: 1-3, mean 2,5; TG2: 2-3, mean 2.9; TG3: 3, mean 3).

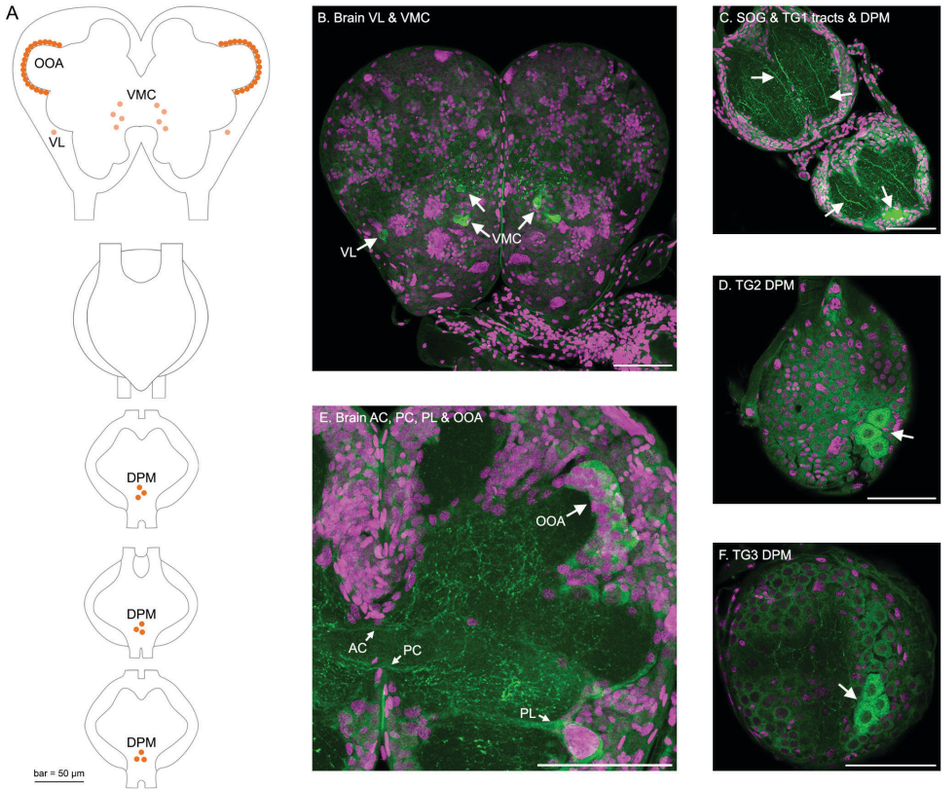

Figure 4. Tyramine (TA) immunoreactivity (IR) in *S. exigua* mid third instar caterpillars. A) overview of TA-active cell bodies and areas in the brain to the third thoracic ganglion (TG3). Light orange dots for the ventral side, and dark orange dots for the dorsal side representing the cell clusters and signal overarching the outer optical anlage (OOA). B-F) show representative CLSM images of TA-IR samples, with arrows indicating identified clusters and cells. B) VMC cluster and VL single cell on the surface of the brain (z-projection of multiple images to visualise all cell bodies). C) the paired projections running through the SOG and TG1 (and further down the following TGs) the DPM cluster (z-projection of multiple images to visualise all cell bodies), which is also visualised in TG2 (D). E) the AC and PC commissures, the PL projection and lastly the signal observed from the OOA in the brain (z-projection of multiple images to visualise all). F) the DPM cluster in TG3. Magenta signal for the TO-PRO-3 nuclei/dsDNA staining, green channel for TA-IR. Scalebars represent 50 µm.

3.3 TßH immunoreactivity

Overall, the TβH staining showed a diffused signal throughout the CNS. However, more intense staining was localised in 3 specific areas in the brain, and a similar intense staining of antigens could not be localised in any of the subsequent ganglia. The VA-cluster was observed in almost all samples predominantly consisting of 1-3 cells (mean 1.9, 19/20) (Figure 5A, B and E; Dataset S3). The VM-cluster was also observed in almost all of the samples examined (1-4, mean 1.3, 19/20), but the TβH-IR signal was most often only at a high enough level to be scored in the most anterior cell bodies (filled circles Figure 5A). In addition, weaker stained cells of the same size and shape, that in many cases formed a circular structure, were observed in this cluster (open circles in Figure 5A). There was a bit of overarching signal in the cells comprising this cluster (4-6 cells per hemisphere), and with the 30 min fixation time most often only 1 of these cells had a high enough signal to be scored for TβH-IR. In 2 out of 19 cases, the TβH-IR signal was high enough for all cells to be regarded proper IR and with the 3 hours fixations steps 4-5 cells per hemisphere in this cluster were scored as TβH-IR (all 3 samples), and no signal was observed in the previously described VA and VM clusters for the samples fixated longer. The clearest projection was the bundle (CA projection) from the superior neuropil (SNP) arborising in two bundles into the calices, it was observed in almost all of the samples (19/20), although in some samples it was more vaguely expressed (Figure 5C).

For the SOG up to TG3, no specific localisation of TβH-IR could be seen, as the signal was not different between cells, but a signal seemed to be present in almost all cells, in the nuclei (colocalisation of TβH-antibodies and TO-PRO-3, Figure 5D and F).

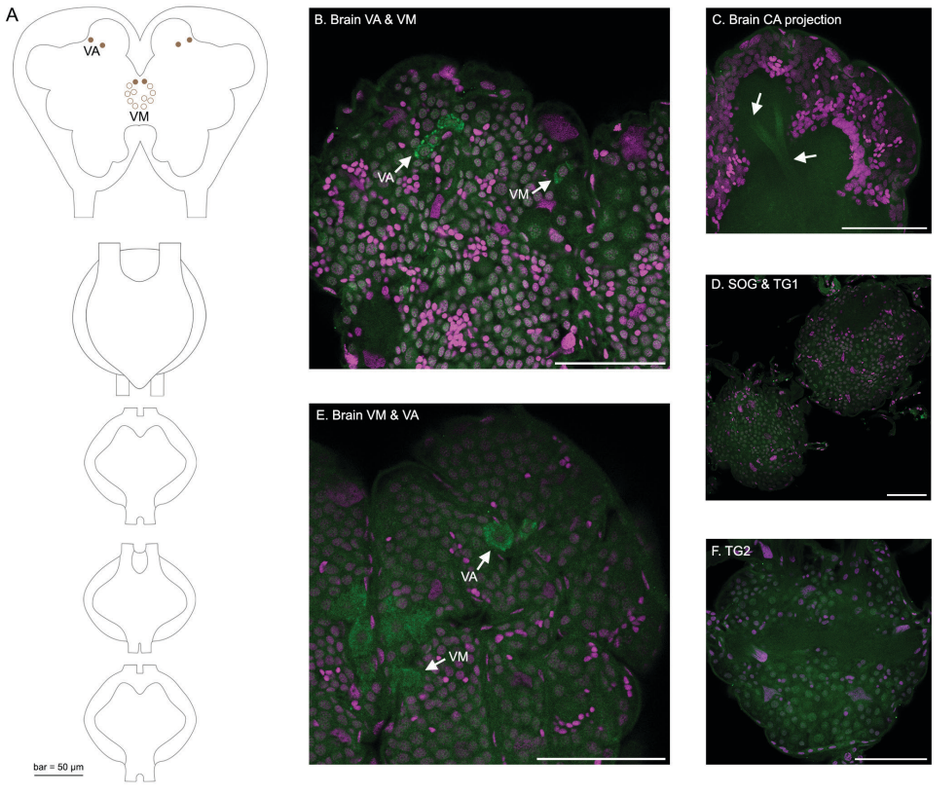

Figure 5. Tyramine beta hydroxylase (TβH) immunoreactivity (IR) in *S. exigua* mid third instar caterpillars. A) overview of TβH-active cell bodies and areas in the brain to the second thoracic ganglion (TG2). Filled circles show the cells that were observed in almost all cases by light brown (ventral side), and open circles indicate the location of the overall circular VM cluster (which did rarely have a high enough-signal level to be scored, but was constituting the cluster (location, size, intensity) where mostly one cell was scored as TβH-IR). B-F) show representative CLSM images of TβH -IR samples, with arrows indicating identified clusters and cells. B) VA-cluster and only one cell is scored for the VM cluster in the brain. C) the major CA projection arborising in the calyx (z-project of multiple stacks to show full observed projection). D) no observed TβH-IR signal in SOG and TG1. E) (in contrast to B)) with all cells from VM was scored as TβH-IR, and VA-cluster in the brain. F) no observed TβH-IR signal in TG2. Magenta signal for the TO-PRO-3 nuclei/dsDNA staining, green channel for TβH-IR. Scalebars represent 50 µm. ›

3.4 OA immunoreactivity

OA-immunoreactivity could be detected throughout the CNS with varicose terminals being observed as vesicle like structures (Figure 6B). Individual cells could only be detected in the DPM cluster in the SOG up toTG3 and in 3 additional ventral clusters in the SOG (Figure 6C-F). Intense staining was also observed in the outer optical anlage (OOA; Huetteroth et al. 2010) (14/17), and PL projections (10/17) similar to those described under the TA-section were observed (3.2; Dataset S4) (Figure 6B).

The DPMs were located on the surface of the ganglia, and the observed cell numbers increased with the more caudally located ganglia, with only a few observations in the SOG (SOG: 1-3, mean 1.5, 4/17; TG1: 1-4, mean 2.2, 17/18; TG2: 2-3, mean 2.9, 16/16; TG3: 3, mean 3, 8/8) (Figure 6C-F). The 3 ventrally paired clusters in the SOG were located in a medial vertical line, with each cluster consisting of mostly 1-2 cell bodies (per hemisphere), leading to the nomenclature of anterior, mid and posterior (VAM, VM and VPM).

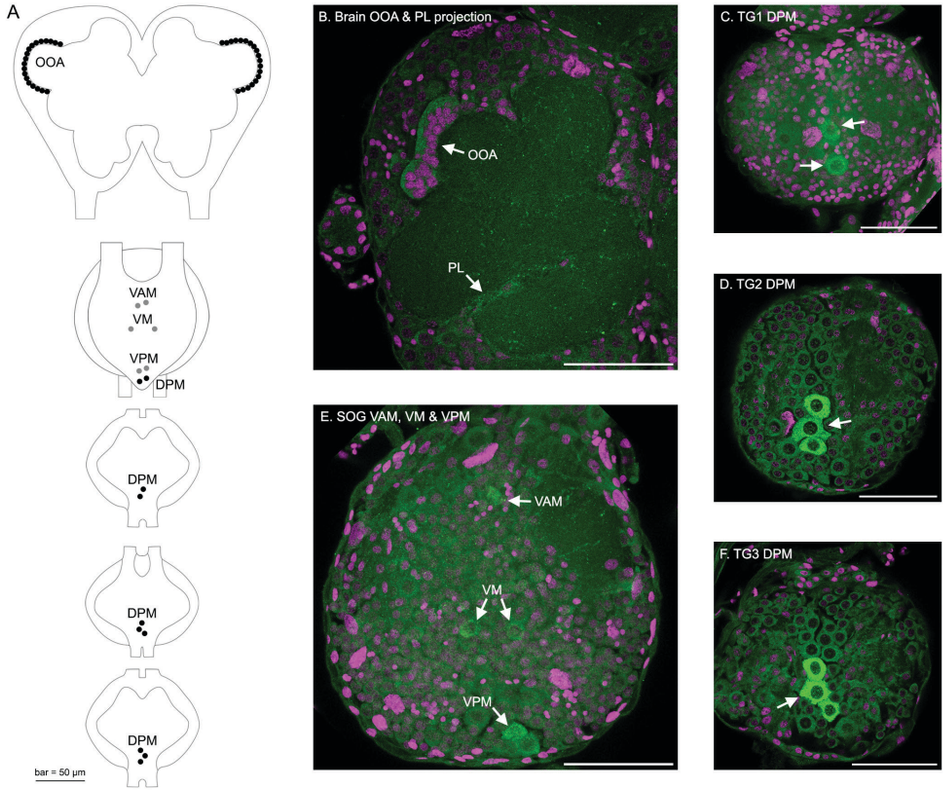

Figure 6. Octopamine (OA) immunoreactivity (IR) in *S. exigua* mid third instar caterpillars. A) overview of OA-active cell bodies and areas in the brain to the third thoracic ganglion (TG3). Grey dots for the ventral side, and black dots for the dorsal side representing the cell clusters and signal overarching the outer optical anlage (OOA). B-F) show representative CLSM images of OA-IR samples, with arrows indicating identified clusters and cells. B) the most prominent OA-IR areas; OOA and the PL projection in the brain. C) DPM clusters in TG1 (z-projection of multiple images) and D) the DPM clusters in TG2. E) the VAM, VM and VPM clusters in the SOG (z-projection of multiple images to visualise all cell bodies). F) DPM cluster in TG3. Magenta signal for the TO-PRO-3 nuclei/dsDNA staining, green channel for OA-IR. Scale-bars represent 50 µm.

3.5 TH immunoreactivity

The TH-immunoreactivity was clearly defined to single cells, cell clusters and projections. The total cell count per brain hemisphere ranged between 31-50 with a mean of 39.8 (N=10). Many clusters and single cells were identified (Dataset S5; Table 1). Described from ventral to dorsal, from anterior to posterior: the VAM cluster, single cell VAL, VAC cluster, VM single cell/cluster, VPM-1, VPM-2, single cell VPL (Figure 7). On the dorsal part, from anterior to posterior: DAM, D-CA located laterally to the calyx, DAL-1, DAL-2 single cell, D-LOC located near LOC (larval optic centre), and DPL single cell (Figure 7). The most prominent clusters (clearest signal) most often found were (ordered ventral to dorsal and by cell numbers): VAM cluster (3-10, mean 5.5, 10/10), VAC cluster (3-4, mean 3.8, 10/10), VPM-1 (4-7, 5.6, 9/10), DAM (2-6, 4, 10/10), D-CA (3-7, 4.8, 10/10), DAL-1 (3-5, 3.4, 10/10), and D-LOC (4-5, 4.2, 10/10) (Dataset S5; Table 1). The most prominent arborisations were projecting from the D-LOC in all of the samples (10/10) and in almost all of the samples for D-CA (9/10). Projections from the VAC (3/10) and DPL (6/10) were less often observed.

Table 1. Overview of TH-immunoreactive single cells and clusters per hemisphere in the brain of *S. exigua* larvae (N=10) for the ventral side and the dorsal side. Minimum and maximum cell counts are given along with the arithmetic mean for each of the single cells and clusters. Bold numbers represent the total number of cell bodies per hemisphere (minimum and maximum), along with the arithmetic mean.

TH	**Ventral**							
Cluster	VAM	VAC	VAL	VM	VPM-1	VPM-2	VPL	Unspecified
Min-max	3-10	3-4	1	1-2	4-7	1-2	1	1-5
Mean	5.5	3.8	1	1.6	5.6	1.4	1	2.5
	Dorsal							**Total**
Cluster	DAL-1	DAL-2	D-CA	DAM	DC	D-LOC	DPL	
Min-max	3-5	1	3-7	2-6	1-4	4-5	1	**31-50**
Mean	3.4	1	4.8	4	1.8	4.2	1	**39.8**

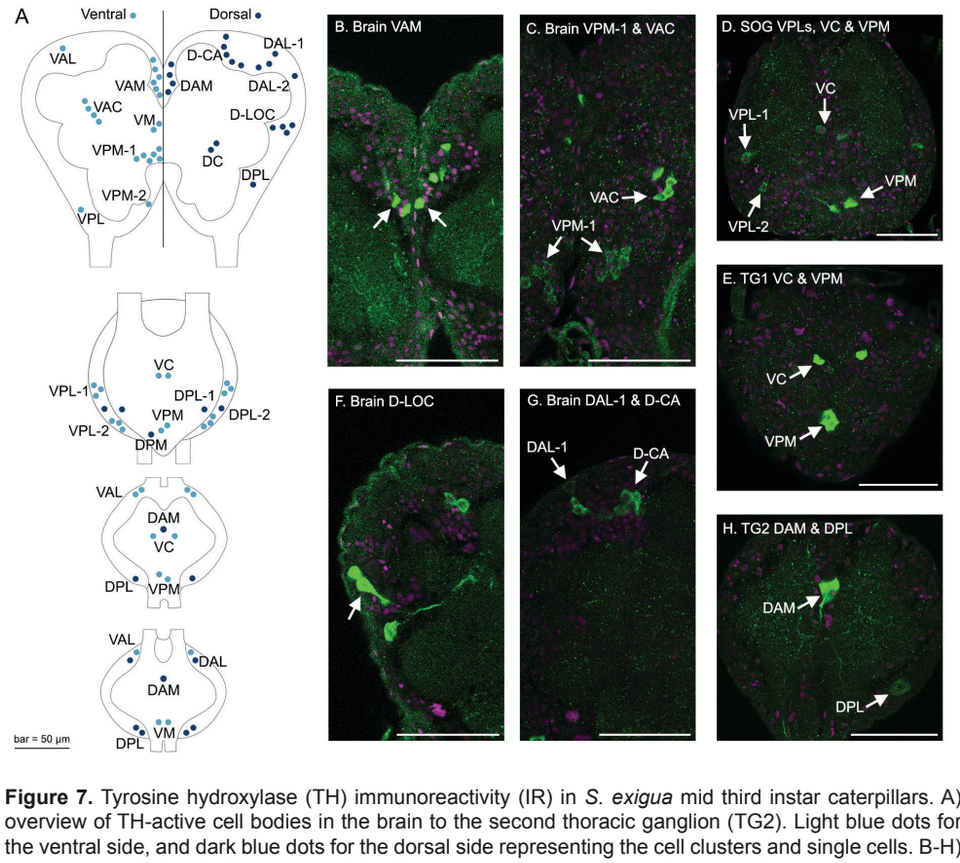

Figure 7. Tyrosine hydroxylase (TH) immunoreactivity (IR) in *S. exigua* mid third instar caterpillars. A) overview of TH-active cell bodies in the brain to the second thoracic ganglion (TG2). Light blue dots for the ventral side, and dark blue dots for the dorsal side representing the cell clusters and single cells. B-H) show representative CLSM images of TH-IR samples, with arrows indicating identified clusters and cells. B) the VAM cluster and C) the VPM-1 and VAC cluster in the brain. D) the VPL-1 and VPL-2 (VPLs), VC and VPM clusters and a clear VPM projection in the SOG. E) the VC and VPM clusters are visualised located in the TG1. F) the D-LOC with a very clear D-LOC projection and G) DAL-1 and D-CA clusters in the brain. H) the dorsally located DAM single cell with projection, and DPL in the TG2. Magenta signal for the TO-PRO-3 nuclei/dsDNA staining, green channel for TH-IR. Scalebar represents 50 µm for the overview, and the CLSM-images.

In the SOG, the single cell VPMs (also referred to as VuM (ventral unpaired medial) (Consoulas *et al.* 1999; Haverkamp and Smid 2014, or the dorsal DuM: Orchard *et al.* 1993)) are placed on both sides of the midline, asymmetrically (Figure 7D). VPM is the most clearly stained cluster in the SOG (referred to as cluster as spanning the midline), followed the VPL-1, VPL-2, the single cells DPL-1 and DPL-2. The single cells VC (4/10) and DPM (6/10) were observed in about half of the observed samples (N=10). Arborisation from the VPM is the most observed projection, followed by longitudinal tracts and lastly projections from DAL-2.

In TG1, VAL, VC, VPM and large single cell DAM were observed in all samples examined, and in many cases DPL as well (7/10) (Figure 7). DPL and the additional cells of more than one cell of the VAL were the least prominent single cells and clusters. Main projections are the tracts and arborisations from the VPM observed in all the samples, and secondarily the projection from the DAM in half of the samples (N=10).

TG2 shared to a great extend single cells and clusters with TG1 as TH-IR was observed in VAL, VM, DAL, DAM and DPL (Figure 7). The large DAM cell and the VM cluster were the most clearly stained. The VM cluster was in most cases centrally located, but in 2-3 samples it had a more posterior location, therefore it was named VM (and not VPM). The main projections are the tracts (9/10), the DAM projection (7/10) and the VM projections (1/10).

3.6 5HT immunoreactivity

The 5HT-immunoreactive signal was observed in clusters, single cells, projections and tracts in each of the investigated ganglia. The signal was clear in cells, but especially in projections when the additional dehydration and rehydration steps were added to the procedure. On the other hand, cell bodies on the surface of the SOG were observed when the additional de- and rehydration steps were not added.

The total cell count per brain hemisphere ranged between 7-21 with a mean at 13.8 (N=9) (Dataset S6; Table 2). The clusters and single cells that were stained most clearly and were the most often observed were VAM, DAM, DAL-2, DPL in nearly all samples (see Table 2). VAL-1, VAL-2, VPM and DAL-1 were observed with a lower frequency (4-5/9), and in some cases VC and VPL were observed (3/9 for both).

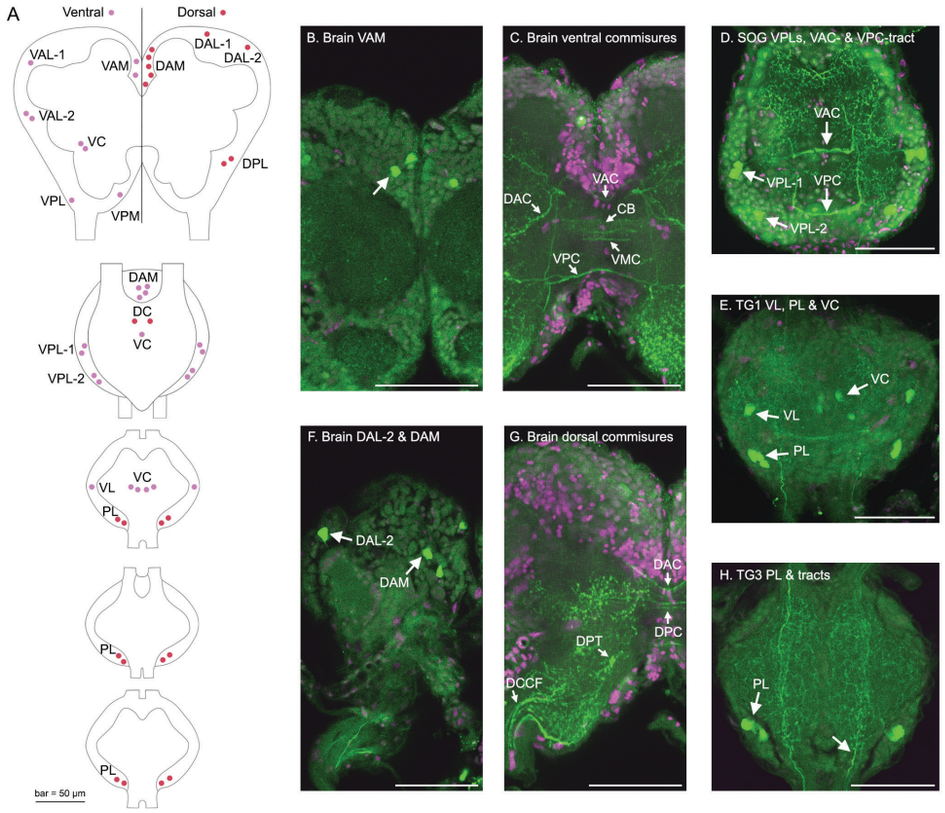

Figure 8. Serotonin (5HT) immunoreactivity (IR) in *S. exigua* mid third instar caterpillars. A) overview of 5HT-active cell bodies in the brain to the third thoracic ganglion (TG3). Pink dots for the ventral side, and red dots for the dorsal side representing the cell clusters and single cells. B-H) show representative CLSM images of 5HT-IR samples, with arrows indicating identified clusters and cells. B) the VAM cluster and C) the ventrally located commissures; VPC, VAC, CB innervation, VMC, and parts of the DAC present both ventrally and dorsally (z-projection of multiple images to visualise all) in the brain. D) the VPL-1, VPL-2 and the commissures VAC and VPC are shown in the SOG (z-project of multiple images). E) VL, PL and VC in TG1 (z-projection of multiple images). F) the dorsally located DAL-2 and DAM and G) the commissures, DCCF, DPT, DAC and DPC (z-projection of multiple images) in the brain. H) the PL and longitudinal tracts in TG3. Magenta signal for the TO-PRO-3 nuclei/dsDNA staining, green channel for 5HT-IR. Scale-bar represents 50 µm for the overview and the CLSM-images

Table 2. Overview of 5HT-immunoreactive single cells and clusters per hemisphere in the brain of *S. exigua* larvae (N=9) for the ventral side and the dorsal side. Minimum and maximum cell counts are given along with the arithmetic mean for each of the single cells and clusters. Bold numbers represent the total number of cell bodies per hemisphere (minimum and maximum), along with the arithmetic mean.

5HT	**Ventral**						**Dorsal**				**Total**
Cluster	VAM	VAL-1	VAL-2	VC	VPM	VPL	DAL-1	DAL-2	DAM	DPL	
Min-max	1-3	1-2	1-2	1-2	1-2	1	1	1	3-7	1-2	7-21
Mean	2.1	1.4	1.8	1.7	1.4	1	1	1	5.4	1.6	13.8

Seven tracts were observed in the *S. exigua* larval brain. These 7 tracts were observed in each of the analysed samples (N=9). Described from ventral to dorsal, anterior to posterior (C stands for commissure, connecting the 2 hemispheres); VAC, VMC, VPC, DAC, DPC, DPT (dorsal posterior tract), DCCF (dorsal cerebro-cervical fascicle). Along with these tracts, innervations of the CBs were observed in all the samples.

In the SOG 8-18 cells (mean 11.7) were found in total (Dataset S6). Prominently stained individual cells and clusters in the SOG were the VPL-1 and VPL-2 (both 1-2, mean 1.9), these were found in all samples examined (N=15). Furthermore, the AL (1-2, mean 1.8) cluster was observed in half of the cases (8/15), the DAM (2, mean 2) cluster was seen in 6 out of 15 samples and the single cell midline located VC and DC (1, mean 1 for both) were only observed in the samples without the additional de- and rehydration step (4/15 and 3/15 respectively). The commissures and tracts were harder to observe in the samples that did not go through the additional de- and rehydration step, but were observed in every single sample that went through these steps. The names and the proportion (combined for both treatments) were; VAC (9/15), VPC (10/15) and DMC (6/15), along with tracts running longitudinally through the ganglia (9/15).

Similarly to the SOG, the TG1 had a total cell count of the ganglia between 4-14, with a mean of 8.9 (Dataset S6) (N=11). The clusters were located differently than in the SOG and major single cells and are the VC (1-2, mean 1.6, 8/11), VL (single cell, 10/11) and PL (2-3, mean 2.3, 11/11). The VPC commissure and the longitudinal tracts were seen in all or all but one of the samples.

In comparison to the above- mentioned parts of the CNS, the 5HT-IR cells in TG2 and TG3 were located at slightly different locations. The total cell count in TG2 resulted in 4-8 5HT-IR cells, with a mean of 4.4 (Dataset S6) (N=10). The major cluster was the PL, located more in the middle, with a consistent cell count of 2. In all the samples the longitudinal tracts were observed and in most cases (6/10) the PC commissure was also observed. For TG3, less samples were analysed (N=4), but the total cell count per ganglia was consistent (4) and the locations of the cell bodies were similar to the patterns observed for TG2, with the PL cluster with a cell count of 2, and the PC commissure (3/4) and longitudinal tracts in all or all but one of the samples.

4 Discussion

The aim of our study was to target each of the four major biogenic amine (TA, OA, DA and 5HT) pathways to provide an overview of the IR in the central nervous system of third instar *S. exigua* caterpillars.

4.1 General overview of immunoreactivity in *S. exigua* larvae

It is difficult to derive the biological function of the stained cells and clusters based on their location within the CNS, we therefore rather focus on the overall cell count here. TH-IR cells and cell clusters were most abundantly present in the brain of *S. exigua*, out of the six different enzymes and biogenic amines targeted in this study (Table 1) (79.6 cells in the whole brain, min-max: 62-100), followed by 5HT-IR cells and cell clusters (27.6, 14-42) (Table 3). This is in line with previous research conducted on honeybees and ants (Harris and Woodring 1992; Cuvillier-Hot and Lenoir 2006). Furthermore, when looking at the overall cell count from brain to TG2, we observed slightly more IR cells for TDC (64.1, 38-90) than for 5HT (56.6, 34-82), which is mainly due to the VA cells that constitute between 10-24 cells in the SOG (Dataset S1). TDC-IR was found as a more dotted signal than 5HT-IR, which made the recognition of signals more difficult and this could have led to an over or under-estimation, meaning that the 5HT-IR and TDC-IR cell quantities might be similar. The TH-IR cell count for the brain to the TG2 ganglion still was the highest observed in our study (87-147 cells), with a mean of 115.6.

Table 3. Overview of cell counts for all six IR targets in third instar larvae of *S. exigua*. Cell numbers are given per ganglion for comparison. Only data where a signal could be observed from individual cells are represented in this table (e.g. excluding the OOA TA-IR and OA-IR signal). The cell counts for TG3 are indicated in grey, as it was not possible to derive TG3s from all targets, and therefore are the totals given from brain to TG2.

	TDC	**TA**	**TβH**	**OA**	**TH**	**5HT**
Brain	10 (6-14)	8.7 (6-12)	6.2 (2-12)	0	79.6 (62-100)	27.6 (14-42)
SOG	18 (6-36)	0	0	4.3 (2-7)	17.5 (13-21)	11.7 (8-18)
TG1	16.8 (12-20)	2.5 (1-3)	0	2.3 (1-4)	10.2 (7-13)	8.9 (4-14)
TG2	20.9 (14-22)	2.9 (2-3)	0	2.9 (2-3)	8.3 (5-13)	4.4 (4-8)
TG3	-	3 (3)	0	3 (3)	-	4 (4)
Total (brain to TG2 incl.)	64.1 (38-90)	14 (9-18)	6.2 (2-12)	9.1 (5-14)	115.6 (87-147)	56.6 (34-82)

For many of the targets (TDC, TA, TH, 5HT and OA to some extend), longitudinal tracts were observed. In most cases, these tracts ran from the brain (see e.g. the 5HT-DCCF, Figure 8) via the connectives between the ganglia, through the ganglia and to the next ganglion through the connectives. For visual purposes these tracts were not represented in the graphical representation (Figure 9). Another aspect that is not visualised in the graphical representation, but can be observed in the images of each of the targets (Figure 4; Figure 7; Figure 8) is the axonal- and commissure staining. TA and 5HT showed the most clearly defined axonal and commissure staining, and differences in the location were observed between them. The commissures observed with 5HT-IR (VAC, VMC, VPC, DAC and DPC) were more clearly defined than with the TA staining. However, we were still able to identify and observe some TA-IR commissures (AC, MC and PC) along with some projections in the SNP. Samples from both targets showed clear staining of the smaller axons branching into the SNP. For 5HT the most dense concentration of axonal arborisation was primarily located laterally and adjacent to the commissures and CB in the centre of the SNP, and another cluster of dense arborisation was located in the most posterior part of the SNP (Figure 8G). For TA, the major concentration of axonal signal did not have the same branching pattern as for 5HT adjacent to commissures and CB, and the two major clusters of arborisation of TA were slightly more anteriorly and posteriorly located compared to the 5HT-axonal cluster adjacent to the commissures and CB (Figure 4E).

For the SOG the biogenic amines producing cells localise more or less around three major areas, which seem to be either in the midline (DAMs, OA-VAM, OA-VM, 5HT-DC, VCs, VPMs and DPMs) and/or at a lateral location such as the most anterior part (DAMs, OA-VAM, TDC-VA and TDC-DAL), and posterior lateral part (VPL-1s, VPL-2s, DPL-1s, DPL-2s, VPMs and DPMs).

Within the signal observed for each of the different targets, overall the locations of IR cells were similar within TG1, TG2 and TG3. TG2 and TG3 are the most alike (at least based on the 5HT-IR samples and based on the TA and OA DPM cell counts), and the locations of single cells and cluster within TG1 have some similarities with the two subsequent TGs, but also have unique features. Based on the 5HT- and TA-IR cells and tracts observed in TG3 along with results from *Drosophila* larvae (Vömel and Wegener 2008; Huser *et al.* 2012), we can state that the location of IR cells in TG3 resembles that of TG2.

Figure 9. Graphical summary of all the immunoreactive (IR) areas for each of the different targets used in our study (see section 3.1-3.6) for *S. exigua* mid third instar caterpillars. Visualised are the cell bodies observed from the brain, to TG2 or TG3 depending on the exact target. Represented is the overview of TDC-IR cell bodies, TA-IR, TβH-IR, OA-IR, TH-IR and lastly 5HT-IR cell bodies. Each of the targets has its own colour scheme, the lighter tone is used for the more ventrally located cell bodies and the darker tones represent the more dorsally located cell bodies. This is done consecutively throughout. TDC (pink and purple), TA (light and darker orange), TβH (lighter and darker brown), OA (grey and black), TH (light and dark blue) and 5HT (pink and red). All overviews are scaled to size and the scalebar represents 50 µm. ›

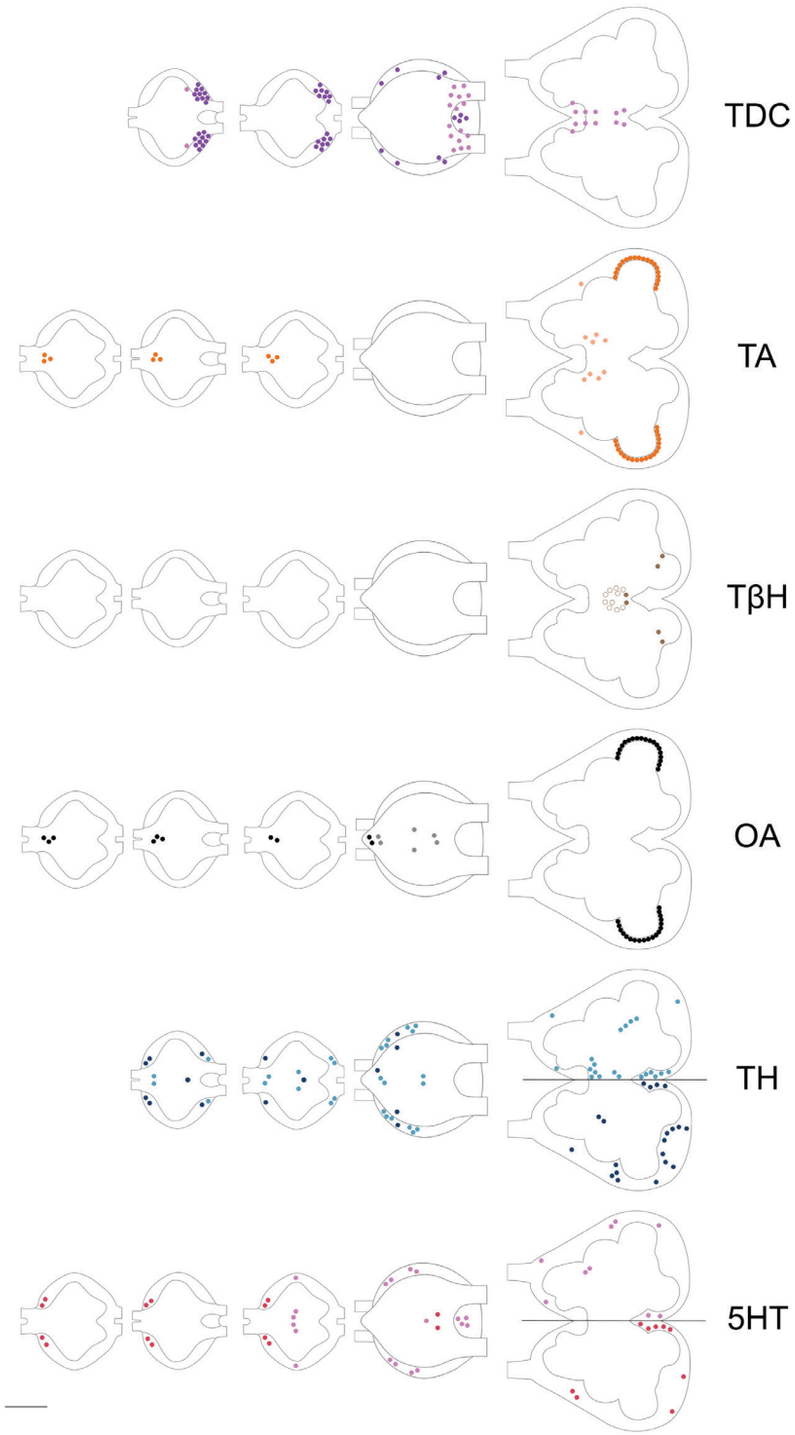

4.2 TDC, TA and OA immunoreactivity

We observed similarities and differences for the OA-IR and TA-IR signal. For both the targets the IR signal was expressed as vesicle-like structures within the neuropil area and this was even more pronounced for OA than for TA. This leads to easier observable longitudinal tracts going through SOG to TG3 for TA than for OA. For both targets the PL projections and the OOA signal were observed. Since we see this clear TA-IR and OA-IR localisation at the OOA, an imaginal disc for the development of the adult optical lobes during metamorphosis (Champlin and Truman 1998), we speculate that TA and OA play a role for halting the proliferation of the neuroblasts.

The AC, MC, PC commissures were only observed for the TA target and the VPC projection and the VMC cluster were also only observed for TA. On the other hand, the VAM, VM, VPM and DPM clusters in the SOG were only observed for OA immunostainings. The presence of three OA-clusters (anterior, mid and posterior) which we detected in the *S. exigua* SOG, were found in other more distant species as well. In adults of *Nasonia vitripennis* and *Nasonia giraulti*, three OA-IR clusters (VAM, VM and VPM) were seen in the corresponding part of the SOG (Haverkamp and Smid 2014), which is likely due to the fact that the SOG results from a fusion of three different neuromeres during development (Rehder 1989). The low number of cells found in our study in comparison to other studies (Homberg *et al.* 2013; Haverkamp and Smid 2014) results from the fact that the CNS of adult insects generally has a higher number of total cells (Levine and Truman 1982; Truman *et al.* 1994).

In our analysis we see a clear similarity of location and size of the DPM TA-IR and OA-IR clusters in TG1, TG2 and TG3. The DPM clusters account for 2-3 DPM cell bodies from TG1 to TG3, with an increasing cell count for the more caudally located ganglia (see section 3.2 and 3.4). In insects such as lepidopterans this cluster is observed on the dorsal side of the ganglia, whereas the neurons are usually found on a ventral position in hymenopterans and dipterans (Rehder 1989). Although TA is a precursor of OA, it is considered as a separate acting biogenic amine (Roeder 2005). Furthermore, TA and OA can couple to different receptors and behavioural outcomes often depend on the ratio between OA and TA (Roeder 2005; Aonuma and Watanabe 2012).

Not many studies have immunolabeled for TDC. Of the few studied that labelled for TDC, we found a similar pattern as observed for our TDC-IR cell bodies (VAM and VPM) in the brain (Figure 3A-B) with cell bodies along the midline in the fruit fly *D. melanogaster* and the desert locust, *Schistocerca gregaria* (Cole *et al.* 2005; Homberg *et al.* 2013). Furthermore, the T6 cluster (Figure 9A) reported in the study by Homberg *et al.* (2013), located an inch more posterior to the protocerebral bridge (PB), shows great similarity in location with the observed TA-IR VMC cluster in *S. exigua* (Figure 4A-B).

4.3 TβH immunoreactivity

Our detected TβH VA-cluster in *S. exigua* seems to be placed at a similar location as the far most ventral OA-cluster in the brain (Fig 3B) of the closely related caterpillar species *Trichoplusia ni* (Malutan *et al.* 2002). In an *in situ* hybridisation study only one cell body was marked (Malutan *et al.* 2002), whereas we saw mostly two. Although Malutan *et al.* (2002) also targeted TβH along with OA, we mainly saw similarities between the TβH-active areas that we found for *S. exigua* and the OA-active areas that they found for *T. ni*. Similarities can also be drawn between the locations and structure of our detected VM-cluster with a circular structured OA-cluster in *T. ni* (Figure 3A brain image) (Malutan *et al.* 2002). In adult *Trichogramma evanescens, N. vitripennis* and *N. giraulti* wasps, circular structured OA-clusters were also observed. Although, the named OA-3 cluster (*T. evanescens*) and G3 cluster (*N. vitripennis* and *N. giraulti*) were found in the middle of the brain surrounding the oesophagus (van der Woude and Smid 2017, Figure 3C; Haverkamp and Smid 2014, Figure 2A and 3A), and the detected cluster in our study is placed on the surface of the brain, the locations are relatively similar as these aspects of "surface or middle" are close to each other taking into account the transformational changes that happen during larval development and during metamorphosis.

4.4 TH immunoreactivity

In our analysis we found between 31-50 TH-IR cells per hemisphere in the brain of *S. exigua*, with a mean of 39.8 cells and an average around 80 per brain. This is similar to the number of DA-IR cells described for others insect larvae or miniaturised parasitic wasp species such as 30 and 4 unpaired cells per hemisphere (64 per brain) in adult *T. evanescens* wasps (van der Woude and Smid 2017), or about 90 TH-IR cells per brain in third instar larvae of *Drosophila* (Selcho *et al.* 2009) (Table 4). However, the above examples for comparison are some of the lowest found. The number of cells in the fly larvae are the most comparable to those in the *S. exigua* larvae, possibly because both concern larval stages of holometabolous insects, whereas other studies have observed higher cell numbers for adult stages, including a range of 200-450 for crickets, 127 (mean of TH-GAL4 positive) to 282 (TH positive) for adult *Drosophila* and 800-900 for *Apis mellifera* (Hörner *et al.* 1995; Mao and Davis 2009; Tedjakumala *et al.* 2017). Due to the miniaturised body size of *T. evanescens*, the cell count was also rather low and differed from other adult wasps (van der Woude and Smid 2017). Comparing our results with hemimetabolous insects such as crickets is valuable as these insects will have approximately the same amount of IR cells throughout their life. Regarding total count of TH active cells in our study for SOG-TG2, these are comparable to the ones described for *G. bimaculatus* (Table 4; Hörner *et al.* 1995).

Table 4. Overview of TH and DA-immunoreactive cells in our study compared to other studies. Cell numbers are given per whole ganglia for comparison. *Spodoptera exigua*: our present study, *T. evanescens*: van der Woude and Smid 2017, *Drosophila* larvae: Selcho *et al.* 2009, *G. bimaculatus*: Hörner *et al.* 1995 (*unclarity about number of samples, 54 TH + 15 DA = 69). N: sample number.

TH	Brain				SOG		TG1		TG2	
Species	*S. exigua*	*T. evanescens*	*Drosophila larvae*	*G. bimaculatus*	*S. exigua*	*G. bimaculatus*	*S. exigua*	*G. bimaculatus*	*S. exigua*	*G. bimaculatus*
Min-max	62-100			180-210	13-21	10-28	7-13	4-10	5-13	2-8
Mean	79.6	64	90	~ 200	17.5	13.3	10.2	6.8	8.3	3.5
N	10	30	6	*	10	*	10	*	10	*

TH-IR cells can be identified in similar locations in other species for DA-immunostaining in the brain and SOG. For example in the brain, the D-CA is at a lateral location and proximate to the calyx, similar to the DA-5a and – 5b, and the VPM-1 or VPM-2 are similar to the DA-3 with a location posterior to the antennal centre (LAC for larvae or AL for adults) as described for *T. evanescens* (van der Woude and Smid 2017). Also, similarities were seen in the SOG between our observed DPM and the DA-4 in *T. evanescens* (van der Woude and Smid 2017), due to their posterior location and their location in the midline, and between our described DPLs and VPLs and the DA-7 in *T. evanescens* (van der Woude and Smid 2017). The TH-projections such as D-LOC and D-CA (section 3.5; Figure 7F) innervating the respective neuropils could point at a role of TH (or indirectly DA) in the integration of sensory information and in associative learning (Tedjakumala *et al.* 2017).

4.5 5HT immunoreactivity

In our analysis we found between 14-42 5HT-IR cells in the brain of *S. exigua*, with a mean of 27.6 cells (Dataset S6; Table 2). The projections described in the brain, such as the innervations of the CB, VAC, VPC, DAC, show a high similarity to those described in other studies for other insect larvae and for related caterpillar species (Mukhopadhyay and Campos 1995; Tang *et al.* 2019). For the SOG, we found between 8-18 5HT-IR cells, with a mean of 11.7 (Dataset S6; Table 5). The quantities of the 5HT-IR cells counted in the brain are similar to those counted for other species, and the IR cell count in the SOG is also similar, although a bit lower. These other species concerned miniaturised adult *T. evanescens* (brain: 76, van der Woude and Smid 2017), larvae of the fly species *Calliphora erythrocephala* (brain: 60, SOG: 22) and *Sarcophaga bullata* (brain: 64, SOG: 22) (both Nässel and Cantera 1985), *M. sexta* larvae (brain: 36-40, SOG: 20; Granger *et al.* 1989 and Griss 1989, respectively), and lastly the closely related *S. frugiperda* larvae (brain: around 40, SOG: around 24; Zhang *et al.* 2022).

Table 5. Overview of 5HT immunoreactive cells in our study compared to other studies, all on insect larvae. Cell numbers are given per whole ganglion for comparison. *S. exigua*: our present study, *H. armigera*: Tang *et al.* 2019, *Drosophila* larvae: Huser *et al.* 2012. N: sample number.

5HT	Brain			SOG			TG1		TG2		TG3	
Species	*S. exigua*	*H. armigera*	*Drosophila*	*S. exigua*	*H. armigera*	*Drosophila*	*S. exigua*	*Drosophila*	*S. exigua*	*Drosophila*	*S. exigua*	*Drosophila*
Min-max	14-42	36-39	21 ± 2,2	8-18	17-22	32 ± 6,2	4-14	6 ± 0	4-8	4 ± 0	4	4 ± 0
Mean	27.6	37		11.7	20		8.9		4.4		4	
N	9	7	10	9	7	10	11	10	10	10	4	10

The single cells and clusters we described in our research are comparable to those found in many other studies. For example, the DAM and VAM are comparable to the PM cluster in fifth instar *M. sexta* and the commissures, DAL-2 and VAL-1 are comparable with the PDL cluster in the same species Granger *et al.* 1989. Similarly, our DAM and VAM are comparable with PR-M, our DAL-2 with PR-L, and our VAL-1 with PR-LD along with the commissures in *H. armigera* larvae (Tang *et al.* 2019).

The 5HT-IR cells localised in the SOG share a high similarity with the clusters reported for the closely related species *M. sexta*, *H. armigera* and *S. frugiperda* (Griss 1989; Tang *et al.* 2019; Zhang *et al.* 2022). In our findings for *S. exigua* compared to *H. armigera,* the AL resembles the GNG-L1, VPL-1 has resemblance in localisation with GNG-L2, our VPL-2 has resemblance with the GNG-L3, DAM resembles the location of GNG-AD and even the less frequently found VC cluster from our study resembles GNG-AV (Tang *et al.* 2019). For all the cell bodies observed in our study, the 5HT-IR cell counts match with the cell counts in the above mentioned studies (except for DC). In *S. exigua* as well as *H. armigera*, three commissures were described (Tang *et al.* 2019).

The pattern of lateral mirrored clusters often in groups of two cells seen in TG1 to TG3, in our study mainly positioned posterior (PL) in either of the ganglia (in some cases anterior; AL), have been observed in other insect larvae as well, such as the T1, T2 and T3 described in *Drosophila,* with very similar cell counts (Table 5) (Vallés and White 1988; Vömel and Wegener 2008; Huser *et al.* 2012).

Conclusion

We managed to successfully stain and identify cells, cell clusters, projections, commissures and tracts for the brain, SOG, TG1, TG2 and TG3 for third instar *S. exigua* caterpillars, with average cell counts ranging from 6.2 for TβH-IR to 115.6 for TH-IR. The cell counts of single cells and clusters along with identifications of projections, commissures and tracts revealed similarities between some of the targets. On the contrary, our results also show a great diversity between biogenic amines, the rate limiting enzymes thereof, and to some extend even between the signal of the target biogenic amine and the rate limiting enzyme leading to it. Further studies could immunolabel directly against DA and TPH to obtain a complete overview. We observed the highest counts of cells for TH, followed by TDC and 5HT. 5HT-IR had the most and the most clearly defined commissures and projections, and TA-IR in commissures and axons were also very well defined. Our study presents a comprehensive overview of biogenic amine-related IR signals in a larval insect, which will further increase our understanding of the evolution and development of the CNS in a comparative context.

Acknowledgements

We thank Els Roode and Dorothy van Leeuwen for maintaining the general rearing of the *S. exigua* population. We would also like to thank Steffi van de Wouw, for initial optimisation of the protocol for TH-immunostaining in *S. exigua*.

Funding

This work was supported by the Dutch Research council (NWO) (grant number: ALWOP.362). V.I.D.R. is supported by an NWO VIDI-grant (VI.Vidi.192.041).

Data accessibility

Analyses reported in this article can be reproduced using the data provided by:
Gasque et al 2023_S1_TDC
Gasque et al 2023_S2_TA
Gasque et al 2023_S3_TBH
Gasque et al 2023_S4_OA
Gasque et al 2023_S5_TH
Gasque et al 2023_S6_5HT

The more I learn, the more I realise how much I do not know.

Isaac Newton
and Albert Einstein

CHAPTER 5

Baculovirus entry into the central nervous system of *Spodoptera exigua* caterpillars is independent of the viral protein tyrosine phosphatase

Simone N. Gasque[1], Yue Han[1], Iris van der Ham[1], Dorothy van Leeuwen[1], Monique M. van Oers[1], Alexander Haverkamp[2], and Vera I.D. Ros[1]

[1]Laboratory of Virology, Wageningen University and Research, Droevendaalsesteeg 1, 6708 PB Wageningen, The Netherlands
[2] Laboratory of Entomology, Wageningen University and Research, Droevendaalsesteeg 1, 6708 PB Wageningen, The Netherlands

Published as:
Gasque SN, Han Y, van der Ham I, van Leeuwen D, van Oers MM, Haverkamp A, Ros VID. 2024. Baculovirus entry into the central nervous system of *Spodoptera exigua* caterpillars is independent of the viral protein tyrosine phosphatase. Open Biol. 13: 230278. doi: 10.1098/rsob.230278.

Abstract

Neuroparasitism concerns the hostile take-over of a host's nervous system by a foreign invader, in order to alter the behaviour of the host in favour of the parasite. One of the most remarkable cases of parasite-induced host behavioural manipulation comprises the changes baculoviruses induce in their caterpillar hosts. Baculoviruses may manipulate caterpillar behaviour in two ways: hyperactivity (increased movement in the horizontal plane) and/or tree-top disease (movement to elevated levels in the vertical plane). Those behavioural changes are followed by liquefaction and death of the caterpillar. In Autographa californica multiple nucleopolyhedrovirus (AcMNPV)-infected *Spodoptera exigua* caterpillars, an enzymatic active form of the virus-encoded protein tyrosine phosphatase (PTP) is needed for the expression of hyperactivity from 3 days post infection (dpi). Using eGFP-expressing recombinant AcMNPV strains we show that infection of the caterpillar's central nervous system (CNS) can be observed primarily from 3 dpi onwards. In addition, we demonstrate that the structural and enzymatic function of PTP does not play a role in infection of the CNS. Instead, we show that the virus entered the CNS via the trachea, progressing caudally to frontally through the CNS and that the infection progressed from the outermost cell layers towards the inner cell layers of the CNS, in a PTP independent manner. These findings help to further understand parasitic manipulation and the mechanisms by which neuroparasites infect the host nervous system to manipulate host behaviour.

1 Introduction

Many parasites and pathogens modify the behaviour of their host to increase transmission (Bethel and Holmes 1973; Helluy 1984; Lafferty and Morris 1996; Berdoy *et al.* 2000; Thomas *et al.* 2002; Andersen *et al.* 2009; Dheilly *et al.* 2015; Małagocka *et al.* 2017; Naundrup *et al.* 2022; Gasque and Fredensborg 2023). A textbook example of behavioural alteration is the one expressed by baculovirus-infected caterpillars (lepidopteran larvae) (Hoover *et al.* 2011; Gasque *et al.* 2019). Baculoviruses have a circular double-stranded genome (81-178 kilo base pairs) that is encompassed in enveloped, rod shaped nucleocapsids (Williams *et al.* 2017a; Ros 2021). Nucleocapsids are packaged into two types of virions; budded virions (BVs) which are responsible for cell-to-cell infections and occlusion-derived virions (ODVs) enclosed in occlusion bodies (OBs) which are needed for host to-host infection (Harrison and Hoover 2012; Blissard and Theilmann 2018). Baculoviruses trigger two forms of parasite-induced behavioural alteration in caterpillars: hyperactivity and tree-top disease (Vasconcelos *et al.* 1996; Goulson 1997; van Houte *et al.* 2014a; Ros *et al.* 2015; Gasque *et al.* 2019). The two behavioural alterations are expressed after the oral infection of caterpillars through virus-contaminated vegetation that the caterpillars feed on and are observed as an increased movement either in the horizontal plane (hyperactivity) or in the vertical plane (tree-top disease). Soon after, the caterpillars liquefy and die. Tree-top disease is argued to be one of the first known cases of parasite-induced behavioural alteration, as it was already reported in 1891 (Goulson 1997).

Although the underlying mechanisms behind behavioural inductions due to parasite/pathogen infections have scarcely been elucidated (Mangold and Hughes 2021), it was within the field of baculoviruses that a parasite gene responsible for an expressed host behaviour was identified for the first time (Kamita *et al.* 2005). Viral protein tyrosine phosphatase (*ptp*) was the factor behind the offset of hyperactivity from 3.75 - 4.75 days post infection (dpi) for Bombyx mori nucleopolyhedrovirus (BmNPV)-infected *Bombyx mori* neonate caterpillars (Kamita *et al.* 2005). Since then, *ptp* has been shown to be involved in the expression of hyperactivity in a few other baculovirus-caterpillar systems (Gasque *et al.* 2019), including Autographa californica multiple nucleopolyhedrovirus (AcMNPV) in caterpillars of the beet armyworm *Spodoptera exigua* (van Houte *et al.* 2012). More specifically, the gene encoding PTP or homologues thereof is found within alphabaculoviruses in the clade termed group I NPVs, and PTP-induced hyperactivity seems a conserved mechanism for this clade (Jehle *et al.* 2006; van Houte *et al.* 2012). PTPs form a large family of enzymes defined by the active-site signature motif HCX5R, where the nucleophile cysteine residue is essential for the catalysis (Takagi *et al.* 1998; Zhang 2002; Tonks 2006). PTPs from baculoviruses belong to the dual-specific PTPs (DUSPs), which can dephosphorylyse phosphotyrosine (pTyr), as well as phosphoserine (pSer) and phosphothreonine (pThr) residues, in contrast to the classical PTPs where pTyr is the only substrate (Zhang 2002; Provost *et al.* 2004; Tonks 2006). Furthermore, PTP encoded by AcMNPV is even more effective as an RNA 5'-triphosphatase (RNA capping enzyme), which classifies it as part of the dual specificity protein phosphatase 11 (DUSP11) subfamily, similar in function to the human PIR1 (Sheng and Chardonneau 1993; Ayres *et al.* 1994; Gross and Shuman 1998; Takagi *et al.* 1998; Tonks 2006; Lu *et al.* 2020; NCBI reference domain: cd17665).

Within baculoviruses, two *ptp* genes are known, *ptp* and *ptp2*, that are phylogenetically unrelated and have low protein similarity, but belong to the same PTP protein family (van Houte *et al.* 2012). While *ptp* is important in behavioural manipulation and is present in all group I NPVs, *ptp2* plays a role in the induction of apoptosis and is present in some but not all baculoviruses (Han *et al.* 2018b). The baculovirus AcMNPV (belonging to group I NPVs of the alphabaculoviruses) encodes for only one PTP (Ayres *et al.* 1994; van Houte *et al.* 2012). The baculoviral *ptp* gene very likely derived from the genome of an ancestral lepidopteran host, and was presumably only incorporated in an ancestral baculoviral genome once, wherefrom it afterwards spread within group I NPVs (van Houte *et al.* 2012).

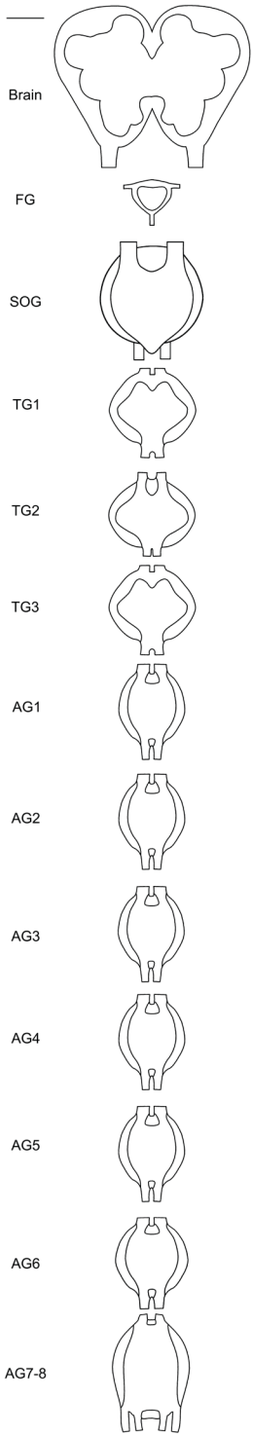

The role of PTP in the expression of hyperactivity in caterpillars seems to be dependent on the virus-host combination. *B. mori* fifth instar caterpillars infected with a mutant BmNPV, which expressed solely the structural properties and not the enzymatic function of PTP, displayed hyperactivity (Katsuma *et al.* 2012). In AcMNPV-infected third instar *S. exigua* caterpillars, in contrast, the enzymatic activity was pivotal for the display of hyperactivity at 3 dpi (van Houte *et al.* 2012). Furthermore, based on the reduced viral propagation in brain tissues after *ptp*-deletion from the BmNPV genome, Katsuma *et al.* (2012) hypothesised that PTP aids in the infection of brain tissues, which would have a direct influence on the expression of hyperactivity. As previous studies have shown the presence of baculoviruses in the host CNS (Knebel-Mörsdorf *et al.* 1996; Herz *et al.* 2003; Torquato *et al.* 2006; Katsuma *et al.* 2012), the modulation of the CNS by baculoviruses forms a needed target of research within this case of baculoviral-induced behavioural changes and more generally in the field of neuroparasitology (Hughes and Libersat 2018). For caterpillars the CNS is organised in different ganglia. Cranially to caudally the CNS starts with the supraoesophageal ganglion (brain) connected to both the much smaller frontal ganglion (which is placed acutely caudally to the brain) and the suboesophageal ganglion (SOG), the latter by the circumoesophageal connectives. The SOG is followed by the first to third thoracic ganglia, and subsequently 7 abdominal ganglia (Chapman 2013) (Figure 1).

Figure 1. Schematic overview of the central nervous system of a mid third instar *S. exigua* caterpillar, consisting of the supraoesophageal ganglion (brain), followed by the suboesophageal ganglion (SOG), 3 thoracic ganglia (TG1 to TG3), and 7 abdominal ganglia (AG1 to AG7-8; abdominal ganglia 7 and 8 are fused). Each ganglion is connected to the adjacent ganglion by two connectives (not fully depicted). The much smaller frontal ganglion (FG) is connected to the brain which it is placed acutely caudally to. Scalebar (top left) represents 50 µm.

Here, we test whether wildtype (WT) AcMNPV can infect the CNS of *S. exigua*, and when and where the virus is visible in the ganglia, and whether it is present on a superficial or internal level. Additionally, we investigate the route of infection by analysing the different ganglia during the course of infection. Moreover, we test whether PTP plays a role in CNS entry by comparing infections by WT AcMNPV and mutant AcMNPV strains either lacking *ptp*, containing a *ptp* gene with an inactivated catalytic site, or where the *ptp* gene deletion has been repaired, respectively. Lastly, we analyse whether any of these strains shows detectable differences in infection patterns for the different ganglia of the CNS. We found that AcMNPV seems to infect the CNS through the trachea and based on the infection levels over time of the different ganglia, the infection progress caudally to frontally. Furthermore, all recombinant viruses tested here could infect *S. exigua* and the CNS, providing further insights into the mechanisms by which baculoviruses can highjack the host's nervous system and express their extended phenotype.

2 Materials and methods

2.1 Insect larvae and cells

Spodoptera exigua larvae (originally derived from Andermatt Biocontrol (Switzerland) in 2014) were reared under a 14h : 10h light : dark photoperiod at 25.5°C and 50% relative humidity on artificial diet (primarily consisting of polenta, wheat germ and yeast) (Simon *et al.* 2021). Disposable plastic trays covered with paper tissue and a lid were used as rearing containers for groups of 50 (smaller instars) to maximum 35 (larger instars) larvae. Late fifth instars were transferred to a plastic tray containing vermiculite to facilitate pupation. Pupae were collected and transferred to cylindrical containers lined with paper sheets for egg deposition, with around 70 pupae per container. Adult moths were provided with water. Collected eggs were surface sterilised using 10% formaldehyde vapor and subsequently put at 28°C until hatching, after which larvae were transferred to 25.5°C.

The *Spodoptera frugiperda* derived cell line Sf9 was cultured as a monolayer in SF900II medium supplemented with 5% fetal bovine serum (FBS) and 50 µg/ml gentamycin (all from Invitrogen) for the subsequent transfection with all recombinant bacmids (section 2.3), except for the AcMNPV Δ*ptp* bacmid (see below), which was transfected into cells cultured in Gibco™ Sf-900™ II serum free medium (Life technologies, Fisher Inv.) and 50 µg/ml gentamycin.

2.2 Generation of recombinant bacmids

The AcMNPV-eGFP:VP39 (WT-eGFP) construct (Mu *et al.* 2014) was used as wildtype (WT) in this study. This construct originates from the WT AcMNPV E2 bacmid (Smith

and Summers 1979; Luckow *et al.* 1993) and contains a fused open reading frame (ORF) for enhanced GFP (eGFP) followed by the coding sequence for the AcMNPV major capsid protein (VP39) under control of the *p10* promotor (Figure 2). The polyhedrin (*polh*) ORF is present downstream of the *polh* promotor. The fusion of eGFP to the N-terminus of VP39 allows subsequent visualisation of the viral nucleocapsids and was shown not to affect viral infectivity, at least in cell culture (Mu *et al.* 2014). In this construct, the original non-fused *vp39* gene is also present, at its normal locus.

In a similar way, a recombinant bacmid carrying the *egfp-vp39* fusion ORF was created using as basis a bacmid from which the *ptp* gene was removed (Figure 2). Here nucleotide positions 509 to 1080 in the AcMNPV E2 bacmid, spanning the complete 507 nucleotides of the *ptp* ORF, were replaced with a zeocin resistance marker gene (Li and Guarino 2008; van Houte *et al.* 2012). The *polh-egfp*:*vp39* expression cassette was transposed from a pFastBacDual construct (Mu *et al.* 2014) into the AcMNPV Δ*ptp* bacmid to generate the recombinant bacmid AcMNPV Δ*ptp*-eGFP:VP39 bacmid (hereafter called AcMNPV Δ*ptp*-eGFP).

To ensure that a potential phenotype after infection with AcMNPV Δ*ptp*-eGFP was not an expression of any additional genomic mutations when deleting the *ptp ORF*, a repair bacmid in which the *ptp* ORF was placed back was created (AcMNPV *ptp* repair). In addition, a recombinant bacmid encoding a catalytically inactive PTP protein (AcMNPV catmut) was created, to test whether the enzymatic activity of PTP is required for entry into the CNS. The catmut has a mutation in the HC signature motif where the Cys-119 residue was replaced with an alanine (C119A) (van Houte *et al.* 2012). The *ptp* ORFs (repair and catmut) were accompanied by an upstream hr1 repeat motif, known to enhance the expression of downstream genes (Blissard 1996; van Houte *et al.* 2012). The two "repair" bacmids were made using the MultiBac Expression system (Berger *et al.* 2004) (Geneva Biotech, Switzerland), as it allows for more than two gene inserts into the *polh* locus of a single bacmid. Both constructs were made starting from the AcMNPV Δ*ptp* bacmid mentioned above (Li and Guarino 2008). First the *polh* ORF was amplified with primers 1 and 2 (Table S1) providing XbaI and PstI sites, respectively, for cloning into the pACEBac1 acceptor vector downstream of its inherent *polh* promoter. The egfp:vp39 fusion mentioned above was amplified with primers 3 and 4 providing XhoI and NcoI sites for cloning behind a *p10* promoter in the pIDK donor vector, while the *ptp* or the *ptp-catmut* ORFs and the upstream *ptp* promotor and hr1 repeat region (as in van Houte *et al.* 2012) were amplified with primers 5 and 6 (Table S1) providing SpeI and NsiI sites, respectively, for cloning into pIDS donor vectors. All amplified fragments were first cloned into pJET 1.2 (Thermo Fischer) and verified by sequence analysis before recloning in the respective acceptor or donor vectors. The pACEbac1-*polh* acceptor vector was fused with the pDK1-egfp:vp39 donor vector by Cre-LoxP recombination (Berger *et al.* 2004). The resulting new acceptor vector was subsequently fused with the pIDS-ptp/catmut donor vector, also via Cre-LoxP recombination. The final transfer vector was used to transform DH10β ΔTN7 cells (Airenne *et al.* 2003) carrying the AcMNPV Δ*ptp* bacmid leading to transposition of the multigene expression cassette into the mini Tn7 acceptor site at the *polh* locus.

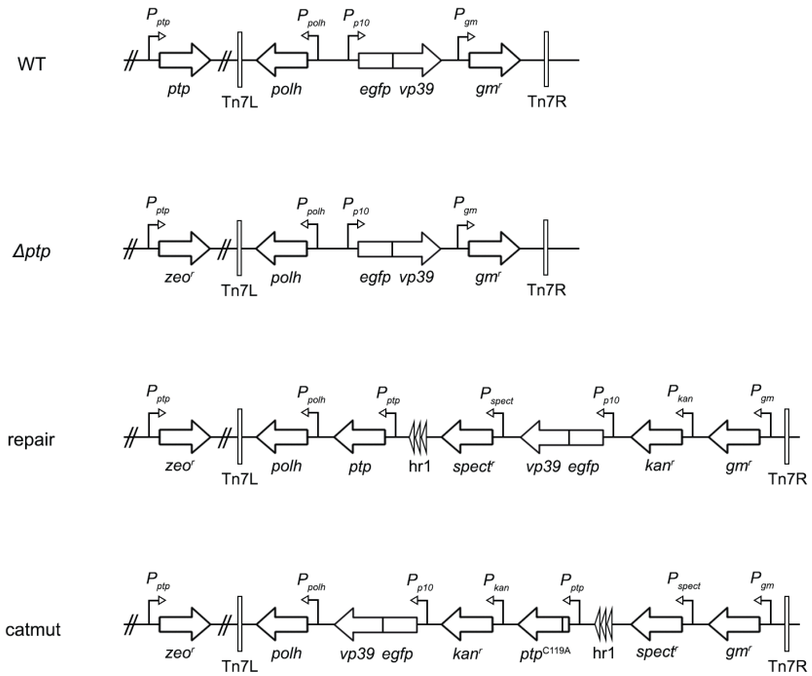

Figure 2. Overview of the modified parts of the recombinant AcMNPV viruses used in this study, including AcMNPV WT-eGFP (WT), AcMNPV Δ*ptp*-eGFP (Δ*ptp*) where *ptp* was replaced by a Zeocin resistance gene (zeor), AcMNPV with *ptp* inserted back into the genome after deletion (repair) and AcMNPV encoding for a catalytic inactive PTP (catmut with the Cys-119 residue replaced with an alanine, C119A)). For all viruses, the polyhedrin (*polh*) gene and the fused *egfp-vp39* genes were inserted between the left and right insertion sites (Tn7L and Tn7R) present in the bacmids. For AcMNPV repair and AcMNPV catmut, the *ptp* gene was inserted with the upstream hr1 repeat region. Antibiotic resistance genes inserted during the different cloning steps (Berger *et al.* 2004) include the gentamicin (gmr), spectinomycin (spectr) and kanamycin (kanr) resistance genes.

2.3 Amplification and purification of virus

An existing OB stock of AcMNPV WT-eGFP (Mu *et al.* 2014) was amplified by oral infection (as described in section 2.4) of early third instar larvae. A fluorescent signal in larvae was visually verified at 3 days post transfection using an UV-lamp under the stereomicroscope (Leica; Wild M3Z and HBO lamp). Liquefied larvae were collected and OBs were isolated by filtration over cheese cloth (van Houte *et al.* 2012).

To obtain a virus stock of AcMNPV Δ*ptp*-eGFP, Sf9 cells were transfected with the bacmid and subsequently OBs were harvested and fed to *S. exigua* larvae. To that aim, the recombinant bacmid AcMNPV Δ*ptp*-eGFP was mixed with ExpreS2-TR Transfection reagent (Expres2ion) and transfected into Sf9 cells cultured in Gibco™ Sf-900™ II serum free medium with 50 µg/ml gentamycin. A fluorescent signal was visible after 3 days post transfection and at 7 days post transfection, OBs were harvested by centrifugation (5 min at 3000 rpm). The pellet, containing the OBs and cell debris, was stored at 4°C and later fed to third instar larvae by droplet feeding (as described in section 2.4). At 6 dpi, OBs were isolated from liquefied larvae by filtration over cheese cloth as described before (van Houte *et al.* 2012).

To obtain OB stocks of AcMNPV repair and AcMNPV catmut, Sf9 cells were transfected with the bacmids as described above, using Lipofectin Reagent (Invitrogen, Fisher Inv.). At 7 days post transfection, BVs were harvested by centrifugation (10 min at 4100 rpm) and supernatant, containing the BVs, was stored at 4°C until intra-haemocoel injection into fourth instar larvae. At 4 dpi, liquefied larvae were collected and OBs were isolated by filtration over cheese cloth (van Houte *et al.* 2012). The concentration of OBs in all stocks was estimated through counting in a haemocytometer (Thoma cytometer).

2.4 Oral infectivity assay

Late first and late second instar *S. exigua* larvae were starved overnight at 25.5°C, to secure ingestion of control (mock) or viral solutions the subsequent morning when the larvae had moulted into early second or early third instars, respectively. The treatments used for infections consisted of a mock 10% (w/v) sucrose solution laced with Patent Blue (Fluka Chemie GmbH), or viral stocks made in the same sucrose/pattern blue mix, where OBs of the 4 viral constructs were diluted to a 108 OBs/ml concentration, known to kill ~90-100% of the larvae (van Houte *et al.* 2012; Mu *et al.* 2014) (corresponding to a >LC95, S.N. Gasque unpublished results). A maximum of 30 larvae were placed in a 9 cm diameter petri dish. The mock and OB suspensions were vortexed and 200 µl was offered as a circle of droplets around the larvae. Larvae were left to feed for a maximum of 15 minutes. The individuals that had ingested the solution (showing a clear blue gut), were placed individually in the wells of a 12-wells plate, each well containing a 8x8x8 mm feed block of artificial diet. Plates were covered by a piece of parafilm, a folded paper towel and the plate lid. Larvae were kept at 27°C until dissections at 1 to 7 dpi. Prior to dissection, eGFP expression was checked under an UV-lamp seen through a stereomicroscope, to ensure proper infection. Only virus-infected larvae expressing eGFP were selected, except for samples taken at 1 dpi where larvae were picked randomly, since eGFP expression was not yet detectable at this timepoint.

2.5 Dissections

Larvae were immobilised by placement on ice. One cold-immobilised larva at the time was decapitated with a sharp sterile scalpel at the second leg pair. Thereby the remaining sample included the head capsule and the pro- and mesothorax. This sample was moved to freshly made 4% PFA (4% paraformaldehyde (Merck) in 0.1 M phosphate buffer, pH 7.2) fixative in a dissection dish and placed under a light microscope (Leica Wild M3Z). The CNS was dissected out with sharpened forceps (Dumont No 5), by first making a rupture on the ventral side of the larvae, removing excess tissue and carefully tearing the oesophagus to facilitate intact circumoesophageal connectives and thereby connected ganglia. Sometimes tearing the oesophagus led to loss of the frontal ganglia and/or no connection between brains and SOGs. Each dissected CNS was carefully moved into fixative in Eppendorf tubes placed on ice, by grasping onto non-essential structures (such as remains of the trachea or connectives after the final attached ganglion), until the desired sample size was reached. The general outline of the fixation protocol has been described earlier (van der Woude and Smid 2017), and was optimised for *S. exigua*.

2.6 Visualisation

For the time course of infection and different ganglia

Dissections were done for 7 consecutive days (1 dpi to 7 dpi). After the overnight fixation step in 4% PFA and 3 subsequent washing steps with phosphate buffered saline (PBS, Oxoid, Dulbecco 'A' tablets), the samples dissected (N=173 larvae) on the first 6 consecutive sampling days were stored in 1% sodium acid (10% in Milli-Q water) in PBS – to prevent fungus growth – until all the dissected CNSs were ready to be taken through the subsequent protocol steps simultaneously. For the 1-6 dpi samples, the washings continued at day 8 with 2 more washings (a total of 6 washings with PBS). The 7 dpi samples were fixed overnight and then washed 6 times (no sodium acid added). To increase permeability of the neural tissue, the samples were incubated in 0.5 mg/ml collagenase (Sigma Aldrich) in PBS for 1 hour at room temperature (RT), to digest the neurolemma. This was followed by 3 washings with PBS-T (0.5% Triton-X) and incubated overnight at 4°C of TO-PRO-3 1:500 to label nuclei, in a 10% normal goat serum in PBS-T (PBS-T-NGS). The subsequent day the counterstain was washed away over 2 hours by 3 washings of PBS-T, and over 2 hours of 3 washings with PBS. The samples were dehydrated 2 minutes each in a series of 50%, 70%, 90%, 96%, 100%, 100% and then cleared by 50% xylene/50% ethanol, 100% xylene and lastly mounted in DPX on microscope slides. Due to the sample multiplicity (173 CNSs) the samples were stored in PBS until they were dehydrated, cleared in xylene and mounted in distyrene plasticiser xylene mixture (DPX, Merck) on one of 3 consecutive days.

For the protein tyrosine phosphatase CNS entry
CNSs for this experiment were dissected in the manner previously mentioned at 4 dpi using freshly made 4% PFA fixative and moved to Eppendorf tubes placed on ice, until the desired sample size was reached and fixed at RT for 2 hours. Six washing steps with PBS (3 quickly and following 3 in total of 1 hour) or one overnight step at 4°C were used to wash off the fixative. Then all samples were incubated simultaneously in 0.5 mg/ml collagenase (Sigma Aldrich) in PBS for 1 hour at RT. Subsequently washing away the collagenase in PBS-T (4 x 10 min), followed by a counterstaining step at 4°C overnight of TO-PRO-3 1:500 to label nuclei in PBS-T-NGS. The following day the samples were rinsed using several changes of PBS-T in a duration of 2 hours and subsequently washed in PBS 4 times during 2 hours. The samples were dehydrated 2 minutes each in a series of 50%, 70%, 90%, 96%, 100%, 100% and then cleared by 50% xylene/50% ethanol, 100% xylene and lastly mounted in DPX on microscope slides.

2.7 Image acquisition and scoring of infection

Confocal laser scanning microscopy and imaging
For image acquisition, a Zeiss LSM 510 confocal laser scanning microscope (CLSM version 3.2 sp2) and a Leica Stellaris 5 CLSM were used. The LSM 510 was equipped with a 458/488-nm argon laser was used to visualise Alexa Fluor 488, and a 633-nm HeNe laser that was used to visualise TO-PRO-3. Scans were made ganglia per ganglia (or when fitting into the frame two at once) with an oil immersion objective; Plan-Neofluar 25x N.A. 0.8, in some cases the Plan-Neofluar 40x N.A. 1.3 was used and for details the Plan-Apochromat 63x N.A. 1.4 was used in very few cases. The resolution was kept at 2048 × 2048 pixels and 8 bits, with a voxel size of 0.078-0.078-1 – 0.225-0.225-2 µm for all images. The Stellaris 5 microscope possess a spectrally flexible white light laser with extended spectral output on the red and near-infrared spectrum (so to reach excitation from 405 up to 685). Samples scanned in similar fashion as at the LSM 510, ganglia per ganglia, now at the 40x N.A. 1.3 magnification comparable to the 25x N.A. 0.8 from the LSM 510 at eGFP at 488 nm and TO-PRO-3 633 nm by the LAS-X software package. In order to account for potential differences between the two confocal microscopes used in this study subgroups of samples were scanned on both microscopes and scored independently; however, no differences in scorings were found between scans at the two microscopes. Further analyses were conducted using the imaging software ImageJ (v 2.9.0, Fiji Distribution; Schindelin *et al.* 2012), the resulting figures were optimised for contrast by the levels command and the schematic overviews of the CNSs were made in Photoshop (v 24.4.1, Adobe).

Scoring of infection
A scoring system was developed to differentiate between different levels of infection. The judgement was made for each intact ganglia for each treatment and sample, and ranged from no infection to the most advanced infection level as follows: 'no eGFP' (no eGFP expression detected at all), tracheal ('tra', eGFP expression detected only in the trachea, not in the CNS, and ganglial appendages), superficial ('sup', eGFP expression detected in the outmost cell layers of the ganglia) and internal ('int', eGFP expression could be detected in cells placed more internally than the outer cells of the ganglia) (see Dataset S3). For each timepoint, we recorded the most advanced level of infection at that moment.

2.8 Statistical analysis

The accumulated percentage of detected fluorescence in larvae of early second instar (eL2) and early third instar (eL3) AcMNPV-infected larvae (AcL2 and AcL3), did not follow a normal distribution. A simple survival analysis (Kaplan-Meier, log rank (Mantel-Cox) test) was used to test the two groups expression of fluorescence for similarity (significance level a=0.05), to see whether the two groups could be considered as one and whether they could be grouped for the following analysis. Statistical tests were run and graphs were made in GraphPad Prism (v 9.5.1).

3 Results

3.1 Progression of virus infection within larvae and within the CNS

Virus progression within larvae (N=225) and within the CNS of individuals from the same group (N=173, which per different ganglia resulted in 700 individual scorings of infection levels) was investigated for AcMNPV WT-eGFP-infected larvae, with mock-infected larvae as a control. In none of the mock-infected larvae an eGFP signal was detected, neither when checking larvae externally under an UV-lamp (n=100), nor in the dissected CNS scanned at the CLSM (n=68). At day 0 and 1 dpi no external eGFP expression could be observed for the AcMNPV-infected larvae by checking under a UV-lamp. This changed at 2 dpi when external eGFP expression was observed in up to 11% of the WT-eGFP infected larvae, increasing to 52-57% at 3 dpi and with a peak at 4 dpi of 71-83% (Figure 3; Dataset S1). The following 2 days (5-6 dpi) the percentage was 77-81%, and at the last recording day (at 7 dpi) this percentage of external eGFP expression was maintained or slightly decreased. On day 6 and 7 some

of the larvae started dying and liquefying (see Figure 7), and eGFP expression ceased (Figure 3). The percentage of larvae observed expressing external fluorescence did not significantly differ between larvae infected as eL2 or eL3 (Figure 3; P = 0.69; Dataset S2), and therefore the data were pooled for the subsequent analyses.

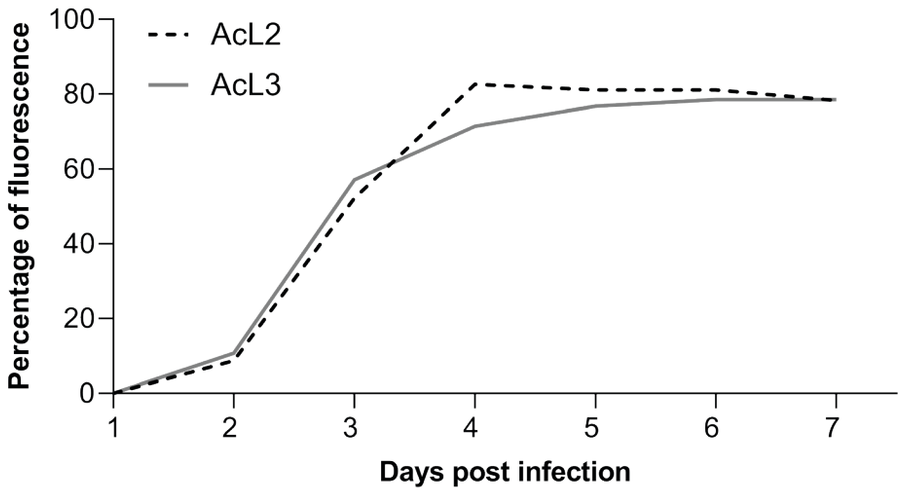

Figure 3. Accumulated percentage of *S. exigua* larvae infected with AcMNPV WT-eGFP (WT) showing external fluorescence. Larvae were examined daily from 1 to 7 days post infection (dpi) under a stereomicroscope with UV-lamp (Leica; Wild M3Z and HBO lamp), using 69 early second instar AcMNPV-infected (AcL2; dashed black line) and 56 early third instar AcMNPV-infected (AcL3; solid grey line) larvae. Percentages of fluorescence was the same during the course of infection for both treatments (Kaplan-Meier analysis, P=0.69). For a few individuals the eGFP expression faded out after liquefaction and death. Neither of the (100) mock-infected individuals (ML2 and ML3) expressed eGFP at any dpi.

For the WT-eGFP-infected larvae, viral infection of the trachea surrounding the CNS became visible from 2 dpi, and at 3 dpi viral infections were observed in the trachea for all larvae and stayed persistent through the observation days (Figure 4; Figure 5; Figure 6). From here onwards (3 dpi) the first viral infections of the cell bodies in the outer layers of the different ganglia could be observed (termed as superficial infection) (Figure 4; Figure 5; Figure 6). Internal infection (in the inner layers of the ganglia) could only be observed in one individual (out of 15) at 3 dpi, in the SOG (Figure 5; Dataset S3). From 4 dpi we started to observe more infections of the internal layers of cell bodies in the different ganglia (54.4%) and from 5 dpi onwards the infection intensified as nearly all ganglia showed infection in the internal neural layers (Figure 4; Figure 5; Figure 6; Dataset S3).

Over the course of infection, a pattern became visible, with certain areas and ganglia being infected earlier than others. Hence, the expression of eGFP was first detectable in the trachea surrounding the CNS, then in the outer cell layers and lastly in the internal layers of the ganglia (Figure 4; Figure 5; Figure 6). Alongside this infection by layers, the infection also progressed with respect to the ganglia (Figure 5). The infections in the superficial cell layers and later the more internal layers were first detected in the abdominal ganglia and the 3 thoracic ganglia, then in the SOG and lastly in the brains along with the frontal ganglia in some occasions (Figure 8).

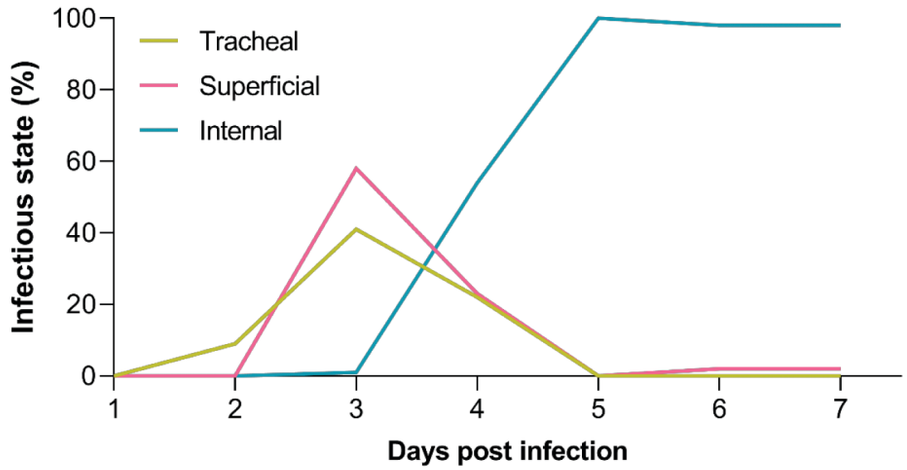

Figure 4. Percentage of AcMNPV WT-eGFP-infected larvae (infected as second and third instars) expressing eGFP only in trachea ('tracheal'; yellow line), or also superficially in the ganglia ('superficial'; pink line), or also internally in ganglia ('internal'; blue-green line) for all the analysed ganglia (brains to first abdominal ganglia) at different days post infection. This figure visualises input data from 413 individual observations of infection levels in different ganglia (n=32 for 1 dpi, 53 for 2 dpi, 69 for 3 dpi, 90 for 4 dpi, 77 for 5 dpi, 51 on 6 dpi and 41 for 7 dpi) from a total of 105 AcMNPV WT-eGFP-infected larvae, and does not include the data from the mock-infected larvae (N=68) as none of the scans of 286 ganglia showed any eGFP expression.

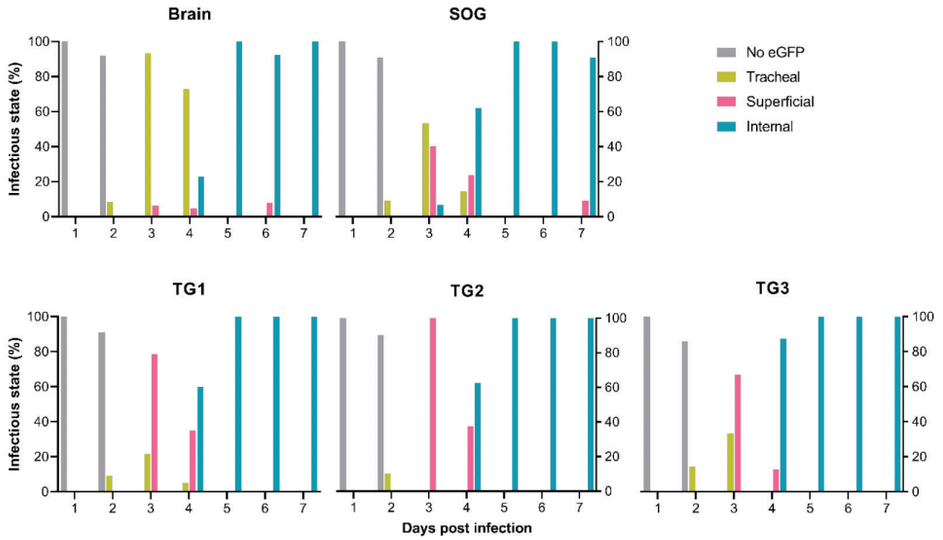

Figure 5. Percentage of AcMNPV WT-eGFP-infected larvae (infected as second and third instars) expressing no eGFP ('No eGFP'; grey bars), eGFP only in trachea ('tracheal'; yellow bars), or also superficially in the ganglia ('superficial'; pink bars), or also internally in ganglia ('internal'; blue-green bars) for the brain, SOG and first to third thoracic ganglia (TG1, TG2 and TG3) at different days post infection. The data represent the most advanced level of infection observed (see section 2.7 scoring of infection). This figure shows data from 402 individual scorings of ganglia (data on AG1 are not represented in this figure).

Figure 6. Confocal laser scanning microscope images of AcMNPV WT infection in the brain, SOG, first, second and third thoracic ganglia (TG1-TG3), and the first abdominal ganglia (AG1; for 3 days post infection (dpi) only) at 1 to 6 days dpi. All images represented here are from *S. exigua* larvae infected as early third instars with a 108 OBs/ml concentration. Magenta channel for the TO-PRO-3 nuclei/dsDNA staining, green channel for AcMNPV WT-eGFP. White signal indicates an overlap and high intensity of the green and magenta channel. Scalebars represent 50 µm. ❯

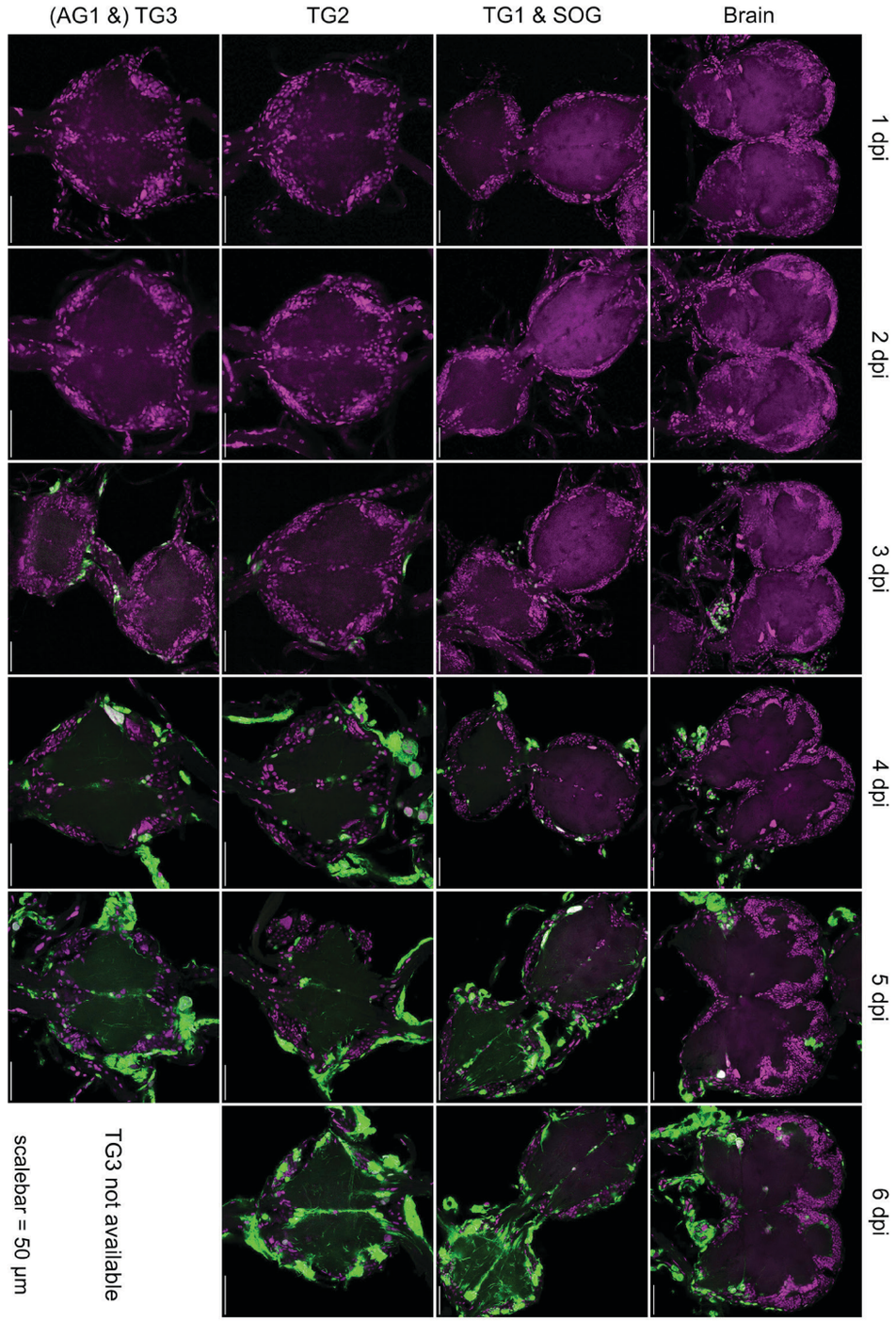

Central nervous systems from liquefied larvae

Of the few liquefied larvae where it was still possible to dissect out complete ganglia (n=13 larvae, n=46 individually scored ganglia), the lysis of cells could be observed by the decreased and fragmented area for the TO-PRO-3 signal (staining dsDNA) and by OBs observed within and outside of cells (eGFP signal) (Figure 7). Some cells are found highly enlarged, just prior to lysis (Figure 7E and 7E'). The "banded" WT-eGFP perinuclear structure superficially located on the ganglia (Figure 7B, C, E and E') had a high resemblance with previously observed patterns in Sf9 cells infected with the same AcMNPV WT-eGFP virus as used in our study (AcMNPV-eGFP:VP39; Mu *et al.* 2014) and in AcMNPV-infected TN-368 cells, where a P10 cage-like structure was seen (Graves *et al.* 2019) (Supplementary Figure S1). The *p10*-gene (ac137) has been described as being transcribed very late in baculovirus infection, and the P10 (10 kDA) cage functions in breaking the nucleus and thereby aids in the OB release (van Oers *et al.* 1993; Harrison and Hoover 2012). We assume that the visualisation of the banded structure is due to precipitation of VP39-eGFP with P10 when the VP39 is overexpressed, e.g. in the example of liquefied larvae (Figure 7).

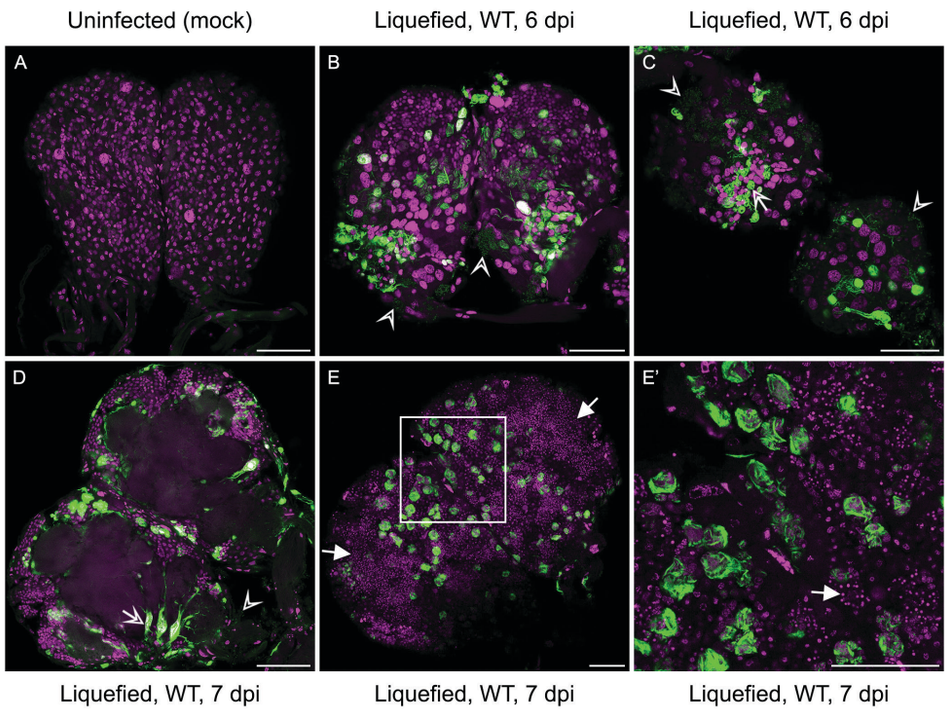

Figure 7. Confocal laser scanning microscope images of parts of the central nervous systems of liquefied *S. exigua* larvae (6 and 7 days post infection (dpi)) upon AcMNPV WT-eGFP infection. Panel A) represents the brain of a mock-infected larvae for comparison with brain B) and SOG and first thoracic ganglion (TG1) C) of 6 dpi liquefied larvae (both from larvae infected as early second instar) and brain of 7 dpi liquefied larvae D), E) and E') (from larvae infected as early third instar). Open arrow heads in B), C) and D) indicate OBs released from cells post lysis, whereas the open arrow in C) and D) indicates OBs still enclosed in cells. Filled arrows in E) and E') indicate lysed cells with fragmented nuclei (TO-PRO-3, magenta channel). E') is a magnification of the square area indicated in E). All panels in the figure represent a stack on the surface of the ganglia, except for D) where the internal infection is visualised from a stack in the midline of the brain. A white signal indicates an overlap and high intensity of the green (AcMNPV WT-eGFP) and magenta channel. Scalebars represent 50 µm.

3.2 Specificity of viral localisation

The observed patterns of viral localisation throughout the analysed ganglia were similar for all samples, with certain cell bodies being infected more frequently than others (Figure 8). In the brain, the cell body in the centre of the superior neuropil (Kato *et al.* 2020) (Figure 8A, B open arrow head) and the cell bodies near the trachea (Figure 8A, B) were frequently infected. When the brain was more heavily infected, we observed infection of the cell bodies surrounding the superior neuropil, e.g. those surrounding the calyx (Figure 8A, B filled arrow). For the SOG (Figure 8A, D) and the subsequent thoracic ganglia and first abdominal ganglion (Figure 8A, E-H), the most frequent pattern was the infection of cell bodies that were localised in a midline of either of the ganglia, or in close proximity to the trachea, connectives and nerves (Figure 8A, E-H). When the SOG and the following ganglia were more heavily infected, the infection could furthermore be localised to cell bodies surrounding the neuropil, similar to what was seen for the brain. In heavily infected brains, the axons could sometimes be seen, but the axon signal was more clearly visible in the SOG or in the first, second, third thoracic ganglia or first abdominal ganglia (see 4-6 dpi in Figure 6; Figure 8E-H). In some occasions superior or internal infections of the frontal ganglia could also be detected (Figure 8A, C).

Figure 8. Schematic overview of AcMNPV WT-eGFP localisation in the CNS (from brain to first abdominal ganglia (AG1)) *of S. exigua* A), with representative images of confocal laser scanning microscope (CLSM) imaging for each of the analysed ganglia B)-H). Based on CLSM images the major localisations of AcMNPV WT-eGFP were visualised with green dots in A) and trachea are visualised as appendages to the ganglia with red-brown lines (viral infections in the trachea are not represented in the schematic overview). B) brain with filled arrow indicating infected cell bodies surrounding the calyx and open arrow head indicating infected cell body in the centre of the superior neuropil, C) frontal ganglion (FG), D) SOG, E) first thoracic ganglion (TG1), F) second thoracic ganglion (TG2), G) third thoracic ganglion (TG3) and H) first abdominal ganglion. B)-H) are from 3-5 dpi; representative images were picked to illustrate the overall trends of viral progression and localisation. Magenta signal for the TO-PRO-3 nuclei/dsDNA staining, green channel for AcMNPV WT-eGFP. Scalebars represent 50 µm. ›

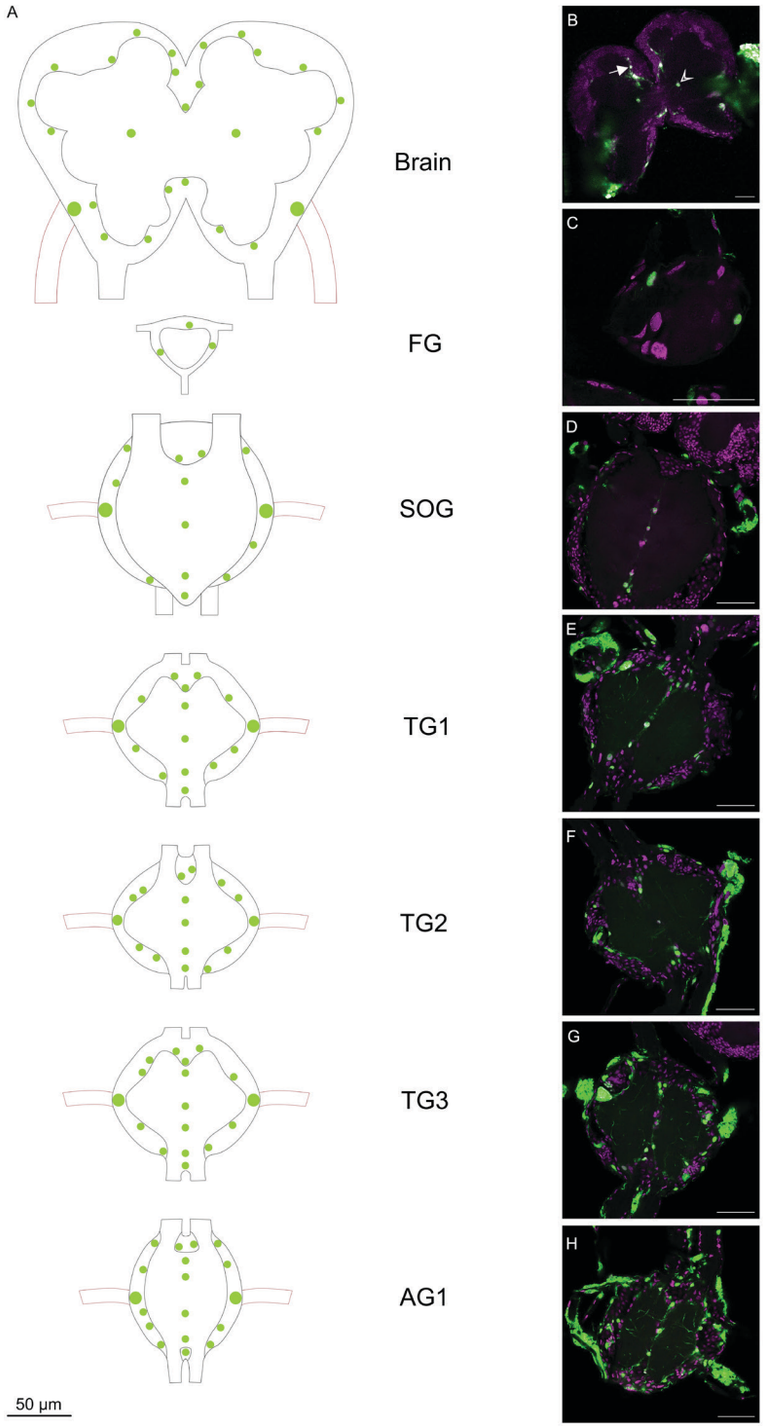

3.3 The role of protein tyrosine phosphatase in CNS entry

Since the enzymatic active form of PTP is essential for the expression of hyperactivity in the AcMNPV-*S. exigua* system (van Houte *et al.* 2012), we tested whether viral entry into the CNS, the area for movement initiation, is dependent on PTP. The earliest and the clearest infections patterns could be detected superficially and internally from 4 dpi in AcMNPV WT-eGFP-infected larvae (Figure 6; see 3.1). We set out to test whether the other AcMNPV-variants could also enter the CNS, and if so, whether there were differences in localisation (described for WT-infected larvae in 3.2). In the CNSs dissected out from larvae orally infected with any of the AcMNPV-variants used in this study, eGFP expression was detectable from 4 dpi (Figure 9). Neither the enzymatic function nor the structural properties of AcMNPV-PTP seemed essential for CNS entry in *S. exigua*, as all recombinant viruses – including the virus without *ptp* – could enter the CNS. Furthermore, no differences were seen for either the superficial or the internal infections of the localisation in the CNS for the different recombinant viruses in this setup.

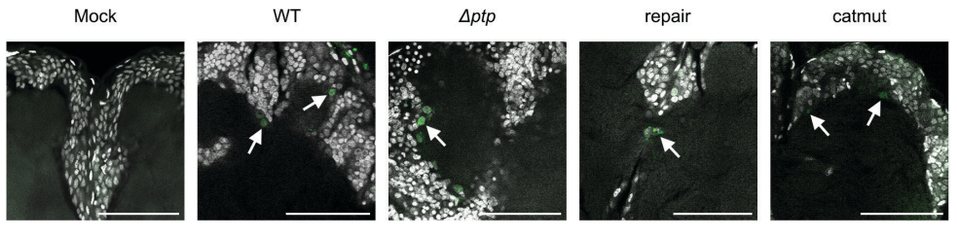

Figure 9. Confocal laser scanning microscope images of the same brain area, showing the calices (all) and/or midline (mock, repair, catmut) of brains dissected at 4 days post infection from larvae infected as early third instar with a mock solution (Mock), or with one of the recombinant AcMNPV viruses expressing eGFP (AcMNPV WT-eGFP (WT), AcMNPV Δ*ptp*-eGFP (Δ*ptp*) lacking *ptp*, AcMNPV with *ptp* repaired back after deletion (repair) and AcMNPV encoding for a catalytic inactive PTP (catmut). White signal for TO-PRO-3 nuclei/dsDNA staining, green channel for eGFP signal from the recombinant viruses described. Scalebars represent 50 µm.

4 Discussion

Baculoviral modification of caterpillar behaviour is a clear example of behavioural alteration by parasites. As the CNS can serve as starting point in the initiation of a range of behaviours, we followed a neuroparasitological approach (Hughes and Libersat 2018) to investigate if, when and where AcMNPV infects the CNS of *S. exigua* caterpillars. Furthermore, we addressed the possible role of viral-PTP in the entry of AcMNPV into the CNS. Since the various ganglia process the reception

and send signals involved in different actions and behaviours, we investigated each ganglion (up to the first abdominal ganglion) separately. Our findings reveal that AcMNPV enters the CNS from 3 dpi onwards, most likely via the trachea. The virus signal in the CNS is first visible in the outer cell layers, e.g. in the cell bodies near the connectives. Subsequently from 3 dpi onwards the infection spreads to the more internal cells. Within the CNS, the first to third thoracic ganglia and the first abdominal ganglion are infected first, followed by the SOG, then the brain and the frontal ganglion. For the internal infections certain cell bodies are infected more frequently than others. In the SOG, thoracic ganglia and abdominal ganglia, the most commonly infected internally layered cell bodies are found in the midlines of the neuropil and in close proximity to the trachea, connectives and nerves. This is the same for the brain, where in addition infected cell bodies are found in close periphery to the superior neuropil or in the centre of the superior neuropil. Neither the enzymatic function, nor the structural properties of AcMNPV-PTP are needed as differences were neither seen in the superficial nor the internal infections by these differently *ptp*-expressing viruses.

4.1 Progression of infection

From 3 dpi onwards we observed superficial infection (followed by internal infection) of the CNS. While in our virus constructs, GFP fused to VP39 is expressed under the *p10* promoter, which is a very late promoter (as reviewed by van Oers 2021), we still think that GFP observations at 3 dpi reflect virus entry into the CNS. Previous studies showed that *p10* transcripts start to be produced from 18 hpi onwards (Chen *et al.* 2013) and that fused and unfused VP39 (which was not removed from the viral genomes and is expressed under its own promoter) are both incorporated into the BVs, as has been shown before (Mu *et al.* 2014). This indicates that fluorescing nucleocapsids (and BVs) will be visible from about 18 hpi. In our earlier work GFP was incorporated in the nucleocapsids, and since the timing of nucleocapsid and BV production has not changed (Mu *et al.* 2014), our observations are likely to reflect AcMNPV entry into the host CNS.

In an earlier study, infections of neural glial cells have been described from 2-3 dpi in the same virus-host system (Knebel-Mörsdorf *et al.* 1996). In our experimental setup, the first signs of viral infection (visible through the cuticle due to eGFP expression) were detectable from 2 dpi onwards and at the same day we started to see infections in the trachea. This corroborates with results from other studies, e.g. for Helicoverpa armigera NPV-infected cotton bollworms, where the first viral infections were detected by GFP-expression at 2 dpi in epithelial cells and trachea (Herz *et al.* 2003). After the initial infection of the midgut epithelial cells, neighbouring cells as well as the tracheal cells along with haemocytes are the first cells to get infected by BVs in the secondary phase of baculoviral infection (Engelhard *et al.* 1994; Barrett *et al.* 1998; Williams *et al.* 2017a; Blissard and Theilman 2018). The trachea have also been shown to be the major route of AcMNPV transmission through *Trichoplusia ni* caterpillars, and as the trachea branch into the CNS by tracheoles this route seems viable (Burrows 1980; Engelhard *et al.* 1994; Torquato *et al.* 2006; Senem *et al.* 2016).

Our study provides data on tracheal infection prior to superficial and internal infections of the different ganglia. The eGFP signal detected from the trachea was a lot stronger than from any of the ganglia and stayed persistent throughout. As the trachea are connected to the ganglia and branch within, the tracheal cells border the two types of glia cells (perineurial and subperineurial) and the neural lamella which comprise the blood-brain barrier surrounding the CNS (Stork *et al.* 2008; Hindle and Bainton 2014; Bittern *et al.* 2020). With our experiment we cannot out rule that other cell types (e.g. haemocytes) are also in direct contact with the cells that comprise the blood-brain barrier and that these cells might also play a role in the infection of the CNS. Due to the BVs mode of infecting neighbouring cells, the baculoviral cell to cell infection could provide an alternative route compared to the route other pathogens must follow to surpass the blood-brain barrier to infect the CNS, such as the Trojan horse strategy (phagocytised by macrophages) (Santiago-Tirado and Doering 2017; van Leeuwen *et al.* 2018; Ash *et al.* 2021). The earlier described banded pattern displayed by VP39-eGFP (Figure 7E and E'; Supplementary Figure S1) in the enlarged cells on the surface of the liquefied brains was also observed in the trachea. The fact that we also found indications for VP39 precipitation on baculoviral P10 structures in tracheal cells (*data not shown)* when VP39-eGFP is over-expressed from the highly active *polh* promoter (similar to what is reported in Supplementary Figure S1) shows that infection proceeds into the very late phase also in trachea. This finding further supports the route of transmission via trachea for surpassing the brain barrier. The fact that our results always indicate a high amount of viral structural proteins (shown by VP39-eGFP) in the trachea, is coherent with previous studies. Increased relative expression of the viral structural gene *gp64* was, for instance, seen in the trachea at 3 and 4 dpi compared to the fat body at 4 dpi of BmNPV-infected *B. mori* caterpillars (Katsuma *et al.* 2012). Due to the fact that we see tracheal infection prior to CNS infection and the strong continuous infection of the trachea compared to the CNS, we hypothesise that the trachea are the route for viral infection of the CNS.

The more caudally (towards the rear end) located ganglia are closer located to the alkaline zone of the midgut (where the OBs dissolve), than the more anterior ganglia (such as the brain and SOG) (Dow 1992). We found a link between increase in infection level connected to increasing days after infection and the order of infection of the different ganglia in the CNS. Generally, the further caudally the ganglia were located, the earlier more advanced infection levels were observed. This positive link between more advanced infection levels of the more caudally located ganglia and the role of thoracic and abdominal ganglia in the initiation of movement (Burrows 1996), suggests that

the infection of these ganglia is also related to the induced changes in behaviour.
Cells involved with movement can be found on the external/superficial part of the ganglia (Weeks and Jacobs 1987), where we also observed virus infections. In many cases we observed an enlargement (compared to neighbouring cells and mock controls) of the infected neural cells adjacent to the trachea. Given the size of the cell bodies these cells could be glia cells, but the enlargement might very well be due to the viral infection and then they could also represent neurons. Interestingly, the infection does not simply spread from initially infected cell to directly neighbouring cells, since we do not see every cell body being infected from the surface of a ganglion to the most internal parts (such as the infections of the midlines of the SOG, first to third thoracic ganglia and the first abdominal ganglion). Also, the infection of a single cell (to a few) in the centre of the superior neuropil of the brain is remarkable. We currently do not know which cell type is infected in the latter, but tracheal cell bodies have been described around the same location in *Drosophila* (Truman *et al.* 1994; Pereanu *et al.* 2007). If these cell bodies are indeed tracheal cell bodies in *S. exigua,* this would further support our theory of viral CNS-infection through the trachea as these cells had been infected in nearly all cases. Furthermore, eGFP signal was detected in some axons indicating that the infection might progress through the axons when having entered the CNS, e.g. to the internally located and centralised cell bodies in the (superior) neuropil in the different ganglia. Axonal invasion and transport via the axons have previously been described for the much smaller RNA virus, Rice yellow stunt virus (RYSV; family *Rhabdoviridae*) in the CNS of the green rice leafhopper (*Nephotettix cincticeps*) (Wang *et al.* 2019).

4.2 Specificity of viral localisation in the CNS

Viral infection of the CNS does not follow a random pattern, in contrast, we found that the virus localises at specific regions in the ganglia (Figure 8). For most of the infected cells in the CNS, the function of these cells is currently unknown and it is also uncertain whether these cells are glial cells or neurons. Further research is needed to see whether AcMNPV specifically infects cells with a particular function, and whether the presence of AcMNPV at these locations has an influence on the induction of hyperactivity. As mentioned above, AcMNPV often infects cells in the midline of the ganglia of the SOG and the ganglia caudally placed, and these are potentially midline glia (MG) cells (Jacobs 2000; Kuehn and Duch 2008). The infected cells in the centre of the superior neuropil in the brain are in close proximity to different parts of the mushroom body (the central processing unit involved in associative learning and memory) and the central complex (involved in vision mediated behaviours and spatial information with locomotor control) (Aso *et al.* 2014; Stropfer 2014; Givon *et al.* 2017), it remains to be studied whether AcMNPV specifically infects those cells to induce hyperactivity.

The viral infection of cell bodies in the rim of the superior neuropil can be further split down to the rim of the calyx (part of the mushroom body), the rim of the optic lobe (perception of signals from the eyes), and the rim of the antennal lobe (perception of signals from the antennae), which indicates that a whole range of different functions could be at play for the viral locations observed in the inner layers of the ganglia. The cells that we detected in the heavier infected samples that are located at the rim surrounding the superior neuropil are likely to be neurons (Burrows 1996) and with the detection of axonal infections we have strong indications of neuronal infections by AcMNPV in *S. exigua*.

Interestingly, the pattern of the above mentioned localisation of AcMNPV-infected cells in the CNS of *S. exigua* seems to overlap with the expression of ecdysone receptors (EcRs) shown for *Drosophila melanogaster* and *Manduca sexta* (Truman *et al.* 1994). Ecdysone receptors A and B1 (EcR-A and EcR-B1) are located in the MG, the glia of the optic lobe, the perineuropilar glia, and in neurons of the mushroom body and of the optic lobe of *D. melanogaster* and *M. sexta* (Truman *et al.* 1994). The insect steroid ecdysone I is required during moulting and metamorphosis, and a peak in relative levels of *D. melanogaster* larval EcR-B1 was detected during the wandering stage (Truman *et al.* 1994; Jacobs 2000). The active state of E, 20-hydroxyecdysone (20E), can be inactivated by ecdysteroid UDP-glucosyl transferase (EGT) (which is present in nearly all baculoviruses) which thereby stalls the normal moulting process of some caterpillars infected by baculoviruses. Furthermore, EGT might play a role in virus-induced tree-top disease and hyperactivity (O'Reilly and Miller 1989; Cory *et al.* 2004; Hoover *et al.* 2011; Ros *et al.* 2015; Zhang *et al.* 2018; reviewed by Gasque *et al.* 2019) and therefore it will be highly interesting to further study the link between AcMNPV-infected cells and the expression of EcRs.

4.3 PTP-induced hyperactivity by baculoviruses

Protein tyrosine phosphatase is a factor needed for initiating hyperactivity in BmNPV-infected *B. mori* caterpillars (Kamita *et al.* 2005). The same is the case for AcMNPV-induced hyperactivity expressed by *S. exigua* at 3 dpi (van Houte *et al.* 2012). Despite the presented similarities, a major difference between the two systems is seen in the exact role of PTP. For BmNPV-infected *B. mori* solely the structural properties of PTP are needed, whereas for AcMNPV-infected *S. exigua* caterpillars the hyperactivity will only be expressed if AcMNPV also encodes for the enzymatic function of PTP (Katsuma *et al.* 2012; van Houte *et al.* 2012). As we have shown in this study, all the eGFP-expressing AcMNPV recombinant viruses could enter the CNS of *S. exigua* including AcMNPV with a deleted *ptp* gene and the virus with a catalytically impaired PTP. We can therefore conclude that for AcMNPV-infected *S. exigua*, PTP is non-essential for CNS entry, and our data therefor does not support the suggested

hypothesis that baculoviral PTP aids in CNS entry of caterpillars (Katsuma *et al.* 2012). Both AcMNPV and BmNPV belong to group I NPVs wherein the *ptp* gene is conserved (van Houte *et al.* 2012). Since group II NPVs also induce hyperactivity (Goulson 1997), but do not encode PTP, it is certain that other mechanisms than solely PTP can induce hyperactivity in the baculoviral-lepidopteran system.

In conclusion, we show the progression of a baculovirus infection in the CNS most likely by the entry via trachea, of initially the more caudally located ganglia placed closer to the alkaline zone of the midgut, followed by the SOG and the brain. Furthermore, we have shown infections of glia cells and neurons, in external and internal layers of all the ganglia, along with AcMNPV's independence of PTP for the entry to the CNS of *S. exigua*. Further research is needed to identify possible interactors of PTP and to disentangle the pathway downstream, but also the search for other possible non-PTP interacting mechanisms that aid to express hyperactivity is needed. Our results demonstrate, that although PTP is not needed for AcMNPV to enter the CNS, the location pattern still suggest a role in manipulating the host nervous system, adding novel insights into the mechanism underlying this intricate host-parasite interaction.

Funding

This work was supported by the Dutch Research council (NWO) (grant number: ALWOP.362). V.I.D.R. is supported by an NWO VIDI-grant (VI.Vidi.192.041).

Acknowledgements

We thank Els Roode for maintaining the general rearing of the *S. exigua* population. Jingfang Mu is thanked for generating the recombinant AcMNPV-eGFP:VP39 (WT-eGFP) construct and Fengqiao Zhou for generating the pACEBac1-pIDK, - *polh* and pIDK-eGFP-*vp39* constructs, which were used for developing the AcMNPV repair and - catmut. We thank Jitte Groothuis for initially demonstrating how to dissect CNSs from *S. exigua*. Nhu Dinh is acknowledged for her contributions to study the PTP variants. We thank Annamaria Mattia, Hans M. Smid and Aidan Williams for giving a helping hand with some dissections and with mountings of samples. Hans M. Smid is also thanked for the introduction to CLSM work and for making the first draft of the *S. exigua* CNS overview.

Data accessibility

Analyses reported in this article can be reproduced using the data provided by:
Dataset S1; Gasque et al 2023_S1_Whole_caterpillar_infections
Dataset S2; Gasque et al 2023_S2_For_survival_analysis
Dataset S3; Gasque et al 2023_S3_Dpi_CNS_infections

Supplementary files

Supplementary Table S1. Primer names and sequences for the utilised primers.

Number	Primer name	Sequence (5' to 3')*
1	*Polh*-XbaI-FW	CCC*TCTAGA*ATGCCGGATTATTCATACCGT CCCACCATCGGGCGTACCTACCT
2	*Polh*-PstI-RV	CCC*CTGCAG*TTAATACGCCGGACCAGTGAA CAGAGGTGCGTCTGGTGCAAACTC
3	*eGFP*-XhoI-FW	CCC*CTCGAG*ACCATGGTGAGCAAGG
4	*Vp39*-NcoI-RV	ACA*CCATGG*CTTAGACGGCTATTCCTCCA
5	*Ptp* cat/rep-SpeI-FW	GAG*ACTAGT*ACATTATCCCTCGATTGTG
6	*Ptp* cat/rep-NsiI-RV	GAG*ATGCAT*CGCTGGAAGAAGCGCAAC

*Restriction sites in italics and underlined

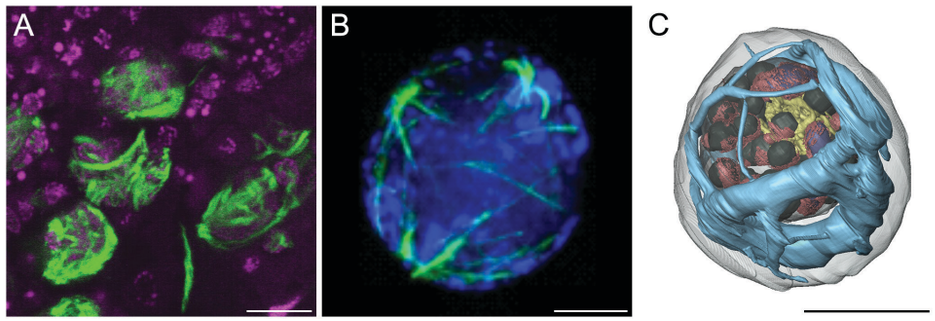

Supplementary Figure S1. Resemblance between banded perinuclear structure observed in our study A) and previous experiments in Sf9 cells B), and a 3D construction of the p10 cage like structure C). A) represents the banded AcMNPV-eGFP:VP39 perinuclear structure superficially located on brain *in vivo* in present study (magenta channel To-pro 3 nuclei/dsDNA staining, green channel AcMNPV-eGFP:VP39), B) represents AcMNPV-eGFP:VP39-infected Sf9 cells from Mu *et al.* (2014) (blue channel Hoechst staining of nuclei, green channel same AcMNPV-eGFP:VP39 construct as in A)), and C) represents a 3D reconstruction of an AcMNPV-infected TN-368 cell at 3 dpi from Graves *et al.* (2019), showing the P10 cage like structure (Zeiss LSM 510 Meta scannings were processed with LSM 5 image Browser). All scalebars 10 µm.

The beauty of science lies in its ability to unravel the complexity of nature and reveal its underlying order.

Rosalind Franklin

CHAPTER 6

Untangling the strings of the puppet master: Investigating the role of biogenic amine signalling cascades in AcMNPV-infected *Spodoptera exigua* caterpillars

Simone N. Gasque[1+], Astrid Bryon[1+], Alexander Haverkamp[2] and Vera I.D. Ros[1]

[1]Laboratory of Virology, Wageningen University and Research, Droevendaalsesteeg 1, 6708 PB Wageningen, The Netherlands

[2] Laboratory of Entomology, Wageningen University and Research, Droevendaalsesteeg 1, 6708 PB Wageningen, The Netherlands

[+] These authors contributed equally to this work

Abstract

Parasites' modifications of host behaviour are detected in a range of systems. The baculovirus Autographa californica multiple nucleopolyhedrovirus (AcMNPV) alters the behaviour of caterpillars of the beet armyworm, *Spodoptera exigua,* into a hyperactive state from around three days post infection (dpi). The viral protein tyrosine phosphatase (PTP) is required for expression of hyperactivity in AcMNPV-infected *S. exigua* caterpillars. We infected early third instar caterpillars with WT AcMNPV or with AcMNPV mutants either expressing a catalytically inactive PTP (catmut) or no PTP (Δ*ptp*), to further investigate the potential role of biogenic amine signalling cascades in AcMNPV-PTP induced behavioural manipulation at 1, 3 and 4 dpi. We measured the concentration in the haemolymph of the three major biogenic amines in invertebrates: serotonin (5HT), dopamine (DA) and octopamine (OA). We further investigated the gene expression of actors involved in the biogenic pathways to these amines along with tyramine (TA), by analysing the gene expression of precursor enzymes, rate-limiting enzymes and the receptors in these major biogenic pathways. We were able to detect an effect of dpi and treatments on the concentration of 5HT and DA and we found that the genes for most of the precursors, rate limiting enzymes and receptors were highest expressed at 1 dpi. Furthermore, the gene encoding for the serotonin receptor 5HT-7 was upregulated in AcMNPV WT-infected larval heads compared to the AcMNPV catmut-, Δ*ptp*-infected and uninfected conspecifics. In addition, when infected with AcMNPV WT, an upregulation of gene encoding the tyramine receptor TAR1 was seen in larval heads, compared to AcMNPV catmut-, Δ*ptp*- infected and uninfected groups. These results suggest that AcMNPV might hijack 5HT-7 and TAR-1 depended signalling pathways to induce hyperactivity. In addition, our results highlight the impact of timing and the host's developmental stage on AcMNPV-induced host manipulation, highlighting the complex influence of the factors.

1 Introduction

Parasitism is a very common lifestyle that is estimated to be employed by more than half of the organisms on earth (Windsor 1998; de Meeûs and Renaud 2002; Weinstein and Kuris 2016). Parasitic manipulation of host behaviour is widespread and can be beneficial to the parasite itself or its progeny (Libersat *et al.* 2009). Numerous examples have been found in natural parasite systems such as suicidal terrestrial insects jumping into water due to infections with horsehair worms (Thomas *et al.* 2002), *Toxoplasma gondii*-infected rodents' fatal attraction to cat urine (Berdoy *et al.* 2000; Webster and McConkey 2010), necrophilic house flies (Naundrup *et al.* 2022) and zombie-ants (Hughes *et al.* 2011; Małagocka *et al.* 2015; de Bekker *et al.* 2021; Gasque and Fredensborg 2023) (Doherty 2020). However, few studies have looked into the underlying mechanisms involved in these behavioural alterations by parasites (Kamita *et al.* 2005; Biron *et al.* 2006; Hoover *et al.* 2011; van Houte *et al.* 2012; de Bekker *et al.* 2017; Will *et al.* 2020; Zhang *et al.* 2018). Baculoviruses manipulate the behaviour of their caterpillar hosts and provide an excellent model system to unravel underlying mechanisms (as reviewed in Gasque *et al.* 2019; Liu *et al.* 2022). The behavioural alteration induced by baculoviruses (circular double-stranded DNA viruses) is distinct from other systems, as it can induce two separately recognised behaviours, with different mechanisms involved (van Houte *et al.* 2014a; Williams *et al.* 2017a; Gasque *et al.* 2019). Upon oral infection with baculoviral occlusion bodies (OBs), lepidopteran larvae (caterpillars) will express hyperactivity, roaming with higher frequency in the horizontal plane, and/or express tree-top disease, climbing the vegetation in the vertical plane (Harrison and Hoover 2012). Independent of each of the two behavioural alterations, as the viral infection progresses, cells will lyse for eruption of newly produced OBs, and the caterpillar will liquefy (Blissard and Theilmann 2018; see lysed cells in Chapter 5). These behavioural alterations are postulated to increase the transmission of OBs to conspecifics, either directly as a consequence of cannibalism and necrophagy (Rebolledo *et al.* 2015) or by subsequent ingestion of OB-contaminated vegetation (Gasque *et al.* 2019). In the field of baculoviruses, for the first time a gene was found to be responsible for a parasite-induced behaviour expressed by the host (Kamita *et al.* 2005). Viral protein tyrosine phosphatase (PTP) induces hyperactivity in a range of baculovirus-caterpillar host systems (Kamita *et al.* 2005; van Houte *et al.* 2012; Katsuma *et al.* 2012; Katsuma 2015). For Autographa californica multiple nucleopolyhedrovirus (AcMNPV)-infected *Spodoptera exigua* third instar larvae, hyperactivity could be observed at 3 days post infection (dpi) (van Houte *et al.* 2012), while in *Bombyx mori* nucleopolyhedrovirus (BmNPV)-infected *B. mori* fourth and fifth instar larvae, hyperactivity was seen at respectively 96 and 90 hours post infection (Katsuma *et al.* 2012; Katsuma 2015). Whether the structural properties and/or the enzymatic function of PTP are pivotal for the expression of hyperactivity differs for these two baculoviral-host systems. While in AcMNPV-infected third instar *S. exigua* larvae the enzymatic activity of PTP was pivotal for the display of hyperactivity, in BmNPV-infected fourth and fifth instar *B. mori* larvae hyperactivity was also seen when an enzymatically inactive PTP was expressed, suggesting that the structural properties of PTP were sufficient to induce hyperactivity (Katsuma *et al.* 2012; van Houte *et al.* 2012; Katsuma 2015). It was therefore suggested that PTP may be needed for entry into the host central nervous system (CNS) as a virion-associated structural protein, however, in Chapter 5 we demonstrated that neither the enzymatic nor the structural properties of AcMNPV-PTP were essential for CNS entry. Parasites may modulate host behaviour by interfering with the synthesis or release of biogenic amines in the host's CNS (Adamo 2002; van Houte *et al.* 2013; Perrot-Minnot and Cezilly 2013; Hughes and Libersat 2018). As biogenic amines are

involved in the offset of a whole variety of behaviours and more specifically being involved in movement, it is therefore highly likely that one or more of these specific biogenic amines and their receptors are involved in parasite-induced behavioural alterations (Helluy and Holmes 1990; Adamo and Shoemaker 2000; Prandovszky *et al.* 2011; Xu *et al.* 2018). For viral induced behavioural change, the modifications can be induced by altered gene expression in the host which lead to the production of molecules, or as an immune response due to the infection (Adamo 2002; Helluy and Thomas 2010; Herbison 2017; Mangold and Hughes 2021; Gasque and Fredensborg 2023). This modification could be induced from specific locations linked to movement e.g. within the CNS itself, or as a modulation secreted throughout the entire body, e.g. by the means of the bloodstream of insects – the hemocoel (Perrot-Minnot and Cézilly 2013). Biogenic amines act not only as nerve signalling molecules within the CNS but are also transported over broader distances as neurohormones by means of the haemolymph. In insects, serotonin (5HT), dopamine (DA), tyramine (TA) and octopamine (OA) are the major biogenic amines (Blenau and Baumann 2001). The synthesis pathways of these biogenic amines involve a range of enzymes. Tyrosine hydroxylase (TH) is known as the rate-limiting enzyme of the biosynthesis pathway leading to DA, tryptophan hydroxylase (TPH) has this role in the 5HT pathway, tyrosine decarboxylase (TDC) first leads the synthesis of tyramine (TA, a separately acting neuromodulator) and lastly TA is hydroxylated by tyramine beta-hydroxylase (TβH) to octopamine (OA) (Figure 1) (see more detail in Chapter 4) (Blenau and Baumann 2001; Rang *et al.* 2016).

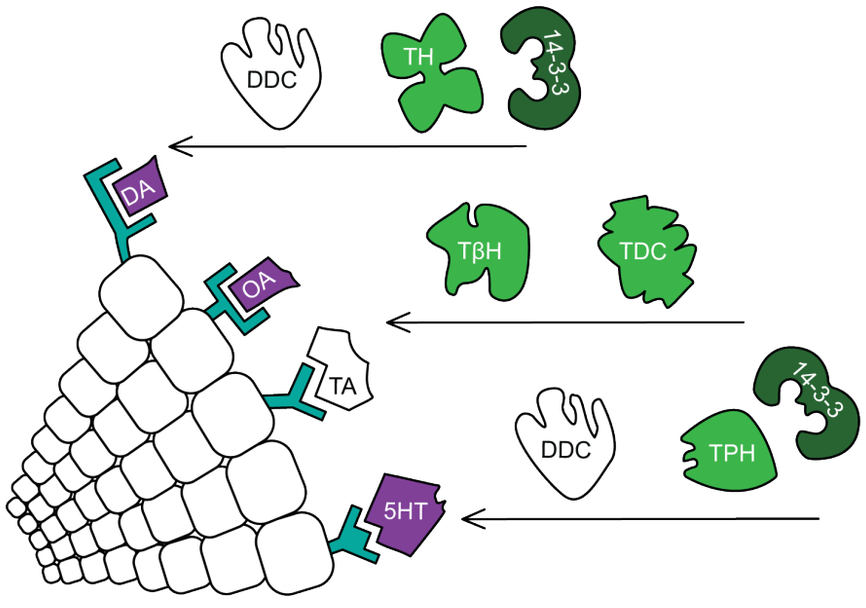

Figure 1. Simplified overview of some of the enzymes, biogenic amines and receptors involved in the biosynthesis pathway for DA, TA, OA and 5HT targeted in this study (only coloured shapes were targeted). The actors in colour (petrol blue, purple and green) are targeted in this study, and the non-coloured (such as DDC and TA) have not been studied in this experiment. 14-3-3 has been added to the figure due to its role as an activator of TH and TDC. Receptors proteins (petrol blue), biogenic amines (purple and white (TA)), enzymes (green and white (DDC)) and 14-3-3 specifically (dark green).

In addition, 14-3-3 proteins are recognised as activators of the rate-limiting enzymes in the biosynthesis of catecholamines (such as TH) (Aitken 1992; Wang and Shakes 1996) and more specifically for TH and tryptophan hydroxylase TPH (Yamauchi *et al.* 1981). The four biogenic amines, DA, 5HT, OA and TA, can activate receptors, some of which are specific to a single biogenic amine (such as TAR2 for TA), while other receptors have an affinity to multiple biogenic amines, such as TAR1 which has an affinity to both TA and OA, although with a higher sensitivity to TA (Farooqui 2007; Tierney *et al.* 2018; Verlinden 2018; Finetti *et al.* 2021a). To unravel and understand the underlying manipulative pathway behind the hyperactivity-induced behavioural change by baculoviruses, we investigated the relative gene expression levels of the 14-3-3 protein family, the rate limiting enzymes leading to the production of the four major biogenic amines (TA, OA, DA and 5HT), and a selection of their receptors over a time course of four days. We compared expression in larvae infected with wildtype (WT) AcMNPV, AcMNPV with the *ptp* gene deleted (Δ*ptp*), AcMNPV expressing an enzymatically inactive PTP (catmut) or with no virus at all (mock infection). Additionally, concentrations of the three major biogenic amines in invertebrates (OA, DA, and 5HT) were measured in the haemolymph of the mock- and virus-infected larvae. Our study aims to elucidate the effect of baculovirus infections and specifically the baculovirus-encoded ptp gene on the pathways and production of three important biogenic amines in infected insect hosts.

2 Materials and methods

2.1 Insect rearing

Spodoptera exigua larvae were reared on artificial diet in a 14h : 10h light : dark regime at 50% relative humidity (Chapter 5). Up to hatching, eggs were kept at 28°C and moved to 25.5°C from first instar and onwards. When larvae reached the late second instar, they were starved overnight for 16h before performing infections.

2.2 Viral constructs and larval infections

In this study, three different viral bacmids of AcMNPV were used, each containing a fused open reading frame (ORF) with enhanced green fluorescent protein (eGFP) followed by the coding sequence for the AcMNPV major capsid protein (VP39) to allow visualisation of successful infections (Mu *et al.* 2014; Chapter 5). The eGFP:VP39 expressing bacmids were originally derived from the WT AcMNPV E2 bacmid (Smith and Summers 1979; Luckow *et al.* 1993), and concerned a wildtype bacmid (WT), a bacmid with the *ptp* gene deleted (Δ*ptp*) and a bacmid containing a catalytically inactive PTP protein (lacking the enzymatic function of PTP but maintaining the structural properties) (catmut) (Chapter 5). Viral OB stocks were obtained from the bacmids as described in Chapter 5. Infections were conducted as described in Chapter 5 and carried out in two rounds. A mock infection (without virus) was taken along as a negative control. Approximately 4700 larvae in the early third larval stage, were orally infected with a concentration of 108 OBs/ml in a 10% w/v sucrose solution with a small amount of Patent Blue (Fluka Chemie GmbH). First, a mock infection was performed, followed by infections with WT, Δ*ptp* and catmut AcMNPV. To ensure the ingestion of the viral suspension, larvae with a blue gut were selected and individual larvae were moved to a single well of a 12-well plate with an 8 x 8 x 8 mm food cube in each well. Plates were covered with parafilm and paper tissue to avoid larval escape. The virus and mock infected larvae were kept at 27°C until the end of the experiment (9 dpi).

2.3 Screening for infection and sampling

Samples were taken from individual larvae, mock-infected or infected with one of the viral constructs (WT, Δ*ptp* or catmut), at three different time points: 1 dpi, 3 dpi and 4 dpi. From samples of the first infection round, haemolymph (for ELISA measurements, see below) was extracted at 1 dpi whereas during the second infection round, haemolymph as well as RNA (see below) was collected at 1, 3 and 4 dpi. Sampling was carried out in three biological replicates and at 3 and 4 dpi, a selection could be carried out for successfully infected larvae by screening the individual larvae for eGFP expression. The expression of eGFP in living larvae was verified on the sampling days with a stereomicroscope (Leica Wild M3Z) and an UV-lamp (Leica HBO lamp). Subsequently, pictures were taken with the Coolsnap digital camera of a selection of the larvae, representing the infection status (Supplementary Figure S1). As eGFP-expression cannot be detected at 1 dpi but firstly from 2 dpi onwards, the selection of larvae expressing eGFP was only possible at the later timepoints (3 and 4 dpi) and therefore, sampling at 1 dpi was conducted at random. Larvae sampled at 1 dpi were late third instar (LL3), at 3 dpi all larvae were mid fourth instar (mL4) and at 4 dpi all virus-infected larvae were still mL4, while the mock-infected individuals had moulted into the early fifth instar (eL5) (Supplementary Figure S1; Supplementary Table S1). Only larvae showing equal levels of eGFP expression at a given dpi were included. Selected larvae were snap-frozen in liquid nitrogen, whereafter they were stored at -80°C until RNA-isolation or haemolymph extractions were conducted. To follow the infection success with the different viruses, 460 larvae were screened for survival or liquefaction due to AcMNPV-infection at 2, 4, 7 and 9 dpi (see Supplementary Table S1).

2.4 Quantitative PCR on genes encoding 14-3-3 proteins and rate-limiting enzymes of the biogenic amines and their receptors

For this study, gene specific primers (Supplementary Table S2) were designed for two viral genes of AcMNPV and 16 *S. exigua* genes involved in the synthesis and reception of dopamine, octopamine and serotonin and two proteins of the 14-3-3 protein family. All primers were designed with Primer3 (version 4.1.0) (Rozen and Skaletsky 1999) to amplify 90-150 base pair fragments of genes encoding for the viral proteins PTP and GP64, the *S. exigua* activator proteins of TH and TPH (14-3-3 zeta and 14-3-3 epsilon), the *S. exigua* rate limiting enzymes for the synthesis of DA, OA and 5HT (TH, TDC and TPH respectively) and a subset of DA, OA and 5HT receptors (5HT1a, 5HT-7, TAR1, TAR2, OCTP1, OCTP2, OCTP3, DOP, DOP1, DOP2 and INDR). Primer design was based on the assembled *S. exigua* genome and transcriptome (Simon *et al.* 2021), which were originally obtained from the rearing present in our laboratory. For all targeted *S. exigua* genes, homologous proteins of related *Spodoptera* species and other Noctuidae were retrieved from NCBI and used as a query against both the transcriptome and genome with the standalone tblastn command (v 14.2.0) Next, transcripts and genomic regions that showed a high similarity with these query proteins were extracted and aligned with MUSCLE (Edgar 2004) revealing the intron-exon pattern in order to design intron-spanning primers, where possible.

2.5 RNA-isolation and quantitative PCR

For each biological sample, five larval heads were cut off at the second thoracic leg pair and RNA was isolated using TRIzol (Ambion). The following steps were conducted on ice. Per sample, 5 heads were grinded using a pestle in an Eppendorf tube with 250 µl TRIzol. To that 72 µl chloroform was added and the sample was incubated for 3 minutes on ice, then briefly vortexed and centrifugated at 4°C at 12.000 rpm for 5 minutes. Then 125 µl of the upper water phase was transferred to new Eppendorf tubes, 125 µl isopropanol was added and the sample was briefly vortexed for 6

seconds. Samples were incubated for 10 minutes at room temperature (RT) and then centrifugated for 10 minutes at 4°C and 12.000 rpm. The supernatant was discarded and the pellet was washed twice by adding 200 µl ice-cold 70% ethanol, centrifugating at 7.500 rpm for 5 minutes at 4°C, and each time discarding the supernatant. The clean pellet was airdried for 10 minutes, dissolved in autoclaved Milli-Q water and incubated at 55°C for maximum 15 minutes. Next, DNA was removed from extracted RNA samples with the DNA-freeTM kit (Ambion) following the supplier's instructions. The quality and quantity of the RNA were checked using the NanoDrop-1000 spectrophotometer (Thermo Fisher Scientific) and by running the RNA samples on a 1% agarose gel. The isolated DNAse-treated RNA was stored at -80°C until cDNA conversion using SuperScript III Reverse Transcriptase (Invitrogen) with oligo dT primers. A standardised amount of 2000 ng RNA input per cDNA conversion reaction was used. Subsequently, a quantitative PCR (qPCR) was conducted on the samples targeting a selection of potential *S. exigua* housekeeping genes (Zhu *et al.* 2014) (β-actin1, β-actin2, *elongation factor 1* (*ef1*), *elongation factor 2* (*ef2*), *glyceraldehyde-3-phosphate dehydrogenase* (*gadph*) and *ribosomal protein L10* (L10)) and a set of viral and *S. exigua* target genes. Suitability of housekeeping genes was tested as described below (section 2.7). All qPCR reactions were prepared with the SYBR™ Select Master Mix following the manufacturer's protocol (Thermo Fisher Scientific Inc.) with a final primer concentration of 0.4 µM per primer in a total volume of 20 µl of which 2 µl of 1/10 diluted cDNA, in the thermal cycler CFX96 Touch Real-Time PCR (Bio-Rad). Reactions were run with the following protocol: initial UDG activation at 50°C for 2 min, initial denaturation at 95°C for 3 min followed by 40 cycles of 95°C for 10 sec, 58°C for 15 sec, 72°C for 1 min. However, for the primer pair targeting the *ptp* gene, an annealing temperature of 62°C was used. At the end of these cycles, a melting curve (from 60°C to 95°C, 1°C per 2 sec) was generated to confirm the absence of non-specific amplification. Standard curves were constructed for every primer pair using different cDNA dilutions from pooled samples to calculate the primer specific amplification efficiency.

2.6 Specific ELISA for OA, DA and 5HT

Haemolymph was extracted from individual virus-infected and mock-infected larvae in three biological replicates at 1 dpi, 3 dpi and 4 dpi. Haemolymph was pooled from 75 larvae at 1 dpi, from 20 larvae at 3 dpi, and from 15 larvae at 4 dpi, per treatment and per replicate. Each pool of haemolymph was mixed 1:3 with methanol, and subsequently aliquoted into 30 µl and stored at -80°C until the three separate ELISA runs (5HT, DA and OA). Samples were centrifuged at 4°C for 10 minutes at 20.000 rcf., whereafter the supernatant was transferred to new tubes, which were placed in a SpeedVac until all the methanol had evaporated with a maximum evaporation of 10 minutes (the described procedure is adapted from Abuhagr *et al.* 2014; Rosero *et al.* 2019; Koyama and Mirth 2021). Five µl of each sample was mixed with 210 µl of a diluent (for 5HT), Milli-Q water (for DA) or PBS (pH 7.5) (for OA) according to the manual of the respective ELISA kits (ImmuSmol for DA and 5HT, MyBioSource for OA). Next, the competitive ELISAs were performed in accordance with the providers' protocols. Each ELISA run included negative controls, two technical replicates for the three biological replicates and the standards included in the kit to determine the concentrations of the target protein in each sample.

2.7 Data and statistical analyses

The qPCR analyses were carried out in QBase+ (v 3.4). Two parameters (geNorm M and geNorm V) were used to select the most stable housekeeping genes (out of six candidates, see 2.5) and the optimal number of housekeeping genes that should be used, respectively. Based on these parameters, two housekeeping genes (β-actin1 and *gadph*) were selected and the obtained geometric mean of these genes were used to calculate the optimal normalisation factor. The primer specific amplification efficiencies ranged from 88-110% for all targeted genes. Per target gene, the normalised relative quantities (NRQs) were calculated. Next, the NRQs were rescaled using the average expression level of a gene across all samples. These rescaled normalised data were exported from QBase+ and used for further analyses. Results of the ELISA experiments were analysed by plotting the measured mean absorbances of the standards provided by the supplier (ImmuSmol, MyBioSource) on the y-axis (linear) against the mean of each standard concentration on the x-axis (logarithmic), generating equations from the linear trendlines that were used for calculation of the unknown samples. The concentrations calculated were inverted with the 10^ function, and were given in ng/ml. For each biogenic amine, the mean of the technical replicates was tested for normality (Shapiro-Wilk test). A two-way ANOVA was performed to analyse the effect of treatment (mock, WT, Δ*ptp*, catmut) and days post infection on the gene expression data and the ELISA measurements. When one of the two factors (treatment and days post infection) or their interaction had a statistically significant effect ($p<0.050$), Tukey's honest significant (HSD) tests were performed as a post hoc test to assess multiple comparisons (Lee and Lee 2018). All datasets were checked for homogeneity of variance and normality. When the assumptions were violated, a log10 transformation was carried out. This transformation was carried out on the NRQs of the gene targets *gp64, tdc, tar1, tbh, octp1, octp2, octp3, th, dop1, dop2, indr, tph, 5ht-1* and *5ht-7* which resulted in the assumptions being fulfilled. Visualisations and statistical analyses were carried out in R (v 4.2.2.) with Rstudio (v 2022.12.0) using the following R packages: car (v 3.1-2), dplyr (v 1.1.3), ggplot2 (v 3.4.0), multcompView (v 0.1-9), and readr (v 2.1.4).

3 Results

3.1 Gene expression of viral genes confirms an increasing virus infection and eGFP-expression during the successive days post infection

To confirm the infection of the larvae by AcMNPV, the gene expression of the viral gene *gp64*, encoding for an essential envelope fusion protein that is required for cell-to-cell transmission of infection (Monsma *et al.* 1996), was tested. *Gp64* is transcribed early in the infection, but also has a late promotor element (van Oers 2021). The gene expression data of *gp64* confirms the replication of AcMNPV at 3 and 4 dpi for all viral treatments and the absence of the virus in the mock infected samples at 1, 3 and 4 dpi. Furthermore, gene expression of *gp64* was not seen in the larval heads at 1 dpi for all treatments, suggesting that the virus is absent in heads of virus-infected larvae at this timepoint. This is in line with the visual eGFP observations absent at 1 dpi, but present at 3 and 4 dpi in virus-infected larvae (Supplementary Figure S1; Supplementary Table S1). The *gp64* expression showed to be dependent on the interaction of treatment and days post infection (df=6, p<0.001). Multiple comparisons confirmed that the expression of *gp64* was undetectable at 1, 3 and 4 dpi for the mock infection and at 1 dpi for all the viral treatments (Figure 2). Furthermore, at 3 and 4 dpi, the level of *gp64* expression was not significantly different between the different viral treatments nor between those days. For larvae infected with AcMNPV WT and catmut, the *ptp* gene was expressed at 3 and 4 dpi and expression was not significantly different between those treatments or between days (Figure 3). In addition, no viral *ptp* expression was detected at 1, 3 and 4 dpi in heads of the mock- or AcMNPV Δ*ptp*-infected larvae.

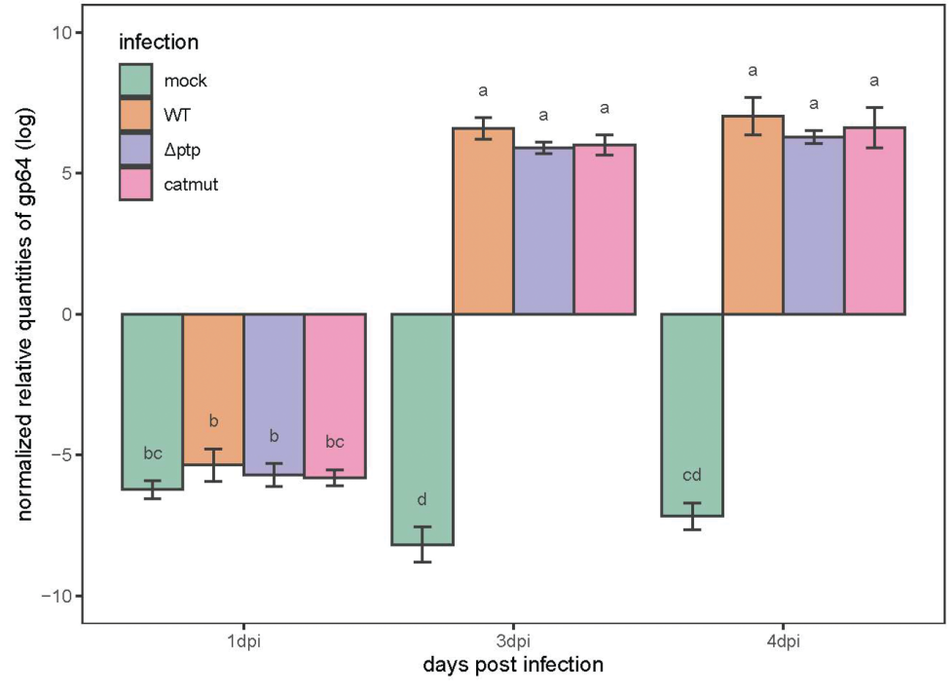

Figure 2. Transcriptional response of the viral *gp64* gene in heads of *S. exigua* larvae infected as early third instar with no virus (mock), WT, Δ*ptp*, or catmut AcMNPV, at 1, 3 and 4 days post infection, quantified by qPCR. The y-axis represents the normalised relative quantities of *gp64* (log transformed), while the x-axis represents the combination of viral infection and days post infection. Error bars represent the standard deviation (n=3). Different letters indicate a significant difference between groups (p=0.05).

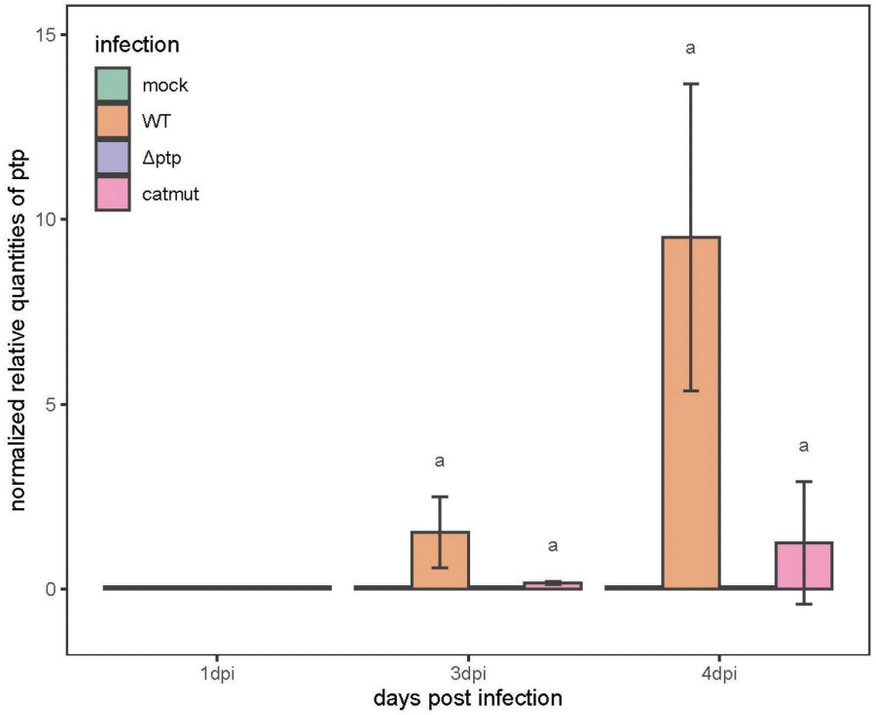

Figure 3. Transcriptional response of the viral *ptp* gene in heads of *S. exigua* larvae infected as early third instar with no virus (mock), WT, Δptp, or catmut AcMNPV, at 1, 3 and 4 days post infection (dpi), quantified by qPCR. The y-axis represents the normalised relative quantities of *ptp*, while the x-axis represents the combination of viral infection and days post infection. Error bars represent the standard deviation (n=3). Different letters indicate a significant difference between groups (p=0.05).

3.2 The activators 14-3-3 epsilon and 14-3-3 zeta

When observing the expression of the gene encoding for the 14-3-3 epsilon protein, it was not significantly affected by the days post infection, the treatment nor their interaction. On the other hand, the transcription levels of the gene encoding for 14-3-3 zeta were significantly influenced by the days post infection (df=2, p<0.001) and the treatment (df=3, p<0.050), but not by the interaction between those two factors. Gene expression of *14-3-3 zeta* was highest at 1 dpi and decreasing towards 3 dpi and 4 dpi (Figure 4). A higher gene expression of the gene *14-3-3 zeta* was also observed when larvae where infected with AcMNPV catmut compared to when an infection with AcMNPV Δ*ptp* was carried out (Figure 5).

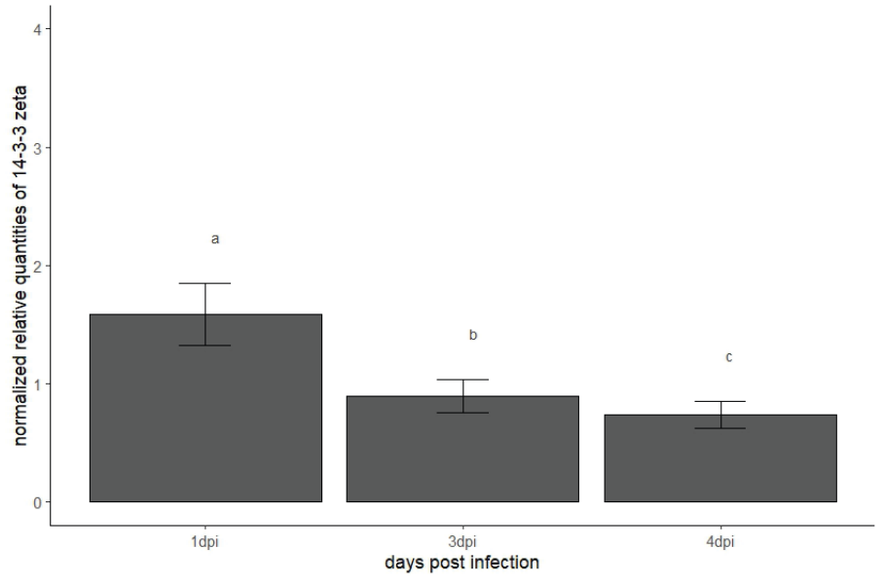

Figure 4. Transcriptional response of the *14-3-3 zeta* gene in heads of *S. exigua* larvae infected as early third instar with no virus (mock), WT, Δ*ptp*, or catmut AcMNPV at 1, 3 and 4 days post infection (dpi) quantified by qPCR. The y-axis represents the normalised relative quantities of *14-3-3 zeta*, while the x-axis represents the different days post infection. Error bars represent the standard deviation (n=3). Different letters indicate a significant difference between days post infection (p=0.05).

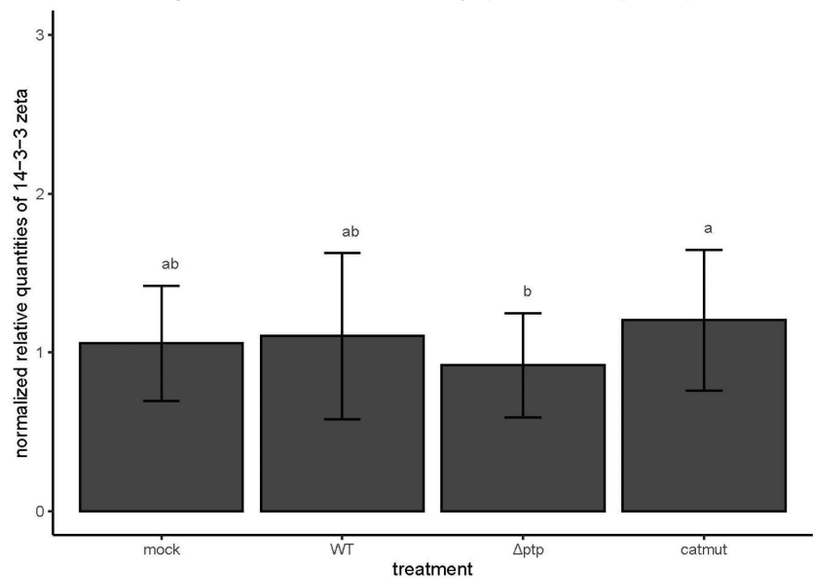

Figure 5. Transcriptional response of the 14-3-3 zeta gene in heads of *S. exigua* larvae infected as early third instar with no virus (mock), WT, Δ*ptp*, or catmut AcMNPV, quantified by qPCR. The y-axis represents the normalised relative quantities of *14-3-3 zeta*, while the x-axis represents the different days post infection. Error bars represent the standard deviation (n=3). Different letters indicate a significant difference between treatments (p=0.05).

3.3 Tyramine

The genes encoding the rate-limiting enzyme (TDC) and one of the receptors (TAR2) for tyramine synthesis and tyramine binding, respectively, showed a significantly higher expression at 1 dpi and then dropped in the following days (3 and 4 dpi) (df=2, p<0.001 and df=2, p<0.001, respectively) (Figure 6; Figure 7). Virus infection had no influence on the gene expression of either *tdc* or one tyramine receptor *tar2*, since expression was not significantly different between heads of mock-infected larvae or of larvae infected with each of the three viruses. However, the gene encoding for another tyramine receptor, *tar1*, displayed a different expression pattern. Significant differences were found between the days post infection (df=2, p<0.050) and different treatments (df=3, p<0.001). At 4 dpi, the *tar1* gen displayed an upregulation compared to 1 dpi (Figure 8). Furthermore, this gene also showed to be higher expressed in heads of all virus-infected larvae compared to heads of mock-infected larvae. In addition, a significantly higher gene expression for the *tar1* gene was seen in heads of AcMNPV WT-infected larvae than those of AcMNPV Δ*ptp*-infected larvae (Figure 9). These results are pointing to an increase of the *tar1* gene expression resulting from a WT viral infection and to a role of the PTP protein in inducing this *tar1* gene upregulation.

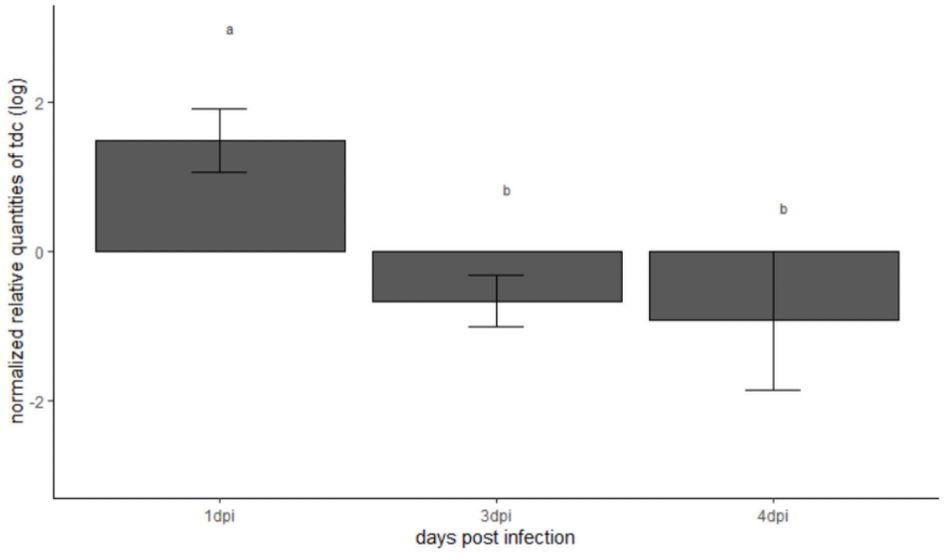

Figure 6. Transcriptional response of the *tdc* gene in heads of *S. exigua* larvae infected as early third instar with no virus (mock), WT, Δ*ptp*, or catmut AcMNPV at 1, 3 and 4 days post infection (dpi) quantified by qPCR. The y-axis represents the log transformation of the normalised relative quantities of *tdc*, while the x-axis represents the different days post infection. Error bars represent the standard deviation (n=3). Different letters indicate a significant difference between days post infection (p=0.05).

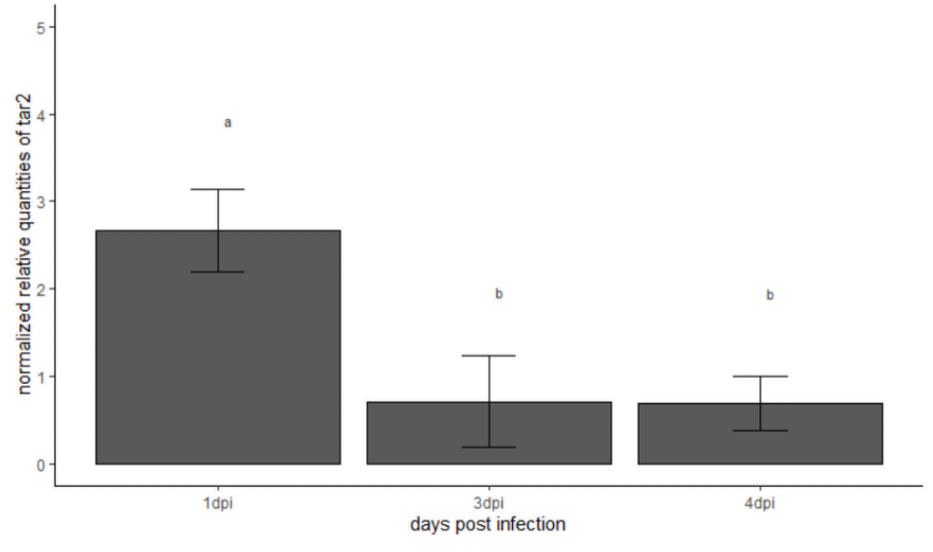

Figure 7. Transcriptional response of the *tar2* gene in heads of *S. exigua* larvae infected as early third instar with no virus (mock), WT, Δ*ptp*, or catmut AcMNPV at 1, 3 and 4 days post infection (dpi), quantified by qPCR. The y-axis represents the normalised relative quantities of *tar2*, while the x-axis represents the different days post infection. Error bars represent the standard deviation (n=3). Different letters indicate a significant difference between days post infection (p=0.05).

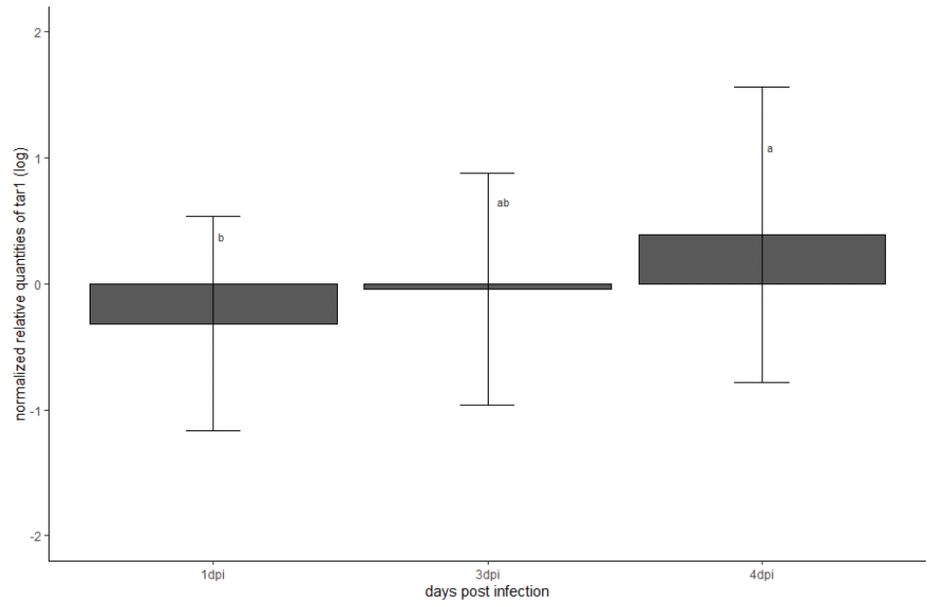

Figure 8. Transcriptional response of the *tar1* gene in heads of *S. exigua* larvae infected as early third instar with no virus (mock), WT, Δ*ptp*, or catmut AcMNPV at 1, 3 and 4 days post infection (dpi), quantified by qPCR. The y-axis represents the normalised relative quantities of *tar2*, while the x-axis represents the different days post infection. Error bars represent the standard deviation (n=3). Different letters indicate a significant difference between days post infection (p=0.05).

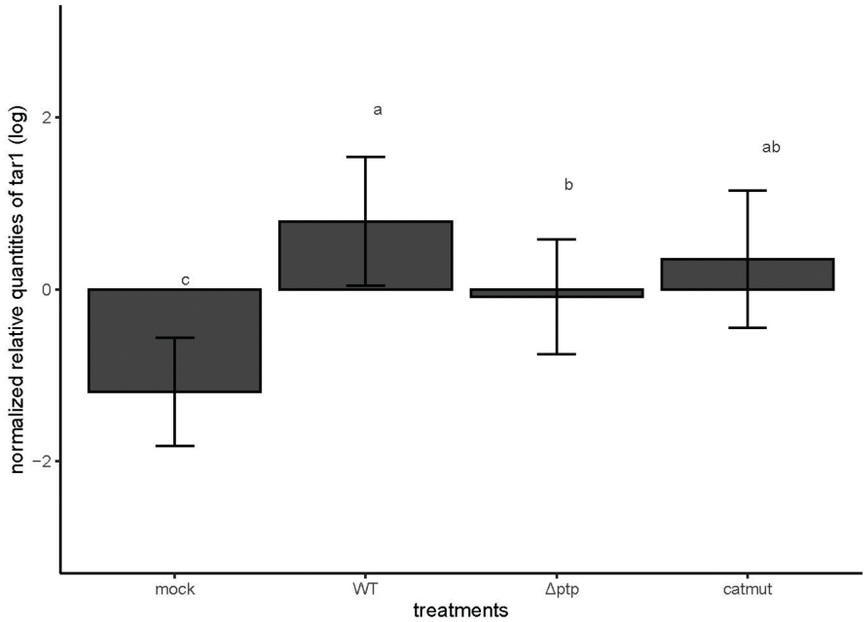

Figure 9. Transcriptional response of the *tar1* gene in heads of *S. exigua* larvae infected as early third instar with no virus (mock), WT, Δ*ptp*, or catmut AcMNPV, quantified by qPCR. The y-axis represents the normalised relative quantities of *tar1*, while the x-axis represents the treatments. Error bars represent the standard deviation (n=3). Different letters indicate a significant difference between treatments (p=0.05).

3.4 Octopamine

Quantitative PCR showed that the gene transcribing the enzyme TBH for the biogenic amine octopamine was affected by the interaction of the days post infection and the treatment (df=6, p<0.050). At 1 dpi, the expression of *tbh* was the highest for all treatments (Figure 10). In addition, the gene expression decreased and reached the lowest level in the larvae of the mock infection at 4 dpi which was significantly different from larvae of the mock infection at 3 dpi, of the AcMNPV WT infection at 3 and 4 dpi and of the AcMNPV catmut infection at 4 dpi.

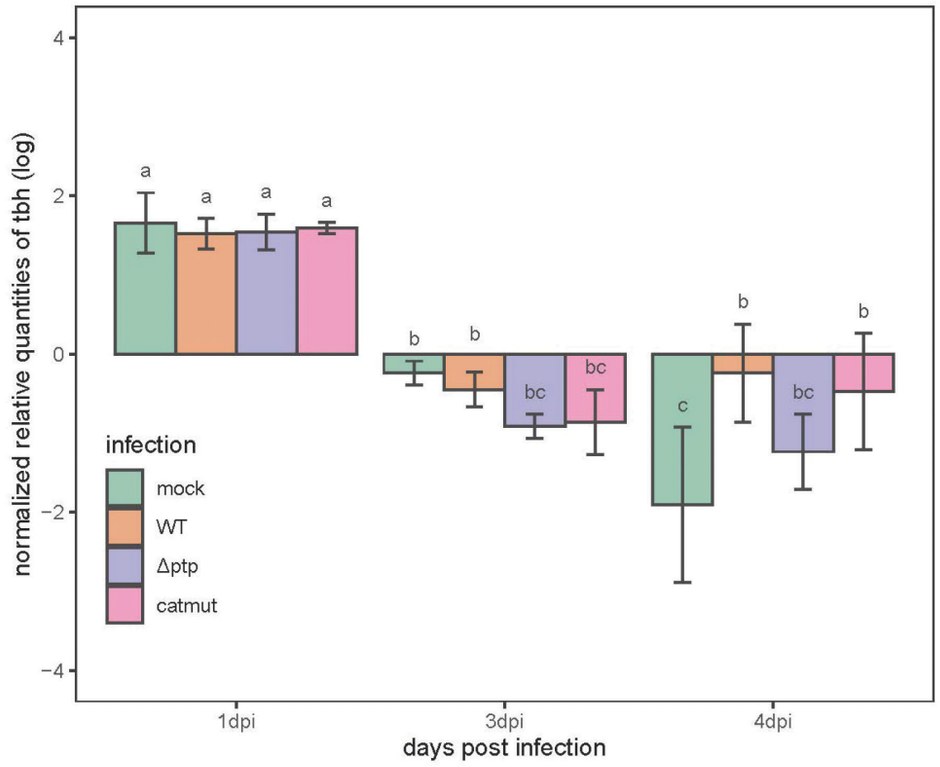

Figure 10. Transcriptional response of the *tbh* gene in heads of *S. exigua* larvae infected as early third instar with no virus (mock), WT, Δ*ptp*, or catmut AcMNPV at 1, 3 and 4 days post infection (dpi), quantified by qPCR. The y-axis represents the log transformation of the normalised relative quantities of *tbh*, while the x-axis represents the combination of viral infection and days post infection. Error bars represent the standard deviation (n=3). Different letters indicate a significant difference between groups (p=0.05).

The expression of the genes encoding two receptors for octopamine (*octp1* and *octp2*) showed a pattern with a significant effect of the days post infection (df=2, p<0.001, df=2, p<0.001, respectively). Moreover, at 1 dpi the expression of *octp1* and *octp2* was significantly higher than at 3 dpi. For *octp1,* the transcripts increased again significantly at 4 dpi however this trend was not observed for *octp2* where expression stayed low until 4 dpi (Figure 11; Figure 12). The expression of the gene encoding octopamine receptor *octp3* was influenced by the interaction of the treatment and the days post infection (df=6, p<0.05). The *octp3* expression of all biological groups (treatment x dpi) were not significantly different among each other except for the expression in mock-infected larvae at 3 dpi which was significantly downregulated compared to the expression in larvae after infection with the AcMNPV catmut at 4 dpi (Figure 13).

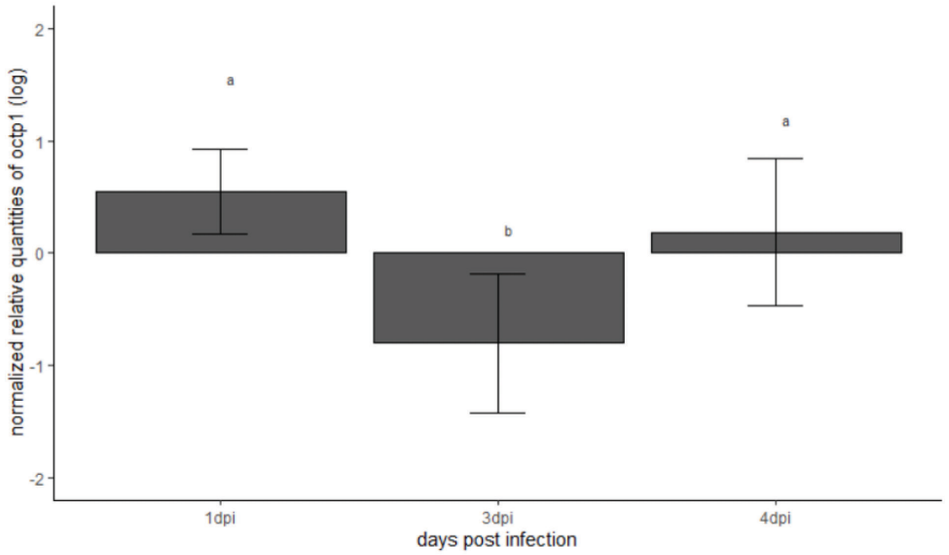

Figure 11. Transcriptional response of the *octp1* gene in heads of *S. exigua* larvae infected as early third instar with no virus (mock), WT, Δ*ptp*, or catmut AcMNPV at 1, 3 and 4 days post infection (dpi), quantified by qPCR. The y-axis represents the log transformation of normalised relative quantities of *octp1*, while the x-axis represents the different days post infection. Error bars represent the standard deviation (n=3). Different letters indicate a significant difference between days post infection (p=0.05).

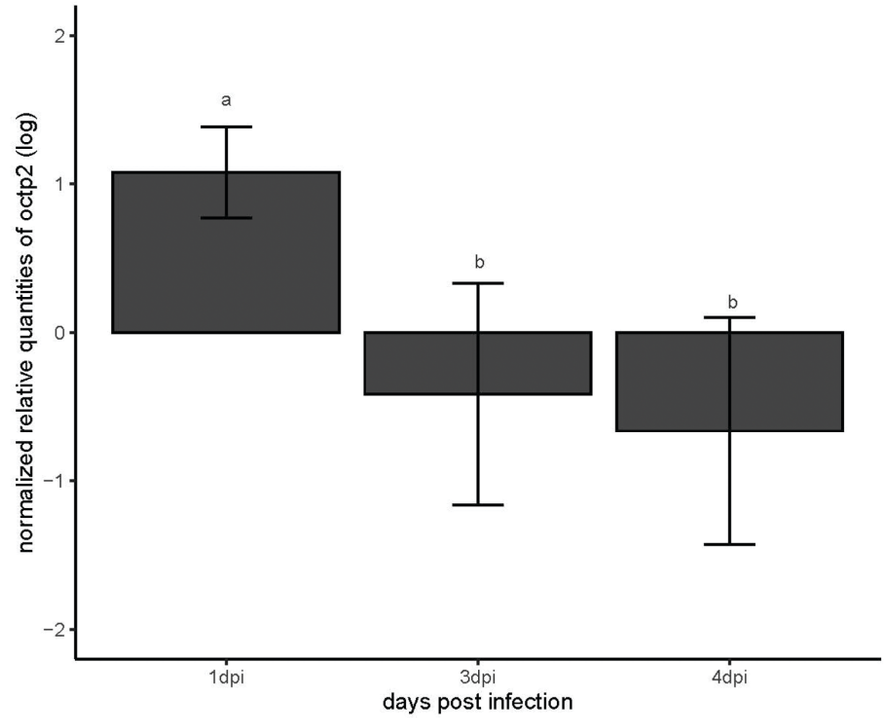

Figure 12. Transcriptional response of the *octp2* gene in heads of *S. exigua* larvae infected as early third instar with no virus (mock), WT, Δ*ptp*, or catmut AcMNPV, at 1, 3 and 4 days post infection (dpi) quantified by qPCR. The y-axis represents the log transformation of the normalised relative quantities of *octp2*, while the x-axis represents the different days post infection. Error bars represent the standard deviation (n=3). Different letters indicate a significant difference between days post infection (p=0.05).

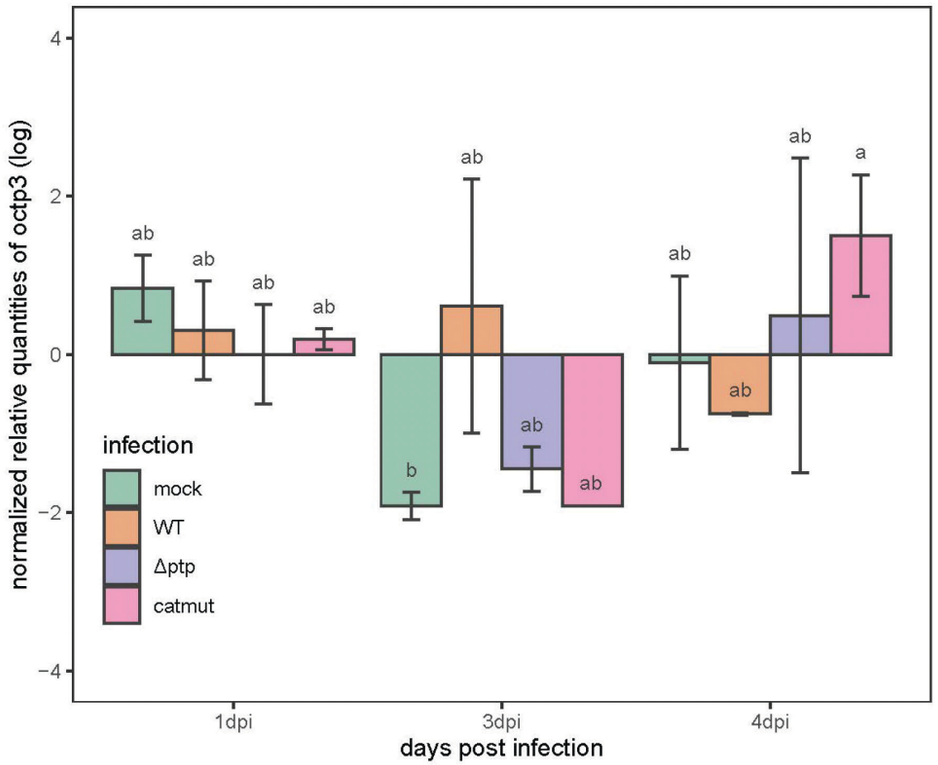

Figure 13. Transcriptional response of the *octp3* gene in heads of *S. exigua* larvae infected as early third instar with no virus (mock), WT, Δ*ptp*, or catmut AcMNPV at 1, 3 and 4 days post infection, quantified by qPCR. The y-axis represents the log transformation of the normalised relative quantities of *octp3*, while the x-axis represents the combination of viral infection and days post infection. Error bars represent the standard deviation (n=3). Different letters indicate a significant difference between groups (p=0.05).

Quantification of octopamine concentrations measured in the larval haemolymph ranged from 0.086 - 0.187 ng/ml (Figure 14) which fell in the range standards provided with the ELISA kit. Neither of the factors, treatment and days post infection, nor their interaction, had a statistically significant effect on the concentrations of octopamine in the haemolymph of larvae.

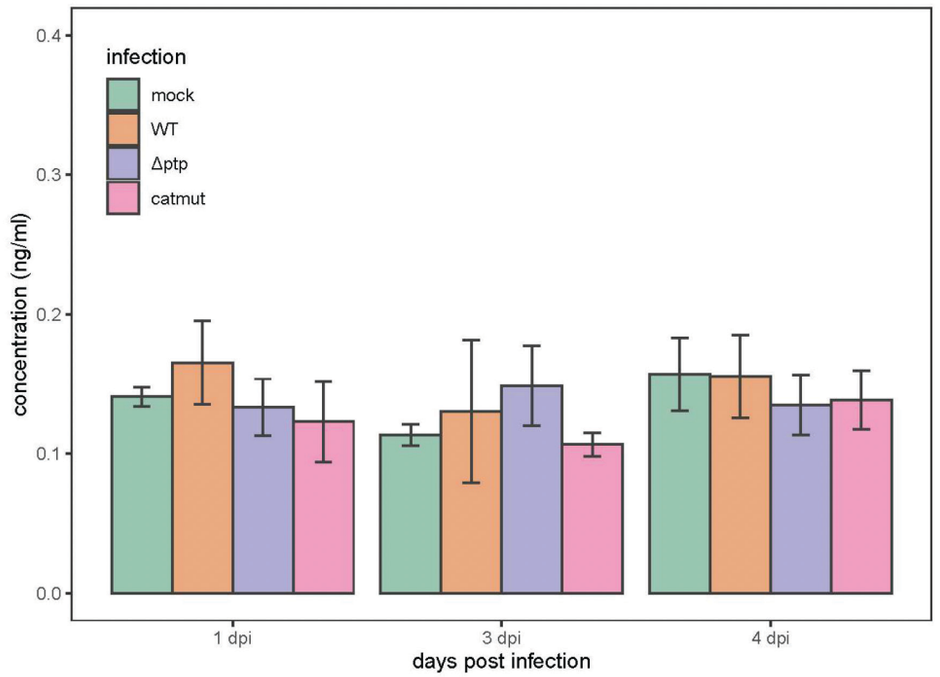

Figure 14. Calculated concentration of octopamine from the haemolymph of *S. exigua* caterpillars infected as early third instar with no virus (mock), WT, Δ*ptp*, or catmut AcMNPV at 1, 3 and 4 days post infection (dpi). The y-axis represents the octopamine concentration (ng/ml), while the x-axis represents the combination of viral infection and days post infection. Error bars represent the standard deviation (n=3). Different letters indicate a significant difference between groups (p=0.05).

3.5 Dopamine

The expression of the gene encoding for the rate-limiting enzyme TH was affected by the interaction of the days post infection and treatment (df=6, p<0.001). Multiple comparisons showed that at 1 dpi, the gene *th* was significantly higher expressed in all treatments than at 3 and 4 dpi (Figure 15). In addition, the *th* expression was significantly downregulated in virus-infected larvae compared to mock-infected larvae at 3 and 4 dpi. Furthermore, three out of four dopamine receptor genes (*dop, dop1, dop2*) targeted showed to be only affected by the days post infections (df=2, p<0.001 for all tests). At 1 dpi, there was an upregulation of *dop, dop1* and *dop2* compared to 3 and 4 dpi (Figure 16; Figure 17; Figure 18). The regulation of the invertebrate dopamine receptor (*indr*) gene was not affected by the days post infection, the treatment nor the interaction of both. Moreover, none of the genes encoding for the dopamine receptors were significantly influenced by virus infections.

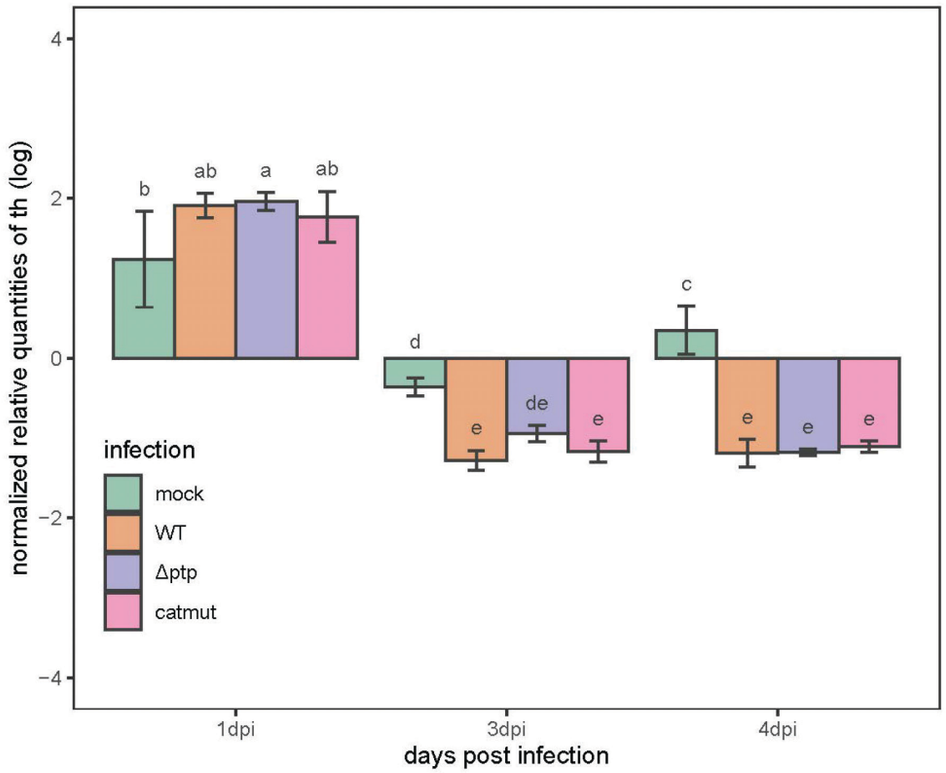

Figure 15. Transcriptional response of the *th* gene in heads of *S. exigua* larvae infected as early third instar with no virus (mock), WT, Δ*ptp*, or catmut AcMNPV at 1, 3 and 4 days post infection (dpi), quantified by qPCR. The y-axis represents the log transformation of the normalised relative quantities of *th*, while the x-axis represents the combination of viral infection and days post infection. Error bars represent the standard deviation (n=3). Different letters indicate a significant difference between groups (p=0.05).

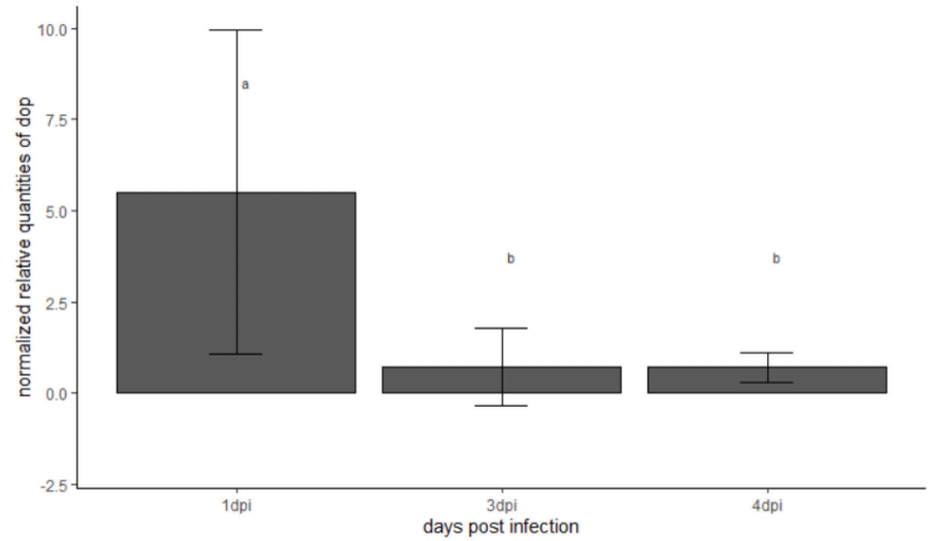

Figure 16. Transcriptional response of the *dop* gene in heads of *S. exigua* larvae infected as early third instar with no virus (mock), WT, Δ*ptp*, or catmut AcMNPV at 1, 3 and 4 days post infection (dpi), quantified by qPCR. The y-axis represents the log transformation of the normalised relative quantities of *dop*, while the x-axis represents the different days post infection. Error bars represent the standard deviation (n=3). Different letters indicate a significant difference between days post infection (p=0.05).

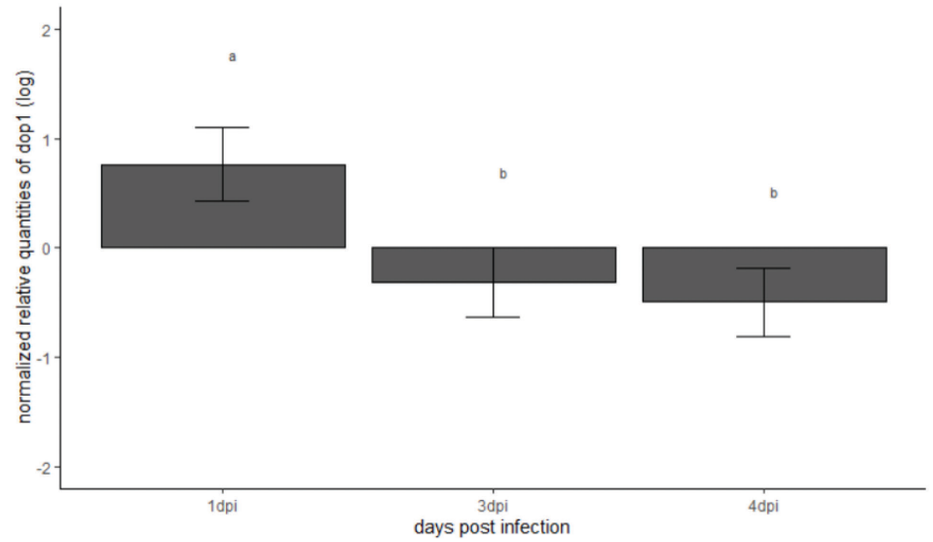

Figure 17. Transcriptional response of the *dop1* gene in heads of *S. exigua* larvae infected as early third instar with no virus (mock), WT, Δ*ptp*, or catmut AcMNPV at 1, 3 and 4 days post infection (dpi), quantified by qPCR. The y-axis represents the log transformation of the normalised relative quantities of *dop1*, while the x-axis represents the different days post infection. Error bars represent the standard deviation (n=3). Different letters indicate a significant difference between days post infection (p=0.05).

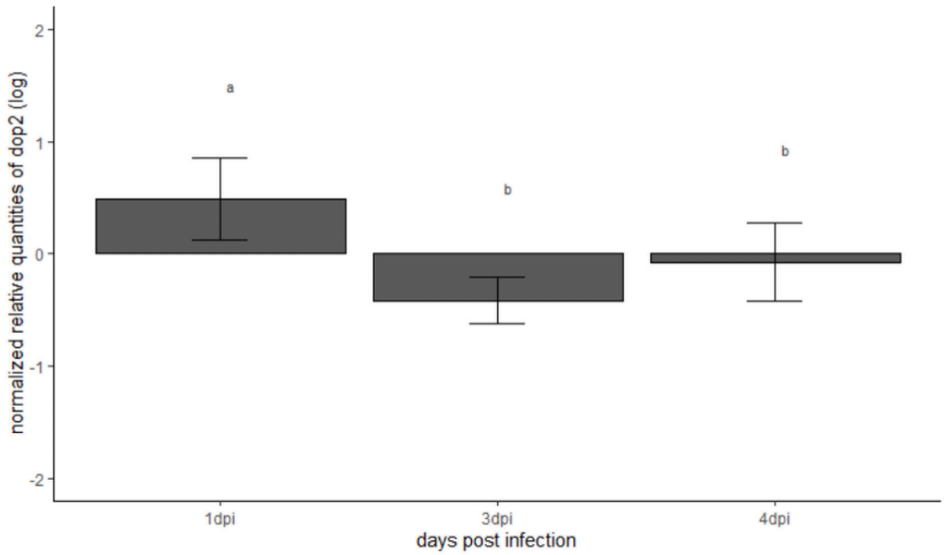

Figure 18. Transcriptional response of the *dop2* gene in heads of *S. exigua* larvae infected as early third instar with no virus (mock), WT, Δ*ptp*, or catmut AcMNPV at 1, 3 and 4 days post infection (dpi), quantified by qPCR. The y-axis represents the log transformation of the normalised relative quantities of *dop2*, while the x-axis represents the different days post infection. Error bars represent the standard deviation (n=3). Different letters indicate a significant difference between days post infection (p=0.05).

The concentrations of dopamine measured in larval haemolymph ranged from 9.02 - 16.15 ng/ml (Figure 19). The concentration of dopamine was highly impacted by the interaction between treatment and days post infection (df=6, p<0.0001,). At 1 dpi, no differences in dopamine concentrations were observed between mock- or any of the virus-infected treatments. At 3 dpi, dopamine concentrations in the haemolymph were significantly lower in AcMNPV WT- and AcMNPV Δ*ptp*-infected larvae compared to mock-infected larvae. At 4 dpi, dopamine concentrations were significantly lower in haemolymph of AcMNPV Δ*ptp*- and catmut-infected larvae compared to mock- and AcMNPV WT-infected larvae.

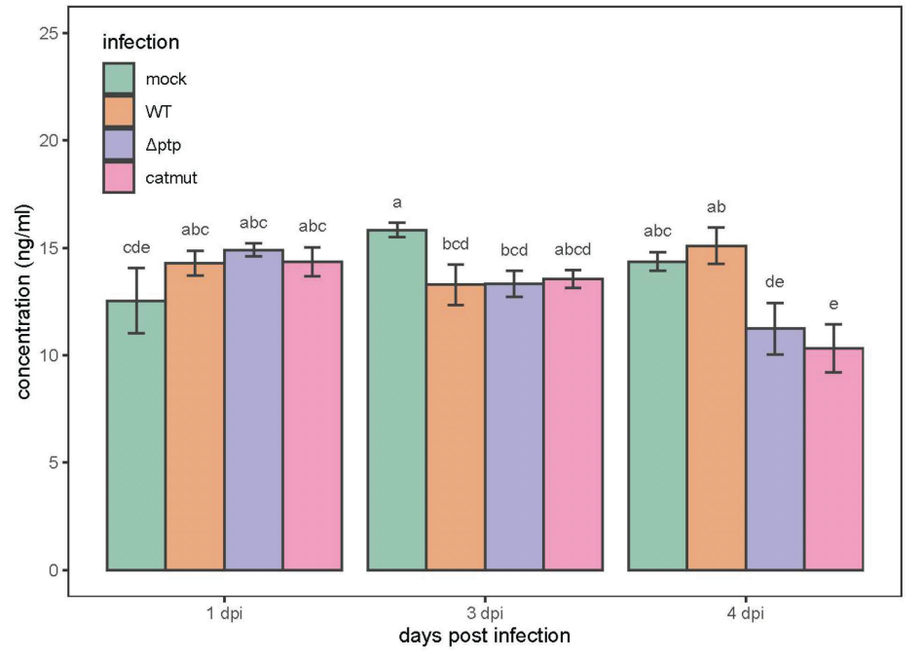

Figure 19. Calculated concentration of dopamine from the haemolymph of *S. exigua* caterpillars infected as early third instar with no virus (mock), WT, Δ*ptp*, or catmut AcMNPV at 1, 3 and 4 days post infection (dpi). The y-axis represents the dopamine concentration (ng/ml), while the x-axis represents the combination of viral infection and days post infection. Error bars represent the standard deviation (n=3). Different letters indicate a significant difference between groups (p=0.05).

3.6 Serotonin

Similarly, to the abovementioned results for the genes encoding the rate-limiting enzymes TDC, TBH and TH, the expression of the gene encoding TPH was greatly influenced by the days post infection (df=2, p<0.001) and not by the treatment nor the interaction of both. At 1 dpi, the *tph* expression showed to be significantly higher than at 3 and 4 dpi (Figure 20). The expression of *5ht-1a* and *5ht-7,* two genes encoding for the serotonin receptors, displayed the same trend based on the days post infection (df=2, p<0.001 and df=2, p<0.050, respectively) (Figure 21; Figure 22), with a higher expression at 1 dpi compared to 3 and 4 dpi. Additionally, the treatments also significantly influenced the gene expression of *5ht-7* (df=3, p<0.050) which resulted in a higher expression of this gene in larvae infected with AcMNPV WT compared to mock infected larvae (Figure 23). While expression levels in larvae infected with either AcMNPV Δ*ptp* or AcMNPV catmut were not significantly different from mock- or AcMNPV WT-infected larvae, a trend can be seen that viral infections increase the gene expression of *5ht-7*. This could point to a role of *ptp*/PTP in affecting the gene expression of the 5HT-7 receptor.

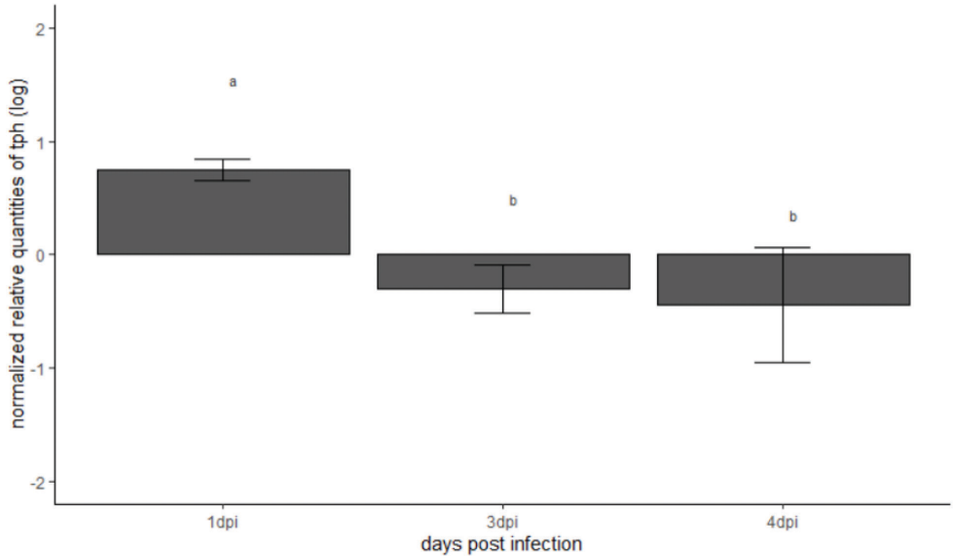

Figure 20. Transcriptional response of the *tph* gene in heads of *S. exigua* larvae infected as early third instar with no virus (mock), WT, Δ*ptp*, or catmut AcMNPV at 1, 3 and 4 days post infection (dpi), quantified by qPCR. The y-axis represents the log transformation of the normalised relative quantities of *tph*, while the x-axis represents the different days post infection. Error bars represent the standard deviation (n=3). Different letters indicate a significant difference between days post infection (p=0.05).

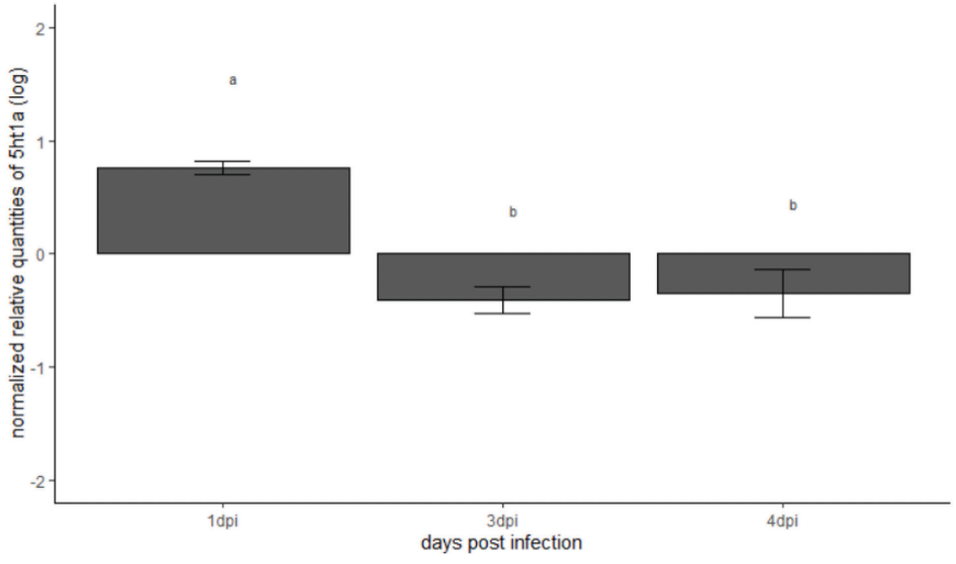

Figure 21. Transcriptional response of the *5ht-1a* gene in heads of *S. exigua* larvae infected as early third instar with no virus (mock), WT, Δ*ptp*, or catmut AcMNPV at 1, 3 and 4 days post infection (dpi), quantified by qPCR. The y-axis represents the log transformation of the normalised relative quantities of *5ht-1a*, while the x-axis represents the different days post infection. Error bars represent the standard deviation (n=3). Different letters indicate a significant difference between days post infection (p=0.05).

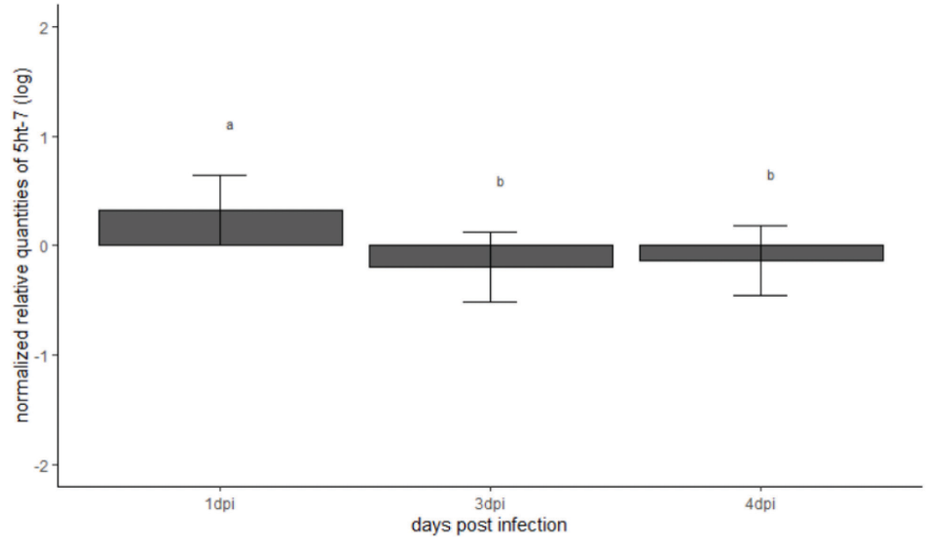

Figure 22. Transcriptional response of the *5ht-7* gene in heads of *S. exigua* larvae infected as early third instar with no virus (mock), WT, Δ*ptp*, or catmut AcMNPV at 1, 3 and 4 days post infection (dpi), quantified by qPCR. The y-axis represents the log transformation of the normalised relative quantities of *5ht-7*, while the x-axis represents the different days post infection. Error bars represent the standard deviation (n=3). Different letters indicate a significant difference between days post infection (p=0.05).

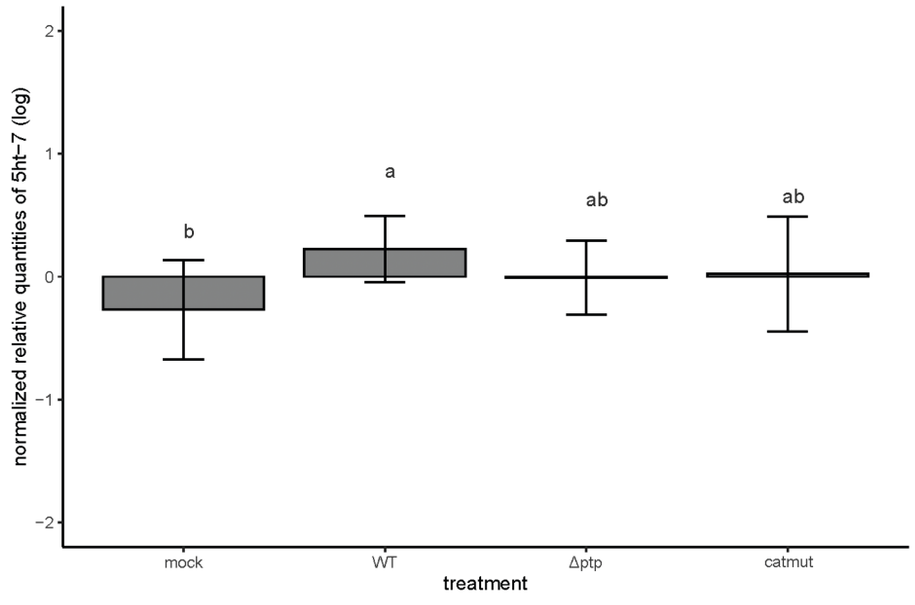

Figure 23. Transcriptional response of the *5ht-7* gene in heads of *S. exigua* larvae infected as early third instar with no virus (mock), WT, Δ*ptp*, or catmut AcMNPV quantified by qPCR. The y-axis represents the log transformation of the normalised relative quantities of *5ht-7*, while the x-axis represents the treatments. Error bars represent the standard deviation (n=3). Different letters indicate a significant difference between treatments (p=0.05).

In the haemolymph of the larvae, the serotonin concentrations were ranging from 1.49 - 3.31 ng/ml and analyses showed that this concentration was highly impacted by the interaction between dpi and treatment (df=6, p<0.0001). Serotonin levels seem higher in virus-infected compared to mock-infected larvae. At both 1 dpi and 4 dpi, serotonin levels were not different between mock- or virus-infected larvae. At 3 dpi, virus infections seem to increase serotonin levels, as levels were significantly higher in the haemolymph of AcMNPV Δ*ptp*- and AcMNPV catmut-infected larvae (but not AcMNPV WT-infected larvae), compared to mock-infected larvae.

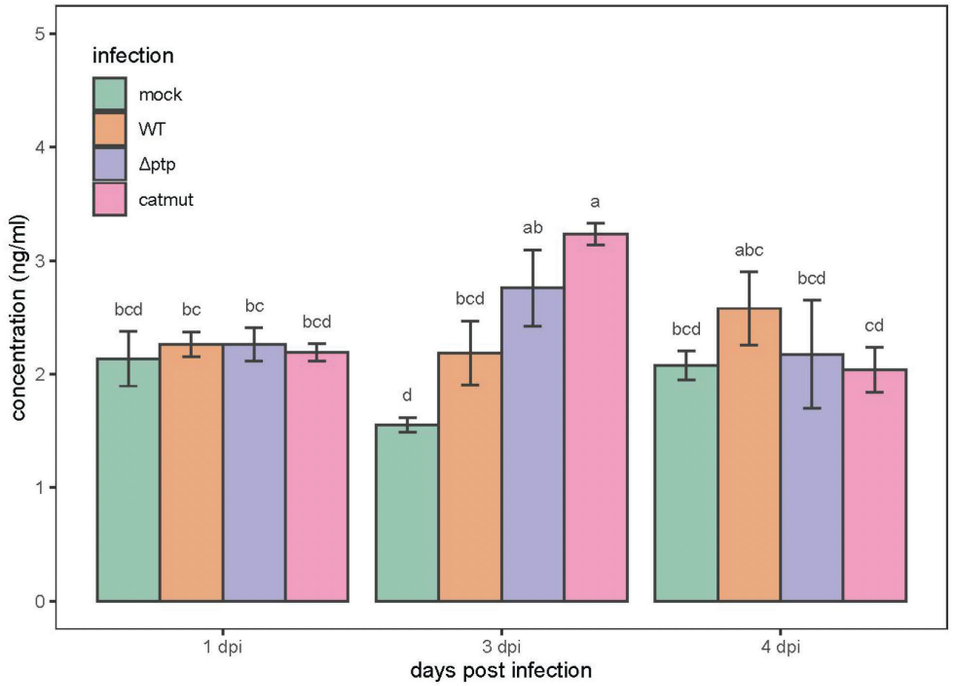

Figure 24. Calculated concentration of serotonin from the haemolymph of *S. exigua* caterpillars as early third instar with no virus (mock), WT, Δ*ptp*, or catmut AcMNPV at 1, 3 and 4 days post infection (dpi). The y-axis represents the dopamine concentration (ng/ml), while the x-axis represents the combination of viral infection and days post infection. Error bars represent the standard deviation (n=3). Different letters indicate a significant difference between groups (p=0.05).

4 Discussion

Biogenic amines can act as neurotransmitters, neuromodulators and neurohormones, orchestrating numerous processes in animals, including development, social interactions, immunity, the contraction properties of muscles and the activity of neurons

(Sinakevitch *et al.* 2018). Changes in biogenic amines like octopamine, dopamine, serotonin and tyramine and their specific receptors is linked to control various behaviours in insects and it is therefore hypothesised that biogenic amines, or their synthesis pathways, are targeted by behaviour-manipulating parasites (Adamo *et al.* 1997; Gasque *et al.* 2019).

In this study, we investigated how an infection with AcMNPV affected the concentration of octopamine, dopamine, serotonin in the *S. exigua* haemolymph and the expression of genes involved in the production and reception of octopamine, dopamine, serotonin and tyramine in *S. exigua* heads, at 1, 3 and 4 days post infection. Since the viral *ptp* gene is known to induce hyperactivity in *S. exigua* larvae, we compared infections by WT AcMNPV, an AcMNPV mutant lacking *ptp* (Δ*ptp*) and AcMNPV expressing a catalytically inactive PTP (catmut). First, we confirmed that an important gene for viral replication, *gp64,* was expressed from 3 dpi onwards in larval heads, which was consistent with the visual observation of eGFP in larvae from this timepoint onwards. This is in accordance with observations in Chapter 5 and in Herz *et al.* (2003), who detected epithelial and tracheal infections by the Helicoverpa armigera single nucleopolyhedrovirus (HaSNPV) in *S. exigua* larvae from 2 dpi. Furthermore, in our study the expression of *ptp* was only found in larvae infected with AcMNPV WT and AcMNPV catmut, and not for AcMNPV Δ*ptp*. Expression of *ptp* was still absent at 1 dpi, but present at 3 and 4 dpi. Although *ptp* expression did not differ significantly between larvae infected with AcMNPV Δ*ptp* and AcMNPV catmut, the qPCR results suggest that expression is higher in AcMNPV WT-infected larvae (Figure 3). This might be related to differences in the infection progression (Supplementary Table S1), although this is not reflected in the *gp64* expression data (Figure 2) which better reflects the progression of the infections.

Expression of genes encoding 14-3-3 zeta, the rate-limiting enzymes TDC and TPH and the receptors TAR2, OCTP1, OCTP2, DOP, DOP1, DOP2 and 5HT-1 was only dependent on the days post infection and showed the highest expression in larval heads at 1 dpi. This indicates that these genes rather fulfil a role in the developmental progression of *S. exigua* than being affected by the viral infections. The genes encoding for 14-3-3 epsilon and the dopamine receptor INDR were not affected by the infection nor the days post infection, pointing at another role than the factors tested in our experiments. The observation that the expression of the *14-3-3* genes was not affected, is in contrast with previous findings that point out the modulation of 14-3-3 proteins during viral infections as a key regulator for the expression of host and viral proteins (Nathan and Lal 2020; Liu *et al.* 2021). 14-3-3 proteins are known to be involved in the innate immunity by recognising the pathogen and inducing intracellular signalling, however, an increased expression of the 14-3-3- transcripts was not observed in our experimental setup. In previous studies, it was also observed that non-structural proteins of viruses bind to specific 14-3-3 proteins that allow

viruses to manipulate and modulate signalling and other cellular processes, yet this could not be confirmed from our analyses (Brockhaus *et al.* 1996). Furthermore, the genes encoding the rate-limiting enzymes TBH (involved in OA synthesis) and TH (involved in DA synthesis) and the octopamine receptor OCTP were affected by the interaction of treatment and the days after infection. For *tbh*, *th* and *octp3,* the highest gene expression was found at 1 dpi for all the infections including mock. When larvae were infected with viruses, no clear effect was detectable for *tbh* and *octp3* transcripts involved in the biosynthesis and reception of octopamine. This was also seen when looking at the octopamine concentrations in the haemolymph, which did not display significant differences related to viral infections. Analyses showed a significant decrease of *th* gene expression at 3 and 4 dpi when larvae where infected with viruses compared to the mock infection, indicating downregulation during viral infection. The dopamine concentrations measured had a similar decreasing trend for AcMNPV WT-infected larvae at 3 dpi and for the AcMNPV-Δ*ptp*- and AcMNPV-catmut-infected larvae at 4 dpi. However, this is contradicting with other studies where it was shown that dopamine increases during infections because of its connection between the immune and nervous system (Adamo *et al.* 2008; Kong *et al.* 2018). Dopamine signalling induces an early activation of the insects' haemocytes (Wu *et al.* 2015) which act in an autocrine way and further stimulate dopamine synthesis. This in its turn supports and stimulates the phagocytic activities, resulting in an increase of total haemocytes (Kong *et al.* 2018; Wu *et al.* 2015). An increase in dopamine has also been observed in the armyworm *Pseudaletia separata* parasitised by the parasitoid wasp *Cotesia kariyaiI* which injects polydnaviruses into the caterpillar (Noguchi *et al.* 1995). This increase of dopamine could be directly linked to the presence of the polydnaviruses and was reproduced by injecting a growth-blocking peptide resulting in a disturbance of normal larval development (Noguchi *et al.* 1995). In the case of *Aedes triseriatus* mosquitoes, an infection with La Crosse virus did not result in a change of dopamine levels, yet a 30% decrease of serotonin was observed in infected mosquitoes. Concentrations of both biogenic amines were analysed by high performance liquid chromatography with electrochemical detection which is known as a more precise technique for measuring dopamine and serotonin concentrations (Yang *et al.* 2019).

A gene involved in serotonin reception, *5ht-7,* showed to have the highest expression at 1 dpi and was upregulated in heads of AcMNPV WT-infected larvae but not in heads of AcMNPV Δ*ptp*- and AcMNPV catmut-infected larvae. Measured levels of serotonin in the haemolymph and in the brain did not show an increase. In insects, three different serotonin receptors, 5HT-1, 5HT-2 and 5HT-7, are known (Vleugels *et al.* 2015). Expression of *5ht-7* has been detected in the honeybee brain and the fly's salivary glands and was suggested to have a role in information processing and learning and inducing saliva secretion, respectively. In grasshoppers (*Locusta migratoria*), 5HT-7 was measured in the midgut and demonstrated to be involved in

the relaxation of the midgut circular muscle, indicating an evolutionary conserved role of muscle relaxation between invertebrates and vertebrates. Like dopamine, serotonin is associated with neural and immune responses in insects. It was reported that 5-HT is involved in haemocyte phagocytosis. 5HT-1 increases phagocytic activity of the insects' haemocytes in both *Pieris rapae* and *Drosophila melanogaster* while 5HT-2 has the opposite effect in *P. rapae* and reduces the activity of haemocyte phagocytosis (Qi *et al.* 2017). The role of 5HT-7 is however not clear in insects, yet seems to be highly expressed in the insects' brains and head in *Tribolium castaneum* (Vleugels *et al.* 2014). A mutant *5ht-7* mosquito uncovered changes in development and reduced motility and stress response to external stimuli (Li *et al.* 2022b) and a knockdown experiment of *5ht-7* in *S. exigua,* displayed immunosuppression and the involvement of these receptor in phagocytosis and nodulation (Hasan *et al.* 2019). The same study also demonstrated that secondary metabolites from a bacterium specifically inhibit this receptor. The observation that the gene expression of *5ht-7* increased in larval heads infected with AcMNPV WT, confirms the role of 5HT-7 in the immune response in *S. exigua*. However, when *ptp* was altered or removed from the viral genome, the increase in *5ht-7* gene expression was only moderate and not significantly different from the expression found in mock-infected larvae, pointing towards an interaction between PTP and 5HT-7 and a potential role of 5HT-7 in the induction of hyperactivity.

Lastly, the TA (and to a lesser extent OA) receptor *tar1* was shown to be significantly higher expressed at 4 dpi than at 1 and 3 dpi. Larvae infected with AcMNPV WT had a significantly higher *tar1* expression than the AcMPNV Δ*ptp*- and mock-infected larvae. TAR1 can both bind TA and OA, but is more sensitive to TA, which is seen for the lepidopteran *B. mori,* where the half maximal effective concentration (EC50) was 8.28 for TA and 5.85 for OA (Ohta *et al.* 2003). TAR1 is a G-protein coupled receptor (GPCR) which activates the signalling cascade in cells via Gi or Gq proteins (Finetti *et al.* 2021a). For *B. mori* and another lepidopteran *Plutella xylostella,* the activation is through the heterotrimeric Gi protein which inhibits the reaction of cyclic adenosine monophosphate (cAMP) from adenosine triphosphate (ATP) through inhibition of adenylyl cyclase (Ohta *et al.* 2003; Ma *et al.* 2019). *Spodoptera exigua* also belongs to the Noctuidae family and therefore it is hypothesised that the *S. exigua* TAR1 also acts through a Gi protein response. In *D. melanogaster* the TAR1 receptors are mainly expressed in the CNS, in the pars intercerebralis, the mushroom bodies, the antennal and olfactory lobes, along with the suboesophageal ganglia (SOG) (Finetti *et al.* 2021a; Finetti *et al.* 2021b). Studies have shown that TAR1 has implications on a range of functions and behaviour in insects like regulating olfactory mediated behaviours, gustatory responses and locomotor control (Finetti *et al.* 2021a). The latter is especially interesting in the scope of the research on elucidating possible mechanisms behind the induction of an altered behaviour in the form of hyperactivity. Removing the *ptp* gene from the virus resulted in a significant decrease

of *tar1* expression that remained significantly different from the expression of *tar1* in the mock infected larvae. Putatively, the absence of *ptp* in the viral genome, results in a decrease of hyperactivity driven by the upregulation of *tar1*. Furthermore, the regulation of the gustatory responses via TAR1 in the insect host could indicate a hijacking onto underlining responses of searching for feed which could lead to an increase in movement.

In conclusion, we found that the 14-3-3 precursor enzymes, the rate-limiting enzymes for the four major biogenic amines and most of their receptors (except for TAR1 and 5HT-7) had the highest transcription at 1 dpi, followed by a significant decline in transcription at 3 and 4 dpi. Additionally, our study could elucidate two gene targets, the OA/TA receptor *tar1* and 5HT receptor *5ht-7* which are potentially involved in hyperactivity after an AcMNPV infection in *S. exigua* larvae.

Funding

This work was supported by the Dutch Research council (NWO) (grant number ALWOP.362 and VI.Vidi.192.041).

Acknowledgements

We would like to thank Els Roode and Dorothy van Leeuwen for maintenance of the *S. exigua* rearing. We would also like to thank Robin Bouwmeester for constructing some of the qPCR primers and for preliminary exploration of the research question. We thank Rick Dekker for his help with the ELISA experiments and Frederik N. Gasque for making Figure 1.

Supplementary file

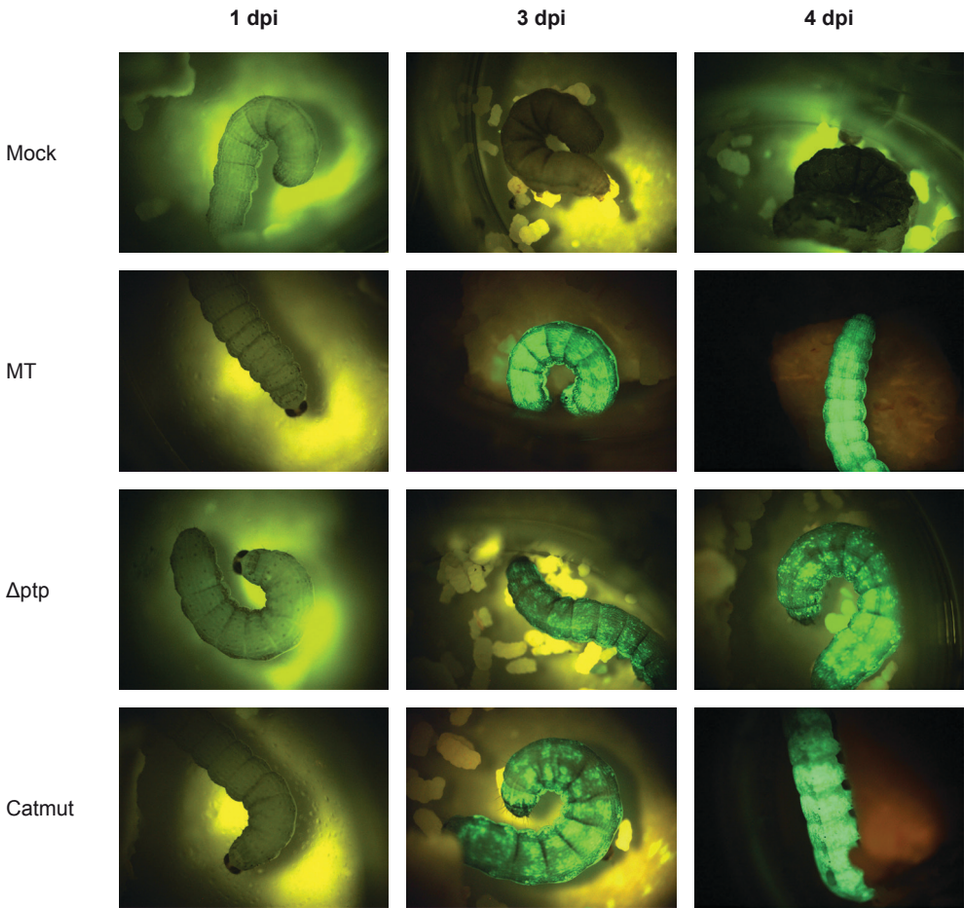

Supplementary Figure S1. Overview and photographic representation of the expression of eGFP in the sampled *S. exigua* infected larvae at 1, 3, and 4 days post infection (dpi). eGFP is not detectable in caterpillars at 1 dpi, and from then onwards only larvae expressing eGFP in the virus-infected larvae (not applicable to the mock treatment) were sampled. Larvae at 1 dpi are all late third instar (LL3) and, at 3 dpi are all mid fourth instar (mL4). At 4 dpi, virus-infected larvae are mL4, while mock-infected larvae are early fifth instar (eL5).

Supplementary Table S1. Overview of the second round of infection for the experiment. The table represents the amount of caterpillars infected with the four treatments (mock, WT, Δ*ptp*, catmut), the percentage of larvae showing eGFP expression in the form of fluorescence (of the caterpillars that were alive, in Chapter 5 we show that fluorescence ceases after death), and the percentage of dead and liquefied caterpillars at different days post infection (dpi).

	Infected larvae	**eGFP expression**			**Liquefaction**			
Dpi	0	1	3	4	2	4	7	9
Mock	300	0 %	0 %	0 %	0 %	0 %	0 %	0 %
WT	618	0 %	72.1%	79.2%	0 %	5.3%	80.3%	80.3%
Δ*ptp*	600	0 %	45.5%	66.7%	0 %	0 %	70.7%	73.0%
Catmut	600	0 %	34.7%	50.8%	0 %	0 %	53.6%	57.1%

Supplementary Table S2. List of gene names and sequences for utilised primers during this study.

Gene name	**Forward primer Sequence, 5'–3'**	**Reverse primer Sequence, 5'–3'**
ptp	TTGGCACAACTATTTACAATGCG	GTTTTACTATCTGTTCTGCGGTC
gp64	AATGTACAGCAGGCTCGAGT	CGTCTCGATGAAGCACAGTG
14-3-3 zeta	CTGAGCAATGAGGAAAGGAACC	AATGGAGGAAATGACACGCC
14-3-3 epsilon	TCAGGTGGAGAAGGAAC	CAGGTATCGGTGGTAATC
tph	TTTCTTCTTCTGACATTTTGGTGG	CTCTTCGCCAGTTTGAGACG
tbh	ACGATTACATTATTGAGGACGGTAC	TACTGGAGTGAAGAGACGCA
th	AGCGTCTGAATTTATCTTTGGCA	GAGCCAGCATCCACCTCTAT
tdc	CAAACCAAACCCAACTTTACTTGA	GGCCTGCAGAAATACGTACG
5ht-1a	GCCCAATACCTGTCAGTAGC	GCGGTCTATGAGGTCAGTCA
5ht-7	CTACACGTTGTATTCGTACTCGC	AATAAATGTGAAGAATGGCGGAG
tar1	CAAAATCGGTGGCGAGCTTA	GCACTCGACAGATATTGGGC
tar2	ATCAAATCGGTTCGTCATCAATCTAC	GATGTCCTCCTGCGCAGA
octp1	GTGACCTGCAGCAAGAGTCC	CCGCACTGAATCCCCTCATT
octp2	AGATGACGAAAAAGATGGCATTCA	TCAAATGGTCGCTGGTTGTG
octp3	CTCAAGATAATGATCAGTTTGGCAG	GGAACACCTTTGATCAAGACGT
dop	ATAATAGCCGGTGGTGTGGG	AATAGCTCCCATCGGCATCA
dop1	TGCTTCCCGAAATTCAGTGT	GTATACCAGATCTGGCGTTCA
dop2	CAACATGCTCGTGATCCTGG	ATCACTACCAACCCCACGAG
indr	TGTTGATAGGTACATTGCAGTAAC	TCAGCCAGACCAGGACTATG

It is hard enough to remember my opinions, without also remembering my reasons for them!

Friedrich Nietzsche

CHAPTER 7

General discussion

The main goal of this dissertation was to better understand the mechanisms behind parasite-induced behavioural alterations, including both the internal aspects of the host in the form of the role of the CNS and what happens on a molecular level, but also the outer abiotic factors that influence the expression of behavioural alterations.

Below an overview of the key findings from this PhD project is outlined (Figure 1) followed by a general discussion of relevant topics linked to these findings.

Key findings

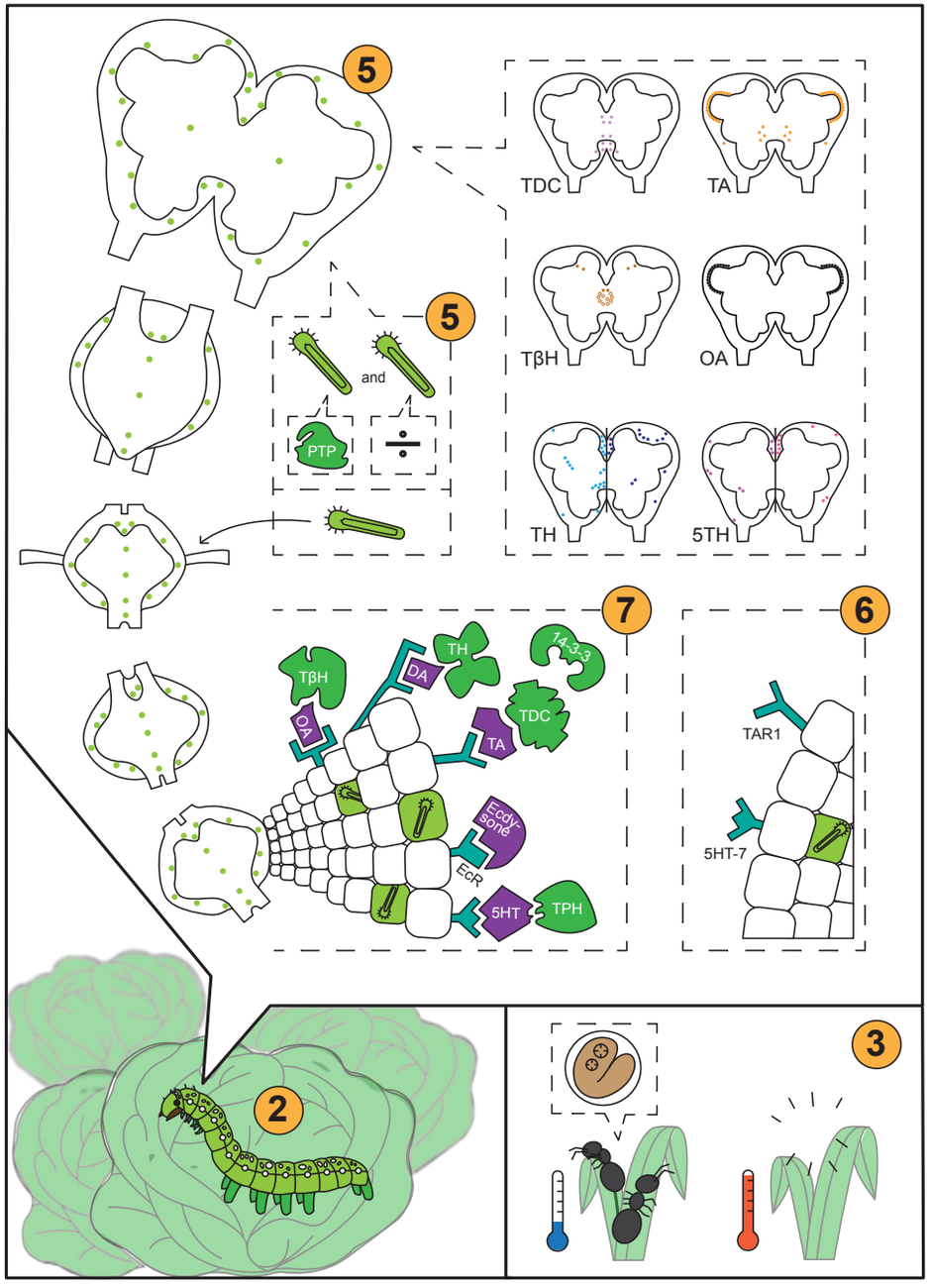

Figure 1. Graphical overview of key findings from this dissertation. Chapter 2 reviewed what was known at the time about behavioural alteration of caterpillars by baculoviruses and posed future perspectives, which paved the route for the direction of this dissertation. Chapter 3 elucidated for the first time that

temperature is the most important abiotic factor in the field (of the studied factors) for the expression of *Dicrocoelium dendriticum*-infected *Formica polyctena* ants. The following chapters zoomed in on the internal aspects in *Spodoptera exigua* caterpillars. In Chapter 4 as many as six targets of biogenic amines and their enzymes were localised in the central nervous system (CNS) of third instar caterpillars. These results showed differences between the targets, but also similarities between some of the targets. In Chapter 5 results supporting the postulated route of baculoviruses into the CNS through infecting tracheal cells was shown, along with analysis of the localisation of Autographa californica multiple nucleopolyhedrovirus (AcMNPV) in the CNS and the progress of infection over time. Furthermore Chapter 5 also revealed that AcMNPV protein tyrosine phosphatase (PTP) does not aid in the entry of AcMNPV into the CNS. In Chapter 6 the key findings were the possible influence on two receptors of biogenic amines TAR1 binding TA and to a lesser extent OA and 5HT-7, a 5HT receptor. In Chapter 7 the information from the previous chapters were linked together and promising future routes of exploration are being suggested. Important molecules and proteins for this dissertation are abbreviated, and orange circles indicate the chapters the content of the visuals can be found in (Chapter 2-7). Idea and initial draft by Simone N. Gasque, and full digital illustration by Frederik N. Gasque.

Abiotic factors and expression of parasite-induced behavioural modifications

Our finding of temperature being the factor *in situ* that has the highest influence (of the studied factors) on the *Dicrocoelium dendriticum* induced behavioural change in the forest ants (Chapter 3) is to my knowledge the first to describe temperature as the factor that has the highest influence on the expression of a parasite induced behavioural change. Other studies have found solar radiation (infected *Gammarus* cases), time of day and circadian clock (*Ophiocordyceps* and *Entomophthora* examples) to be the major factors for the expression of the parasite induced behavioural change (Bethel and Holmes 1973; Helluy 1984; Andersen *et al.* 2009; Hughes *et al.* 2011; Andriolli *et al.* 2019). I hypothesise that the major reason that we see this split of the most influential factors (temperature or solar radiation and circadian clock) in the field is due to which organismal group the parasite belongs to and the lifecycle of the parasite. Are we dealing with a parasitic organism that will kill the host in a relative short time and has a direct lifecycle (e.g. fungi and baculoviruses) then extreme temperatures might not be an issue. Or are we dealing with a parasite with a complex lifecycle that needs to have a window for transmission to the next environment or host, and until succeeding needs to keep the current host and itself alive (e.g. Acanthocephalan- and trematode-infected *Gammarus* cases, and *D. dendriticum* in ants) (Bethel and Holmes 1973; Ponton *et al.* 2006; Botnevik *et al.* 2016; Chapter 3). For the fungi, factors such as solar cues and circadian clocks of the hosts are speculated to correlate with optimal conditions for fungal spore maturation and release (Andersen *et al.* 2009; Hughes *et al.* 2011). For *D. dendriticum*, I measured temperatures in the field that were around the ant host's thermal limits (Kadochová *et al.* 2017). Avoiding these temperatures is necessary to keep the host alive (and maybe to ensure that the metacercariae are in a viable state too). The time of the day at which the highest proportions of the infected ants are biting to the vegetation correlates with

low temperatures, which is at dawn and dusk, and this coincides with the crepuscular feeding times of a possible final host in the Danish forests, the European roe deer (Stache *et al.* 2013). On a day with a higher daily temperature range, or when there is a limited temperature range and when it is cold, the ants stay attached most of the day, see Chapter 3.

Unfortunately, the larvae of the *S. exigua* population that was available in our laboratory, were not very mobile and attempts to record differences in locomotion between AcMNPV-infected caterpillars and non-infected individuals were not successful (Pleiter 2020; Sajadi 2023). However, in our studies a different set-up was used to record hyperactivity, with well-plates instead of a large arena (van Houte *et al.* 2012), and further research needs to investigate whether this affects the hyperactivity observations. In the previous population with reported hyperactivity at 3 days post infection (dpi) (van Houte *et al.* 2012), movement recordings at 4 dpi were not included as the caterpillars started to become moribund. In the population available during my PhD project, the caterpillars started being moribund later than reported in van Houte *et al.* (2012) with caterpillars dying and liquefying at 6-7 dpi (see Dataset S1 in Chapter 5). This could indicate that the hyperactivity would for our population also be expressed at a later timepoint than in the population used by van Houte (2012). In chapter 5, I present the observation that AcMNPV can internally infect the central nervous system (CNS) from 3 dpi onwards. In this experiment this was a single case of infection in a SOG, whereas at 4 dpi more internal infections were observed. In previous experiments conducted 2-3 years ago (so during another status of the *S. exigua* population) I observed internal infection in the brain and with a higher intensity already at 3 dpi (unpublished results, S.N. Gasque). This indicate intricate links between the internal state of the caterpillar (due to instar and where it is in the development e.g. close to a moult), the caterpillar population, CNS entry and expression of hyperactivity. Therefore, the timing of hyperactivity should be re-investigated for the current population to further study the link between the progress of CNS infection and hyperactivity.

Parasite entry into the insect CNS and the role of PTP

Looking closer at neuroparasites, only viruses and trematodes have been described to be in direct contact with the CNS of insects before or during the manipulation of host behaviour (Hughes and Libersat 2018). So far, within these systems no examples of behavioural manipulation to be induced from the inner structures of the CNS opposing merely the outmost cell layers of the CNS were known (Romig *et al.* 1980; Knebel-Mörsdorf *et al.* 1996; Herz *et al.* 2003; Torquato *et al.* 2006; Katsuma *et al.*

2012; Dheilly *et al.* 2015; Martín-Vega *et al.* 2018). Our study shows that baculoviruses do infect cells from the outermost cell layers to the inner cell layers of the CNS, however, further research is needed to unravel how this might aid the manipulation of host behaviour. In Chapter 5, I show clear AcMNPV-infections of tracheal cell before infections of the CNS occur. The tracheoles branch within the CNS, so the tracheal cells are in very close contact to the blood-brain barrier (BBB). The findings of prior and persisting trachea cell infection support my postulation of AcMNPV to cross the BBB by infecting the brain cells constituting the BBB from adjacent tracheal cells (Figure 4; Figure 5; and Figure 6 in Chapter 5). Previous studies have postulated the same route of infection (Burrows 1980; Engelhardt *et al.* 1994; Torquato *et al.* 2006; Senem *et al.* 2016). The repeated observation of one or more AcMNPV-infected cell bodies in the centre of the superior neuropil (SNP), seems to overlap with the location of tracheal cells described for *Drosophila melanogaster* larvae (Truman *et al.* 1994; Pereanu *et al.* 2007). A confirmation of these AcMNPV-infected cells being tracheal, would emphasise the efficacy of utilising the tracheal route with these deep innervations into the brain of the host. Conducting tracheal staining in the CNS (as described by Pereanu *et al.* 2007; Yuan *et al.* 2020) of *S. exigua* larvae could further reveal this infection route. Another organism that, as I have previously argued (see Chapter 1 and Chapter 3), should be regarded as a neuroparasite is *Entomophthora muscae,* as the fungus infects the CNS while the host is still alive and is exhibiting the parasite-induced behavioural change (Elya *et al.* 2018). Elya and colleagues (2018) showed that when exposing *Drosophila* flies to the entomophthoralean *E. muscae* 'Berkley', the fungal cells were present in the CNS of all but one fly at 48 hrs after exposure. In another study it was observed that the BBBs of the infected flies were more permeable in the late stages of the infection (Elya *et al.* 2023). These findings highlight a different way for a neuroparasite to infect the CNS, in contrast to our postulated route for baculoviruses from one tracheal cell to the next and crossing the BBB (see Chapter 5). The tracheal route is also only possible for organisms that can exploit cell to cell infections in this way, which the release of the baculovirus budded virus (BV) phenotype permits. Elya and colleagues (2023) found by metabolomic analysis a difference in compounds present in the haemolymph between the entomophthoralean-infected and non-infected flies. When haemolymph from infected flies was transfused to non-infected conspecifics, a burst of movement was observed, indicating that factors for induction of the hyperactivity can be found in the haemolymph in this system (Elya *et al.* 2023).

It was hypothesised that the virally encoded PTP plays a role in baculoviral entry into the CNS, as shown for BmNPV-infected *Bombyx mori* caterpillars (Katsuma *et al.* 2012). Additional results showed that in AcMNPV-infected *S. exigua* larvae the enzymatic activity of PTP was needed for induction of hyperactivity expressed at 3 dpi (van Houte *et al.* 2012). When adding these two aspects together, the AcMNPV mutants utilised in Chapter 5 with a deletion of PTP or lacking the enzymatic activity

of PTP should not be able to enter the brain of *S. exigua*. As I showed in Chapter 5 all AcMNPV mutants tested, even the strain lacking PTP, could enter the CNS. This shows that at least in this specific AcMNPV-*S. exigua* system PTP is not needed for CNS entry and therefore we speculate that also other factors are involved in the induction of the behavioural modification. It was already known that other factors than PTP could induce hyperactivity in the caterpillar host, as the *ptp* gene is only present in group I nucleopolyhedroviruses (NPVs) of the alphabaculoviruses, to which for example AcMNPV and Bombyx mori (BM) NPV belong (van Houte *et al.* 2012), but group II NPVs can also induce hyperactivity (Goulson 1997). PTP is not solely a protein that has been shown to play a role in the induction of a behavioural change in baculovirus-infected caterpillars, but data also points to it having a role as an inducer of behavioural change in other systems as discussed. Another behaviour-altering fungus is the hypocrealean *Ophiocordyceps unilateralis* (*sensu latol*) where the fungus enters the brain of its ant host, but firstly after death of the host (so thereby not regarded as a neuroparasites by the definition) (Hughes *et al.* 2011; Fredericksen *et al.* 2017; Mangold *et al.* 2019). The *O. unilateralis*-infected carpenter ants (*Camponotus* genus) initially express altered movement behaviour in the horizontal plane in the form of non-directed and arrhythmic movements (Hughes *et al.* 2011; Trinh *et al.* 2021). Around solar noon the movement switches from horizontal to vertical as the infected ants move up the vegetation, and at a specific height and direction (seemingly based on illumination and dependent on the fungus-host system) bite with the mandibles and grasp the legs onto the vegetation in a death grip (Andersen *et al.* 2009; Hughes *et al.* 2011; Loreto *et al.* 2018; Andriolli *et al.* 2019). This location provides the right microclimate for a fruiting body to grow from the host and for subsequent spore maturation and release onto the ant sisters walking below their infected and death sibling (Andersen *et al.* 2009; Andriolli *et al.* 2019). Although, this parasite-host phenotype has more in common with baculoviral tree-top disease due to movement in the vertical plane rather than the horizontal movement of hyperactivity, there is a link between the hyperactivity-required *ptp* gene and the fungal *O. unilateralis* death grip. Along with regulations of other genes (e.g. genes encoding enterotoxins, tyrosinases, terpenoids) a >110 fold upregulation of a putative *ptp* gene in the manipulated biting state of *O. unilateralis*-infected *C. castaneus* ants was found along with a smaller but significant subsequent downregulation afterwards (> 5-fold) (de Bekker *et al.* 2015). Furthermore, two additional ant genes putatively encoding PTP were significantly higher expressed in the ant heads (compared to fungal growth culture). A latter experiment showed similar tendencies in two other *Ophiocordyceps-Camponotus* systems and showed that the ant's *takeout* gene was downregulated (Will *et al.* 2020). The *takeout* gene encodes for a juvenile hormone (JH) – carrying protein (TO) involved in the circadian clock, which has been hypothesised as a (in)direct intermediate for the action of PTP (van Houte *et al.* 2013). Juvenile hormone has been suggested to have opposing effects to 20-hydroxyecdysone (20E) through ecdysone receptors (EcRs) (in the active form as heterodimers with

ultraspiracle protein receptors (USP)), on a set of micro RNAs (miR-8 and miR-429) and the *BrZ2* gene which inhibits tree-top disease expressed in HaSNPV-infected *Helicoverpa armigera* larvae (Yao *et al.* 1992; Zhang *et al.* 2018). Another suggested pathway for the action of PTP is through cGMP-dependent protein kinase (PKG), encoded by the *for* (foraging) gene (van Houte *et al.* 2013; Allen and Sokolowski 2021).

With comparisons between the above mentioned systems where PTP has either been shown to be pivotal, like for the induction of baculovirus-induced hyperactivity in caterpillars, or could play a role in the fungal-induced death grip, as suggested by the upregulation of *ptp* during the manipulated biting state in ants - the parasite-host phenotype (hyperactivity versus death grip) seems very different. However, new studies highlight that particular enzymes from the large PTP family may not only be involved in the baculovirus-induced hyperactivity, but also in the induction of tree-top disease. A knockdown of the PTEN gene (encoding a lipid phosphatase belonging to the PTP family and also belonging to the dual-specific PTPs like AcMNPV-PTP) of *Lymantria dispar* (Ld) MNPV (group II NPV), disrupted the expression of tree-top disease of *Lymantria dispar* caterpillars (Tonks *et al.* 2006; Alonso *et al.* 2016; Li *et al.* 2022a). However, van Houte *et al.* (2014a) demonstrated that the *ptp* gene of AcMNPV was not involved in inducing tree-top disease in *S. exigua* larvae.

Biogenic amines and parasites location in the CNS of larval instars

In Chapter 4, I analysed and illustrated the locations and quantities of immunoreactivity (IR) of six different targets of biogenic amines and their rate limiting enzymes; tyrosine decarboxylase (TDC), tyramine (TA), tyramine beta-hydroxylase (TβH), octopamine (OA), tyrosine hydroxylase (TH) and serotonin (5HT). Overlap in locations of cell bodies, their numbers and overall similarity (e.g. shape and size of cell bodies) was observed to the greatest extend for the TA-IR and OA-IR. To some extend there were also proximities of locations of TH-IR and 5HT-IR cell bodies. Regarding the projections and commissures, TA-IR and 5HT-IR were the most similar. The locations of the observed cell bodies and projections are similar in location and number to those in CNSs of other insect species, but mostly to the instars of closely related lepidopteran species (Granger *et al.* 1989; Tang *et al.* 2019; Zhang *et al.* 2022). Combining the results of locations of the biogenic amines and their rate limiting enzymes with the location of AcMNPV in the CNS of mid third instar *S. exigua* larvae, there does not seem to be a one to one overlap between virus and location of the biogenic amine-producing in exactly the same cell bodies (Figure 2). Some viral locations are in close proximity to some of the locations of the targets, but there is not an exact overlap of all the immunoreactive areas from one of the targets analysed and the viral locations.

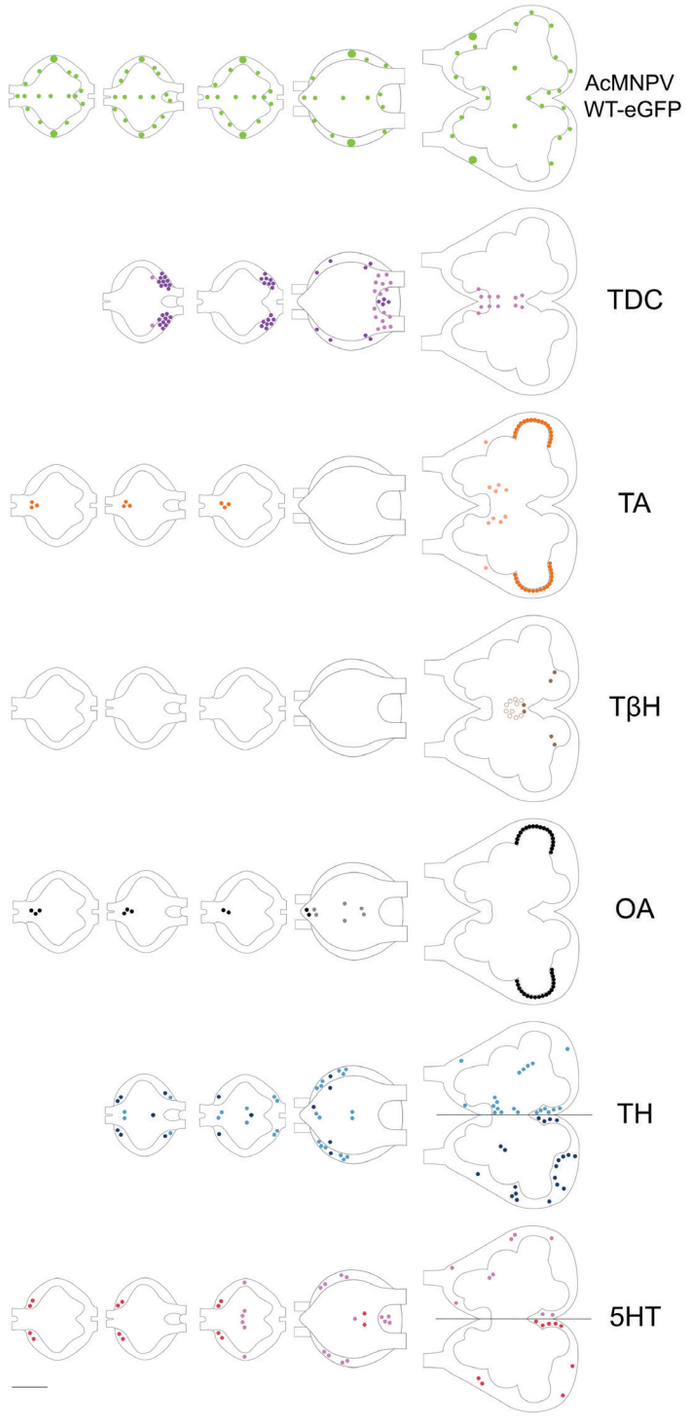

Figure 2. Schematic overview of the results gathered in Chapter 4 and Chapter 5 of the third instar *Spodoptera exigua* caterpillar CNS from brain to TG2 (for TDC and OA) or TG3 (for all other targets). As shown, there is no clear indication of a specific co-localisation of the Autographa californica multiple nucleopolyhedrovirus wildtype-expressing eGFP (AcMNPV WT-eGFP) and either of the six targets; tyrosine decarboxylase (TDC), tyramine (TA), tyramine beta-hydroxylase (TβH), octopamine (OA), tyrosine hydroxylase (TH) and serotonin (5HT). Scalebar represent 50 µm.

I wanted to make sure that the lack of overlap observed when combining the individual biogenic amines experiments and the AcMNPV experiment separately, was the full picture observed and that the locations of the IR of the targets would not change due to the infection (not expected). As a check-up I therefor conducted co-immunolabelling experiments combining AcMNPV infection followed by immunolabelling of one of three of the targets. In these co-immunolabelling experiments, firstly infected early third instar *S. exigua* caterpillars with AcMNPV WT-eGFP (as described in Chapter 5), thereafter at 4 dpi dissected the CNS out, following the protocol described in Chapter 4, and lastly scanned the prepared slides at the confocal laser scanning microscope and analysed the results. The immunocytochemistry was conducted for TDC, TH, and 5HT, to cover representatives from the different biogenic pathways along with a mix of both biogenic amines and enzymes.

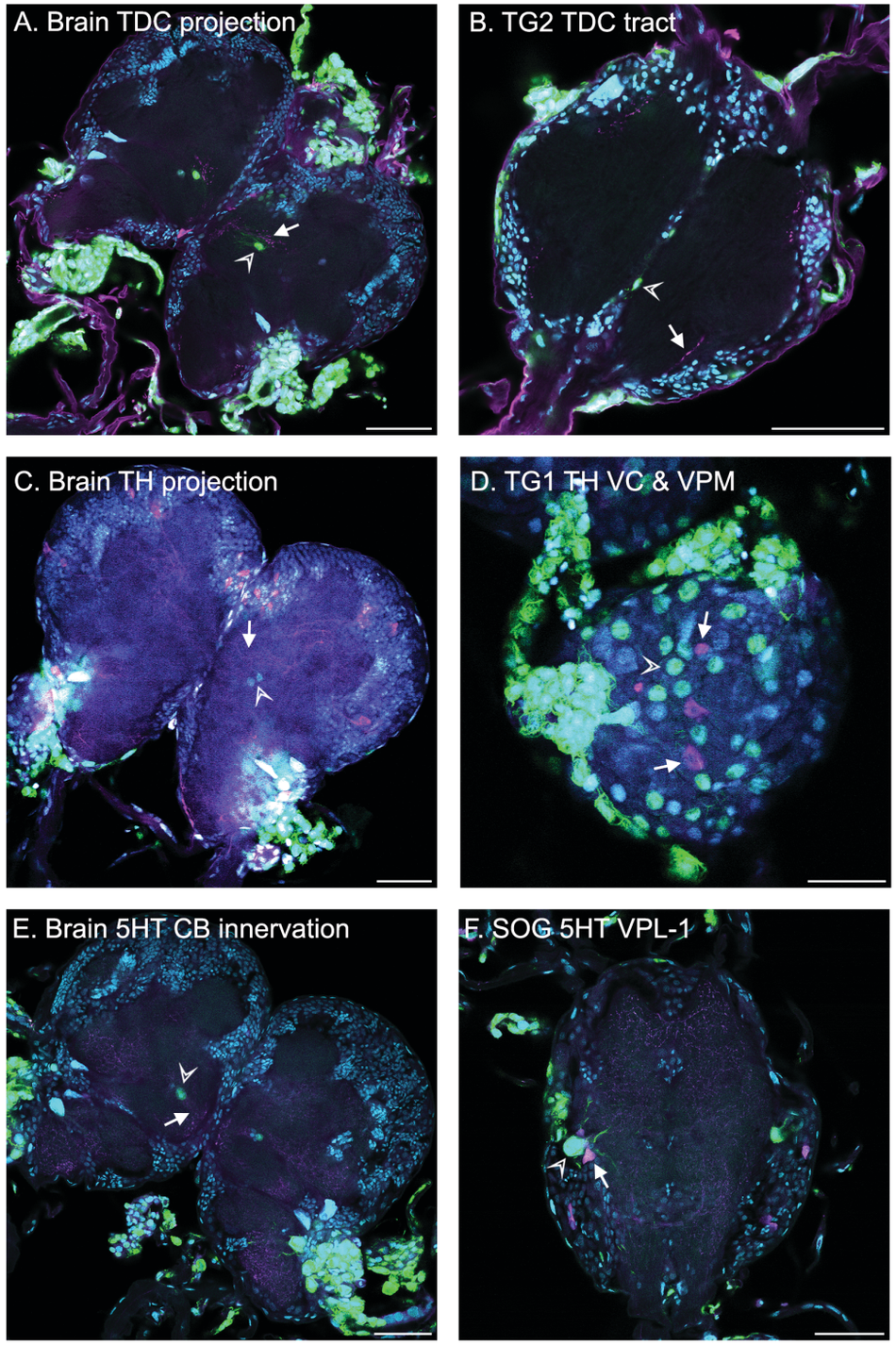

Figure 3. Co-immunolabelling experiment of AcMNPV-WT expressing eGFP and one of targets (TDC, TH or 5HT) in the CNS of third instar *Spodoptera exigua* larvae. Arrow heads indicate AcMNPV WT-eGFP, whereas arrows indicates immunoreactivity (IR) of one of the three targets. A) brain with TDC projections in close proximity to the virus infected cells in the centre of the superior neuropil (SNP) and B) TDC signal in the second thoracic ganglion (TG2). C) brain with TH projections in close proximity to the virus infected cells in the centre of the superior neuropil (SNP) and the TH-IR VC and VPM clusters on the surface of a TG1 D) with many virus infected cells near. E) brain with 5HT signal innervating the central body (CB), which terminates at where the virus infected cell in the centre of the SNP is located and F) big virus infected cell innervating the neuropil adjacent to the VPL-1 5HT-IR cells (see Chapter 4). Cyan signal for the TO-PRO-3 nuclei/dsDNA staining, green channel for AcMNPV WT eGFP, and magenta for each of the three targets; TDC, TH or 5HT (see specifications above and in panels). Scalebars represents 50 µm.

The results from the co-immunolabeling experiments showed that the location of these three targets of TDC, TH, and 5HT (which were the targets with the most abundant cell counts) did not change from the locations of the same targets observed in their uninfected con-specifics (Figure 3). The co-immunolabelling experiments did make it easier to confirm the proximity of virus-infected cells and IR-cells and projections for either of the targets.

The viral infected midline glial cells (Figure 3B) in the SOG and following thoracic and abdominal ganglia possess ecdysone receptors (EcR-A and EcR-B1) for the insects steroid ecdysone required during metamorphosis (Jacobs 2000). The active state of ecdysone, 20E, can be inactivated by ecdysteroid UDP-glucosyl transferase (EGT) (which is present in nearly all baculovirus) which thereby stalls the normal moulting process of some caterpillars infected by baculoviruses and can in some species induce tree-top disease (Gasque *et al.* 2019). The above mentioned case of stalling of moulting which thereby changes the feeding-associated behaviours, could also be under influence in the expression of hyperactivity, or by the possible sequential expression of both hyperactivity and tree-top disease (Gasque *et al.* 2019). A range of cells involved in movement are found at the external/superficial part of the ganglia, where we also have seen viral infections. A preliminary experiment of dissecting the CNS out of mid third instar *S. exigua*, for labelling against ecdysone receptor EcR-B1 was conducted (4% PFA fixation protocol as described used for TDC and 5HT in Chapter 4, but now with a mouse anti EcR-B1 primary antibody (10F1, DSHB), and a secondary goat anti mouse Alexa-488 (Jackson)) (Robinow *et al.* 1993; Truman *et al.* 1994). The results showed that there was no detectable staining in the brain with the concentrations used, but a signal was detected in the SOG, as an ventral anterior medial (VAM) cluster with a cell body signal (about four-five cells) and projections from there into the midline and bilateral projections (Figure 4) (Kuehn and Duch 2008). Another cluster was observed on the surface of the SOG, localised dorsal medial (DM) and consisted of about six to eight cells. Furthermore, a diffused projection signal was observed in the first thoracic ganglion in the neuropil, but running close to the rim of the cell bodies. The projections into the midline and most medial longitudinal tracts are located next to where AcMNPV WT-eGFP was found, but not with a closer location to any of the other targets described in Chapter 4.

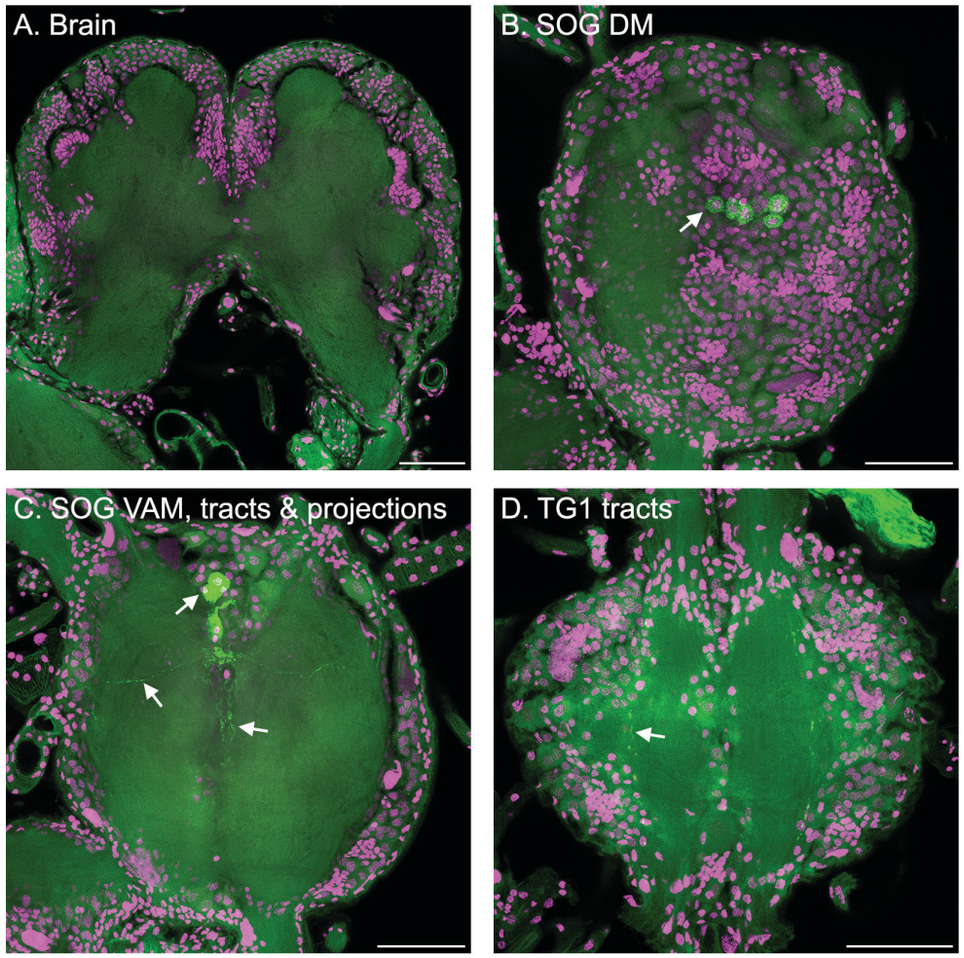

Figure 4. Ecdysone receptor B1 (EcR-B1) staining in the CNS of third instar *Spodoptera exigua* caterpillars from a preliminary experiment. A) No EcR-B1 immunoreactivity is observed in the brain. One EcR-B1 cluster located dorsal medial (DM) B) (z-projection of multiple images to visualise all cell bodies), another cluster located ventral anterior medial (VAM), two rows of longitudinal tracts and projections C) (z-projection of multiple images to visualise all) are observed in the SOG. D) Lateral longitudinal tracts were also observed in the first thoracic ganglion (TG1) (z-projection of multiple images) and in the second thoracic ganglion. Arrows indicating identified clusters, projections and longitudinal tracts. Magenta signal for the TO-PRO-3 nuclei/dsDNA staining, green channel for EcR-B1. Scalebars represents 50 µm.

Of all the areas and cells that AcMNPV-infected in the *S. exigua* CNS, I would like to highlight one specific area, due to the repeated observations and due to its location deep into the brain (therefor highly unlikely this location is a mere chance). One or several AcMNPV-infected cell bodies were observed in the centre of the SNP of *S. exigua,* located in the area of the centrally located end of the central body (CB) and the noduli, which is at the central complex (CX) (Wolff *et al.* 2015). As mentioned in

Chapter 5, I very often observed these cells being infected. This is of interest as the CX is considered to be involved in coordinating locomotor behaviour and to control the insects' motivation to walk (Libersat and Gal 2014; Wolff *et al.* 2015). Since we know that AcMNPV induces behavioural changes in the form of movement (hyperactivity and tree-top disease) these exact cells might play a role. Also, the CX in the cockroach *Periplaneta americana* is targeted by another manipulating parasite the emerald jewel wasp *Ampulex compressa* (Gal and Libersat 2008; Libersat and Gal 2014). Of the targets immunolabelled in Chapter 4, these virus-infected CX cells are in close proximity to the VC-TDC projection, for TA to the AC, MC and PC commissures, and for 5HT to both the VMC and DPC commissures. As these cells are located at the end of the CB, I propose to first look deeper into the role of TA and 5HT innervations of the CB, and of other projections and commissures in the CX overall. In this regard 5HT showed the strongest and most clear innervation of the CB.

In the jewel wasp case described above the mother injects venom into the SOG and in and around the CX (Libersat and Gal 2014), thereby induces first grooming behaviour in the cockroach that was stung, which later becomes lethargic and will not initiate spontaneous walking (Gal and Libersat 2008). The wasp grabs the cockroach by the antennae and leads it to a nest, where it lays eggs in the cockroach and subsequently seals the nest (Gal and Libersat 2008). Injecting venom into the CNS in this way classifies the jewel wasp as a neuroparasite, although the parasitoid induces this manipulating from a distance in regards to not staying in the CNS or the body of the host (Hughes and Libersat 2018). As AcMNPV and *E. muscae* are both neuroparasites that induce hyperactivity by being present in their insect host (although *E. muscae* also expresses summiting behaviour, but the same applies for baculovirus-infected *S. exigua* caterpillars in the form of tree-top disease), these models serve as good systems for comparisons. A recent study shows that the main area of the adult brain that the fungus infects is the superior medial protocerebrum (SMP) (placed anterior to the CX) (Phillips-Portillo and Strausfeld 2012; Elya *et al.* 2023). Projections from the central body of adult flies both innervate and branch within the SMP, where *E. muscae* was mainly found, but also the neighbouring neuropils such as the superior intermediate (SIP) and lateral protocerebrum (SLP) (Phillips-Portillo and Strausfeld 2012; Elya *et al.* 2023). The similar location of AcMNPV and *E. muscae* in the brain indicates that these parasites may induce locomotion from the same location in the CNS by deploying motivation of locomotion speculated to be induced in the CX. Elya *et al.* (2023) also found infections of the DN1p circadian neurons by the fungus, which is not so surprisingly considering the circadian timing of the burst of locomotion, summiting and time of kill by *E. muscae*. The circadian clock has shown to play a role of induction of the altered behaviour in other fungal systems such as *Ophiocordyceps unilateralis* infecting and modifying the behaviour of the carpenter ant hosts (Andersen *et al.* 2009; Hughes *et al.* 2011; de Bekker *et al.* 2015; Andriolli *et al.* 2019; de Bekker *et al.* 2021). *Entomophthora muscae* was

also found in the pars intercerebralis to corpora allatum projecting neurons and in corpora allatum itself (Elya *et al.* 2023), corpora allatum is solely responsible for JH synthesis and release.

Where are we standing now? And where to go?

Not only did I visualise candidate biogenic amines and enzymes, as mentioned in the previous section, by immunotargeting these in the CNS and comparing their location in the CNS to that of AcMNPV, I also found areas in the brain that are of special interest, using co-immunolabeling. In Chapter 6, we revealed some of the actors that might be involved in AcMNPV-induced change in host behaviour, as we saw differences in concentrations or transcript levels of specific biogenic amines and proteins that are part of particular biogenic amine pathways. As a result of the analysis we detected an interaction between the treatment (mock-, WT-, Δ*ptp*- or catmut-infected larvae) and the days post infection (dpi; 1, 3 or 4 dpi) for the concentration of 5HT and DA (also targeted for locations in the CNS in Chapter 4). Looking closer at the biological groups, at 4 dpi the concentration of DA was significantly lower for the WT-infected larvae compared to the Δ*ptp*- and catmut-infected larvae. We found the highest expression of the serotonin receptor 5HT-7 in AcMNP WT-infected caterpillars, compared to AcMNPV-Δ*ptp* and AcMNPV-catmut infected at 1 dpi. Furthermore, we found a significant difference between the transcript levels of tyramine receptor 1 (TAR1) when comparing between the different treatments (mock-, WT-, Δ*ptp*- or catmut-infected). Since the mentioned candidates are parts of three different biogenic pathways, future studies should look further into this, also as potential targets for PTP. Applying both a proteomics and metabolomics approach by targeting both the biogenic amines and the enzymes and receptors thereof could aid in revealing more about these candidates (Barylyuk *et al.* 2020; Parksepp *et al.* 2020). In addition, a pharmacological approach using receptor antagonists or a molecular approach using receptor knock-out mutants could be used to further study the role of biogenic amines in the behavioural manipulation of the caterpillar by the virus (Szczuka *et al.* 2013; Vinauger *et al.* 2018).

As we know that PTP is needed for the expression of hyperactivity in *S. exigua* (van Houte *et al.* 2012), but in Chapter 5 I showed that this is not due to a possible role of PTP aiding the CNS entry (as even viral constructs not encoding PTP could enter the CNS), then the quest for finding the interactors of PTP is even more interesting. Previous studies have looked into the interactors of baculoviral PTP, such as AcMNPV-PTP (van Houte *et al.* 2014a; Han *et al.* 2018a) by utilising viral constructs where PTP has been changed so it binds the interactors, but the catalysis cannot happen as the interactors are trapped in the pocket site, working as a trap. In the constructs used,

GFP was added to PTP as the tag for protein purification (Han *et al.* 2018a). In these experiments the input materials were pooled whole larvae or pooled larvae heads. Due to the miniaturised size of the CNS compared to the previous way of sampling, it would most likely not be possible to detect the interactors of PTP in the CNS only, as the amount of PTP present in the samples when working with dissected CNSs might be very low (even after pooling from 10 or 100 individuals). Instead, the proximity labelling biotinylation approach (Turbo-ID; Branon *et al.* 2018) would be a more viable way forward. Turbo-ID works while only low levels of biotin are active, and due to the success of its use in studies concerning minuscule areas in other insects (e.g. strip of cells in imaginal wing disc of *D. melanogaster* larvae) and parasite host interactions this approach seems promising (Branon *et al.* 2018; Zhou *et al.* 2021).

Above I showed preliminary evidence that EcRs have proximity to the viral locations of AcMNPV in the CNS of *S. exigua* as the biogenic amines and their enzymes. This along with the fungal *E. muscae* infections of corpora allatum (which is solely responsible for JH synthesis and release) (Elya *et al.* 2023), shows further venues of the option of parasites to hijack the intricate and already existing pathways expressed during an insects life by e.g. hormone levels. When pulling together the information presented above from Chapter 4, Chapter 5 and Chapter 6, regarding biogenic amines, their rate limiting enzymes and the receptors thereof we do see responses to neuroparasites altering the behaviour of the host. With the significant differences of AcMNP-WT infected larvae compared to their Δ*ptp*- and catmut-infected conspecifics regarding the concentrations of DA, the expression levels of 5HT-7 and TAR1 and the proximity of immunoreactive areas of TDC, TH, TA and 5HT with AcMNPV in the CNS, specifically at the central complex in the brain, I have in this project provided indications for a role of these actors in the behavioural manipulation by AcMNPV in the *S. exigua* caterpillar host. I have demonstrated that PTP is not necessary for the virus to enter the caterpillar CNS and that AcMNPV likely acts by directly manipulating the intrigued network of neuromodulators and developmental processes that govern the behaviour of an insect. Through these results I have added new insights into the complex mechanisms exploited by baculoviruses in specific, and by neuroparasites in general.

Acknowledgements

I would like to thank Vera I.D. Ros, Alexander Haverkamp and Monique M. van Oers for constructive feedback on an earlier version of this chapter. I would also like to extend my gratitude to Frederik N. Gasque for visualising my ideas on a sketch, into the key findings overview in Figure 1.

I shall be telling this with a sigh
Somewhere ages and ages hence:
Two roads diverged in a wood, and I,
I took the one less travelled by,
And that has made all the difference.

Robert Frost
last strophe of The Road Not Taken

References

Abuhagr AM, Blindert JL, Nimitkul S, Zander IA, Labere SM, Chang SA, Maclea KS, Chang ES, Mykles DL. 2014. Molt regulation in green and red color morphs of the crab Carcinus maenas: gene expression of molt-inhibiting hormone signaling components. J Exp Biol. 217: 796-808. doi: 10.1242/jeb.093385.

Acheson NH. 2011. Introduction to Virology. In NH Acheson (Ed.) Fundamentals of Molecular Virology. Wiley. ISBN: 9780470900598.

Adamo SA, Linn CE, Hoy RR. 1995. The role of neurohormonal octopamine during 'fight or flight' behaviour in the field cricket Gryllus bimaculatus. J Exp Biol. 198: 1691-1700. doi: 10.1242/jeb.198.8.1691.

Adamo SA, Linn C, Beckage N. 1997. Correlation between changes in host behaviour and octopamine levels in the tobacco hornworm Manduca sexta parasitized by the gregarious braconid parasitoid wasp Cotesia congregata. J Exp Biol. 200: 117-127. doi: 10.1242/jeb.200.1.117.

Adamo SA and Shoemaker KL. 2000. Effects of parasitism on the octopamine content of the central nervous system of Manduca sexta: a possible mechanism underlying host behavioural change. Can J Zool. 78: 1580-1587. doi: 10.1139/z00-096.

Adamo SA. 2002. Modulating the modulators: Parasites, neuromodulators and the host behavioural change. Brain Behav Evol. 60: 370-377. doi: 10.1159/000067790.

Adamo SA, Roberts JL, Easy RH, Ross NW. 2008. Competition between immune function and lipid transport for the protein apolipophorin III leads to stress-induced immunosuppression in crickets. J Exp Biol. 211: 531-538. doi: 10.1242/jeb.013136.

Adamo SA and Baker JL. 2011. Conserved features of chronic stress across phyla: the effects of long-term stress on behavior and the concentration of the neurohormone octopamine in the cricket, Gryllus texensis. Horm Behav. 60: 478-483. doi: 10.1016/j.yhbeh.2011.07.015.

Adamo SA. 2013. Parasites: evolution's neurobiologists. J Exp Biol. 216: 3-10. doi: 10.1242/jeb.073601.

Adamo SA, Easy RH, Kovalko I, MacDonald J, McKeen A, Swanburg T, Turnbull KF, Reeve C. 2017. Predator exposure-induced immunosuppression: trade-off, immune redistribution or immune reconfiguration? J Exp Biol. 220: 868-875. doi: 10.1242/jeb.153320.

Airenne, KJ, Peltomaa E, Hytönen VP, Laitinen OH, Ylä-Herttuala S. 2003. Improved generation of recombinant baculovirus genomes in Escherichia coli. Nucleic Acids Res. 31: e101. doi: 10.1093/nar/gng102.

Aitken A, Collinge DB, van Heusden BP, Isobe T, Roseboom PH, Rosenfeld G, Soll J. 1992. 14-3-3 proteins: a highly conserved, widespread family of eukaryotic proteins. Trends Biochem Sci. 17: 498-501. doi: 10.1016/0968-0004(92)90339-b.

Akasaka S, Sasaki K, Harano K, Nagao T. 2010. Dopamine enhances locomotor activity for mating in male honeybees (Apis mellifera L.). J Insect Physiol. 56: 1160-1166. doi: 10.1016/j.jinsphys.2010.03.013.

Allen AM and Sokolowski MB. 2021. Expression of the foraging gene in adult Drosophila melanogaster. J Neurogenet. 35: 192-212. doi: 10.1080/01677063.2021.1941946.

Alonso A, Nunes-Xavier CE, Bayón Y, Pulido R. 2016. The extended family of protein tyrosine phosphatases. In Pulido R (Eds.): Protein tyrosine phosphatases, methods and protocols. Humana Press. ISBN 978-1-4939-3746-2. doi : 10.1007/978-1-4939-3746-2.

Andersen SB, Gerritsma S, Yusah KM, Mayntz D, Hywel-Jones NL, Billen J, Boomsma JJ, Hughes DP. 2009. The life of a dead ant: the expression of an adaptive extended phenotype. Am Nat. 174: 424-433. doi: 10.1086/603640.

Andriolli FS, Ishikawa NK, Vargas-Isla R, Cabral TS, de Bekker C, Baccaro FB. 2019. Do zombie ant fungi turn their hosts into light seekers? Behav Ecol. 30: 609-616. doi: 10.1093/beheco/ary198.

Aonuma H and Watanabe T. 2012. Changes in the content of brain biogenic amine associated with early colony establishment in the queen of the ant, Formica japonica. PLoS One. 7: e43377. doi: 10.1371/journal.pone.0043377.

Ash MK, Al-Harthi L, Schneider JR. 2021. HIV in the Brain: identifying viral reservoirs and addressing the challenges of an HIV Cure. Vaccines. 9: 867. doi: 10.3390/vaccines9080867.

Aso Y, Hattori D, Yu Y, Johnston RM, Iyer NA, Ngo TT, Dionne H, Abbott LF, Axel R, Tanimoto H, Rubin GM. 2014. The neuronal architecture of the mushroom body provides a logic for associative learning. ELife. 3: e04577. doi: 10.7554/eLife.04577.

Aubert M, Setiawan P, Oktaviana AA, Brumm A, Sulistyarto PH, Saptomo EW, Istiawan B, Ma'rifat TA, Wahyuono VN, Atmoko FT, Zhao J-X, Huntley J, Taçon PSC, Howard DL, Brand HEA. 2018. Palaeolithic cave art in Borneo. Nature. 564: 254-257. doi: 10.1038/s41586-018-0679-9.

Ayres MD, Howard SC, Kuzio J, Lopez-Ferber M, Possee RD. 1994. The complete DNA sequence of Autographa californica nuclear polyhedrosis virus. Virol. 202: 586-605. doi: 10.1006/viro.1994.1380.

Azidah AA and Sofian-Azirun M. 2006. Life history of Spodoptera exigua (Lepidoptera: Noctuidae) on various host plants. Bull Entomol Res. 96: 613-618. doi: 10.1017/ber2006461.

Badie A, Vincent M, Morel-Varieille, Rondelaud D. 1973. Cycle de Dicrocoelium dendriticum (Rudolphi, 1819) en Limousin: ethologie des fourmis parasitees par les metacercaires. C R Seances Soc Biol Fil. 167: 725–727.

Badie A. 1975. Cycle annuel d'activité des fourmis parasitées par les métacercaires de Dicrocoelium lanceolatum (Ruddolphi 1819). Ann Rech Vet. 6: 259-264.

Badie A and Rondelaud D. 1988. Les fourmis parasitées par Dicrocoelium lanceolatum, Rudolphi en limousin. Les relation avec le support végétal. Rev. Méd. Vét. 6: 629-633.

Bao X, Wang B, Zhang J, Yan T, Yang W, Jiao F, Liu J, Wang S. 2010. Localization of serotonin/tryptophan-hydroxylase-immunoreactive cells in the brain and suboesophageal ganglion of Drosophila melanogaster. Cell Tissue Res. 340: 51-59. doi: 10.1007/s00441-010-0932-5.

Barrett JW, Brownwright AJ, Primavera MJ, Palli SR. 1998. Studies of the nucleopolyhedrovirus infection process in insects by using the green fluorescence protein as a reporter. J Virol. 72: 3377-3382. doi: 10.1128/jvi.72.4.3377-3382.1998.

Barylyuk K, Koreny L, Ke H, Butterworth S, Crook OM, Lassadi I, Gupta V, Tromer E, Mourier T, Stevens TJ, Breckels LM, Pain A, Lilley KS, Waller RF. 2020. A comprehensive subcellular atlas of the Toxoplasma proteome via hyperLOPIT provides spatial context for protein functions. Cell Host Microbe. 28: 752-766.e9. doi: 10.1016/j.chom.2020.09.011.

Berdoy M, Webster JP, Macdonald DW. 2000. Fatal attraction in rats infected with Toxoplasma gondii. Proc R Soc B. 267: 1591-1594. doi: 10.1098/rspb.2000.1182.

Berger I, Fitzgerald D, Richmond T. 2004. Baculovirus expression system for heterologous multiprotein complexes. Nat Biotechnol, 22: 1583–1587. doi: 10.1038/nbt1036.

Bergold GH. 1943. Über Polyederkrankheiten bei Insecten. Biologische Zeintralblatt. 63: 1-55.

Bethel WM and Holmes JC. 1973. Altered evasive behavior and responses to light in amphipods harboring acanthocephalan cystacanths. J Parasitol. 59: 945-956. doi: 10.2307/3278623.

Bhattarai MK, Bhattarai UR, Feng JNA, Wang D. 2018a. Effect of different light spectrum in Helicoverpa armigera larvae during HearNPV induced tree-top disease. Insects. 9: 183. doi: 10.3390/insects9040183.

Bhattarai UR, Bhattarai MK, Li FJ, Wang D. 2018b. Insights into the temporal gene expression pattern in Lymantria dispar larvae during the baculovirus induced hyperactive stage. Virol Sin. 33: 345-358. doi: 10.1007/s12250-018-0046-x.

Bhattarai UR, Li FJ, Bhattarai MK, Masoudi A, Wang D. 2018c. Phototransduction and circadian entrainment are the key pathways in the signaling mechanism for the baculovirus induced tree-top disease in the lepidopteran larvae. Sci Rep. 8: 17528. doi: 10.1038/s41598-018-35885-4.

Biron DG, Joly C, Galeotti N, Ponton F, Marché L. 2005a. The proteomics: a new prospect for studying parasitic manipulation. Behav Process. 68: 249-253. doi: 10.1016/j.beproc.2004.08.016.

Biron DG, Marché L, Ponton F, Loxdale HD, Galéotti N, Renault L, Jolyland C, Thomas F. 2005b. Behavioural manipulation in a grasshopper harbouring hairworm: a proteomics approach. Proc Biol Sci. 272: 2117-2126. doi: 10.1098/rspb.2005.3213.

Biron DG, Ponton F, Marché L, Galéotti N, Renault L, Demey-Thomas E, Poncet J, Brown SP, Jouin P, Thomas F. 2006. 'Suicide' of crickets harbouring hairworms: a proteomics investigation. Insect Mol Biol. 15: 731-742. doi: 10.1111/j.1365-2583.2006.00671.x

Bittern J, Pogodalla N, Ohm H, Brüser L, Kottmeier R, Schirmeier S, Klämbt C. 2020. Neuron-glia interaction in the Drosophila nervous system. Dev Neurobiol. 81: 438-452. doi: 10.1002/dneu.22737.

Blenau W and Baumann A. 2001. Molecular and pharmacological properties of insect biogenic amine receptors: lessons from Drosophila melanogaster and Apis mellifera. Arch Insect Biochem Physiol. 48: 13-38. doi: 10.1002/ARCH.1055.

Blissard GW. 1996. Baculovirus-insect cell interactions. Cytotechnology. 20: 73-93. doi: 10.1007/BF00350390.

Blissard GW and Theilmann DA. 2018. Baculovirus entry and egress from insect cells. Annu Rev Virol. 5: 113-139. doi: 10.1146/annurev-virology-092917-043356.

Botnevik CF, Malagocka J, Jensen AB, Fredensborg BL. 2016. Relative effects of temperature, light, and humidity on clinging behavior of metacercariae-infected ants. J Parasitol. 102: 495-500. doi: 10.1645/16-53.

Branon TC, Bosch JA, Sanchez AD, Udeshi ND, Svinkina T, Carr SA, Feldman JL, Perrimon N, Ting AY. 2018. Efficient proximity labeling in living cells and organisms with TurboID. Nat Biotechnol. 36: 880-887. doi: 10.1038/nbt.4201.

Brockhaus K, Plaza S, Pintel DJ, Rommelaere J, Salomé N. 1996. Nonstructural proteins NS2 of minute virus of mice associate in vivo with 14-3-3 protein family members. J Virol. 70: 7527-7534. doi: 10.1128/JVI.70.11.7527-7534.1996.

Burke CJ, Huetteroth W, Owald D, Perisse E, Krashes MJ, Das G, Gohl D, Silies M, Certel S, Waddell S. 2012. Layered reward signalling through octopamine and dopamine in Drosophila. Nature. 492: 433-437. doi: 10.1038/nature11614.

Burrows M. 1980. The tracheal supply to the central nervous system of the locust. Proc R Soc B. 207: 63–78. http://www.jstor.org/stable/35401

Burrows M. 1996. The Neurobiology of an Insect Brain, first edition. Oxford University Press. Oxford, UK. ISBN: 9780198523444.

Cardona A, Saalfeld S, Schindelin J, Arganda-Carreras I, Preibisch S, Longair M, Tomancak P, Hartenstein V Douglas RJ. 2012. TrakEM2 software for neural circuit reconstruction. PLoS One. 7: e38011. doi: 10.1371/journal.pone.0038011.

Caroll L. 1871. Through the Looking-Glass, and What Alice Found There. Macmillan & Co. London.

Cederlund G. 1989. Activity patterns in moose and roe deer in a north boreal forest. Ecography. 12: 39-45.

Champlin DT and Truman JW. 1998. Ecdysteroid control of cell proliferation during optic lobe neurogenesis in the moth Manduca sexta. Development. 125: 269-277. doi: 10.1242/dev.125.2.269.

Chapman RF. 2013. The insects: Structure and function, fifth edition. Cambridge University Press. Cambridge, UK. ISBN: 9780521113892.

Chen Y-R, Zhong S, Fei Z, Hashimoto Y, Xiang JZ, Zhang S, Blissard GW. 2013. The transcriptome of the baculovirus Autographa californica multiple nucleopolyhedrovirus in Trichoplusia ni cells. J Virol. 87: 6391-6405. doi: 10.1128/JVI.00194-13.

Chen Y, Wu H, Li J, Hu Z, Wang M, Zhang H. 2023. Cysteines 128 and 250 are essential for the functions of the baculovirus core gene ac109. Virol. 587: 109857. doi: 10.1016/j.virol.2023.109857.

Chung T-Y, Sun P-F, Kuo J-I, Lee Y-I, Lin C-C, Chou J-Y. 2017. Zombie ant heads are oriented relative to solar cues. Fungal Ecol. 25: 22-28. doi: 10.1016/j.funeco.2016.10.003.

Clem RJ and Passarelli AL. 2013. Baculoviruses: sophisticated pathogens of insects. PLoS Pathog. 9: e1003729. doi: 10.1371/journal.ppat.1003729.

Cole SH, Carney GE, McClung CA, Willard SS, Taylor BJ, Hirsh J. 2005. Two functional but noncomplementing Drosophila tyrosine decarboxylase genes: distinct roles for neural tyramine and octopamine in female fertility. J Biol Chem. 280: 14948-14955. doi: 10.1074/jbc.M414197200.

Combes C. 2001. Parasitism: the Ecology and Evolution of Intimate Interactions. University of Chicago Press. Chicago, USA. ISBN: 9780226114460.

Consoulas C, Johnston RM, Pflüger HJ, Levine RB. 1999. Peripheral distribution of presynaptic sites of abdominal motor and modulatory neurons in Manduca sexta larvae. J Comp Neurol. 410: 4-19. doi: 10.1002/(sici)1096-9861(19990719)410:1<4::aid-cne2>3.0.co;2-w.

Cory JS, Wilson KR, Hails RS, O'Reilly DR. 2001. Host manipulation by Insect Pathogens: the Effect of the Baculovirus egt Gene on the Host-Virus Interaction. In JP Edwards and RJ Weaver (eds.): Endocrine Interactions of Insect Parasites and Pathogens. Garland Science. 233-244. ISBN: 9781859962176.

Cory RJ. 2003. Ecological Impacts of virus insecticides: host range and non-target organisms. In Hokkanen HMT and Hajek AE (eds): Environmental Impacts of Microbial Insecticides. Progress in Biological Control. Vol 1. Springer. Dordrecht. doi: 10.1007/978-94-017-1441-9_5.

Cory JS, Clarke EE, Brown ML, Hails RS, O'Reilly DR. 2004. Microparasite manipulation of an insect: the influence of the egt gene on the interaction between a baculovirus and its lepidopteran host. Funct Ecol. 18: 443-450. doi: 10.1111/j.0269-8463.2004.00853.x.

Criscione CD, van Paridon BJ, Gilleard JS, Goater CP. 2020. Clonemate cotransmission supports a role for kin selection in a puppeteer parasite. Proc Natl Acad Sci. USA. 117: 5970-5976. doi: 10.1073/pnas.1922272117.

Cuvillier-Hot V and Lenoir A. 2006. Biogenic amine levels, reproduction and social dominance in the queenless ant Streblognathus peetersi. Naturwissenschaften. 93: 149-153. doi: 10.1007/s00114-006-0086-1.

Dacks AM, Christensen TA, Agricola HJ, Wollweber L, Hildebrand JG. 2005. Octopamine-immunoreactive neurons in the brain and subesophageal ganglion of the hawkmoth Manduca sexta. J Comp Neurol. 488: 255-268. doi: 10.1002/cne.20556.

Dawkins R and Krebs JR. 1979. Arms races between and within species. Proc R Soc Lond B. 205: 489-511. doi: 10.1098/rspb.1979.0081.

Dawkins R. 1982. The Extended Phenotype. Oxford: W. H. Freeman.

de Bekker C, Ohm RA, Loreto RG, Sebastian A, Albert I, Merrow M, Brachmann A, Hughes DP. 2015. Gene expression during zombie ant biting behavior reflects the complexity underlying fungal parasitic behavioral manipulation. BMC Genomics. 16: 620. doi: 10.1186/s12864-015-1812-x.

de Bekker C, Will I, Hughes DP, Brachmann A, Merrow M. 2017. Daily rhythms and enrichment patterns in the transcriptome of the behavior-manipulating parasite Ophiocordyceps kimflemingiae. PLoS One. 12: e0187170. doi: 10.1371/journal.pone.0187170.

de Bekker C, Will I, Das B, Adams RMM. 2018. The ants (Hymenoptera: Formicidae) and their parasites: effects of parasitic manipulations and host responses on ant behavioral ecology. Myrmecol News. 28: 1-24. doi: 10.25849/myrmecol.news_028:001.

de Bekker C, Beckerson WC, Elya C. 2021. Mechanisms behind the madness: how do zombie-making fungal entomopathogens affect host behavior to increase transmission? mBio 12: e0187221. doi: 10.1128/mBio.01872-21.

de Meeûs T and Renaud F. 2002 Parasites within the new phylogeny of eukaryotes. Trends Parasitol. 18: 247-251. doi: 10.1016/S1471-4922(02)02269-9.

Dheilly NM, Maure F, Ravallec M, Galinier R, Doyon J, Duval D, Leger L, Volkoff AN, Missé D, Nidelet S, Demolombe V, Brodeur J, Gourbal B, Thomas F, Mitta G. 2015. Who is the puppet master? Replication of a parasitic wasp-associated virus correlates with host behaviour manipulation. Proc Biol Sci. 282: 20142773. doi: 10.1098/rspb.2014.2773.

Dingha BN, Moar WJ, Appel AG. 2004. Effects of Bacillus thuringiensis cry1c toxin on the metabolic rate of cry1c resistant and susceptible Spodoptera exigua (lepidoptera: noctuidae). Physiol Entomol. 29: 409-418. doi: 10.1111/j.0307-6962.2004.00409.x.

Doherty J-F. 2020. When fiction becomes fact: exaggerating host manipulation by parasites. Proc R Soc B. 287: 20201081. doi: 10.1098/rspb.2020.1081.

Dow JAT. 1992. pH gradients in lepidopteran midgut. J Exp Biol. 172: 355-375. doi: 10.1242/jeb.172.1.355.

Dunphy GB and Downer RGH. 1994. Octopamine, a modulator of the haemocytic nodulation response of non-immune Galleria mellonella larvae. J Insect Physiol. 40: 267-272. doi: 10.1016/0022-1910(94)90050-7.

Dunton AD, Göpel T, Ho DH, Burggren W. 2021. Form and function of the vertebrate and invertebrate blood-brain barriers. Int J Mol Sci. 22: 12111. doi: 10.3390/ijms222212111.

Edgar RC. 2004. MUSCLE: multiple sequence alignment with high accuracy and high throughput. Nucleic Acids Res. 32: 1792-1797. doi: 10.1093/nar/gkh340.

Eilenberg J, Gasque SN, Ros VID. 2017. Natural enemies in insect production systems. In van Huis A and Tomberlin JK (eds.): Insects as food and feed: from production to consumption. Wageningen Academic Publishers. The Netherlands. 201-223. doi: 10.3920/978-90-8686-849-0.

Elya C, Lok TC, Spencer QE, McCausland H, Martinez CC, Eisen M. 2018. Robust manipulation of the behavior of Drosophila melanogaster by a fungal pathogen in the laboratory. Elife 7: e34414. doi: 10.7554/eLife.34414.

Elya C, Lavrentovich D, Lee E, Pasadyn C, Duval J, Basak M, Saykina V, de Bivort B. 2023. Neural mechanisms of parasite-induced summiting behavior in 'zombie' Drosophila. Elife. 12: e85410. doi: 10.7554/eLife.85410.

Engelhard EK, Kam-Morgan LN, Washburn JO, Volkman LE. 1994. The insect tracheal system: a conduit for the systemic spread of Autographa californica M nuclear polyhedrosis virus. PNAS. 918: 3224-3227. doi: 10.1073/pnas.91.8.3224.

Entwistle PF, Forkner AC, Green BM, Cory JS. 1993. Avian dispersal of nuclear polyhedrosis viruses after induced epizootics in the pine beauty moth, Panolis flammea (Lepidoptera: Noctuidae). Biol Control. 3: 61-69. doi: 10.1006/bcon.1993.1010.

Farooqui T. 2007. Octopamine-mediated neuromodulation of insect senses. Neurochem Res. 32: 1511-1529. doi: 10.1007/s11064-007-9344-7.

Finetti L, Roeder T, Calò G, Bernacchia G. 2021a. The insect type 1 tyramine receptors: from structure to behavior. Insects. 12: 315. doi: 10.3390/insects12040315.

Finetti L, Tiedemann L, Zhang X, Civolani S, Bernacchia G, Roeder T. 2021b. Monoterpenes alter TAR1-driven physiology in Drosophila species. J Exp Biol. 224: jeb232116. doi: 10.1242/jeb.232116.

Fredericksen MA, Zhang Y, Hazen ML, Loreto RG, Mangold CA, Chen DZ, Hughes DP. 2017. Three-dimensional visualization and a deep-learning model reveal complex fungal parasite networks in behaviorally manipulated ants. PNAS. 114: 12590-12595. doi: 10.1073/pnas.1711673114.

Fritz SR. 1982. Selection for host modification by insect parasitoids. Evolution. 36: 283-288. doi: 10.1111/j.1558-5646.1982.tb05043.x.

Froelick S, Gramolini L, Benesh DP. 2021 Comparative analysis of helminth infectivity: growth in intermediate hosts increases establishment rates in the next host. Proc R Soc B. 288: 20210142. doi:10.1098/rspb.2021.0142.

Gal R and Libersat F. 2008. A parasitoid wasp manipulates the drive for walking of its cockroach prey. Curr Biol. 18: 877-882. doi: 10.1016/j.cub.2008.04.076.

Gaskell EA, Smith JE, Pinney JW, Westhead DR, McConkey GA. 2009. A unique dual activity amino acid hydroxylase in Toxoplasma gondii. PLoS One. 4: e4801. doi: 10.1371/journal.pone.0004801.s.

Gasque SN. 2017. Influential abiotic factors in situ and neuromodulation underlying behavioural manipulations by Dicrocoelium dendriticum in the Formica polyctena host. Masters dissertation, University of Copenhagen.

Gasque SN, Poinar GO, Fredensborg BL. 2018. Ant (Hymenoptera: Formicidae) parasitism by Neoneurinae wasps (Hymenoptera: Braconidae) in Denmark. Ent Medd vol. 86: 27-30. (ISSN: 0013-8851).

Gasque SN, van Oers MM, Ros VID. 2019. Where the baculoviruses lead, the caterpillars follow: baculovirus-induced alterations in caterpillar behaviour. Curr Opin Insec Sci. 33: 30-36. doi: 10.1016/j.cois.2019.02.008.

Gasque SN and Fredensborg BL. 2023. Expression of trematode-induced zombie-ant behavior is strongly associated with temperature. Behav Ecol. 34: 960-968. doi: 10.1093/beheco/arad064.

Georgievska L, Hoover K, van der Werf W, Munoz D, Caballero P, Cory JS, Vlak JM. 2010. Dose dependency of time to death in single and mixed infections with a wildtype and egt deletion strain of Helicoverpa armigera nucleopolyhedrovirus. J Invertebr Pathol. 104: 44-50. doi: 10.1016/j.jip.2010.01.008.

Givon LE, Lazar AA, Yeh C-H. 2017. Generating executable models of the Drosophila central complex. Front. Behav Neurosci. 11: 102. doi: 10.3389/fnbeh.2017.00102.

Glaser RW and Chapman JW. 1916. The nature of the polyhedral bodies found in insects. Biol Bulletin. 30: 367-390. doi: 10.2307/1536363.

Goulson D. 1997. Wipfelkrankheit: modification of host behaviour during baculoviral infection. Oecologia. 109: 219-228. doi: 10.1007/s004420050076.

Granger NA, Homberg U, Henderson P, Towel A, and Lauder JM. 1989. Serotonin-immunoreactive neurons in the brain of Manduca sexta during larval development and larval-pupal metamorphosis. Int J Dev Neurosci. 7: 55-72. doi: 10.1016/0736-5748(89)90044-0.

Graves LP, Hughes LC, Irons SL, Possee RD, King LA. 2019. In cultured cells the baculovirus P10 protein forms two independent intracellular structures that play separate roles in occlusion body maturation and their release by nuclear disintegration. PloS Pathog. 15: e1007827. doi: 10.1371/journal.ppat.1007827.

Greenfield S. 1998. The human brain: a guided tour. Weidenfeld & Nicholson. Phoenix, USA. ISBN: 9780753801550.

Griss C. 1989. Serotonin-immunoreactive neurons in the suboesophageal ganglion of caterpillar of the hawk moth Manduca sexta. Cell Tissue Res. 258: 101-109. doi: 10.1007/bf00223149.

Gross CH and Shuman S. 1998. Characterization of a baculovirus-encoded RNA 5'-triphosphatase. J Virol. 72: 7057-7063. doi: 10.1128/JVI.72.9.7057-7063.1998.

Gullan PJ and Cranston PS. 2010. The Insects: An Outline of Entomology, fourth edition. Wiley-Blackwell. Chichester, UK. ISBN: 9781444330366.

Haase S, Sciocco-Cap A, Romanowski V. 2015. Baculovirus insecticides in Latin America: historical overview, current status and future perspectives. Viruses. 7: 2230-2267. doi: 10.3390/v7052230.

Hamanaka Y and Mizunami M. 2018. Tyrosine hydroxylase-immunoreactive neurons in the mushroom body of the field cricket, Gryllus bimaculatus. Cell Tissue Res. 376: 97-111. doi: 10.1007/s00441-018-2969-9.

Han Y, van Houte S, Drees GF, van Oers MM, Ros VID. 2015a. Parasitic manipulation of host behaviour: baculovirus SeMNPV EGT facilitates tree-top disease in Spodoptera exigua larvae by extending the time to death. Insects. 6: 716-731. doi: 10.3390/insects6030716.

Han Y, van Oers MM, van Houte S, Ros VID. 2015b. Virus-Induced Behavioural Changes in Insects. In H Mehlhorn (ed.): Host Manipulation by Parasites and Viruses. Springer International Publishing. 149-174. ISBN: 9783319229355. doi: 10.1007/978-3-319-22936-2_10.

Han Y, Boeren S, Ros VID, van Oers MM. 2018a. Substrate identification of baculovirus portein tyrosine phosphatase. Chapter 6 of PhD dissertation, Wageningen University.

Han Y, van Houte S, van Oers MM, Ros VID. 2018b. Baculovirus PTP2 functions as a pro-apoptotic protein. Viruses. 10: 181. doi: 10.3390/v10040181.

Han Y, van Houte S, van Oers MM, Ros VID. 2018c. Timely trigger of caterpillar zombie behaviour: temporal requirements for light in baculovirus-induced tree-top disease. Parasitol. 145: 822-827. doi: 10.1017/S0031182017001822.

Harris JW and Woodring J. 1992. Effects of stress, age, season, and source colony on levels of octopamine, dopamine and serotonin in the honey-bee (Apis mellifera L) brain. J Insect Physiol. 38: 29-35. doi: 10.1016/0022-1910(92)90019-A.

Harrison R and Hoover K. 2012. Baculoviruses and Other Occluded Insect Viruses. In EF Vega and HK Kaya (eds.): Insect Pathology. 73-131. Elsevier Inc. doi: 10.1016/B978-0-12-384984-7.00004-X.

Harrison RL, Herniou EA, Jehle JA, Theilmann DA, Burand JP, Becnel JJ, Krell PJ, van Oers MM, Mowery JD, Bauchan GR, ICTV Report Consortium. 2018. ICTV virus taxonomy profile: Baculoviridae. J Gen Virol. 99: 1185-1186. doi: 10.1099/jgv.0.001107.

Hasan A, Yeom HS, Ryu J, Bode HB, Kim Y. 2019. Phenylethylamides derived from bacterial secondary metabolites specifically inhibit an insect serotonin receptor. Sci Rep. 9: 20358. doi: 10.1038/s41598-019-56892-z.

Haverkamp A and Smid HM. 2014. Octopamine-like immunoreactive neurons in the brain and subesophageal ganglion of the parasitic wasps Nasonia vitripennis and N. giraulti. Cell Tissue Res. 358: 313-329. doi: 10.1007/s00441-014-1960-3.

Helluy S. 1983. Relations hôtes–parasite du trématode Microphallus papillorobustus (Rankin 1940). II. Modifications du comportement des Gammarus hôtes intermédiaires et localisation des métacercaires. Ann Parasitol Hum Comp. 58: 1-17.

Helluy S. 1984. Relations hôtes–parasite du trématode Microphallus papillorobustus (Rankin 1940). III. Facteurs impliqués dans les modifications du comportement des Gammarus hôtes intermédiaires et tests de prédation. Ann Parasitol Hum Comp. 59: 41-56. doi: 10.1051/parasite/1984591041.

Helluy S and Holmes JC. 1990. Serotonin, octopamine, and the clinging behavior induced by the parasite Polymorphus paradoxus (Acanthocephala) in Gammarus lacustris (Crustacea). Can J Zool. 68 : 1214-1220. doi: 10.1139/z90-18.

Helluy S and Thomas F. 2003. Effects of Microphallus papillorobustus (Platyhelminthes: Trematoda) on serotonergic immunoreactivity and neuronal architecture in the brain of Gammarus insensibilis (Crustacea: Amphipoda). Proc R Soc Lond B. 270: 563-568. doi:10.1098/rspb.2002.2264.

Helluy S and Thomas F. 2010. Parasitic manipulation and neuroinflammation: evidence from the system Microphallus papillorobustus (Trematoda) - Gammarus (Crustacea). Parasit Vectors. 3: 38. doi: 10.1186/1756-3305-3-38.

Herbison REH. 2017. Lessons in mind control: trends in research on the molecular mechanisms behind parasite-host behavioral manipulation. Front Ecol Evol. 5: 102. doi: 10.3389/fevo.2017.00102.

Herz A, Kleespies RG, Huber J, Chen XW, Vlak JM. 2003. Comparative pathogenesis of the Helicoverpa armigera single-nucleocapsid nucleopolyhedrovirus in noctuid hosts of different susceptibility. J Invertebr Pathol. 83: 31-36. doi: 10.1016/s0022-2011(03)00034-x.

Hindle S and Bainton R. 2014. Barrier mechanisms in the Drosophila blood-brain barrier. Front Neurosci. 8: 414. doi: 10.3389/fnins.2014.00414.

Homberg U, Seyfarth J, Binkle U, Monastirioti M and Alkema MJ. 2013. Identification of distinct tyraminergic and octopaminergic neurons innervating the central complex of the desert locust, Schistocerca gregaria. J Comp Neurol. 521: 2025-2041. doi: 10.1002/cne.23269

Hoover K, Grove M, Gardner M, Hughes DP, McNeil J, Slavicek J. 2011. A gene for an extended phenotype. Science. 333: 1401. doi: 10.1126/science.1209199.

Hörner M, Spörhase-Eichmann U, Helle J, Venus B, Schürmann FW. 1995. The distribution of neurones immunoreactive for β-tyrosine hydroxylase, dopamine and serotonin in the ventral nerve cord of the cricket, Gryllus bimaculatus. Cell Tissue Res. 280: 583-604. doi: 10.1007/BF00318362.

Huetteroth W, el Jundi B, el Jundi S, Schachtner J. 2010. 3D-reconstructions and virtual 4D-visualization to study metamorphic brain development in the sphinx moth Manduca sexta. Front Syst Neurosci. 4: 1-15. doi: 10.3389/fnsys.2010.00007.

Hughes DP, Andersen S, Hywel-Jones NL, Himaman W, Bilen J, Boomsma JJ. 2011. Behavioral mechanisms and morphological symptoms of zombie ants dying from fungal infection. BMC Ecology 11: 13. doi: 10.1186/1472-6785-11-13.

Hughes DP and Libersat F. 2018. Neuroparasitology of parasite–insect associations. Ann Rev Entomol. 63: 471-487. doi: 10.1146/annurev-ento-020117-043234.

Huser A, Rohwedder A, Apostolopoulou AA, Widmann A, Pfitzenmaier JE, Maiolo EM, Selcho M, Pauls D, Essen Av, Gupta T, Sprecher SG, Birman S, Riemensperger T, Stocker RF, Thum AS. 2012. The serotonergic central nervous system of the Drosophila larva: anatomy and behavioral function. PLoS One. 7: e47518. doi: 10.1371/journal.pone.0047518.

ICTV. 2023a, December 2. Circoviridae. https://ictv.global/report_9th/ssDNA/Circoviridae

ICTV 2023b, December 2. Parvoviridae. https://ictv.global/report_9th/ssDNA/Parvoviridae

ICTV. 2023c, December 2. Picornavirales. https://ictv.global/report_9th/RNApos/Picornavirales

Ito K, Shinomiya K, Ito M, Armstrong JD, Boyan G, Hartenstein V, Harzsch S, Heisenberg M, Homberg U, Jenett A, Keshishian H, Restifo LL, Rössler W, Simpson JH, Strausfeld NJ, Strauss R, Vosshall LB. 2014. A systematic nomenclature for the insect brain. Neuron. 81: 755-765. doi: 10.1016/j.neuron.2013.12.017.

Jacobs JR. 2000. The midline glia of Drosophila: a molecular genetic model for the developmental functions of glia. Prog Neurobiol. 62: 475-508. doi: 10.1016/s0301-0082(00)00016-2.

Javed MA, Biswas S, Willis LG, Harris S, Pritchard C, van Oers MM, Donly BC, Erlandson MA, Hegedus DD, Theilmann DA. 2017. Autographa californica multiple nucleopolyhedrovirus AC83 is a per os infectivity factor (PIF) protein required for occlusion-derived virus (ODV) and budded virus nucleocapsid assembly as well as assembly of the PIF complex in ODV envelopes. J Virol. 91: e02115-16. doi: 10.1128/JVI.02115-16.

Jehle JA, Blissard GW, Bonning BC, Cory JS, Herniou EA, Rohrmann GF, Theilmann DA, Thiem SM, Vlak JM. 2006. On the classification and nomenclature of baculoviruses: a proposal for revision. Arch Virol. 151: 1257-1266. doi: 10.1007/s00705-006-0763-6.

Johnson PTJ, Lunde KB, Thurman EM, Ritchie EG, Wray SN, Sutherland DR, Kapfer JM, Frest TJ, Bowerman J, Blaustein AR. 2002. Parasite (Ribeiroia ondatrae) infection linked to amphibian malformations in the western united states. Ecol Monogr. 72: 151-168. doi: 10.1890/0012-9615(2002)072[0151:PROILT]2.0.CO;2.

Kadochová S, Frouz J, Roces F. 2017. Sun basking in red wood ants Formica polyctena (Hymenoptera, Formicidae): individual behaviour and temperature-dependent respiration rates. PLoS ONE. 12: e0170570. doi: 10.1371/journal.pone.0170570.

Kalafati E, Papanikolaou E, Marinos E, Anagnou NP, Pappa KI. 2022. Mimiviruses: giant viruses with novel and intriguing features (review). Mol Med Rep. 25: 207. doi: 10.3892/mmr.2022.12723.

Kamhi JF and Traniello JFA. 2013. Biogenic amines and collective organization in a superorganism: neuromodulation of social behaviour in ants. Brain Behav Evol. 82: 220-236. doi: 10.1159/000356091.

Kamhi JF, Gronenberg W, Robson SKA, Traniello JFA. 2016. Social complexity influences brain investment and neural operation costs in ants. Proc R Soc B. 283: 20161949. doi: 10.1098/rspb.2016.1949.

Kamita SG, Nagasaka K, Chua JW, Shimada T, Mita K, Kobayashi M, Maeda S, Hammock BD. 2005. A baculovirus-encoded protein tyrosine phosphatase gene induces enhanced locomotory activity in a lepidopteran host. PNAS. 102: 2584-2589. doi: 10.1073/pnas.0409457102.

Karnkowska A, Vacek V, Zubáčová Z, Treitli SC, Petrželková R, Eme L, Novák L, Žárský V, Barlow LD, Herman EK, Soukal P, Hroudová M, Doležal P, Stairs CW, Roger AJ, Eliáš M, Dacks JB, Vlček Č, Hampl V. 2016. A eukaryote without a mitochondrial organelle. Curr Biol. 26: 1274-1284. doi: 10.1016/j.cub.2016.03.053.

Kato K, Orihara-Ono M, Awasaki T. 2020. Multiple lineages enable robust development of the neuropil-glia architecture in adult Drosophila. Development. 147: dev184085. doi: 10.1242/dev.184085.

Katsuma S, Koyano Y, Kang WK, Kokusho R, Kamita SG, Shimada T. 2012. The baculovirus uses a captured host phosphatase to induce enhanced locomotory activity in host caterpillars. PLoS Pathog. 8: e1002644. doi: 10.1371/journal.ppat.1002644.

Katsuma S. 2015. Phosphatase activity of Bombyx mori nucleopolyhedrovirus PTP is dispensable for enhanced locomotory activity in B. mori larvae. J Invertebr Pathol. 132: 228-232. doi: 10.1016/j.jip.2015.11.002.

Knebel-Mörsdorf D, Flipsen JTM, Roncarati R, Jahnel F, Kleefsman AWF, Vlak JM. 1996. Baculovirus infection of Spodoptera exigua larvae: lacZ expression driven by promoters of early genes pe38 and me53 in larval tissue. J Gen Virol. 77: 815-824. doi: 10.1099/0022-1317-77-5-815.

Kong H, Dong C, Tian Z, Mao N, Wang C, Cheng Y, Zhang L, Jiang X, Luo L. 2018. Altered immunity in crowded Mythimna separata is mediated by octopamine and dopamine. Sci Rep. 8: 3215. doi: 10.1038/s41598-018-20711-8.

Koyama T and Mirth CK. 2021. Ecdysone quantification from whole body samples of Drosophila melanogaster larvae. Bio Protoc. 11: e3915. doi: 10.21769/BioProtoc.3915.

Kristensen T, Nielsen AI, Jørgensen AI, Mouritsen KN, Glenner H, Christensen JT, Høeg JT. 2012. The selective advantage of host feminization: a case study of the green crab Carcinus maenas and the parasitic barnacle Sacculina carcini. Mar Biol. 159: 2015-2023. doi: 10.1007/s00227-012-1988-4.

Kuehn C and Duch C. 2008. Expression of two different isoforms of fasciclin II during postembryonic central nervous system remodeling in Manduca sexta. Cell tissue res. 334: 477-498. doi: 10.1007/s00441-008-0703-8.

Kwon M, Cho HM, Ahn YJ. 2006. Relationship between feeding damage by beet armyworm, Spodoptera exigua (Lepidoptera: Noctuidae) and leaf trichome density of potato. J Aisa-Pacific Entomol. 9: 361-367. doi: 10.1016/S1226-8615(08)60315-5.

Labaude S, Cézilly F, De Marco L, Rigaud T. 2020. Increased temperature has no consequence for behavioral manipulation despite effects on both partners in the interaction between a crustacean host and a manipulative parasite. Sci Rep. 10: 11670. doi: 10.1038/s41598-020-68577-z.

Lacey LA, Grzywacz D, Shapiro-Ilan DI, Frutos R, Brownbridge M, Goettel MS. 2015. Insect pathogens as biological control agents: back to the future. J Invertebr Pathol. 132: 1-41. doi: 10.1016/j.jip.2015.07.009.

Lafferty KD and Morris AK. 1996. Altered behavior of parasitized killifish increases susceptibility to predation by bird final hosts. Ecology. 77: 1390-1397. doi: 10.2307/2265536.

Lafferty KD, Allesina S, Arim M, Briggs CJ, De Leo G, Dobson AP, Dunne JA, Johnson PTJ, Kuris AM, Marcogliese DJ, Martinez ND, Memmott J, Marquet PA, McLaughlin JP, Mordecai EA, Pascual M, Poulin R, Thieltges DW. 2008. Parasites in food webs: the ultimate missing links. Ecol Lett. 11: 533-546. doi: 10.1111/j.1461-0248.2008.01174.x.

Lafferty KD and Shaw JC. 2013. Comparing mechanisms of host manipulation across host and parasite taxa. J Exp Biol. 216: 56-66. doi: 10.1242/jeb.073668.

Lazcano A and Peretó J. 2017. On the origin of mitosing cells: a historical appraisal of Lynn Margulis endosymbiotic theory. J Theor Biol. 434: 80-87. doi: 10.1016/j.jtbi.2017.06.036.

Lee S and Lee DK. 2018. What is the proper way to apply the multiple comparison test? Korean. J. Anesthesiol. 71: 353-360. doi: 10.4097/kja.d.18.00242.

Levine RB and Truman JW. 1982. Metamorphosis of the insect nervous system: changes in morphology and synaptic interactions of identified neurones. Nature. 299: 250-252. doi: 10.1038/299250a0.

Li Y and Guarino LA. 2008. Roles of LEF-4 and PTP/BVP RNA triphosphatases in processing of baculovirus late mRNAs. J Virol. 82: 5573-5583. doi: 10.1128/JVI.00058-08.

Li F, Liu L, Yu X, Rensing C, Wang D. 2022a. The PI3K/AKT Pathway and PTEN gene are involved in "Tree-Top Disease" of Lymantria dispar. Genes. 13: 247. doi: 10.3390/genes13020247.

Li M, Zhang L, Wu Y, Li Y, Chen X, Chen J, Wang Q, Liao C, Han Q. 2022b. Deletion of the serotonin receptor 7 gene changed the development and behavior of the mosquito, Aedes aegypti. Insects. 13: 671. doi: 10.3390/insects13080671.

Lianguzova AD, Ilyutkin SA, Korn OM, Miroliubov AA. 2020. Specialised rootlets of Sacculina pilosella (Rhizocephala: Sacculinidae) used for interactions with its host's nervous system. Arthropod Struct Dev. 60: 101009. doi: 10.1016/j.asd.2020.101009.

Libersat F, Delago A, Gal R. 2009. Manipulation of host behavior by parasitic insects and insect parasites. Ann Rev Entomol. 54: 189-207. doi: 10.1146/annurev.ento.54.110807.090556.

Libersat F and Gal R. 2014. Wasp voodoo rituals, venom-cocktails, and the zombification of cockroach hosts. Integr Comp Biol. 54: 129-142. doi: 10.1093/icb/icu006.

Libersat F, Kaiser M, Emanuel S. 2018. Mind control: how parasites manipulate cognitive functions in their insect hosts. Front Psychol. 9: 572. doi: 10.3389/fpsyg.2018.00572.

Liu J, Cao S, Ding G, Wang B, Li Y, Zhao Y, Shao Q, Feng J, Liu S, Qin L, Xiao Y. 2021. The role of 14-3-3 proteins in cell signalling pathways and virus infection. J Cell Mol Med. 25: 4173-4182. doi: 10.1111/jcmm.16490.

Liu X, Tian Z, Cai L, Shen Z, Michaud JP, Zhu L, Yan S, Ros VID, Hoover K, Li Z, Zhang S, Liu X. 2022. Baculoviruses hijack the visual perception of their caterpillar hosts to induce climbing behaviour thus promoting virus dispersal. Mol Ecol. 31: 2752-2765. doi: 10.1111/mec.16425.

Loreto RG, Araujo JPM, Kepler RM, Fleming KR, Moreau CS, Hughes DP. 2018. Evidence for convergent evolution of host parasitic manipulation in response to environmental conditions. Evolution. 72: 2144-2155. doi: 10.1111/evo.13489.

Lu S, Wang J, Chitsaz F, Derbyshire MK, Geer RC, Gonzales NR, Gwadz M, Hurwitz DI, Marchler GH, Song JS, Thanki N, Yamashita RA, Yang M, Zhang D, Zheng C, Lanczycki CJ, Marchler-Bauer A. 2020. CDD/SPARCLE: the conserved domain database in 2020. Nucleic Acids Res. 48: D265-D268. doi: 10.1093/nar/gkz991.

Luckow VA, Lee SC, Barry GF, Olins PO. 1993. Efficient generation of infectious recombinant baculoviruses by site-specific transposon-mediated insertion of foreign genes into a baculovirus genome propagated in Escherichia coli. J Virol. 67: 4566-4579. doi: 10.1128/JVI.67.8.4566-4579.1993.

Ma H, Huang Q, Lai X, Liu J, Zhu H, Zhou Y, Deng X, Zhou X. 2019. Pharmacological properties of the type 1 tyramine receptor in the Diamondback moth, Plutella xylostella. Int J Mol Sci. 20: 2953. doi: 10.3390/ijms20122953.

Małagocka J, Grell MN, Lange L, Eilenberg J, Jensen AB. 2015. Transcriptome of an entomophthoralean fungus (Pandora formicae) shows molecular machinery adjusted for successful host exploitation and transmission. J Invertebr. Pathol. 128: 47-56. doi: 10.1016/j.jip.2015.05.001.

Małagocka J, Jensen AB, Eilenberg J. 2017. Pandora formicae, a specialist ant pathogenic fungus: new insights into biology and taxonomy. J Invertebr Pathol. 143: 108-114. doi: 10.1016/j.jip.2016.12.007.

Malutan T, McLean H, Caveney S, Donly C. 2002. A high-affinity octopamine transporter cloned from the central nervous system of cabbage looper Trichoplusia ni. Insect Biochem Mol Biol. 32: 343-357. doi: 10.1016/s0965-1748(01)00114-x.

Manga-González MY, González-Lanza C, Cabanas E, Campo R. 2001. Contributions to and review of dicrocoeliosis, with special reference to the intermediate hosts of Dicrocoelium dendriticum. Parasitology. 123: 91-114. doi: 10.1017/s0031182001008204.

Manga-González MY and González-Lanza C. 2005. Field and experimental studies on Dicrocoelium dendriticum and dicrocoeliasis in northern Spain. J Helminthol. 79: 291-302. doi: 10.1079/joh2005323.

Mangold CA, Ishler MJ, Loreto RG, Hazen ML, Hughes DP. 2019. Zombie ant death grip due to hypercontracted mandibular muscles. J Exp Biol. 222: jeb200683. doi: 10.1242/jeb.200683.

Mangold CA and Hughes DP. 2021. Insect behavioral change and the potential contributions of neuroinflammation—a call for future research. Genes. 12: 465. doi: 10.3390/genes12040465.

Mao Z and Davis RL. 2009. Eight different types of dopaminergic neurons innervate the Drosophila mushroom body neuropil: anatomical and physiological heterogeneity. Front. Neural Circuits. 3: 1-17. doi: 10.3389/neuro.04.005.2009.

Mapes CR and Krull WH. 1952. Studies on the biology of Dicrocoelium dendriticum (Rudolphi, 1819) looss, 1899 (Trematoda: Dicrocoeliidae), including its relation to the intermediate host, Cionella lubrica (Müller). VII. The second intermediate host of Dicrocoelium dendriticum. Cornell Vet. 42: 603-604.

Martín-Vega D, Garbout A, Ahmed F, Wicklein M, Goater CP, Colwell DD, Hall MJR. 2018. 3D virtual histology at the host/parasite interface: visualization of the master manipulator, Dicrocoelium dendriticum, in the brain of its ant host. Sci Rep. 8: 8587. doi: 10.1038/s41598-018-26977-2.

Maynard BJ, DeMartini L, Wright WG. 1996. Gammarus lacustris harboring Polymorphus paradoxus show altered patterns of serotonin-like immunoreactivity. J Parasitol. 82: 663-666.

Miroliubov AA, Borisenko I, Nesterenko M, Lianguzova A, Ilyutkin S, Lapshin N, Dobrovolskij A. 2020. Specialized structures on the border between rhizocephalan parasites and their host's nervous system reveal potential sites for host-parasite interactions. Sci Rep 10: 1128. doi: 10.1038/s41598-020-58175-4.

Momohara Y, Aonuma H, Nagayama T. 2018. Tyraminergic modulation of agonistic outcomes in crayfish. J Comp Physiol A. 204: 465-473. doi: 10.1007/s00359-018-1255-3.

Monsma SA, Oomens AG, Blissard GW. 1996. The GP64 envelope fusion protein is an essential baculovirus protein required for cell-to-cell transmission of infection. J Virol. 70: 4607-4616. doi: 10.1128/JVI.70.7.4607-4616.1996.

Moore J. 2002. Parasites and the Behavior of Animals, first edition. Oxford University Press. Oxford, UK. ISBN: 9780195146530.

Mu J, Lent JMV, Smagghe G, Wang Y, Chen X, Vlak JM, van Oers MM. 2014. Live imaging of baculovirus infection of midgut epithelium cells: a functional assay of per os infectivity factors. J Gen Virol. 95: 2531-2539. doi: 10.1099/vir.0.068262-0.

Mukhopadhyay M and Campos AR. 1995. The larval optic nerve is required for the development of an identified serotonergic arborization in Drosophila melanogaster. Dev Biol. 169: 629-643. doi: 10.1006/dbio.1995.1175.

Nathan KG and Lal SK. 2020. The multifarious role of 14-3-3 family of proteins in viral replication. Viruses. 12: 436. doi: 10.3390/v12040436.

Naundrup A, Bohman B, Kwadha CA, Jensen AB, Becher PG, de Fine Licht HH. 2022. Pathogenic fungus uses volatiles to entice male flies into fatal matings with infected female cadavers. ISME J. 16: 2388-2397. doi: 10.1038/s41396-022-01284-x.

Nässel DR and Cantera R. 1985. Mapping of serotonin-immunoreactive neurons in the larval nervous system of the flies Calliphora erythrocephala and Sarcophaga bullata. A comparison with ventral ganglion in adult animals. Cell Tissue Res. 239: 423-434. doi: 10.1007/bf00218023.

Noguchi H, Hayakawa Y, Downer RGH. 1995. Elevation of dopamine levels in parasitized insect larvae. Insect Biochem Mol Biol. 25: 197-201. doi: 10.1016/0965-1748(94)00054-L.

Ohta H, Utsumi T, Ozoe Y. 2003. B96Bom encodes a Bombyx mori tyramine receptor negatively coupled to adenylate cyclase. Insect Mol Biol. 12: 217-223. doi: 10.1046/j.1365-2583.2003.00404.x.

Orchard I, Ramirez J-M, Lange AB. 1993. A multifunctional role for octopamine in locust flight. A Rev Ent. 38: 227-249. doi: 10.1146/annurev.en.38.010193.001303.

O'Reilly DR and Miller LK. 1989. A baculovirus blocks insect molting by producing ecdysteroid udp-glucosyl transferase. Science. 245: 1110-1112. doi: 10.1126/science.2505387.

O'Reilly DR and Miller LK. 1991. Improvement of a baculovirus pesticide by deletion of the egt gene. Bio Technol. 9: 1086-1089. doi: 10.1038/nbt1191-1086.

O'Reilly DR. 1999. The baculovirus egt gene: focused on the Baculoviridae: current research and future directions. RIKEN Rev. 22: 17-19.

Paraschivescu D and Raicev C. 1980. Experimental ecological investigations on the tetany of the species Formica pratensis complementary host of the trematode Dicrocoelium dendriticum. Trav Mus Hist Nat "Grigore Antipa". 22: 299-302.

Parker GA, Ball MA, Chubb JC, Hammerschmidt K, Milinski M. 2009. When should a trophically transmitted parasite manipulate its host? Evolution. 63: 448-458. doi: 10.1111/j.1558-5646.2008.00565.x.

Parksepp M, Leppik L, Koch K, Uppin K, Kangro R, Haring L, Vasar E, Zilmer M. 2020. Metabolomics approach revealed robust changes in amino acid and biogenic amine signatures in patients with schizophrenia in the early course of the disease. Sci Rep. 10: 13983. doi: 10.1038/s41598-020-71014-w.

Pereanu W, Spindler S, Cruz L, Hartenstein V. 2007. Tracheal development in the Drosophila brain is constrained by glial cells. Dev Biol. 302: 169-180. doi: 10.1016/j.ydbio.2006.09.022.

Perrot-Minnot MJ and Cézilly F. 2013. Investigating candidate neuromodulatory systems underlying parasitic manipualtion: concepts, limitations and prospects. J Exp Biol. 216: 134-141. doi: 10.1242/jeb.074146.

Phillips-Portillo J and Strausfeld NJ. 2012. Representation of the brain's superior protocerebrum of the flesh fly, Neobellieria bullata, in the central body. J Comp Neurol. 520: 3070-3087. doi: 10.1002/cne.23094.

Pleiter S. 2020. Going around in circles: designing and testing new methods to measure and compare hyperactive behaviour caused by Autographa californica multiple nucleopolyhedrovirus in Spodoptera exigua larvae. Masters dissertation, Wageningen University.

Ponton F, Lefevre T, Lebarbenchon C, Thomas F, Loxdale HD, Marché L, Renault L, Perrot-Minnot MJ, Biron DG. 2006. Do distantly related parasites rely on the same proximate factors to alter the behaviour of their hosts? Proc Biol Sci. 273: 2869-2877. doi: 10.1098/rspb.2006.3654.

Poulin R. 1995. "Adaptive" changes in the behaviour of parasitized animals: a critical review. Int J Parasitol. 25: 1371-1383. doi: 10.1016/0020-7519(95)00100-x.

Poulin R. 2007. Evolutionary Ecology of Parasites, second edition. Princeton University Press. New Jersey, USA. ISBN: 9780691120850.

Prandovszky E, Gaskell E, Martin H, Dubey JP, Webster JP, McConkey GA. 2011. The neurotropic parasite Toxoplasma gondii increases dopamine metabolism. PLoS One. 6: e23866. doi: 10.1371/journal.pone.0023866.

Provost B, Varricchio P, Arana E, Espagne E, Falabella P, Huguet E, La Scaleia R, Cattolico L, Poirié M, Malva C, Olszewski JA, Pennacchio F, Drezen JM. 2004. Bracoviruses contain a large multigene family coding for protein tyrosine phosphatases. J Virol. 78: 13090-13103. doi: 10.1128/JVI.78.23.13090–13103.2004.

Qi YX, Jin M, Ni XY, Ye GY, Lee Y, Huang J. 2017. Characterization of three serotonin receptors from the small white butterfly, Pieris rapae. Insect Biochem Mol Biol. 87: 107-116. doi: 10.1016/j.ibmb.2017.06.011.

Rang HP, Ritter JM, Flower RJ, Henderson G. 2016. Rang and Dale's Pharmacology, eighth edition. China: Elsevier.

Rebolledo D, Lasa R, Guevara R, Murillo R, Williams T. 2015. Baculovirus-induced climbing behavior favors intraspecific necrophagy and efficient disease transmission in Spodoptera exigua. PLoS One. 10: e0136742. doi: 10.1371/journal.pone.0136742.

Rehder V. 1989. Sensory pathways and motoneurons of the proboscis reflex in the suboesophageal ganglion of the honey bee. J Comp Neurol. 279: 499-513. doi: 10.1002/cne.902790313.

Riddiford LM, Hiruma K, Zhou XF, Nelson CA. 2003. Insights into the molecular basis of the hormonal control of molting and metamorphosis from Manduca sexta and Drosophila melanogaster. Insect Biochem Mol Biol. 33: 1327-1338. doi: 10.1016/j.ibmb.2003.06.001.

Robinow S, Talbot WS, Hogness DS, Truman JW. 1993. Programmed cell death in the Drosophila CNS is ecdysone-regulated and coupled with a specific ecdysone receptor isoform. Development. 119: 1251-1259. doi: 10.1242/dev.119.4.1251.

Robinson GS, Ackery PA, Kitching I, Beccaloni GW, Hernández LM. 2023. HOSTS (from HOSTS - a database of the world's lepidopteran hostplants) [data set resource]. Natural History Museum. https://data.nhm.ac.uk/dataset/hosts/resource/877f387a-36a3-486c-a0c1-b8d5fb69f85a

Roeder T. 2005. Tyramine and octopamine: ruling behavior and metabolism. Annu Rev Entomol. 50: 447-477. doi: 10.1146/annurev.ento.50.071803.130404.

Romig T, Lucius R, Frank W. 1980. Cerebral larvae in the second intermediate host of Dicrocoelium dendriticum (Rudolphi, 1819) and Dicrocoelium hospes Looss, 1907 (Trematodes, Dicrocoeliidae). Z Parasitenkd. 63: 277-286. doi: 10.1007/BF00931990.

Ros VID, van Houte S, Hemerik L, van Oers MM. 2015. Baculovirus-induced tree-top disease: how extended is the role of egt as a gene for the extended phenotype? Mol Ecol. 24: 249-258. doi: 10.1111/mec.13019.

Ros VID. 2021. Baculoviruses: General Features (Baculoviridae). In DH Bamford and M Zuckerman (eds.): Encyclopedia of Virology. fourth edition. 739-746. Elsevier Ltd. ISBN: 9780128145166.

Rosero MA, Abdon B, Silva NJ, Cisneros Larios B, Zavaleta JA, Makunts T, Chang ES, Bashar SJ, Ramos LS, Moffatt CA, Fuse M. 2019. Divergent mechanisms for regulating growth and development after imaginal disc damage in the tobacco hornworm, Manduca sexta. J Exp Biol. 222: jeb200352. doi: 10.1242/jeb.200352.

Rozen S and Skaletsky H. 1999. Primer3 on the WWW for general users and for biologist programmers. Methods Mol Biol. 132: 365-386. doi: 10.1385/1-59259-192-2:365.

Sagan L. 1967. On the origin of mitosing cells. J Theor Biol. 14: 255-274. doi: 10.1016/0022-5193(67)90079-3.

Sajadi T. 2023. Expression of AcMNPV-infection by means of behavioural alteration in S. exigua populations. Masters dissertation, Wageningen University.

Santiago-Tirado FH and Doering TL. 2017. False friends: phagocytes as trojan horses in microbial brain infections. PLoS Pathog. 13: e1006680. doi: 10.1371/journal. ppat.1006680.

Schindelin J, Arganda-Carreras I, Frise E, Kaynig V, Longair M, Pietzsch T, Preibisch S, Rueden C, Saalfeld S, Schmid B, Tinevez JY, White DJ, Hartenstein V, Eliceiri K, Tomancak P, Cardona A. 2012. Fiji: an open-source platform for biological-image analysis. Nat Methods. 9: 676-682. doi: 10.1038/nmeth.2019.

Schmidt-Rhaesa A and Ehrmann R. 2001. Horsehair worms (Nematomorpha) as parasites of praying mantids with a discussion of their life cycle. Zool Anz. 240: 167-179. doi: 10.1078/0044-5231-00014.

Selcho M, Pauls D, Han KA, Stocker RF, Thum AS. 2009. The role of dopamine in Drosophila larval classical olfactory conditioning. PLoS One. 4: e5897. doi: 10.1371/journal.pone.0005897.

Senem JV, Torquato EFB, Ribeiro LdFC, Brancalhão RMC. 2016. Cytopathology of the trachea of Bombyx mori (Lepidoptera: Bombycidae) to Bombyx mori nucleopolyhedrovirus. Micron. 80: 39-44. doi: 10.1016/j.micron.2015.09.005

Shaw JC, Korzan WJ, Carpenter RE, Kuris AM, Lafferty KD, Summers CH, Øverli Ø. 2009. Parasite manipulation of brain monoamines in California killifish (Fundulus parvipinnis) by the trematode Euhaplorchis californiensis. Proc Biol Sci. 276: 1137-1146. doi: 10.1098/rspb.2008.1597.

Sheng Z and Charbonneau H. 1993. The baculovirus Autographa californica encodes a protein tyrosine phosphatase. JBC. 268: 4728-4733. doi: 10.1016/S0021-9258(18)53457-8.

Simon S, Breeschoten T, Jansen HJ, Dirks RP, Schranz ME, Ros VID. 2021. Genome and transcriptome analysis of the beet armyworm Spodoptera exigua reveals targets for pest control. G3. 11: jkab311. doi: 10.1093/g3journal/jkab311.

Sinakevitch IT, Wolff GH, Pflüger HJ, Smith BH. 2018. Editorial: biogenic amines and neuromodulation of animal behavior. Front Syst Neurosci. 12: 31. doi: 10.3389/fnsys.2018.00031.

Slack J and Arif BM. 2007. The baculoviruses occlusion-derived virus: virion structure and function. Adv Virus Res. 69: 99-165. doi: 10.1016/S0065-3527(06)69003-9.

Smirnoff WA. 1965. Observations on the effect of virus infection on insect behavior. J Invertebr Pathol. 7: 387-388. doi: 10.1016/0022-2011(65)90017-0.

Smith GE and Summers MD. 1979. Restriction maps of five Autographa californica MNPV variants, Trichoplusia ni MNPV, and Galleria mellonella MNPV DNAs with endonucleases SmaI, KpnI, BamHI, SacI, XhoI, and EcoRI. J Virol. 30: 828-838. doi: 10.1128/JVI.30.3.828-838.1979.

Smits PH. 1987. Nuclear polyhedrosis virus as biological agent of Spodoptera exigua. Chapter 1 in Doctoral dissertation. Wageningen Agricultural University.

Spindler E, Zahler M, Loos-Frank B. 1986. Behavioural aspects of ants as second intermediate hosts of Dicrocoelium dendriticum. Z Parasitenkd. 72: 689-692. doi: 10.1007/BF00925492.

Stache A, Heller E, Hothorn T, Heurich M. 2013. Activity patterns of European roe deer (Capreolus capreolus) are strongly influenced by individual behavior. Folia Zool. 62: 67-75. doi: 10.25225/fozo.v62.i1.a10.2013.

Steinhaus EA. 1946. Insect Microbiology: An Account of the Microbes Associated with Insects and Ticks with Special Reference to the Biologic Relationships Involved. Comstock Publishing Company. London, UK.

Stork T, Engelen D, Krudewig A, Silies M, Bainton RJ, Klämbt C. 2008. Organization and function of the blood-brain barrier in Drosophila. J Neurosci. 28: 587-597. doi: 10.1523/JNEUROSCI.4367-07.2008.

Stropfer M. 2014. Central processing in the mushroom bodies. Curr Opin Insec. 6: 99-103. doi: 10.1016/j.cois.2014.10.009.

Szczuka A, Korczyńska J, Wnuk A, Symonowicz B, Gonzalez Szwacka A, Mazurkiewicz P, Kostowski W, Godzińska EJ. 2013. The effects of serotonin, dopamine, octopamine and tyramine on behavior of workers of the ant Formica polyctena during dyadic aggression tests. Acta Neurobiol Exp. 73: 495-520. doi: 10.55782/ane-2013-1955.

Tain L, Perrot-Minnot MJ, Cézilly F. 2006. Altered host behaviour and brain serotonergic activity caused by acanthocephalans: evidence for specificity. Proc Biol Sci. 273: 3039-3045. doi: 10.1098/rspb.2006.3618.

Takagi T, Taylor GS, Kusakabe T, Charbonneau H, Buratowski S. 1998. A protein tyrosine phosphatase-like protein from baculovirus has RNA 5′-triphosphatase and diphosphatase activities. PNAS. 95: 9808-9812. doi: 10.1073/pnas.95.17.9808.

Tang Q-B, Song W-W, Chang Y-J, Xie G-Y, Chen W-B, Zhao X-C. 2019. Distribution of serotonin-immunoreactive neurons in the brain and gnathal ganglion of caterpillar Helicoverpa armigera. Front Neuroanat. 13: 56. doi: 10.3389/fnana.2019.00056.

Tarry DW. 1969. Dicrocoelium dendriticum: the life cycle in Britain. J Helminthol. 43: 403-416. doi: 10.1017/S0022149X00004971.

Tedjakumala SR, Rouquette J, Boizeau ML, Mesce KA, Hotier L, Massou I, Giurfa M. 2017. A tyrosine-hydroxylase characterization of dopaminergic neurons in the honey bee brain. Front Syst Neurosci. 11: 47. doi: 10.3389/fnsys.2017.00047.

Thamm M, Balfanz S, Scheiner R, Baumann A, Blenau W. 2010. Characterization of the 5-HT1A receptor of the honeybee (Apis mellifera) and involvement of serotonin in phototactic behavior. Cell Mol Life Sci. 67: 2467-2479. doi: 10.1007/s00018-010-0350-6.

Thomas F, Schmidt-Rhaesa A, Martin G, Manu C, Durand P, Renaud F. 2002. Do hairworms (Nematomorpha) manipulate the water seeking behavior of their terrestrial hosts? J Evol Biol. 15: 356-361. doi: 10.1046/j.1420-9101.2002.00410.x.

Tierney AJ. 2018. Invertebrate serotonin receptors: a molecular perspective on classification and pharmacology. J Exp Biol. 221: jeb184838. doi: 10.1242/jeb.184838.

Tonks, N. 2006. Protein tyrosine phosphatases: from genes, to function, to disease. Nat Rev Mol Cell Biol. 7: 833-846. doi: 10.1038/nrm2039.

Torquato EF, Neto MH, Brancalhão RM. 2006. Nucleopolyhedrovirus infected central nervous system cells of Bombyx mori (L.) (Lepidoptera: Bombycidae). Neotrop Entomol. 35: 70-74. doi: 10.1590/s1519-566x2006000100010.

Trinh T, Ouellette R, de Bekker C. 2021. Getting lost: the fungal hijacking of ant foraging behaviour in space and time. Anim Behav. 181: 165-184. doi: 10.1016/j.anbehav.2021.09.003.

Truman JW, Talbot WS, Fahrbach SE, Hogness DS. 1994. Ecdysone receptor expression in the CNS correlates with stage-specific responses to ecdysteroids during Drosophila and Manduca development. Development. 120: 219-234. doi: 10.1242/dev.120.1.219.

Tsuji E, Aonuma H, Yokohari F, Nishikawa M. 2007. Serotonin-immunoreactive neurons in the antennal sensory system of the brain in the carpenter ant, Camponotus japonicus. Zoolog Sci. 24: 836-849. doi: 10.2108/zsj.24.836.

Vallés AM and White K. 1988. Serotonin-containing neurons in Drosophila melanogaster: development and distribution. J Comp Neurol. 268: 414–428. doi: 10.1002/cne.902680310.

van der Woude E and Smid HM. 2017. Maximized complexity in miniaturized brains: morphology and distribution of octopaminergic, dopaminergic and serotonergic neurons in the parasitic wasp, Trichogramma evanescens. Cell Tissue Res. 369: 477–496. doi: 10.1007/s00441-017-2642-8.

van Houte S, Ros VID, Mastenbroek TG, Vendrig NJ, Hoover K, Spitzen J, van Oers MM. 2012. Protein tyrosine phosphatase-induced hyperactivity is a conserved strategy of a subset of baculoviruses to manipulate lepidopteran host behavior. PLoS One. 7: e46933. doi: 10.1371/journal.pone.0046933.

van Houte S, Ros VID, van Oers MM. 2013. Walking with insects: molecular mechanisms behind parasitic manipulation of host behaviour. Mol Ecol. 22: 3458-3475. doi: 10.1111/mec.12307.

van Houte S, Ros VID, van Oers MM. 2014a. Hyperactivity and tree-top disease induced by the baculovirus AcMNPV in Spodoptera exigua larvae are governed by independent mechanisms. Naturwissenschaften. 101: 347-350. doi:10.1007/s00114-014-1160-8.

van Houte S, van Oers MM, Han Y, Vlak JM, Ros VID. 2014b. Baculovirus infection triggers a positive phototactic response in caterpillars to induce 'tree-top' disease. Biol Letters. 10: 20140680. doi: 10.1098/rsbl.2014.0680.

van Houte S, van Oers MM, Han Y, Vlak JM, Ros VID. 2015. Baculovirus infection triggers a positive phototactic response in caterpillars: a response to Dobson et al. (2015). Biol Letters. 11: 20150633. doi: 10.1098/rsbl.2015.0633.

van Leeuwen LM, Boot M, Kuijl C, Picavet DI, van Stempvoort G, van der Pol SMA, de Vries HE, van der Wel NN, van der Kuip M, van Furth AM, van der Sar AM, Bitter W. 2018. Mycobacteria employ two different mechanisms to cross the blood–brain barrier. Cell Microbiol. 20: 1-17. doi: 10.1111/cmi.12858.

van Oers MM, Flipsen JTM, Reusken CBEM, Sliwinsky EL, Goldbach RW, Vlak JM. 1993. Functional domains of the p10 protein of Autographa californica nuclear polyhedrosis virus. J Gen Virol. 74: 563-574. doi: 10.1099/0022-1317-74-4-563.

van Oers MM. 2021. Baculoviruses: Molecular Biology and Replication (Baculoviridae). In DH Bamford and M Zuckerman (eds.): Encyclopedia of Virology. fourth edition. Elsevier Ltd. ISBN: 9780128145166.

van Valen L. 1973. A new evolutionary law. Evol Theory. 1: 1-30.

Vasconcelos SD, Cory JS, Wilson KR, Sait SM, Hails RS. 1996. Modified behavior in baculovirus-infected lepidopteran larvae and its impact on the spatial distribution of inoculum. Biol Control. 7: 299-306. doi: 10.1006/bcon.1996.0098.

Verlinden H. 2018. Dopamine signalling in locusts and other insects. Insect Biochem Mol Biol. 97: 40-52. doi: 10.1016/j.ibmb.2018.04.005.

Vinauger C, Lahondère C, Wolff GH, Locke LT, Liaw JE, Parrish JZ, Akbari OS, Dickinson MH, Riffell JA. 2018. Modulation of host learning in Aedes aegypti mosquitoes. Curr Biol. 28: 333-344.e8. doi: 10.1016/j.cub.2017.12.015.

Vleugels R, Lenaerts C, Vanden Broeck J, Verlinden H. 2014. Signalling properties and pharmacology of a 5-HT7-type serotonin receptor from Tribolium castaneum. Insect Mol Biol. 23: 230-243. doi: 10.1111/imb.12076.

Vleugels R, Verlinden H, Vanden Broeck J. 2015. Serotonin, serotonin receptors and their actions in insects. Neurotransmitter. 2: e314. doi: 10.14800/nt.314.

Vömel M and Wegener C. 2008. Neuroarchitecture of aminergic systems in the larval ventral ganglion of Drosophila melanogaster. PLoS One. 3: e1848. doi: 10.1371/journal.pone.0001848.

Waddell S. 2013. Reinforcement signalling in Drosophila; dopamine does it all after all. Curr Opin Neurobiol. 23: 324-329. doi: 10.1016/j.conb.2013.01.005.

Wang W and Shakes DC. 1996. Molecular evolution of the 14-3-3 protein family. J Mol Evol. 43: 384-398. doi: 10.1007/BF02339012.

Wang GB, Zhang JJ, Shen YW, Zheng Q, Feng M, Xiang XW, Wu XF. 2015. Transcriptome analysis of the brain of the silkworm Bombyx mori infected with Bombyx mori nucleopolyhedrovirus: a new insight into the molecular mechanism of enhanced locomotor activity induced by viral infection. J Invertebr Pathol. 128: 37-43. doi: 10.1016/j.jip.2015.04.001.

Wang H, Wang J, Zhang Q, Zeng T, Zheng Y, Chen H, Zhang XF, Wei T. 2019. Rice yellow stunt nucleorhabdovirus matrix protein mediates viral axonal transport in the central nervous system of its insect vector. Front Microbiol. 10: 939. doi: 10.3389/fmicb.2019.00939.

Webster JP and McConkey GA. 2010. Toxoplasma gondii-altered host behaviour: clues as to mechanism of action. Folia Parasitol. 57: 95-104. doi: 10.14411/fp.2010.012.

Weeks JC and Jacobs GA. 1987. A reflex behavior mediated by monosynaptic connections between hair afferents and motoneurons in the larval tobacco hornworm, Manduca sexta. J Comp Physiol A. 160: 315-329. doi: 10.1007/BF00613021.

Weinstein SB and Kuris AM. 2016 Independent origins of parasitism in animalia. Biol Lett. 12: 20160324. doi: 10.1098/rsbl.2016.0324.

Wesołowska W and Wesołowski T. 2014. Do Leucochloridium sporocysts manipulate the behaviour of their snail hosts? J Zool. 292: 151-155. doi: 10.1111/jzo.12094.

Will I, Das B, Trinh T, Brachmann A, Ohm R, de Bekker C. 2020. Genetic underpinnings of host manipulation by Ophiocordyceps as revealed by comparative transcriptomics. G3. 10: 2275-2296. doi: 10.1534/g3.120.401290.

Williams T, Bergoin M, van Oers MM. 2017a. Diversity of large DNA viruses of invertebrates. J Invertebr Pathol. 147: 4-22. doi: 10.1016/j.jip.2016.08.001.

Williams T, Virto C, Murillo R, Caballero P. 2017b. Covert infection of insects by baculoviruses. Front Microbiol. 8: 1337. doi: 10.3389/fmicb.2017.01337.

Windsor DA. 1998. Most of the species on earth are parasites. Int J Parasitol. 28: 1939-1941. doi: 10.1016/S0020-7519(98)00153-2.

Wolff T, Iyer NA, Rubin GM. 2015. Neuroarchitecture and neuroanatomy of the Drosophila central complex: a GAL4-based dissection of protocerebral bridge neurons and circuits. J Comp Neurol. 523: 997-1037. doi: 10.1002/cne.23705.

Wright GA, Mustard JA, Simcock NK, Ross-Taylor AA, McNicholas LD, Popescu A, Marion-Poll F. 2010. Parallel reinforcement pathways for conditioned food aversions in the honeybee. Curr Biol. 20: 2234-2240. doi: 10.1016/j.cub.2010.11.040.

Wu SF, Xu G, Stanley D, Huang J, Ye GY. 2015. Dopamine modulates hemocyte phagocytosis via a D1-like receptor in the rice stem borer, Chilo suppressalis. Sci Rep. 5: 12247. doi: 10.1038/srep12247.

Xie G-Y, Ma B-W, Liu X-L, Chang Y-J, Chen W-B, Li G-P, Feng H-Q, Zhang Y-J, Berg BG, Zhao X-C. 2019. Brain organization of Apolygus lucorum: a hemipteran species with prominent antennal lobes. Front Neuroanat. 13: 70. doi: 10.3389/fnana.2019.00070.

Xu L, Jiang H-B, Chen X-F, Xiong Y, Lu X-P, Pei Y-X, Smagghe G, Wang J-J. 2018. How tyramine β-hydroxylase controls the production of octopamine, modulating the mobility of beetles. Int J Mol Sci. 19: 846. doi: 10.3390/ijms19030846.

Yamauchi T, Nakata H, Fujisawa H. 1981. A new activator protein that activates tryptophan 5-monooxygenase and tyrosine 3-monooxygenase in the presence of Ca2+-, calmodulin-dependent protein kinase. Purification and characterization. J Biol Chem. 256: 5404-5409. doi: 10.1016/S0021-9258(19)69215-X.

Yang F, Chan K, Brewster CC, Paulson SL. 2019. Effects of La Crosse virus infection on the host-seeking behavior and levels of two neurotransmitters in Aedes triseriatus. Parasit Vectors. 12: 397. doi: 10.1186/s13071-019-3658-6.

Yao TP, Segraves WA, Oro AE, McKeown M, Evans RM. 1992. Drosophila ultraspiracle modulates ecdysone receptor function via heterodimer formation. Cell. 71: 63-72. doi: 10.1016/0092-8674(92)90266-f.

Yao Z and Scott K. 2022. Serotonergic neurons translate taste detection into internal nutrient regulation. Neuron. 110: 1036-1050.e7. doi: 10.1016/j.neuron.2021.12.028.

Yuan X, Sipe CW, Suzawa M, Bland ML, Siegrist SE. 2020. Dilp-2–mediated PI3-kinase activation coordinates reactivation of quiescent neuroblasts with growth of their glial stem cell niche. PLoS Biol. 18: e3000721. doi: 10.1371/journal.pbio.3000721.

Zhang ZY. 2002. Protein tyrosine phosphatase: structure and function, substrate specificity, and inhibitor development. Annu Rev Pharmacol Toxicol. 42: 209-234. doi: 10.1146/annurev.pharmtox.42.083001.144616.

Zhang S, An S, Hoover K, Li Z, Li X, Liu X, Shen Z, Fang H, Ros VID, Zhang Q, Liu X. 2018. Host miRNAs are involved in hormonal regulation of HaSNPV-triggered climbing behaviour in Helicoverpa armigera. Mol Ecol. 27: 459-475. doi: 10.1111/mec.14457.

Zhang J-J, Sun L-L, Wang Y-N, Xie G-Y, An S-H, Chen W-B, Tang Q-B, Zhao X-C. 2022. Serotonergic neurons in the brain and gnathal ganglion of larval Spodoptera frugiperda. Front. Neuroanat. 16: 844171. doi: 10.3389/fnana.2022.844171.

Zhou LJ, Peng J, Chen M, Yao LJ, Zou WH, He CY, Peng HJ. 2021. Toxoplasma gondii SAG1 targeting host cell S100A6 for parasite invasion and host immunity. iScience. 24: 103514. doi: 10.1016/j.isci.2021.103514.

Zhu X, Yuan M, Shakeel M, Zhang Y, Wang S, Wang X, Zhan S, Kang T, Li J. 2014. Selection and evaluation of reference genes for expression analysis using qRT-PCR in the beet armyworm Spodoptera exigua (Hübner) (Lepidoptera: Noctuidae). PLoS One. 9: e84730. doi: 10.1371/journal.pone.0084730.

Zimmer C. 2001. Parasite Rex: Inside the Bizarre World of Nature's Most Dangerous Creatures. Atria. New York, USA. ISBN: 9780743200110.

Øverli Ø, Páll M, Borg B, Jobling M, Winberg S. 2001. Effects of Schistocephalus solidus infection on brain monoaminergic activity in female three-spined sticklebacks Gasterosteus aculeatus. Proc Biol Sci. 268: 1411-1415. doi: 10.1098/rspb.2001.1668.s.

Summary

X

Parasite-induced modification of host behaviour which increase transmission to the next host is a common phenomenon. Two of the most remarkable cases of parasite-induced host behavioural manipulation comprise the changes baculoviruses induce in their caterpillar hosts in the form of hyperactivity and tree-top disease, and trematode-infected ants climbing into vegetation and biting onto it. These two systems are great examples of parasites that go a step further in their manipulation: they do so by invading the central nervous system (CNS) of the host. This hostile take-over of a host's nervous system by a foreign invader, in order to alter the behaviour of the host in favour of the parasite, is termed neuroparasitism.

Chapter 2 of this thesis, reviews what was known at the time about baculoviral manipulation of their caterpillar hosts' behaviour. Baculoviruses are well-known for inducing hyperactivity (enhanced locomotion) and/or tree-top disease (climbing to elevated positions prior to death). Baculoviruses can be easily mutated, allowing an optimal experimental setup in comparative studies, where for instance host gene expression can be compared between insects infected with wild-type (WT) viruses or with mutant viruses lacking genes involved in behavioural manipulation. We here addressed results from recent studies that revealed the first insight into the underlying molecular pathways that lead to the typical behaviour of baculovirus-infected caterpillars and into the role of light therein. Since host behaviour in general is mediated through the host's CNS, we postulated promising future steps to study how baculoviruses regulate the neuronal activity of the host.

In **Chapter 3**, I focused on the factors, which influence the expression of behavioural alteration, induced by a brain-infecting trematode in its natural habitat in the forest. This chapter examines the effects of temperature, relative humidity (RH), time of the day, date, and an irradiation-proxy on behavioural modification of the ant *Formica polyctena* by the lancet liver fluke *Dicrocoelium dendriticum*. This fluke induces ants to climb and bite to vegetation by the mandibles in a state of temporary tetany. A total of 1264 individual ants expressing the modified behaviour were observed over 13 non-consecutive days and a sub-set of those ants was individually marked to track attachment and release of infected ants in relation to variation in temperature. Infected ants primarily attached to vegetation early and late in the day corresponding to low temperature and high RH, presumably coinciding with the grazing activity of potential mammalian herbivores, the definitive hosts of the liver fluke. Temperature was the single most important determinant for the induced phenotypic change. On warm days, infected ants altered between the manipulated and non-manipulated state multiple times, while on cool days many infected ants remained attached to the vegetation all day. The results from this chapter suggest that temperature-sensitivity of these naturally infected ants serves the dual-purpose of exposing infected ants to the next host at an opportune time, while protecting them from exposure to high temperatures, which might increase host (and parasite) mortality.

Chapter 4 represents an in depth analysis of the CNS of *Spodoptera exigua* caterpillars. While the CNS of insects has been studied to some extent, the focus has been mainly on brains of adult insects and the larval CNS has received little attention so far. This chapter presents an overview of immunoreactive areas of the major biogenic amines in the CNS of mid third instar larvae of the beet armyworm *S. exigua*. The major biogenic amines of insects and the rate limiting enzymes involved in their biosynthesis were targeted, as it has been suggested that these are involved in the induction of a wide range of behavioural traits. I identified and described the immunoreactive neurons and projections and their location in the CNS of *S. exigua* for tyrosine decarboxylase (TDC), tyramine (TA), tyramine beta-hydroxylase (TβH), octopamine (OA), tyrosine hydroxylase (TH) and serotonin (5HT). The analysis from this chapter aided in filling knowledge gaps for the CNS of larval insects, and thereby facilitates future research on lepidopteran larvae, their CNS and their behaviour, including the studies in the next two chapters.

In **Chapter 5** the focus is on the most well-studied baculovirus Autographa californica multiple nucleopolyhedrovirus (AcMNPV) and CNS entry. Upon infection of AcMNPV in *S. exigua* caterpillars, an enzymatically active form of the virus-encoded protein tyrosine phosphatase (PTP) is needed for the expression of hyperactivity from 3 days post infection (dpi). Using eGFP-expressing recombinant AcMNPV strains I showed that infection of the caterpillar's CNS can be observed primarily from 3 dpi onwards. In addition, the chapter demonstrates that PTP does not play a role in the infection of the CNS. It is shown that the virus entered the CNS via the trachea, progressing caudally to frontally through the CNS and that the infection progressed from the outermost cell layers towards the inner cell layers of the CNS, in a PTP-independent manner.

Chapter 6 builds onto the knowledge acquired in the past two chapters, and we dived further into the underlying mechanisms of behavioural alteration. In this chapter early third instar caterpillars were orally infected with WT AcMNPV or with AcMNPV mutants either expressing a catalytically inactive PTP (catmut) or no PTP (Δ*ptp*), to further investigate the potential role of biogenic amine signalling cascades in AcMNPV-PTP induced behavioural manipulation at 1, 3 and 4 dpi. We measured the concentration in the haemolymph of the three major biogenic amines in invertebrates: 5HT, OA and dopamine (DA). In addition, we investigated the gene expression of actors involved in the biogenic pathways to these amines along with TA, by analysing the gene expression of precursor enzymes, rate-limiting enzymes and the receptors in these major biogenic pathways. We were able to detect an effect of dpi and treatments on the concentration of 5HT and DA and we found the genes for most of the precursors, rate limiting enzymes and receptors were highest expressed at 1 dpi. Furthermore, the gene encoding for the serotonin receptor 5HT-7 was upregulated in AcMNPV WT-infected larval heads compared to the AcMNPV

catmut- and AcMNPV Δ*ptp*-infected conspecifics. In addition, when infected with AcMNPV WT, an upregulation of the gene encoding the tyramine receptor TAR1 was seen in larval heads compared to heads of larvae infected with AcMNPV catmut- or AcMNPV Δ*ptp*.

In the last **Chapter 7**, I discussed the above mentioned findings from the thesis by placing the results into the scientific field and I revealed some additional preliminary results. When pulling together the information presented above from Chapter 4, 5 and 6 regarding biogenic amines, their rate limiting enzymes and the receptors thereof we do see a potential role of these actors in host behavioural manipulation by neuroparasites. With the significant differences of AcMNPV WT-infected larvae compared to their AcMNPV Δ*ptp*- and catmut-infected conspecifics regarding the concentrations of DA, the expression levels of 5HT-7 and TAR1 and the proximity of immunoreactive areas of TDC, TH, TA and 5HT with AcMNPV in the CNS, I have in this project provided indications of the role of these actors in the behavioural manipulation by AcMNPV of the *S. exigua* caterpillar host. I have demonstrated that PTP is not necessary for the virus to enter the caterpillar CNS and that AcMNPV likely acts by directly manipulating the intriguing network of neuromodulators and developmental processes that govern the behaviour of an insect. Through these results I have added new insights into the complex mechanisms exploited by baculoviruses in specific, and by neuroparasites in general.

Samenvatting

Parasiet-geïnduceerde veranderingen van gastheergedrag die de transmissie naar de volgende gastheer vergroten, zijn een veelvoorkomend verschijnsel. Opvallende gevallen van parasiet-geïnduceerde manipulaties van gastheergedrag treffen we aan bij baculovirussen, die veranderingen induceren in rupsen in de vorm van hyperactiviteit en 'tree-top disease', en bij trematode-geïnfecteerde mieren, die omhoog klimmen in de vegetatie en zich erin vastbijten. Deze twee systemen zijn aansprekende voorbeelden, waarin de parasieten ver gaan om hun manipulatie te bewerkstelligen: ze doen dat door het centrale zenuwstelsel (CZS) van hun gastheer binnen te dringen.

Hoofdstuk 2 van dit proefschrift geeft een overzicht van wat bekend was over manipulatie van rupsengedrag door baculovirussen. Baculovirussen staan bekend om het induceren van hyperactiviteit (verhoogde locomotie) en 'tree-top disease' (klimmen naar hoge posities voorafgaand aan de dood). In het laboratorium zijn baculovirussen makkelijk te muteren en dit maakt een optimale experimentele set-up mogelijk voor vergelijkende studies, waarin bijvoorbeeld de genexpressie van de gastheer vergeleken kan worden tussen insecten geïnfecteerd met het wildtype (WT) virus dan wel met mutante virussen die genen missen die mogelijk betrokken zijn bij de gedragsmanipulatie. We refereren aan resultaten van recente studies die een eerste inzicht geven in de onderliggende moleculaire signaaltransductie routes die leiden tot het typische gedrag van baculovirus-geïnfecteerde rupsen en de rol van licht hierin. Omdat gastheergedrag in het algemeen aangestuurd wordt via het CZS van die gastheer benoemen we veelbelovende manieren om te kunnen bestuderen hoe baculovirussen de neuronale activiteit van de gastheer reguleren.

In **Hoofdstuk 3** focus ik op de factoren in een natuurlijke bosomgeving die de expressie van gedragsveranderingen in mieren beïnvloeden als gevolg van een hersen-infecterende trematode . In dit hoofdstuk onderzoek ik de effecten van temperatuur, relatieve luchtvochtigheid (RV), tijd van de dag, datum en van een bestralingsindicator op de gedragsmanipulatie van de mier *Formica polyctena* door de kleine leverbot *Dicrocoelium dendriticum*. Deze leverbot zet mieren aan tot klimmen en zorgt ervoor dat de mieren zich met hun monddelen in de vegetatie vastbijten n een staat van tijdelijke verkramping. Een totaal van 1264 mieren, die alle het veranderde gedrag lieten zien, werd geobserveerd in 13 niet-opeenvolgende dagen. Een subset van de geïnfecteerde mieren werd individueel gemarkeerd om de vasthechting en loslating in relatie tot variaties in temperatuur te kunnen volgen. Geïnfecteerde mieren hechtten zich voornamelijk vast aan vegetatie vroeg en laat op de dag, overeenkomend met een lage temperatuur en een hoge RV, wat vermoedelijk samenvalt met de graasactiviteit van mogelijke zoogdier herbivoren, de uiteindelijke gastheren van de leverbot. Temperatuur was de belangrijkste bepalende factor voor de geïnduceerde fenotypische veranderingen. Op warme dagen wisselden de geïnfecteerde mieren meermaals tussen de gemanipuleerde en niet-gemanipuleerde status, terwijl op koelere dagen

veel geïnfecteerde mieren de hele dag vastgehecht bleven zitten aan de vegetatie. De resultaten van dit hoofdstuk suggereren dat de temperatuurgevoeligheid van deze op een natuurlijk manier geïnfecteerde mieren een tweeledig doel dient: het op een geschikt tijdstip blootstellen van geïnfecteerde mieren aan de volgende gastheer van de leverbot en tegelijkertijd de mieren beschermen tegen te hoge temperaturen om zo sterfte van gastheer (en parasiet) te voorkomen.

Hoofdstuk 4 laat een diepgaande analyse zien van het CZS van rupsen van de Florida uil *Spodoptera exigua*. Hoewel het CZS van insecten tot op zeker hoogte bestudeerd was, was de focus vooral gericht op hersenen van volwassen insecten, terwijl het larvale CZS tot dusver weinig aandacht heeft gekregen. Dit hoofdstuk presenteert een overzicht van de immunoreactieve gebieden in het CZS van midden-derde stadium larven van de *S. exigua* ten aanzien van de voornaamste biogene aminen. Deze biogene aminen en de snelheidsbeperkende enzymen betrokken bij hun biosynthese werden bestudeerd, omdat deze vermoedelijk betrokken zijn bij de inductie van een breed scala aan gedragseigenschappen. Ik heb de immunoreactieve neuronen en projecties geïdentificeerd, en hun locatie beschreven in het CZS van de *S. exigua* larven voor tyrosine decarboxylase (TDC), tyramine (TA), tyramine beta-hydroxylase (TβH), octopamine (OA), tyrosine hydroxylase (TH) en serotonine (5HT). De analyse beschreven in dit hoofdstuk draagt bij aan het opvullen van hiaten in de kennis over het CZS van larvale insecten en faciliteert daarmee toekomstig onderzoek aan larven van de orde Lepidoptera, hun CZS en gedrag, inclusief de studies in de twee volgende hoofdstukken van deze thesis.

In **Hoofdstuk 5** ligt de nadruk op het meest bestudeerde baculovirus Autographa californica multiple nucleopolyhedrovirus (AcMNPV) en hoe dit het CZS binnendringt. Na infectie van *S. exigua* rupsen met AcMNPV is een enzymatisch-actieve vorm van het viraal-gecodeerde eiwit 'protein tyrosine phosphatase' (PTP) nodig voor de expressie van hyperactiviteit vanaf 3 dagen na infectie. Door recombinante AcMNPV varianten die eGFP tot expressie brengen te gebruiken, laat ik zien dat de infectie van het CZS van de rupsen voornamelijk waar te nemen is vanaf 3 dagen na infectie. Daarnaast laat het hoofdstuk zien dat PTP niet nodig is voor de infectie van het CZS. Het virus komt het CZS binnen via de tracheeën, van caudaal naar frontaal en de infectie vordert van de buitenste cellagen naar de binnenste cellagen van het CZS, onafhankelijk van PTP.

Hoofdstuk 6 bouwt voort op de kennis vergaard in de twee voorafgaande hoofdstukken, en ik richt mij hier op de onderliggende mechanismen van gedragsveranderingen. In dit hoofdstuk werden vroeg-derde stadium rupsen oraal geïnfecteerd met WT AcMNPV of met AcMNPV mutanten die of een katalytische inactieve PTP (catmut) of geen PTP (Δ*ptp*) tot expressie brachten, om de mogelijke rol van signaal cascades van biogene aminen verder te bestuderen in de door AcMNPV-PTP

geïnduceerde gedragsveranderingen op 1, 3 en 4 dagen na infectie. Daartoe is de concentratie in de hemolymfe gemeten van de drie voornaamste biogene aminen in ongewervelden: 5HT, OA en dopamine (DA). Daarnaast is de genexpressie onderzocht van factoren betrokken bij de biosynthese-routes die leiden tot de productie van deze amines en ook van TA, door de expressie te analyseren van genen coderend voor de voor enzymen nodig voor de vorming van de benodigde substraten, voor snelheidsbeperkende enzymen en voor de receptoren van de voornaamste biogene amines. We waren in staat om een effect van het aantal dagen na infectie en van de behandelingen te meten op de concentratie van 5HT en DA, en we vonden dat het merendeel van de genen coderend voor de enzymen nodig voor de vorming van de substraten, de snelheidsbeperkende enzymen en de receptoren het hoogst tot expressie kwamen op 1 dag na infectie. Daarnaast was het gen coderend voor de serotonine receptor 5HT-7 actiever in de kop van AcMNPV WT-geïnfecteerde larven dan in de kop van AcMNPV catmut- en AcMNPV Δ*ptp*-geïnfecteerde soortgenoten. Aanvullend was in de kop van AcMNPV WT-geïnfecteerde larven een verhoogde activiteit te zien van het gen voor de tyramine receptor TAR1 ten opzichte van larven die met AcMNPV catmut of AcMNPV Δ*ptp* waren geïnfecteerd.

In het laatste **Hoofdstuk 7** bediscussieer ik de bovengenoemde bevindingen van dit proefschrift door de resultaten in een breder wetenschappelijke kader te plaatsen en laat ik enkele aanvullende preliminaire resultaten zien. Wanneer ik de informatie uit hoofdstuk 4 tot 6 die hierboven gepresenteerd is samenvoeg betreffende snelheidsbeperkende enzymen en hun receptoren, zie ik een potentiële rol van deze actoren in de manipulatie van het gastheergedrag door neuroparasieten. Op grond van de significante verschillen tussen AcMNPV WT-geïnfecteerde larven en hun AcMNPV Δ*ptp*- en catmut-geïnfecteerde soortgenoten betreffende de concentraties van DA, de expressie van 5HT-7 en TAR1, en de nabijheid van AcMNPV en de immunoreactieve gebieden voor TDC, TH, TA en 5HT in het CZS, presenteer ik in dit hoofdstuk aanwijzingen voor de rol van deze actoren in de gedragsmanipulatie van de *S. exigua* rupsen door AcMNPV. Ik heb laten zien dat PTP niet noodzakelijk is voor het binnengaan van het virus in het CZS van de rupsen en daarom is de hypothese nu dat AcMNPV waarschijnlijk acteert door een netwerk van neuromodulatoren en ontwikkelingsprocessen die het insectengedrag aansturen rechtstreeks te manipuleren. Deze onderzoeksresultaten hebben nieuwe inzichten verschaft in de complexe mechanismen gebruikt door baculovirussen in het bijzonder en door neuroparasieten in het algemeen om het gedrag van hun gastheren te beïnvloeden.

I would like to acknowledge Vera I.D. Ros for making this ‘Samenvatting’; Dutch translation.

Referat

Parasit-induceret adfærdsændringer der øger transmissionen til den næste vært er et almindeligt fænomen. To af de mest mærkværdige eksempler på parasit-inducerede adfærdsændringer er de ændringer som baculovirus inducerer in deres møllarve vært i form af hyperaktivitet og trætop sygdom, og fladorme-inficerede myrer som klatrer op i vegetationen og bider sig fast til den. Disse to systemer er fantastiske eksempler på parasitter der går et skridt videre i deres manipulation: det gør det ved at invadere centralnervesystemet (CNS) i deres vært. Dette fjendtlige overtag af værtens nervesystem udført af en anden organisme, der udnytter værtens ændrede adfærd til egen fordel, kaldes neuroparasitisme.

Kapitel 2 af denne afhandling, er en sammenfatning af hvad man vidste på gældende tidspunkt om baculovirus manipulation af deres møllarve værts adfærd. Baculovirus er velkendt for at inducere hyperaktivitet (forøget bevægelse) og/eller trætop sygdom (klatrer opad før døden indtræffer). Baculovirus kan nemt muteres, hvilket øger mulighederne for optimal eksperimentel opsætning ved komparative studier mellem insekter inficeret med vildtyper (WT) af virus eller med mutant vira som mangler bestemte gener, der er involveret i adfærds manipulation. Vi satte her fokus på resultater fra nylige studier som for første gang løftede sløret for de underliggende molekylære sammenhænge som førte til de typiske adfærdsmønstre af baculovirus inficerede møllarver og i deres rolle heri. Da værtens adfærd generelt er reguleret gennem værtens CNS, postulerede vi lovende fremtidige skridt til at studere hvordan baculovirus regulerer værtens nerve aktivitet.

I Kapitel 3, fokuserede jeg på de faktorer som influerer udtrykkelsen af adfærdsændringer, induceret af en hjerne inficerende fladorm i dens naturlige habitat i skoven. Dette kapitel undersøger effekterne af temperatur, relativ luftfugtighed (RH), tid på dagen, dato, og en indstrålings-proxy på adfærdsændringer hos myren *Formica polyctena* induceret af den lille leverikte *Dicrocoelium dendriticum*. Denne fladorm får myrer til at klatre op og bide sig fast i vegetationen med deres kæber i et stadie af tetanus. En total af 1264 individuelle myrer som udtrykte den inducerede adfærd blev observeret over 13 ikke konsekutive dage og en mindre del af disse fik også individuelt sat mærkater på, for at følge når de bed og gav slip i relation til variationer i temperaturen. Inficerede myrer bed sig primært fast til vegetationen tidligt og sent på dagen, hvilket passer med lav temperatur og høj RH, formentlig sammenhængende med græsningsadfærden hos græsædende pattedyr, hvilket er de endelige værter for den lille leverikte. Temperaturen var den vigtigste faktor for den inducerede fænotypiske ændring. På varme dage ændrede de inficerede myrer adfærd mange gange, hvorimod på kolde dage blev mange inficerede myrer siddende med kæberne fastlåst til vegetationen hele dagen. Resultaterne fra dette kapitel indikerer at temperatur-sensitivitet af disse naturligt inficerede myrer har to formål ved at udsætte inficerede myrer for den næste vært på et passende tidspunkt, samtidig med at de beskyttes mod for høje temperaturer på andre tidspunkter, hvilket kan øge værts- (og parasit-) dødeligheden.

Kapitel 4 er en dybdegående analyse af CNS af *Spodoptera exigua* møllarver. Tidligere studier af CNS hos insekter er primært undersøgt på voksne individer, mens larvernes CNS indtil videre kun har fået ringe opmærksomhed. Dette kapitel præsenterer en oversigt over de immunoreaktive områder af de primære signalstoffer i CNS af mellem tredje larve stadie af smalvinget ugle, *S. exigua*. De vigtigste signalstoffer af insekter og deres hastighedsbegrænsende enzymer som er involveret i biosyntesen blev målt, da det har været foreslået at disse er involveret i en bred vifte af adfærdstyper. Jeg identificerede og beskrev de immunoreaktive neuroner og deres projektioner og lokation i CNS af *S. exigua* for tyrosin decarboxylase (TDC), tyramin (TA), tyramin beta-hydroxylase (TβH), octopamin (OA), tyrosin hydroxylase (TH) og serotonin (5HT). Analysen fra dette kapitel hjalp til at udfylde det videnskabelige hul der er for CNS af insekt larver, og danner derved udgangspunkt for fremtidige studier af lepidoptera larver, deres CNS og deres adfærd samt studierne i de næste to kapitler.

Kapitel 5 fokuserer på den bedst kendte baculovirus Autographa californica multiple nucleopolyhedrovirus (AcMNPV) og invasionsveje til CNS. Under infektion med AcMNPV i *S. exigua* møllarver, er der brug for en enzymatisk aktiv form af et virus protein kaldet protein tyrosine phosphatase (PTP) for at udtrykke hyperaktivitet 3 dage post infektionen (dpi). Ved at bruge forbedret Grønt Fluorescerende Protein (eGFP)-udtrykkende rekombinante AcMNPV stammer viste jeg at man kunne observere infektion af møllarvernes CNS fra 3 dpi og fremefter. Ydermere, demonstrerer kapitlet at PTP ikke spiller nogen rolle i infektionen af CNS. Der vises at virus kommer ind i CNS via trachea, og infektionen udvikles caudalt til frontalt igennem CNS og fra de yderste cellelag til de inderste cellelag af CNS, uafhængigt af PTP.

Kapitel 6 bygger videre på den viden som blev erhvervet i de to tidligere kapitler med studier af de underliggende mekanismer bag adfærdsændringer. I dette kapitel inficerede jeg det tidlige tredje stadie af møllarver oralt med WT AcMNPV eller med AcMNPV mutanter som enten udtrykte en katalytisk inaktiv PTP (catmut), eller ingen PTP (Δ*ptp*), for at undersøge den potentielle rolle af monoaminers signal vej i AcMNPV-PTP induceret adfærds manipulation ved 1, 3 og 4 dpi. Vi målte koncentrationen i hæmolymfen af de tre vigtigste monoaminer i invertebrater: 5HT, OA og dopamine (DA). Endvidere, undersøgte vi genekspressionen af aktører involveret i biosyntesen af de førnævnte monoaminer samt for TA, ved at analysere genekspressionen af "precursor" enzymer, hastighedsbegrænsende enzymer, og receptorer i disse vigtige signalveje. Vi kunne måle en effekt af dpi og behandling på koncentrationen af 5HT og DA og vi fandt at for de fleste af generne, at enzymerne og receptorerne var højest udtrykt ved 1 dpi. Ydermere, var generne som koder for serotonin receptor 5HT-7 opreguleret i AcMNPV WT inficerede møllarve hoveder sammenlignet med AcMNPV catmut- og AcMNPV Δ*ptp*-inficerede artsfæller. Når møllarverne var inficeret med AcMNPV WT kunne vi detektere en opregulering af generne der koder for tyramin receptoren TAR1 sammenlignet med larver inficeret med AcMNPV catmut- og AcMNPV Δ*ptp*.

I det sidste **Kapitel 7**, diskuterede jeg de ovenstående fund fra afhandlingen ved at placere resultaterne i konteksten af det eksisterende videnskabelige område og jeg præsenterede yderligere foreløbige resultater. Når man samler informationen præsenteret i Kapitel 4, 5 og 6 omkring monoaminer, deres hastigheds begrænsende enzymer og deres receptorer ser vi en potentiel rolle for disse aktører i værts adfærds manipultation hos neuroparasitter. Med den signifikante forskel af AcMNP WT-inficerede larver sammenlignet med deres AcMNPV Δ*ptp*- og catmut-inficerede artsfæller angående koncentrationen af DA, deres ekspressions niveau af 5HT-7 og TAR1 og tætheden af immunoreaktive områder af TDC, TH, TA og 5HT med AcMNPV i CNS, har jeg i dette projekt givet indikatorer for rollen af disse aktører i adfærds manipulation af AcMNPV på *S. exigua* møllarve værten. Jeg har demonstreret at PTP ikke er nødvendig for virusen i invasionen af møllarvens CNS og at AcMNPV sandsynligvis handler ved direkte manipulation af netværket af neuromodulatorer og udviklingsprocesser, der styrer et insekts adfærd. Gennem disse resultater har jeg tilføjet ny indsigt i de komplekse mekanismer, der udnyttes af baculovira i specifikke tilfælde og af neuroparasitter generelt.

Publications

Before PhD dissertation

Eilenberg J, **Gasque SN**, Ros VID. 2017. Natural Enemies in Insect Production Systems. In A van Huis and JK Tomberlin (eds.): Insects as Food and Feed: From Production to Consumption. Wageningen Academic Publishers. The Netherlands. 201-223. doi: 10.3920/978-90-8686-849-0.

Fredensborg BL and **Gasque SN.** 2018. Parasitter og adfærd – på opdagelse hos naturens hjerneforskere. Kaskelot. 219: 20-23. (Parasites and behaviour – on exploration with natures brain surgeons). https://www.kaskelot.dk/parasitter-kaskelot-219/

Gasque SN, Poinar GO, Fredensborg BL. 2018. Ant (Hymenoptera: Formicidae) parasitism by Neoneurinae wasps (Hymenoptera: Braconidae) in Denmark. Ent Medd. 86: 27-30. https://www.researchgate.net/publication/334469511_Ant_Hymenoptera_Formicidae_parasitism_by_Neoneurinae_wasps_Hymenoptera_Braconidae_in_Denmark

Non-scientific

Two chapters in:
EEH productions. 2020. Snapshots: An Anthology of True Stories. GVO Drukkers & Vormgevers. Wageningen, the Netherlands. ISBN: 9789463327114.

In this dissertation

Gasque SN, van Oers MM, Ros VID. 2019. Where the baculoviruses lead, the caterpillars follow: baculovirus-induced alterations in caterpillar behaviour. Curr Opin Insect Sci. 33: 30-36. doi: 10.1016/j.cois.2019.02.008.

Gasque SN and Fredensborg BL. 2023. Expression of trematode-induced zombie-ant behavior is strongly associated with temperature. Behav Ecol. 34: 960-968. doi: 10.1093/beheco/arad064.

Gasque SN, Han Y, van der Ham I, van Leeuwen D, van Oers MM, Haverkamp A, Ros VID. 2024. Baculovirus entry into the central nervous system of *Spodoptera exigua* caterpillars is independent of the viral protein tyrosine phosphatase. Open Biol. 13: 230278. doi: 10.1098/rsob.230278.

About the author

Simone Nordstrand Gasque was born on September 1, 1990 in Hundested, Denmark - growing up in idyllic surroundings overlooking the Kattegat. She always loved nature and maybe due to her dad's interest in insects, hers got spiked at an early age. Her interest in natural science was noticed as she was offered a spot on a natural science week for selected young kids from this part of the country. She took the high school exam in 2009, where she in the end became a student tutor in mathematics. She was a teacher at a primary/secondary school for more than a year. During this time she acquired the necessary skills for working with humans and for teaching.

In 2011 she started a bachelor's degree in Biology at the University of Copenhagen (KU). One year in, she got hired as a custodian at the Natural History Museum, where she worked mostly part-time for the following five years. She advanced to a guide and was responsible for the manuals and specimens, for children's programs and for the guided tours. Furthermore, she was also responsible for the bones that were delivered to the museum for identification, and on special occasions she presented knowledge about smelly Sumatran plants (see picture, *Amorphophallus titanum*) to the general public.

During a six months exchange to James Cook University (JCU) in Townsville (Queensland, Australia), her interest for parasites got a boost. The knowledge she acquired during courses from JCU and KU, she shared with the guests the following years at another side-job as a marine biologist (at "Pet a Fish") at the harbour of her hometown. As edible insects were an upcoming theme and her current interest was to make a project of this and parasites, under the guidance of Prof. Dr Jørgen Eilenberg she wrote a literature review covering the parasites known in four of the most consumed insects species worldwide. This was followed by a short employment to create a list of Danish edible insects. This project was ordered by the company supplying research to the number one restaurant in the world; Noma. Simone graduated with a bachelor in Biology in 2014.

Simone continued with a Master in Parasitology at the University of Copenhagen, at the same time being a student assistant on four BSc-courses. When deciding on the topic of her MSc-thesis project, she had to follow her heart and performed a project on her favourite parasite *Dicrocoelium dendriticum,* the lancet liver fluke. In this project she elucidated the main abiotic driver of the expression of the parasitic induced behaviour of the host in the field, and investigated the mechanisms behind said behaviour in the laboratory. This was done under the supervision of Prof. Dr Brian Lund Fredensborg. During one of many ant dissections she found a parasitoid wasp larva inside an individual, which until then had not been found in this host species and its presence had not been described in Denmark before. This lead to a short note with Dr George Poinar Jr., who is behind the idea of extracting DNA from ancient insects embedded in amber - the idea on which the Jurassic Park movies are based upon. Towards the end of the thesis she was awarded the Nordic OIKOS student travel award, to present the results from her MSc-thesis in Trondheim, Norway. In the spare time of the MSc-thesis, the knowledge acquired during her BSc-thesis was put together into a book chapter with her BSc-supervisor Prof. Dr Jørgen Eilenberg and with Dr Vera I.D. Ros. The latter later became her daily supervisor at the department of Virology, at Wageningen University and Research (WUR) on a project resulting in this dissertation you are reading now.

During Simone's time as a PhD candidate at WUR, she was an arranging member of the Wageningen Evolution and Ecology Seminars (WEES). In 2022 she received both the Uyttenboogaart-Eliasen Stichting (UES), Symposia of Invertebrate Pathology (SIP)-travel award and the Rob Goldbach Fund to participate in conferences planned for Denmark and South Africa that year. She became known as the athlete from Denmark at the first day at the calisthenics park where she started training with the Goaltrainers, and she also became one of the steady storytellers at the Wageningen Storytelling scene, where she shared personal stories for about four years. Simone was one of the presenters during the first Pint of Science held in Wageningen. For this she constructed a Pokémon inspired game about parasite induced behavioural alteration, to get the audience excited about parasite-host interactions. Towards the end of her PhD, Chapter 3 in this dissertation got published. Likely due to the catchy usage of the word "zombie-ants" in the title, the article got a lot of attention from different news sites around the world. This lead to an invitation to present the results, and Simone left Wageningen on a flight ticket to be one of eight scientist to present new results of the year at the Science gala arranged by the Natural History Museum of Denmark. This was where she used to work at, giving her a feeling of completing a circle going back to where she fully got interested in science communication. With an audience accounting 400 people of all backgrounds and ages, she feels well equipped to give the laymen's speech about this thesis you are now holding in your hands.

Training and education statement

X

PE&RC training and education statement

With the training and education activities listed below the PhD candidate has complied with the requirements set by the C.T. de Wit Graduate School for Production Ecology and Resource Conservation (PE&RC) which comprises of a minimum total of 32 ECTS (= 22 weeks of activities)

Review/project proposal (6 ECTS)

• Where the baculoviruses leads, the caterpillars follow: Baculovirus-induced changes in caterpillar behaviour
• Insane in the brain: How a virus manipulates a caterpillar's brain function and behaviour to enhance transmission

Post-graduate courses (7 ECTS)

• Chemical and genomic insight to parasitic and mutualistic host-microbe interactions; PhD School of Science, University of Copenhagen (2018)
• Electron microscopy course the basics: From A to W; UMC and WUR (2018)
• Introduction to R and R studio; PE&RC (2021)

Invited review of journal manuscripts (1 ECTS)

• Journal of Insects as Food and Feed; Comparison of volatile aroma compounds in and processing aptitude of edible insects: Breeding in plastic and glass cages (2022)

Deficiency, refresh, brush-up courses (9 ECTS)

• Fundamentals of genetics and molecular biology (2019)
• Fundamental and applied virology (2019)

Competence, skills and career-oriented activities (5.608 ECTS)

• Competence assessment; PE&RC (2018)
• Searching and organising literature; PE&RC (2018)
• Introduction to the Netherlands; PE&RC (2018)
• Scientific artwork/vector graphics and images; PE&RC (2018)
• PhD workshop carousel; WGS (2019)
• Supervising BSc and MSc thesis students; WUR (2019)
• Stress identification and management; WGS (2019)
• Storytelling workshop and many additional storytelling events (2019-2023)
• Multiple sessions; Studium Generale (2019-2023)
• Efficient writing strategies; WGS (2020)
• Ethics and animal sciences; WGS (2021)
• Brain friendly working; WGS (2021)

• Scientific artwork; data visualisation and infographics with Adobe illustrator; WGS (2022)
• Grant applications: how to write a winning impact paragraph?; WUR (2023)
• Last stretch of PhD programme and propositions writing; WGS (2023)

PE&RC Annual meetings, seminars and the PE&RC retreat (3 ECTS)

• PE&RC Weekend first year (2018)
• PE&RC Day (2019, 2021)
• PE&RC Weekend midterm (2020)
• PE&RC Weekend last year (2022)

Discussion groups/local seminars or scientific meetings (10.7 ECTS)

• Rob Goldbach lectures (2018-2022)
• Dutch annual virology symposium (2019)
• WUR PhD symposium (2019)
• Dutch entomology day (2020-2022)
• WEES (2020-2022)
• NERN (2022)

International symposia, workshops and conferences (9.1 ECTS)

• SIP (2019, 2021, 2022)
• ICOPA (2022)

Societally relevant exposure (1.69 ECTS)

• Pint of science: Insect brain surgeons (2023)
• Podcast interview for Decodificando la Ciencia about parasites and neuroparasites (2023)
• Interview Washington Post, and for other media (2023)
• Invited speaker at Science gala at the Natural History Museum of Denmark/ University of Copenhagen (2023)

Lecturing/supervision of practicals/tutorials (9.75 ECTS)

• Fundamental and applied virology (2019)
• Biological control of insects (2019)
• Integrated pest management (2019)
• Ecological aspects of bio interactions (2019-2021)

BSc/MSc thesis supervision (20 ECTS)

• Dopaminergic cell cluster identification and AcMNPV localisation in *Spodoptera exigua* larval brains
• The involvement of PTP in insect virus entry to hosts' brain
• Losing their minds: Octopaminergic cell cluster identification and AcMNPV locali sation in *Spodoptera exigua* larval brains
• Going around in circles: Designing and testing new methods to measure and compare hyperactive behaviour caused by Autographa californica multiple nucleopolyhedrovirus in *Spodoptera exigua* larvae
• The mechanism behind baculovirus-induced host behavioural changes in *S. exigua*; the role of neuroreceptors, rate limiting enzymes and the 14-3-3 protein family
• Expression of AcMNPV-infection by means of behavioural alteration in *S. exigua* populations
• Influence of AcMNPV infection and its hyperactivity needed viral protein tyrosine phosphatase on relative serotonin precursor- and - receptor gene expression in *Spodoptera exigua*

Acknowledgements

The last pages of my dissertation is dedicated to the people supervising my PhD-journey, collaborating and who helped me and were present near and far away during the process. These people are the rocks of the foundation that you do not see at first glimpse when looking at the dissertation. But whom have been crucial for me during the process.

The first person I would like to thank, is one I specifically could not have done this without. My daily supervisor during this long journey, **Vera**. For your invaluable knowledge about Insect Virology. For supervising me through my bad and better ideas. Always providing a sharp eye on the details and untiring feedback loops on drafts and articles. I am happy that we many years ago got an email collaboration up and working over our book chapter. Without that I am not sure we would have been where we are today. **Monique**, thank you for being my supervisor. For always having an eye out on the bigger picture, for your endless knowledge within virology and providing super quick feedback on emails and drafts, specifically in the last stretch of my project when it was extra needed. This work would also not have been possible without you **Alexander**. Thank you for your expertise on insect neuroscience. For the many discussion over how to structure chapters, and your patience with me when I got ideas for experiments or came by with ”quick questions” about links or explanations for results. **Hans**, thank you for being a human neuro-insect encyclopaedia, remarkable photographer, great illustrator and always having time to helping me out with the issues I had in photoshop. **Astrid**, thank you for your late afternoon help on tricky calculations, for initially teaching me and my students about primer design, qPCR etc. And finally for the intense 1-2 weeks of working on Chapter 6. I am happy with what we got from it.

Brian, tak for den evigt gode vejledning både under min MSc og senere karriere beslutninger. Jeg sætter umindeligt pris på at du altid har vægtet min mening og behandlet mig som en lige-mand/kvinde i al den tid jeg har kendt dig. Tak for tålmodigheden i vores mangeårige samarbejde omkring vores *D. dendriticum* artikel. Den artikel betyder noget helt særligt for mig. Og wow en interesse der var for vores studie omkring zombie-myrer. **Per**, et tak skal lyde for din statistiske bistand i forbindelse med denne artikel. Tak for din tålmodighed og kørsel af SAS koder når mit eget program stoppede med at fungere. **Jørgen**, tak for at være min første vejleder i min akademiske karriere og særligt for at have anset mig som en uafhængig forsker selv under en BSc. Jeg værdsætter at du anså min viden inden for parasitter/patogener i insekter relevant nok til at deltage i samarbejdet med Vera, som blev til min første publikation - vores bogkapitel. Et kapitel der gav mig erfaring med scientific writing, og nok gav mig blod på tanden til mere.

A special thanks to my two paranymhs whom has been doing a great job helping me out arranging aspects around the invitation, defence etc.

Annamaria, thank you for being such a good friend both at work and in private life. You always put other people’s needs higher than your own, a quality that makes you a great friend and colleague, but something that might be a challenge in academia and life in general. I am happy to see that you are putting your own needs in priority more and more. I wish you all the best in finalising your PhD – you can do this! **Julian**, you were the first one to be confused about my nationality (a common feature for people at the laboratory of Entomology it seems ;)) – but after a few years it seemed that you accepted that I am not German. Thank you for being a constant hurricane swirling around in a hurry between Ento and Viro, but never too busy for checking in on how people are doing or getting the latest progress updates on experiments or articles. The times we shared was always good fun!

Being a PhD candidate at the **department of Virology** learned me many valuable lessons, both in-depth knowledge, and soft skills of working in a multicultural group. I would like to thank the whole department for a pleasant work environment, specifically for all the great outings we had such as the lab-uitje and the international dinners thanks to **Jan, Rene, Emilyn, Cristina, Corinne, Marleen** (I hope you will forgive me one day for every year wearing the same red sweater at the group picture), **Richard, Gorben, Jelke, Jeroen, Marry, Dennis** and **Mark**. I would like to thank the other PhDs and post docs that had an overlap with me, for the experiences we shared both at work and at social gatherings. Thanks to **Corien, Magda, André, Irene, Min, Mandy, Janna, John, Marcelle, Sharella, Haidong, Giel, Sandra, Linda, Miao, Jerome, Lisa, Joyce, Linda, Kristel, Sophie, Wessel** and **Carmen**.

Specifically I would like to extend my thanks to the **Virus Insect group**, for all the interesting discussion at our weekly meetings, conferences and seminars we joined together. I would like to thank late **Hanke, Els** and **Dorothy**, you are the corner stones of keeping the lab and the insect rearing running. For the PhDs and post docs that I shared time with, in the later hours of the day in the lab or during the weekends; **Han, Irene, Hannah, Melissa, Caroline, Jirka, Jozsef** and **Sam. Luis** (Liru) Hernandez Pelegrin, my Spanish brother. I am happy you came to Wageningen and we had so many fun experiences together such as our visit to the big city of Amsterdam during Pride 2022. **Ahmed**, thank you for being my desk buddy, for suggestions on different statistical test and giving second opinions on the small things, but the ones that matters in life, such as versions of different figures. **Bob**, thank you for being my first desk buddy, and for teaching me many things in the lab when I started. For always being such a happy and good spirited guy – although when you get so well spirited you speak Dutch and I do not know what you are talking about. Sjonge Jonge! I enjoyed our trip to Valencia along with **Gabriela**. I look fondly at our trip to Valencia, and all the times I passed by your house unannounced, which ended up lasting for hours, staying for dinner and even Elinor’s sleepover invitations. And

thank you for trusting me so much as to be the first babysitter of Elinor. **Jitte** thank you for initially introducing me to *S. exigua* brain dissections and later in life for inviting me along as you co-speaker at Pint of Science, and for support in my mad ideas regarding science communication.

Having a project overlapping different fields meant I was fortunate to not only being part of one, but two groups. I would like to thank my second family, the **Entomology group**, for all the good discussions about projects, ideas and social gatherings such as the annual lab trips, WEDays, Sinterklaas and the YELREM. Thanks to: **Marcel, Joop, Karen, Sander, Eveline, Pieter, Martine, Erik, Angelique, Hariëtte, Rieta, Gerard, Gabe, Jeroen** and **Janneke**. More specifically I would like to thank all the PhDs and postdocs who I shared this journey with: **Peter, Daan, Stijn, Quint, Yidong, Julia, Davy, Thibault, Kay, Alessia, Helen, Shaphan, Julien, Mitchel, Bram, Max, Kathe, Els, Parth, Hanneke, Emily, Marieke, Jeanine, Anna, Kelly, Yvonne, Zulema, Marcella, Mariska, Helena, Lena, Sarah, Kris, Zoe, Natalia, Carlotta, Sami, Maxence,** and **Charlotte. Rody** thank you for being my eyes on colours in figures and graphs, for sharing cool (animal) stickers and for always being up for a beer. **Luuk** for being the most direction and number confused person in Ento (Syd! Fjorten!) and for the fun times we shared at concerts. **Alessandro**, thank you for all the nice trips we had around the country and joining me on our salsa adventure. **Mitchel** thank you for always checking in and spreading good vibes when bouncing around in the hallways. **Fillipo**, for always being such a good sport helping out with whatever I could not find in the Ento molecular lab and always providing such random topics for fun conversations. You are indeed the best breakdancer (... straight after Sander). **Pedro**, thank you for taking some days out of your busy agenda to help me run the Random Forest method on my data set. Your constant kindness on my emails and texts at random times were much appreciated. **Aidan, Qi** and **Stefan** thank you for good company and for all the random talks and listening to all sorts of music in the Brain lab during brain dissections. **Rick**, thank you for your innovative ideas of stitching things together for the purpose we might have. Thanks for being my partner in crime during the ELISA endeavour. I think back on our intense week of ELISA runs and our quote stickers with a smile on my face. **Tessa**, thank you for your kindness and always being ready to provide ideas of how to solve Prism issues or just pressing exactly the right buttons!

Thanks to both **Henk** Schipper from EZO and **Norbert** de Ruijter from the WLMC Facility, for maintaining the CLSM microscopes and the help when the machines behaved interesting. This dissertation would not be what it is today without these machines that I have used so many hours in front of.

Thanks to my graduate school **PE&ER**, for arranging a great first year weekend and other following courses, and **Claudius** for great feedback on my propositions.

Part of doing a PhD is also about the learning experiences of supervising others. During my PhD I supervised both BSc and MSc projects, and I learned from each and every one of these people and experiences. Results obtained in some of these projects, even made it to parts of this dissertation. Thanks to **Steffi, Nhu, Simon, Sarah, Robin, Tina** and **Lisanne** for picking a project under my supervision and for the lessons we learned together.

Thanks to all past and present members of **WEES**, for the afternoons shared on planning and arranging great and interesting seminars.

Drawing a line between whom to acknowledge on a professional basis and on a personal note has been hard for me to draw. As an expat moving to a new country to conduct this project, making friends and a support system is as much part of a successful finalisation of a PhD, as the guidance and help you get in the lab and the office. Therefor I would also like to thank all the people involved in keeping me sane, by being part of my alternate worlds, being my friends, my support system here and lastly my original by blood family.

For sharing many good days, afternoons, evenings and much more, I would like to thank all the people involved in any of my multiple alternate worlds. Thanks to **Goaltrainers** (**Guido, Bassou, Don, Erik, Daan, Myrthe**) and the friends I made during the nights and sunny Sunday afternoons at our lovely park. **Simone**, thanks for introducing me to- and being the instructor on my other alternate world; salsa dancing. For our many walks and talks about nothing and everything. **Jana**, for the evenings shared at GT and the fun trip we shared to Dordrecht. Thanks to the **Wageningen-Storytelling community**, but specifically to you **Emma**. For first having faith in me as a storyteller, for always wanting to hear my weird stories about life and lastly for being a good friend. I enjoyed the project of writing a book during the lockdown period. A pity we never got started on our podcast – that might be for another chapter.

Thanks to the **Meisjes; Irene** and **Isabelle**. For your friendship, all the dinners, the trips to the cinema, walks and much more. We had so many good times and trips together e.g. to Maastricht, den Bosh, the tulip fields in Nordwijkerhout, and my all-time favourite trip to Ameland.

Some people had and extra influence on making my first few months in Wageningen an extra joyful time, thanks to **Davide, Marielle** and **Barnardo,** we did not have much time together, but in the time we made stories for the books! **Remnants/weekend muts**: thank you for all our nice brunches, dinners and much more e.g. at H3 arranged by Bernardo. **Rajan**, thank you for being exactly who you are; a preacher for the ministry of Pakistan and for inviting us all to Pakistan

(and being such a good and kind host to us), to take us into your family and for my Pakistani-princess adventure. **Anouk** and **Raul** I enjoyed our monthly visits to Diels to treat ourselves with fancy three course dinners during the lockdown, and all our bubble-brunches. Raul a specific thanks to you for managing to live in the same house with me during the hard lockdown and for a great trip to Rio and Pakistan.

Henry, thank you for becoming a good friend of mine and bringing me into your awesome friendship group, I really appreciate that. Thanks to the rest of the **Drunk division; David, Rosie, Mark, Michael, Lorenzo, Rutger, Dilara, Tjark, Nilesh, Céline** and **Rushabh** for all the fun experiences we shared, for our great trips to Zeeland, Belgium and Ireland. A special thanks to you **Heleen**. For becoming such a good and dear friend to me, willing to go the extra mile to visit me in Wageningen when you could, and for the extra experiences we shared in Denmark and the fields of Nijkerk. Even coming all the way to Wageningen to spend the last time I had in the country, and bringing me all the way to the airport.

Mie, tak for at række ud og ville bruge så meget af din fritid på at digitalt illustrere, og farvelægge min idé til forsiden. Tak for din tålmodighed i feedback processen. Jeg er helt vild med det endelige produkt! **Kenneth** Sømark, tak for at gøre mig selvskab på overnatningen i Bidstrupskoven til 24-timers studiet af mine zombie-myrer, for din entusiasme over en helt bestemt myre med nummer på (rød 14). Plastik **Lene**. Jeg er glad for at lige præcis du og jeg endte med at tage fra KU til James Cook i Australien. Det var en fantastisk tid vi delte dér og som blev starten på et stabilt og langt venskab. Selvom først du var i Australien af flere omgange, og jeg sidenhen flyttede til Holland, så har det altid været det samme gode venskab når vi så hinanden. At sende random videoer i tide og utide – det er sand kærlighed og støtte langvejs fra. Tak til mine "gamle" venskaber fra før afrejse til Holland og de nye venskaber jeg er ved at bygge op i Danmark.

Tak til hele min **Gasque familie** i Danmark og andre steder i verden. Særligt tak til **Claus**, for at designe den fine figur i Kapitel 2, samt for tålmodighed og rettelser når en liquified møllarve lige skal se noget mere flydende ud. Tak til **Nordstrand klanen**, jeg er så glad for at jeg er vokset op i så stor en familie som den vi har. Særligt tak til **Tante Trine**, for de kærlige beskeder langvejs fra, for vores mystiske indfald, så som at sende postkort skrevet med venstre hånd til hinanden og tak til dig og **Jørgen** for besøget i sommers, det var sådan en god overraskelse!

Drengene; **André** og **Frederik**. I to fjolle hoveder. Utroligt at to mennesker som har delt en livmoder i ni måneder kan være så forskellige og skønne på hver jeres måde. I er så meget fra en anden generation end mig, men heldigvis har jeg I jeres tidlige år gjort tingene på en måde der passede jeres interesser og niveau. Jeg ved ikke om det har gået den anden vej senere i livet. Men jeg har lært meget af at være jeres storesøster og de senere år med alle de smarte hjemmesider og gadgets I kender til. Ja Simo lyder gammel. **André** tak for din evige omsorg for folk omkring dig, man kan se hvor utroligt mange ting der sker inde i dit kloge hovede. Tak for dine pudsige og mystiske indfald, som kan få os andre til at måbe over hvor den sætning kom fra. Tak for lån af støjreducerende hovedtelefoner i hele den sidste del af min skrive process, og for din tålmodighed når jeg kom ind og forstyrrede dig ved fx bare at stå og hoppe på dit værelse :) Og **Frederik** dit morgensure, kreative menneske. Tak for at være lige præcis dig selv – uanset hvor meget det kunne stikke ud fra mængden, det er en god kvalitet at have. Og ekstra mange tusinde tak for at sætte hele min bog op i InDesign det var en kæmpe hjælp! Og tak for at visualisere mine ideer til figurer i forskellige kapitler (Kapitel 1: Figur 5; Kapitel 4: Figur 1; og Kapitel 7: Figur 1) – de er simpelthen så flotte!

Mor og **Far**, tak for at I opdragede mig som I gjorde. Mange værdigfulde lektier lærte jeg tidligt i livet. Lektier som jeg sidenhen i livet er blevet klar over og begyndt at sætte særligt pris på i mødet med andre mennesker, andre kulturer og andre måder at gøre ting på. **Mor**, tak for din evige mødre bekymring for alle dine kyllinger, for din varme, og for dit kritiske hårde blik af bekymring som kan skære ind i én uden at du endnu har sagt noget. Tak for alle hæklerierne og glæden ved andres gode og tætte relationer. For din følsomhed, som nu kan føre til tårer når man får eller snakker om; lavendel gaver, zombie-myrer artikler, videnskabsgalla og meget mere. Lad os håbe at du kan holde det i dig til forsvaret er overstået :) **Far**, tak for at give din rejselyst videre til mig, for glæden ved at udforske ting, steder mm. For at kaste dig over projekter på den måde du gør og for altid at ville ud til vandet og kigge på det samme hav hver eneste dag, og tjekke om noget sand mon har rykket sig. Og tak for at tage mig med på dit gale båd eventyr. Ja der er nok ikke andre end dig og mig der er tossede og eventyrslystne nok til at kaste sig over sådan et projekt. I to lærte mig et niveau af inklusion tidligt i livet, som jeg har opdaget er en søjle i mine værdier. I lærte mig navne på sommerfugle, en tække med planter, og en indsigt i at vide noget om ting er fedt, som nok har ført til min nørdede side. Samt at det er okay at nørde noget. En værdi som nok kendetegner mig, men også kendetegner mange mennesker i den akademiske verden og dem som vælger at lave en PhD. I gav mig en evig tro på mig selv og at hvis man knokler på, skal man nok nå de mål man sætter sig.

Den her afhandling vil jeg gerne tilegne min nære familie; drengene og mine forældre, som har skulle undvære mig i deres daglige liv de sidste fem år.

This dissertation, I would like to dedicate to my close family; my brothers and my parents, whom had to do without me in their daily life for the last five years.

The research described in this thesis was performed at the Laboratory of Virology and Laboratory of Entomology of Wageningen University and Research (WUR) and financially supported by the Dutch Research Council (NWO, ALWOP.362). Financial support from Wageningen University for printing this thesis is gratefully acknowledged.

Cover design by Simone Nordstrand Gasque and Mie Branick Jacobsen.
Layout by Simone Nordstrand Gasque and Frederik Nordstrand Gasque.
Printed on FSC-certified paper by Gildeprint, Enschede, the Netherlands.